

A METHODOLOGY FOR GENERATION CAPACITY AND NETWORK REINFORCEMENT PLANNING

Panagis Vovos



Thesis submitted for the degree of
Doctor of Philosophy
University of Edinburgh

2005



ABSTRACT

This thesis presents a novel methodology for generation expansion planning. The method is based on Optimal Power Flow (OPF), a common tool for the economic operation of power systems. New generation capacity is simulated by means of virtual generators located at the candidate connection points, so OPF is used to plan generation expansion with respect to operating constraints of the existing network.

Further research examined the bounds set on generation penetration by the specification of existing switchgear equipment, specifically switchgear and the contribution of additional generation to fault levels. Initially, the new constraints were considered in a three-step iterative generation allocation process. In each iteration, potential generators are gradually downsized from their original OPF allocation, which ignores expected fault currents, in proportion to their contribution to violations of switchgear equipment specifications. The process iterates until both system and fault constraints are satisfied.

However, the iterative nature of the above approach cannot guarantee optimality for the final solution. Therefore, a new method had to be developed for the direct incorporation of switchgear constraints in generation expansion. The modelling of new capacity with virtual generators gives access to power flow control variables. Binding constraints for generation expansion can be expressed as constrained functions of those variables. Accordingly, expected fault currents were expressed as functions of OPF variables and switchgear equipment specification were converted to constraints for these functions. Thereafter, the allocation of new capacity by the OPF directly respects both system and fault constraints. The iterative approach has been proven less efficient than the later approach, but still maintains some advantages should the method be commercially exploited.

Generator voltage control policies can also be converted to OPF constraints. The functionality of the suggested generation capacity allocation method was expanded to operate as an assessment tool of their impact on the amount of new capacity that a network can absorb. The method was expanded further, so as to consider the impact of capacity allocation on transmission losses. With a minor reformulation of the original method a new tool was designed for the optimal siting of reactive power compensation banks for the improvement of network headroom.

Finally, a network planning method is presented based on the LaGrange multipliers, sensitivity by-products of the OPF solution method, which connect network constraints with generation expansion. Generation expansion is planned simultaneously with network reinforcement, so the overall optimum is achieved. The main conclusion of this work is that OPF can be used as a powerful planning, as well as operating tool. Its flexible formulation allows the incorporation of emerging constraints in generation and network expansion, such as those imposed by switchgear.

DECLARATION OF ORIGINALITY

The research recorded within this thesis and the thesis itself is, except where indicated to the contrary, the original and sole work of the author.

—Panagis Vovos

ACKNOWLEDGEMENTS

I would like to thank my supervisor Professor Janusz Bialek and second supervisor Dr Gareth Harrison for their support and supervision over the duration of this research. Also, I am grateful to the staff and postgraduate students of the Institute for Energy Systems for their ideas and suggestions during the course of my work. I would also like to thank my family and friends for their loving support. Last, but certainly not least, I would like to thank my girlfriend Ela for enduring my ups and downs through these difficult three years.

“If A equals success, then the formula is: $A = X+Y+Z$. X is work. Y is play. Z is keep your mouth shut.”

Albert Einstein

To stubbornness.

ABBREVIATIONS

AC	Alternating Current
AVPFC	Automatic Voltage / Power Factor Control
AVR	Automatic Voltage Regulator
B	Shunt capacitance
CEL	Capacity Expansion Location
CVC	Central Voltage Control
D-FLCOPF	Direct - Fault Level Constrained Optimal Power Flow
DG	Distributed Generator
DNO	Distribution System Operator
E/IP	Export / Import Point
ECVC	Emergency Central Voltage Control
FACTS	Flexible Alternating Current Transmission Systems
FLC	Fault Level Constraints
FLCOPF	Fault Level Constrained Optimal Power Flow
FLCRA	Fault Level Constraints Reduction Algorithm
GROA	Generator Reactance Optimisation Algorithm
NP	Nonlinear Programming
NSO	Network System Operator
OF	Objective Function
OPF	Optimal Power Flow
p.f.	power factor
R	Resistance
RES	Renewable Energy Sources
RMS	Root Mean Square
RPCB	Reactive Power Compensation Bank
RPM	Reinforcement Planning Mechanism
SCC	Short Circuit Capacity
S-M-W	Sherman - Morrison - Woodbury
SQP	Sequential Quadratic Programming
TF	Target Function
TSO	Transmission System Operator
X	Reactance
GHz	Gigahertz
kA	Kiloamperes
kV	Kilovolts
MVA	Megavolt-amperes

MVA	Megavars
MW	Megawatts
p.u.	per unit

SYMBOLS

$^{\circ}$	Degrees
$*$	Conjugate of a complex number
P_g	Real power output of generator located at bus g (in MW)
P_T	Real power import/export from/to connection point T to external network (in MW)
Q_g	Reactive power output of generator located at bus g (in MVar)
Q_T	Reactive power import/export from/to connection point T to external network (in MVar)
S_g	Capacity of generator located at bus g (in MVA)
S_t	Apparent power of transmission line t (in MVA)
$C(x)$	Cost function of variable x
φ_b	Voltage angle of bus b with respect to a reference bus voltage angle (in degrees)
θ_G	Voltage angle of generator bus g with respect to a reference bus voltage angle (in degrees)
Z_f	Fault impedance (in p.u. with respect to the system impedance base)
I_f	Fault current through fault impedance (in p.u. with respect to the system current base)
Z_{bus}	Impedance matrix
Y_{bus}	Admittance matrix
z_{ij}	i,j element of impedance matrix (in p.u. with respect to the system impedance base)
y_{ij}	Element i,j of admittance matrix (in p.u. with respect to the system impedance base)
$\bar{z}_{q,r}$	Impedance of line connecting buses q and r (in p.u. with respect to the system impedance base)
$I_{i,j}^f$	Fault current flowing through line i,j for a fault at bus f (in p.u. with respect to the system current base)
S_b	System base (for p.u. calculations, 100MVA)
X_G	Steady state reactance of generator G (in p.u. with respect to the system impedance base)
X'_G	Transient reactance of generator G (in p.u. with respect to the system impedance base)
X''_G	Subtransient reactance of generator G (in p.u. with respect to the system

	impedance base)
$X_{p.u.}''(S^G)$	p.u. subtransient reactance of generator G with respect to its capacity
$FSF_{i,j}^f$	Fault Sensitivity Factors of transmission line i,j for a fault at bus f
K^x	Real part of complex variable K
K^y	Imaginary part of complex variable K
Z_{RPCB}	Impedance of Reactive Power Compensation Bank (RPCB) (in p.u. with respect to the system impedance base)
V_{RPCB}	Voltage of RPCB bus (in p.u. with respect to the voltage base at the part of the network where the RPCB is)
Q_{RPCB}	MVAr size of RPCB
$P_{k,m}^{losses}$	Transmission losses of line k,m (in MW)
P_{lines}^{losses}	System transmission losses (in MW)
λ_i	LaGrange multiplier of constraint i
L_i	Complex power consumption of load located at bus i (in MW/MVAr or p.u. with respect to the system MVA base)
d_i	Percentage increase of load at bus i per time unit

CONTENTS

TABLE OF CONTENTS

1. INTRODUCTION.....	1
1.1 GENERATION CAPACITY	1
1.2 GENERATION CAPACITY ALLOCATION.....	1
1.3 NETWORK REINFORCEMENT.....	2
1.4 DISTRIBUTED GENERATION IMPACT ON DISTRIBUTION NETWORK OPERATION	3
1.5 ALLOCATION OF NEW GENERATION CAPACITY IN A DEREGULATED ELECTRICITY MARKET	4
1.6 THESIS STATEMENT.....	4
1.7 LITERATURE REVIEW	5
1.7.1 Generation capacity allocation methods.....	5
1.7.2 The theory of optimal power flow.....	8
1.7.3 Network expansion and network reinforcement planning.....	8
1.8 STRUCTURE OF THESIS	10
2. FAULT LEVEL CONSTRAINED OPTIMAL POWER FLOW AS A TOOL FOR NETWORK CAPACITY ANALYSIS	12
2.1 INTRODUCTION	12
2.2 POWER FLOW ANALYSIS.....	12
2.3 ECONOMIC DISPATCH.....	14
2.4 OPTIMAL POWER FLOW	14
2.5 OPF MODEL FOR GENERATION CAPACITY ALLOCATION	16
2.5.1 Sinks and sources	16
2.5.2 System Constraints.....	18
2.5.3 Objective function	20
2.5.4 OPF target function	20
2.6 FAULT STUDIES	21
2.6.1 Rationale	21
2.6.2 Types of generators and fault studies	21
2.6.3 Focus on balanced faults	21
2.6.4 Fault system analysis.....	22
2.6.5 Reactance of synchronous generators during fault.....	22
2.6.6 Generator capacity and subtransient reactance.....	24
2.6.7 Example fault analysis.....	25
2.6.8 General formulation of line currents during faults	26
2.6.9 Fault analyses and evaluation of switchgear adequacy	27
2.6.9.1 Capacity.....	27
2.6.9.2 Breaking capability.....	27
2.7 INCORPORATION OF FAULT LEVEL CONSTRAINTS IN OPF	28
2.7.1 Why add fault level constraints to OPF?	28
2.7.2 Fault Level Constrained OPF algorithm.....	29
2.7.3 Maximization of generation capacity using OPF	30
2.7.4 Limiting fault currents using Generator Reactance Optimisation Algorithm.....	31
2.7.5 Changing the bounds of new capacities	33
2.7.6 Algorithm implementation	34
2.8 EXAMPLE	35
2.8.1 Topology	35
2.8.2 Constraints.....	37
2.8.3 Assumptions about Capacity Expansion Locations.....	37
2.8.4 Algorithm-specific settings	39
2.8.5 Test case 1: no preferences for locations.....	40
2.8.5.1 Results	40

2.8.6	Test case 2 : locational preferences	45
2.8.6.1	Results	45
2.8.7	Analysis of Results	50
2.9	CHAPTER SUMMARY	51
3.	DIRECT INCORPORATION OF FAULT LEVEL CONSTRAINTS IN OPTIMAL POWER FLOW AS A TOOL FOR NETWORK CAPACITY ANALYSIS.....	53
3.1	INTRODUCTION	53
3.2	DEFINING THE PROBLEM	54
3.3	CONNECTING EXPECTED FAULT CURRENTS WITH NEW GENERATION SIZE	55
3.4	CALCULATING THE DERIVATIVES OF FAULT LEVEL CONSTRAINTS	57
3.4.1	Derivatives of fault currents with respect to bus voltages	58
3.4.1.1	If $f \neq i$ and $f \neq j$	59
3.4.1.2	If $f = i$	61
3.4.1.3	If $f = j$	62
3.4.2	Derivatives of fault currents with respect to real and reactive power of generators	63
3.5	DECREASING THE NUMBER OF FAULT LEVEL CONSTRAINTS IN CAPACITY ALLOCATION	65
3.6	EXAMPLE	66
3.6.1	Topology	67
3.6.2	Constraints	69
3.6.3	Assumptions about Capacity Expansion Locations	69
3.6.4	Test case 1: no preferences for locations	69
3.6.4.1	Results	70
3.6.5	Test case 2 : preference for specific CEL	72
3.6.5.1	Results	73
3.6.6	Analysis of results	76
3.7	CHAPTER SUMMARY	77
4.	COMPARISON BETWEEN FLCOPF AND D-FLCOPF.....	78
4.1	INTRODUCTION	78
4.2	CONNECTION CAPACITY	78
4.3	ALLOCATION PREFERENCES VS. BENEFIT	79
4.4	CONVERGENCE	81
4.5	RELIABILITY AND COMMERCIAL USE	83
4.6	THE NEED FOR A NEW CAPACITY PLANNING MECHANISM	84
4.7	CHAPTER SUMMARY	86
5.	EXTENSIONS OF THE OPF MODEL FOR CAPACITY ALLOCATION.....	87
5.1	INTRODUCTION	87
5.2	REACTIVE POWER COMPENSATION BANKS	87
5.2.1	Steady-state model	88
5.2.2	Contribution to Fault Levels	88
5.2.3	Cost model	90
5.2.4	Example	91
5.2.4.1	Strategy A	94
5.2.4.2	Strategy B	98
5.2.5	Limitations	101
5.3	ALTERNATIVE VOLTAGE CONTROL OF DISTRIBUTED GENERATORS	101
5.3.1	Automatic Voltage / Power Factor Control	102
5.3.2	Central Voltage Control	103
5.3.3	Steady-state behaviour	103
5.3.3.1	Intelli-Gens	104
5.3.3.2	CVC-Gens	106
5.3.3.3	ECVC-Gens	107
5.3.4	Contribution to fault levels	109
5.3.5	Cost model	109
5.3.6	Example	109
5.3.7	Transmission losses	113

5.3.8	Limitations	114
5.4	CHAPTER SUMMARY	114
6.	CONSIDERING THE IMPACT OF NEW CAPACITY ON LOSSES.....	116
6.1	INTRODUCTION	116
6.2	CALCULATION OF LOSSES	117
6.3	EXPRESSING LOSSES AS A FUNCTION OF OPF VARIABLES	118
6.4	CONSIDERING LOSSES DURING ALLOCATION OF NEW CAPACITY	119
6.5	FINDING THE DIRECTION TO OPTIMUM ALLOCATION	119
6.6	EXAMPLE	120
6.7	CHAPTER SUMMARY	123
7.	REINFORCEMENT PLANNING MECHANISM	125
7.1	INTRODUCTION	125
7.2	SEQUENTIAL QUADRATIC PROGRAMMING	126
7.3	MEANING OF LAGRANGE MULTIPLIERS IN THE OPF SOLUTION.....	127
7.4	NETWORK REINFORCEMENT PLANNING MECHANISM BASED ON LAGRANGE MULTIPLIERS ..	128
7.4.1	Step 1: Creating a list of realistic investments.....	128
7.4.2	Step 2: Allocating new generation capacity with the OPF	129
7.4.3	Step 3: 'Discretising' marginal reinforcement	129
7.4.4	Step 4: Defining the cost of investment.....	131
7.4.5	Step 5: Optimum investment	132
7.4.6	Step 6: Updating investment plan and cost	133
7.5	PLANNING LOOP.....	134
7.6	CONSIDERING LONG-TERM LOAD FORECASTS	136
7.7	CONSIDERING THE RETIREMENT OF GENERATORS	136
7.8	EXAMPLE	137
7.8.1	Investment economics	137
7.8.2	Results	138
7.8.2.1	Investment plan under strict power factor control	138
7.8.2.2	Investment plan under widespread use of Intelli-Gens	143
7.8.2.3	Investment plan under widespread use of ECVC-Gens	149
7.8.2.4	Investment plan under widespread use of CVC-Gens	153
7.8.3	Comparison of results.....	157
7.9	CHAPTER SUMMARY	162
8.	THE IMPACT OF FAULT LEVELS ON THE ECONOMIC OPERATION OF POWER SYSTEMS.....	163
8.1	INTRODUCTION	163
8.2	INCORPORATION OF FLCs IN OPF AS AN OPERATING TOOL	164
8.3	EXAMPLE	166
8.3.1	Average load (1st scenario).....	167
8.3.2	Light load (2nd scenario)	168
8.3.3	Heavy load (3rd scenario)	169
8.3.4	Planned network maintenance (4th scenario).....	170
8.3.5	Constrained remote switchgear (5 th scenario).....	170
8.4	EFFECT OF FLCs ON OPF BUS VOLTAGE PATTERN.....	172
8.5	PERFORMANCE OF OPF WITH FLCs	178
8.6	CHAPTER SUMMARY	178
9.	CONCLUSIONS	179
9.1	INTRODUCTION	179
9.2	OPTIMAL CAPACITY ALLOCATION	179
9.3	INCORPORATION OF FAULT LEVEL CONSTRAINTS	179
9.4	STUDYING THE IMPACT OF REACTIVE POWER INJECTIONS ON THE ALLOCATION OF NEW CAPACITY	180
9.5	NETWORK REINFORCEMENT PLANNING MECHANISM.....	181
9.6	IMPACT OF FLCs IN THE ECONOMIC OPERATION OF POWER SYSTEMS	182

9.7	THESIS LIMITATIONS, CONCLUSIONS AND FUTURE WORK	182
10.	REFERENCES.....	184
A.	APPENDIX.....	191
A.1	THE SHERMAN-MORRISON-WOODBURY FORMULA EXTENSION TO MATRIXES OF COMPLEX NUMBERS	191
A.2	CALCULATION OF THE DERIVATIVES OF FAULT LEVEL CONSTRAINTS.....	192
A.2.1	Derivatives of fault currents with respect to voltage magnitudes and angles.....	192
A.2.2	Derivatives of fault currents with respect to real and reactive power of generators.....	198
A.3	DERIVATIVES OF TRADITIONAL NON-LINEAR CONSTRAINED FUNCTIONS IN THE OPTIMAL POWER FLOW FORMULATION	201
A.3.1	Apparent power flows constrained by lines thermal limits	201
A.3.2	Power imbalance at buses equal to zero	201
B.	PUBLISHED/SUBMITTED PAPERS CONNECTED WITH THESIS	203

LIST OF FIGURES

Figure 2.1 Typical current response of a short circuited generator.	23
Figure 2.2 Typical variation of generator reactance and RMS fault current response.	24
Figure 2.3 Fault analysis example case.	25
Figure 2.4 Thevenin equivalent of example case.	25
Figure 2.5 Flowchart of Fault Level Constrained OPF algorithm.	30
Figure 2.6 Generator reactance (p.u.) vs. generator capacity (MVA).	32
Figure 2.7 The 12-bus 14-line test case.	35
Figure 2.8 New generators' p.u. reactance with respect to their MVA base.	38
Figure 2.9 New generators' p.u. reactance with respect to the system MVA base.	39
Figure 2.10 Voltage pattern contours of the initial allocation (a) and the FLCOPF reallocation (b) of new capacity, superimposed on the test case graph. No locational preferences.	42
Figure 2.11 Capacity reallocation sequence at the CELs and the E/IP.	43
Figure 2.12 Capacity bounds imposed by GROA vs. iteration number.	44
Figure 2.13 Update of bounds at the end of each iteration loop.	44
Figure 2.14 Voltage pattern contours of the initial capacity allocation (a) and the FLCOPF reallocation (b), superimposed on the test case graph. Preference for CEL 1.	47
Figure 2.15 Capacity reallocation sequence at the CELs and the E/IP.	48
Figure 2.16 Capacity bounds imposed by GROA vs. iteration number.	49
Figure 2.17 Update of bounds at the end of each iteration loop.	49
Figure 3.1 Selection of 'active' fault level constraints using FLCRM.	66
Figure 3.2 The 12-bus 14-line test case.	67
Figure 3.3 Voltage pattern contours of the initial capacity allocation (a) and the D-FLCOPF reallocation (b), superimposed on the test case graph. No preferences.	72
Figure 3.4 Voltage pattern contours of the initial capacity allocation (a) and the D-FLCOPF reallocation (b), superimposed on the test case graph. Preference for CEL 1.	75
Figure 4.1 Loss of benefit with respect to forced new capacity at CEL 1.	81
Figure 4.2 'Iterations' of FLCOPF (a) and D-FLCOPF (b).	82
Figure 5.1 Cost optimisation of RPCB elements.	91
Figure 5.2 The 12-bus 15-line test case with RPCBs at buses 6 and 8.	92
Figure 5.3 Cost of capacitor bank vs. rating, using capacitor costs from Table 5.1.	93
Figure 5.4 Typical cost of LV RPCBs. Positive/negative MVar represent capacitors/reactors.	94
Figure 5.5 Generation capacity allocation at CELs and expected exports at E/IP with respect to the available RPCBs budget. No preferences are expressed over CELs.	95
Figure 5.6 RPCBs allocation with respect to the available RPCBs budget. Negative and positive values indicate RPCBs consisted of reactors and capacitors, respectively. No preferences are expressed over CELs.	95
Figure 5.7 Generation capacity allocation at CELs and expected exports at E/IP with respect to the available RPCBs budget. Preference expressed for CEL at bus 1.	96
Figure 5.8 RPCBs allocation with respect to the available RPCBs budget. Negative and positive values indicate RPCBs consisted of reactors and capacitors, respectively. Preference expressed for CEL at bus 1.	96
Figure 5.9 Voltage magnitude of the controlled voltage at bus 9 and the tap ratio of the transformer with respect to the available budget. No preferences are expressed over CELs.	97
Figure 5.10 Voltage magnitude of the controlled voltage at bus 9 and the tap ratio of the transformer with respect to the available budget. Preference expressed for CEL at bus 1.	98
Figure 5.11 AVPFC response.	103
Figure 5.12 Voltage control strategy of Intelli-Gens.	105
Figure 5.13 'Smoothing' of control strategy transition for Intelli-Gens.	106
Figure 5.14 Central voltage control region of DGs.	107
Figure 5.15 'Smoothing' of control strategy transition from PFC to CVC when the DNO performs ECVC.	108
Figure 5.16 Shifting of Voltage/PF operating points of new generators operating under a) AVPFC and b) ECVC for $V_{threshold} = 1.05$ p.u. due to the introduction of FLCs.	112

Figure 5.17 Shifting of Voltage/PF operating points of new generators operating under a) AVPFC and b) ECVC for $V_{threshold}=1.035$ p.u. due to the introduction of FLCs.	112
Figure 5.18 Shifting of Voltage/PF operating points of new generators operating under a) AVPFC and b) ECVC for $V_{threshold}=1.065$ p.u. due to the introduction of FLCs.	113
Figure 7.1 Estimation of objective function increase due to investment.	129
Figure 7.2 Cost of upgrading equipment in discrete steps.	132
Figure 7.3 Flowchart of the iterative algorithm implementing the RPM.	135
Figure 7.4 Investment plan created by the RPM assuming strict PFC for new generators.	140
Figure 7.5 Benefit for the network operator vs. cost of investment.	141
Figure 7.6 Expected tap ratio and regulated voltage of the transformer with automatic tap changer vs. cost of investment.	142
Figure 7.7 Investment plan created by the RPM assuming widespread deployment of Intelli-Gens.	145
Figure 7.8 Benefit for the network operator vs. cost of investment.	146
Figure 7.9 Investment cost and increase of benefit for a) the first investment and b) the last investment on T4-9.	147
Figure 7.10 Expected tap ratio and regulated voltage of the transformer with automatic tap changer vs. cost of investment.	148
Figure 7.11 Investment plan created by the RPM assuming widespread deployment of ECVC-Gens.	150
Figure 7.12 Benefit for the network operator vs. cost of investment.	151
Figure 7.13 Expected tap ratio and regulated voltage of the transformer with automatic tap changer vs. cost of investment.	152
Figure 7.14 Investment plan created by the RPM assuming widespread deployment of CVC-Gens.	154
Figure 7.15 Benefit for the network operator vs. cost of investment.	155
Figure 7.16 Expected tap ratio and regulated voltage of the transformer with automatic tap changer vs. cost of investment.	156
Figure 7.17 Total new capacity vs. cost of investment under different voltage control policies.	160
Figure 7.18 Benefit for the network operator vs. cost of investment under different voltage control policies.	161
Figure 8.1 The 12-bus test case network.	166
Figure 8.2 Production cost vs. breaking capacity of switchgear connected to remote bus 6.	172
Figure 8.3 Initial (a) and final (b) bus voltage pattern for the 1 st scenario (average load).	173
Figure 8.4 Initial (a) and final (b) bus voltage pattern for the 2 nd scenario (light load).	174
Figure 8.5 Initial (a) and final (b) bus voltage pattern for the 3 rd scenario (high load).	175
Figure 8.6 Initial (a) and final (b) bus voltage pattern for the 4 th scenario (planned network maintenance).	176
Figure 8.7 Initial (a) and final (b) bus voltage pattern for the 5 th scenario (constrained remote switchgear).	177

LIST OF TABLES

Table 2.1 Switching speed of switchgear and impact of direct current component.	28
Table 2.2 Line and transformer data.	36
Table 2.3 Demand characteristics.	36
Table 2.4 CEL benefit function coefficients.	40
Table 2.5 E/IP benefit function coefficients.	40
Table 2.6 Allocation of generation capacity at CELs.	41
Table 2.7 Bus voltage pattern of the initial and FLCOPF capacity allocation.	41
Table 2.8 CEL benefit function coefficients, expressing a preference for bus 1.	45
Table 2.9 E/IP benefit function coefficients.	45
Table 2.10 Allocation of generation capacity at CELs.	45
Table 2.11 Bus voltage pattern of the initial and FLCOPF capacity allocation, when there is a preference for the CEL at bus 1.	46
Table 2.12 Benefit functions used in test cases.	50
Table 2.13 Capacity allocation and transfers to E/IP in the two test cases.	50
Table 2.14 Calculation of total benefits for both test cases.	51
Table 3.1 Transformer and line characteristics.	68
Table 3.2 Demand characteristics.	68
Table 3.3 CEL cost function coefficients when no preferences are expressed.	69
Table 3.4 E/IP cost function coefficients.	70
Table 3.5 Allocation of generation capacity at CELs.	70
Table 3.6 Initial and D-FLCOPF capacity allocation, when there is no preference for any CEL.	71
Table 3.7 CEL cost function coefficients, expressing a preference for bus 1.	72
Table 3.8 E/IP cost function coefficients.	73
Table 3.9 Allocation of generation capacity at CELs.	73
Table 3.10 Bus voltage pattern of the initial and D-FLCOPF capacity allocation, when there is a preference for the CEL at bus 1.	74
Table 3.11 Capacity allocation and transfers to E/IP in the two test cases.	76
Table 3.12 Calculation of total benefits for both test cases.	76
Table 4.1 Calculation of total benefits for both test cases.	78
Table 4.2 Calculation of loss of benefit when new capacity is allocated at CEL 1.	80
Table 4.3 Summary of convergence attributes of FLCOPF and D-FLCOPF.	82
Table 4.4 First-come-first-served capacity allocation.	84
Table 4.5 Release of capacity certificates for the D-FLCOPF allocation.	85
Table 5.1 Typical fixed costs of LV capacitors.	92
Table 5.2 Scenarios of preferences under which Strategy B will be tested.	100
Table 5.3 D-FLCOPF allocation results for the RPCBs test case.	100
Table 5.4 Initial capacity allocation (FLCs ignored).	110
Table 5.5 Reallocation of capacity considering FLCs.	111
Table 5.6 Transmission losses as a percentage of the total new capacity.	113
Table 6.1 Initial capacity allocation (FLCs ignored) under strict PFC.	120
Table 6.2 Allocation of new Intelli-Gens, CVC-Gens and ECVC-Gens when FLCs are ignored.	121
Table 6.3 Reallocation of capacity under strict PFC due to FLCs.	122
Table 6.4 Reallocation of new Intelli-Gens, CVC-Gens and ECVC-Gens due to FLCs.	122
Table 6.5 Transmission losses as a percentage of total new capacity when losses are considered during capacity allocation.	123
Table 7.1 Comparative analysis of reinforcement plans.	157
Table 8.1 Initial and final solutions of first scenario.	167
Table 8.2 Initial and final solutions of second scenario.	168
Table 8.3 Initial and final solutions of third scenario.	169
Table 8.4 Initial and final solutions of fourth scenario.	170
Table 8.5 Initial and final solutions of fifth scenario.	171

1. INTRODUCTION

1.1 Generation capacity

A basic axiom in physics is energy conservation. Upon this axiom is based the main operation rule in power systems: supply of energy must always meet demand. Since large scale energy storage is not an economically viable solution yet, there must be enough electric power available to cover consumption at all times. Unfortunately, consumption is not constant, even in the short term. It fluctuates according to the electric energy needs throughout a time period. However, there must be enough installed generation to cover the highest demand, even if this is experienced for only a few hours or minutes per day. This means that the sum of generators' capacity must always be equal, or for security reasons higher, than expected demand. Otherwise, either the supply will be disrupted or part of the demand must be disconnected to prevent unacceptable reduction in system frequency (load shedding). 'Generation capacity' or for simplicity 'capacity' is the maximum power output of a generator.

1.2 Generation capacity allocation

In the long term, demand constantly increases, thus, new generation capacity is needed. The equipment of the transmission and distribution network sets several technical limitations to the location and size of new capacity or the expansion of the existing plants. For example, both power flows in lines and voltages on buses rise as new generation is installed. The new power system, which is created after the connection of a new generator onto the grid, must operate within thermal limits of existing transmission and distribution lines and bus voltage statutory limits. Hereafter, these limitations of network infrastructure will be referred to as network constraints. Capacity allocation is the problem of defining the location and capacity of new generation, so that the available system will not violate the constraints of the existing network.

Usually the allocation of network capacity for generation is done in a heuristic manner, some times based solely on engineering experience. The candidate locations for new capacity are few, so a small number of power flow studies for the suggested expansion options is enough to determine if the future system will respect system constraints. Loads are considered equal to their lowest values, because it is assumed (not always true) that this case corresponds to the highest power flows. However, as Distributed Generation (DG) increases the candidate

locations become numerous. So a more concise method is needed to coordinate the allocation of new capacity on the network in order to exploit the existing network capabilities to the maximum [1]. Optimal capacity allocation is the capacity allocation that maximises an objective function, for example total new capacity, with respect to network constraints.

Capacity allocation becomes even more complicated when it is performed on small-scale generation connected to distribution networks. As it will be proven later, the number of such applications increased significantly following the latest drive towards renewable energy (see Section 1.4). The distribution network was not originally designed to accommodate generation. Therefore, additional constraints that were not practically binding in the transmission level now have to be considered. One major problem from the installation of generators in low voltage networks is the raising of fault levels. The specifications of the existing switchgear equipment have to be respected if the operation of the distribution network is to remain reliable and safe. It is a new challenge for power engineers to design a capacity allocation method that respects security constraints, such as the ones imposed by switchgear equipment.

1.3 Network reinforcement

As it was mentioned before, the installation of new generation capacity brings the network closer to its operational limits. One way to remedy this problem is to invest in the network, so that those limits are increased. However, the deregulation of the energy sector followed by increased competition between energy companies has reduced profit margins and with it available investment budgets (see Section 1.5). Therefore, a mechanism is needed to plan the limited investment on the grid in the most efficient way. Since the problem is caused by the rise of capacity, due to demand growth, it is logical to seek the foundation of the new mechanism close to the theory of capacity allocation and even find a combined approach for the optimum overall result. Such a combinational approach of capacity planning and network investment is formally suggested by TSOs for the integration of booming wind power into the grid without compromising reliable operation [2].

Finally, political and environmental reasons often hinder or even prohibit the expansion of existing networks. Therefore, the mechanism could be simplified, without significantly limiting its applicability, by focusing on the reinforcement of the existing infrastructure rather than its expansion.

1.4 Distributed generation impact on distribution network operation

Environmental concerns push governments to encourage the exploitation of 'cleaner' energy sources, particularly Renewable Energy Sources (RES). Unfortunately, RES are mostly located in remote or rural areas. The load is low and sparse at these areas, mostly served from radial distribution networks. Therefore, the new renewable generation connects to networks, which were not originally designed to accommodate power injections.

The technological mismatch between the original purpose and the usage of the distribution networks creates a wide range of technical problems in their operation [3], [4]. Several corrective measures have to be taken to maintain the reliability and quality of supply. The distribution equipment is possibly re-regulated or even upgraded to facilitate bidirectional power flows or voltage rise during normal operation. The existence of generation in the distribution power system increases the expected fault currents and alters transient stability. Therefore, the upgrade of switchgear equipment and their coordination mechanisms may be crucial for secure and reliable operation.

When there is a request for connection of new generation capacity, Distribution Network Operators (DNOs) consider the above measures by examining the impact the new capacity will have on the network operation under worst case conditions. The dominant factor constraining generation capacity in radial networks, such as the rural distribution networks, is local voltage rise. In this context, voltage rise is caused by the reverse power flows injected from the new generators. The maximum reverse power flow, thus highest voltage rise, is attained when the new generation capacity is operating at full capacity whilst local load is at a minimum.

If the DNO decides there is a need for network upgrading to maintain quality and reliability of supply, the generator bears the financial responsibility. Therefore, DNOs' current policy in issuing connection permits on a first-come-first-serve basis without properly exploiting the existing network capabilities may result in high connection costs that could repel investment in distributed generation.

The above analysis emphasises the need for a method that would identify the maximum potential connection capacity. New capacity should be optimally allocated to the connection points, with respect to the existing network's constraints and security restrictions (i.e. fault levels). DNOs could use the results of such a method to guide investment to the points of spare connection capacity in an efficient manner in order to utilize fully the existing network.

1.5 Allocation of new generation capacity in a deregulated electricity market

In a regulated environment, a central authority plans the expansion of all three layers of a power system: generation, transmission and distribution. Knowing the limits of the transmission and distribution network, forecasting the increase of demand and managing a specific investment budget, it coordinates the development of the power system in the most efficient way.

As the electricity markets continue to move to a deregulated electricity generation environment, the need for enhanced capacity allocation increases. The private sector takes over the investment in new generation capacity and an independent authority¹ operates the transmission system. The legal frameworks currently used in deregulated markets encourage investment in new generation capacity, especially from RES. Some may also adequately protect the system from crossing its operating limits due to misplaced capacity. However, they are generally inadequate in providing appropriate incentives, to guide the process of installing new generation in an efficient manner, concerning both rate of development and location. Inadvertently, they potentially limit the capability of the network to absorb new generation capacity.

Any capacity planning method should direct financial incentives towards the correct location and size of new capacity rather than directly 'allocate it'. In a deregulated environment only the investment force can implicitly allocate new capacity in an efficient manner. The TSO seems to be the most appropriate authority to provide such economic signals (e.g. subsidies) for efficient allocation of new capacity, as it possesses a largely complete picture of the status of the power system and predictions of future increases in demand.

1.6 Thesis statement

This thesis has three consecutive targets. They are consecutive in the sense that previous targets have to be achieved before the next one is attempted.

Allocation of new capacity is currently done in a heuristic manner with no theoretical grounds of efficiency. The first target is to create a more sound methodology for the optimum allocation of new capacity; the definition of 'optimum' is also to be determined. If the objective of the allocation is to maximize total new capacity with respect to the limitations imposed by the existing network infrastructure, then optimum coincides with

¹ The independent authority responsible for the maintenance, operation and expansion of the transmission system is usually called Transmission System Operator or TSO.

making use of available network capacity or headroom.

Most of the applications of such a methodology would be on the allocation of DGs, where there are many possible connection points and the network is not even designed to accommodate generation. However, one of the major problems created by the penetration of DG is rising of fault level. Therefore, additional constraints such as the ones imposed by the specifications of existing switchgear equipment should be taken into account during the allocation of new capacity. The second target of this research is to extend the methodology of capacity allocation, so that constraints imposed by switchgear equipment are also considered.

The third target is to investigate the possibility of exploiting the method developed for allocation of new capacity in order to provide economic signals for efficient investment on the network. Again, 'efficient' depends on the objective of investment strategies. The objective for most strategies is the maximization of profit, but this raises the question 'profit from what?', or better, 'who pays for what'.

Consequently, even if the targets of this research are clear, the statement of the thesis leaves plenty of space for extensions, some of them in the engineering and some of them in the economic field.

1.7 Literature review

1.7.1 Generation capacity allocation methods

Generation expansion planning is a challenging problem due to its large-scale, non-linear nature. Due to the lack of sufficient computational tools, until recently engineers were forced to rely on their intuition and experience to solve it. With the rapid advance of computers, several methodologies have been developed for the efficient allocation of new generation capacity to an existing network.

The accumulated experience gathered by engineers in planning can be translated to a large set of rules connecting generation expansion scenarios with the properties of the power system under development. The theory of expert systems can use those rules in order to solve the problem of generation expansion planning [5]. One of the first approaches was developed by Farghal, who used the decision tree technique to emulate the one-at-a-time problem-solving approach of human experts [6]. Several other rule-based expert systems followed, capable of handling economic and environmental constraints, besides technical constraints on planning [7], [8].

However, expert systems are incapable of handling uncertainties, such as the ones existing in investment policies implemented by expansion planning, simply because they mimic responses from an existing knowledge base. Fuzzy logic is more appropriate in facilitating decision making in uncertain environments. David and Zhao used fuzzy logic to formulate a portion of the decision making procedure in their expert system, which contained uncertainty [9]. Another hybrid approach was developed by Su et al., which involved dynamic programming as the optimisation technique [10]. Methodologies purely derived from fuzzy set theory have also been developed [11], [12], [13].

Keane and O'Malley in [14] use linear programming to find the optimal allocation of distributed generation. However, they are forced to make several assumptions in order to convert non-linear constraints, such as the ones imposed by existing switchgear equipment on expected fault currents, to linear constraints. This approximation may result in reduced accuracy of the final solution and possibly even not finding a global optimal solution.

Several methods based on metaheuristic techniques attempt to directly trace the globally optimum allocation. In reference [15], a method based on tabu-search is suggested for the optimal placement of distributed generators. Kannan et al. exploited the global search characteristics of evolutionary programming [16], in order to overcome the highly nonlinear nature of generation expansion constraints [17]. Sasaki et al. expressed the relationship between expansion constraints and decision variables by the weighting factors of a neural network. An iterative scheme was then used to train the network, so that it will produce the optimum expansion plan that satisfies all constraints [18].

Nevertheless, genetic algorithms and simulated annealing are probably the most promising heuristic techniques [19]. They are capable of solving large-scale non-linear problems, avoiding local minima and in many cases obtaining better solutions than the other heuristic approaches [20]. K. Wong and Y. Wong attempted to combine the strengths of those two promising techniques by creating a hybrid method with the primal target of solving the generation scheduling problem, but with direct extensions to planning [16]. Kuri et al extended methodologies based on genetic algorithms, so that it considers the impact of the allocation on network operation and expected losses [21]. Improved algorithms were soon developed in order to reduce the computational power needed to perform these large scale combinatorial genetic processes [22], [23].

Even if all the above methods produce satisfactory results for most practical cases they do have two significant disadvantages:

- a) They do not provide any kind of indication, as to which part of equipment on the network limits the penetration of new generation.
- b) They are based on bespoke algorithms which most power engineers are not familiar

with.

Harrison and Wallace in [4],[24],[25] provide a different approach using a widely known commercial Optimal Power Flow (OPF) package software to allocate new capacity by simulating new generators as negative loads. They use the inherent capability of the software to perform load shedding to minimize the loss of load, i.e. maximise negative load representing new generation capacity. By practically maintaining the concept of the original tool, which is based on power flow analysis, this method attempts to simulate the planning process of generation expansion performed by engineers up to now. Traditionally, generation expansion planning is done by the solution of numerous power flows, each of them assessing the impact of an expansion option on system operation. When OPF is used to do the allocation of new capacity, it practically seeks the bundle of options, which if it was implemented would maintain acceptable system operation.

The method suggested in this thesis is also based on the OPF. However, a basic difference between the two approaches is that here new generators are simulated as virtual generators, rather than loads, located at the candidate connection points. This basically gave access to the OPF variables which are used during optimisation. Thereafter, it became feasible to create a mathematical link between new generation and additional constraints not currently handled by the original tool (OPF), such as expected fault currents, or even consider conditions not currently addressed by existing planning tools, such as losses or different voltage control policies. The OPF solution method used is Nonlinear Programming, because it directly handles the non-linear constraints [26] and produces signals about the extent to which they restrict the optimal solution (see Section 7.3).

Another interesting advantage of simulating new capacity with virtual generators is connected with the inherent capability of the OPF to use the different production cost functions attached to each generator in order to decide the optimal generation pattern. Lower or higher production costs attached to different virtual generators carry the meaning of preferences between candidate locations for the allocation of new capacity. For example, a lower cost attached to the virtual generator simulating a future wind farm will result in a higher permitted capacity at this point in the expense of lower total new capacity.

Lately, several research teams have investigated ways to improve the available planning mechanisms, so that they are capable of handling uncertainties due to competition in generation [27]. Park et al. presented a genetic algorithm which deals with the conflicting objectives between independent generation companies that are willing to invest in new capacity [28]. Gnansounou et al. designed an agent-based model, which considers the interaction among participants in electricity markets [29]. Bresesti et al. claim that there are common factors affecting both generation and transmission market-based expansions [30].

1.7.2 The theory of optimal power flow

Optimal Power Flow is the process of dispatching the electric power system variables in order to minimize an operation criterion (usually the minimisation of generation production cost), while attending load and feasibility according to the restrictions imposed by the power system operating capabilities. It was introduced by Carpenter [31],[32] and extended by Dommel [33]. Since then, several approaches have been suggested for successful solution due to its complicated mathematical nature [34].

Initially, the solution algorithms focused on analytical mathematics. Sun et al. exploited the close link between the formulation of the OPF and simple power flow and created an extension of the Newton method, widely applied in power flow analysis [35]. Alsac et al. presented several practical assumptions in order to linearise the non-linear constraints in OPF and solve it using linear programming [36]. Mukherjee and Douligeris completed the applicability of the method by incorporating constraints for the slack bus, which to some extent were ignored in the previous approach [37]. Karmaker presented a new algorithm in linear programming, which had the ability to handle numerous inequality constraints [38]. Narger et al. successfully applied the interior point method, as it was termed later, to the solution of the OPF [39].

However, if no simplifications or approximations are made to linearise its constraints, OPF is a non-linear programming problem. Non-analytical mathematics has been employed in attempts to overcome the problems of divergence and local optimality created by the non-linear nature of the OPF. Genetic algorithms, neural networks and simulated annealing, all stochastically seek the optimal point of operation for power systems [40].

In this thesis a non-linear programming algorithm solves the OPF. Sequential quadratic programming outperforms every other tested non-linear programming method in terms of efficiency, accuracy, and percentage of successful solutions over a large number of test problems [41]. It still has to be tested, though, on large-scale networks where many highly non-linear constraints co-exist. Linear Programming methods have already proven their robustness in this field that is why they are currently used by most commercial OPF solving software (e.g. PowerWorld or PSS/E).

1.7.3 Network expansion and network reinforcement planning

Network expansion is the process of expanding the existing network infrastructure by building new transmission lines, upgrading substations etc. The target is to increase the operating capabilities of the power system, so that it can serve the future demand in a reliable and secure manner. It is a difficult technical and economic problem, which increased in

complexity as the transmission systems expanded across vast geographical areas and became interconnected.

Until recently network expansion was manually planned by experienced engineers. Therefore, it is logical for most approaches to be based on this accumulated experience. Reference [42] suggests a generic planning framework aiming to meet the requirements of distribution companies with particular regard to embedded generation. This framework has been developed from an extensive survey of standard planning practices and methodologies. Kandil et al. present a hybrid mathematical and rule-based expert system to expand the transmission system in open access schemes [43]. The interesting point in this paper is that the authors acknowledge the importance of a combined approach to generation expansion and network planning. In this thesis, the connection between new generation capacity and network operating capability is also acknowledged. The difference, though, between the two is that the former finds sets of generation allocations and respective optimum network investments, whereas the later plans optimum investment on the network as generation expands gradually. In other words, this work exploits the interdependence of the two planning functions in order to find the overall optimum, rather than trying to find the optimum for one of the two after the other is defined.

Carvalho and Ferreira formulated the planning problem as a stochastic decision problem [44]. Then, they exploited the property of radial networks, which have a power flow monotonic with the generation profile, in order to convert the stochastic problem into a two-scenario under uncertainty problem. They solved the multiple-scenario problem using a new evolutionary algorithm, which has the interesting feature of producing information related with the robustness of each plan in the context of distribution deregulation. However, the applicability of this approach is limited to radial networks. The method suggested in this thesis can be applied indistinguishably to radial and highly meshed networks.

The decision complexity involved in network planning inspired the automation engineers, who provided methodologies based on modern control theories. An interesting example is the state-of-the-art genetic algorithm presented by Danhong et al. The algorithm introduces an adaptive generation gap in order to consider the specific characteristics of electric network planning [45]. A second example of network planning based on computational intelligence techniques was introduced by Mori and Iimura. They proposed a two-layered tabu search method that deals with the optimal location of new generation at the first layer and the feeders and substations at the second [46]. Another interesting approach not based on analytical mathematics is the one presented by Orths. In order to consider the new planning requirements created by competition in deregulated markets he designed an effective multi-criteria optimisation method based on game theory [47].

The advantage of the above 'intelligent' methods is that they can handle non-engineering

parameters, such as financial incentives or competition. However, the solution processes are not entirely 'understandable' by planning engineers. This leaves too little space for intervention under special planning conditions or when new technical problems arise, e.g. increase of fault levels due to high penetration of distributed generation. Levi and Calovic break the investment problem into a) a subproblem dealing with initial power flows encompassing security aspects only and b) a second subproblem solving superimposed power flows that take into account the economy of the suggested solutions [48]. Similarly, Hashimoto et al. uses a logic similar to the one used in system operation in order to gradually include the network constraints which become binding in the planning horizon [49]. The small number of constraints included in the final solution is resolved using a linear programming algorithm.

Haffner et al. attempted to transfer the experience gained from similar path-planning models, such as transportation, to network planning [50]. The simplification attained from those models made planning of very large networks feasible, but compromised simulation accuracy. For example, in Haffner's model only Kirchhoff's current law is depicted. Siddiqi and Baughman proved that for transmission system planning where reactive power flows and voltage constraints are important, it is imperative that an AC power flow model must be used [51]. The limitations of their own oversimplified approach were later acknowledged by Haffner's team [52]. The method developed in this thesis not only implements a full AC power flow analysis in order to consider investments which counteract traditional security constraints, but the formulation has been extended so that investment options on constrained switchgear equipment are also taken into account.

1.8 Structure of thesis

The results from this research are presented in the following eight Chapters with necessary appendices.

In the second Chapter, a method of modelling new generation capacity and expected power transfers to external networks will be presented, so that Optimal Power Flow (OPF) can be used as a tool for generation capacity allocation. The allocation respects network constraints, which are inherent in the OPF formulation, but the method relied on an iterative procedure to convert constraints imposed by switchgear equipment to bounds on new capacity.

In Chapter three, a methodology for the incorporation of those constraints directly into the OPF set of constraints was developed. Henceforth, OPF can be used directly as a tool of capacity allocation, which considers the impact of new generation on fault levels.

The next Chapter, Chapter four, compares the two methods of fault level constrained

capacity allocation in terms of efficiency, speed and commercial usability. It also constrains a simplistic mechanism of distributing available connecting capacity among investors that the network operator can use in order to fully exploit the capabilities of the existing infrastructure.

In Chapter five, the flexibility of OPF as a tool for capacity allocation is demonstrated by two practical extensions: a) Optimal allocation of reactive power compensation banks with the objective of increasing the ability of the network to absorb new generation capacity and b) Considering generators voltage control policies, while assessing the ability of the network to absorb new generation capacity.

The theme of Chapter six was inspired by the previous Chapter, when several allocations under different voltage control policies resulted in very high transmission losses. In this Chapter, a possible way of considering the impact of new capacity on losses is analysed. It is also discussed why losses should be considered by the network operator during capacity planning.

In Chapter seven, a mechanism that uses economic signals produced by OPF for constraint equipment during capacity allocation in order to suggest a network reinforcement plan is introduced.

Chapter eight investigates the impact of expected fault currents on the economic operation of power systems. It also demonstrates how fault level constraint OPF can be used for the coordination of system apparatus during maintenance or other extreme cases (e.g. very low or high demand), so that failure of switchgear can be avoided.

Chapter nine concludes this research by highlighting the most significant results of the previous Chapters, so that the reader can have an overview of its contribution to knowledge. Finally, the potential of the methodologies described throughout the thesis is stated and the direction to future work is suggested.

2. FAULT LEVEL CONSTRAINED OPTIMAL POWER FLOW AS A TOOL FOR NETWORK CAPACITY ANALYSIS

2.1 Introduction

This Chapter starts with a brief description of two basic theories in power systems: power flow analysis and economic dispatch. Optimal Power Flow (OPF), a basic tool for the economic operation of power systems, is then presented as a combination of those two concepts. However, later a method for modelling new capacity is obtained, so that OPF can be used for planning generation expansion. Finally, an algorithm is presented which iteratively converts the constraints imposed by the specifications of switchgear equipment to constraints on the allocation of new capacity by the optimal power flow. A simple example demonstrates the efficiency of the suggested methods and the impact of the additional constraints on capacity allocation.

2.2 Power flow analysis

The aim of power flow analysis is to estimate the steady-state operating point of a power system under specific loading conditions [53]. The operating point is defined by all bus voltages and power flows sustained on transmission lines and transformers.

Power flow analysis is usually applied on one-line equivalent circuits, because power systems are supposed to be balanced and operating in the steady state. Let us examine the net power intake of random bus i of a n -bus system. Generally, on this bus there may be a generator producing complex power S_i^G , loads consuming complex power S_i^L , and transmission lines exporting complex power S_i^T to other buses. The powers flowing in and out of the bus are connected with the following equation:

$$S_i = S_i^G - S_i^L = S_i^T \quad (2.1)$$

where S_i is defined as the net power injected into bus i .

The response of the network with n buses is described with the following equation, which is practically the result of the method of nodes:

$$I_{bus} = Y_{bus} \cdot V_{bus} \quad (2.2)$$

where I_{bus} is the $1 \times n$ vector of currents I_i injected into buses 1 to n , V_{bus} is the $n \times 1$ vector of bus voltages with respect to a reference bus and Y_{bus} is the $n \times n$ admittance matrix describing the passive elements of the network.

I_i can be expressed as a function of admittance matrix elements and system bus voltages:

$$I_i = \sum_{j=1}^n (y_{ij} \cdot V_j) \quad (2.3)$$

where y_{ij} is the i,j element of the Y_{bus} .

By definition the complex power exported from bus i is equal to:

$$S_i^T = V_i \cdot \left[\sum_{j=1}^n (y_{ij} \cdot V_j) \right]^* \quad (2.4)$$

Equations like (2.4) can be written for all system buses and they show the complex power balance that must exist in each of them. They are known as *the power flow equations in complex form*. If the product of $V_i \cdot \left[\sum_{j=1}^n (y_{ij} \cdot V_j) \right]^*$ is analysed in a real and an imaginary part and the complex power intake of each bus in (2.1) is also analysed in its real ($P_i = P_i^G - P_i^L$) and reactive ($Q_i = Q_i^G - Q_i^L$) power terms, then (2.4) can be broken down in two equations: one for the real and one for the imaginary parts of each side.

$$\left. \begin{aligned} P_i^G - P_i^L &= \text{Real} \left\{ V_i \cdot \left[\sum_{j=1}^n (y_{ij} \cdot V_j) \right]^* \right\} \\ Q_i^G - Q_i^L &= \text{Imag} \left\{ V_i \cdot \left[\sum_{j=1}^n (y_{ij} \cdot V_j) \right]^* \right\} \end{aligned} \right\} \quad (2.5)$$

The new equations are equivalent to the power flow equations in complex form, but they are between real quantities only. Thus, they are known as *the power flow equations in real form*.

Power flow analysis is a common tool for power engineers during planning of modifications or extensions of existing power systems. It allows power engineers to assess their impact on system operation, but also analyse and compare the efficiency of different planning options. For example, when a new generator requests to connect to a specific point on the network, the network operator is obliged to run a series of power flows with a model of the prospective generator connected to the system under all possible loading conditions. If the analysis guarantees that system security is not significantly compromised, then the connection permission is granted. Otherwise, a new series of power flows is run to determine

which of the network reinforcement options available tackles the problems rising from the connection in the most efficient way.

2.3 Economic dispatch

The target of economic dispatch is to define the power outputs of generation plants, so that total electricity production equals demand in the most economic way. This is mathematically formulated by the following expressions:

$$\min \sum_{i=1}^n C_i(P_i) \quad (2.6)$$

$$\sum_{i=1}^n P_i = \sum_{j=1}^k L_j \quad (2.7)$$

where $C_i(P_i)$ is the production cost of generator i at a power output of P_i and L_j is the real power consumption of load j . n and k are the total numbers of generators and loads, respectively. In this simple formulation of economic dispatch, the balance between production and consumption of reactive power is neglected.

In addition, the power output of each generator i must be greater than the minimum permitted P_i^{\min} and less than the maximum permitted P_i^{\max} . In order to keep the analysis simple, losses were neglected from the original economic dispatch formulation. However, it must be noted that other operating limits are not stated in the original formulation as well.

2.4 Optimal power flow

In the preceding Sections we introduced two basic concepts in power systems: power flow analysis and economic dispatch. The first is purely technical. It calculates the electrical state of the system to a particular set of loads and generator unit outputs [54]. The second reflects the economics of combining different power resources in order to meet consumption [55]. The OPF is a combination of those two concepts, aiming to satisfy both technical and economic targets in power system operation. The solution of the OPF requires balance throughout the entire power flow, but at the same time this has to be achieved for the minimum generation cost.

Mathematically, this amalgam of concepts is expressed by the replacement of (2.7) from economic dispatch with (2.4) from power flow analysis. In other words, the single balance between generation and demand is substituted with a set of power balances for every system bus. The target of optimisation remains (2.6), which forms the system state with the

minimum operating cost. Additionally, since the power flow equations are included in the optimisation procedure, several other system operating limits can be formulated by constraining functions of variables used in those equations, e.g. the reactive power capability of generators or lines thermal limits. Therefore, it can be claimed that Optimal Power Flow is actually the process of dispatching the electric power system variables in order to minimize an operation criterion, while generation meets demand and no system operating limits are violated (expressed by constrained functions of those variables). A conceptual formulation of the problem is briefly described below.

It is generally assumed that the following are known: active and reactive power generation capabilities and costs, fixed loads sizes, elastic loads benefit functions, transmission and distribution line capacities, specification of fixed transformers and other power system devices. The *control variables* c , which are regulated during optimisation, are usually the ones at the disposal of system operators:

- a) The generators' active and reactive power output.
- b) The tap ratios and/or phase shifts of transformers with tap changers and/or phase shifting capabilities.
- c) The settings of switched shunt devices, such as capacitor or inductor banks.
- d) The active power transferred from DC links.
- e) The shedding of elastic loads

However, in order to completely define the state of the system, more variables have to be introduced. The *state variables* s are:

- a) The voltage phase angles at every bus.
- b) The voltage magnitudes at load buses.

The equation linking variables c and s is the power system load flow equation:

$$EqCon(c, s) = 0 \quad (2.8)$$

It can be analysed to a number of *equality constraints*, one for each bus, expressing the power balance between the active/reactive power injected and withdrawn from the bus. Practically, it is either implemented by (2.4) with complex power quantities or, equivalently, by (2.5) as a set of real and reactive power quantities.

Additional *inequality constraints* on functions with OPF variables describe the operating limits of the power system (e.g. lines thermal limits, generator capacity etc.):

$$IneqCon(c, s) < 0 \quad (2.9)$$

Such constraints are line flow limits, active and reactive power generation capability bounds,

bandwidth of tap changers or phase shifters and voltage limits at buses. Additional operational constraints may be easily added, using expressions of the c and s variables describing operating violations, if they are valued as critical for the system security.

The operation criterion to be minimized by the OPF optimisation process is called the *objective function* $f(c, s)$. In most cases, the objective function to be minimised is the short term cost of electricity production. The OPF optimisation process aims to find the variables c and s that minimise the objective function, subject to the sets of equality and inequality constraints expressed by (2.8) and (2.9), respectively. It is a typical problem of nonlinear programming:

$$\min f(c, s) \quad (2.10)$$

$$\text{subject to } EqCon(c, s) = 0$$

$$\text{and } IneqCon(c, s) < 0$$

OPF solution algorithms are commonly used in power system operation planning. They facilitate the development of optimal economic dispatch schedules and control settings that will result in flows that are within the capabilities of the network infrastructure.

2.5 OPF model for generation capacity allocation

Several methods [25], [15] have been developed to identify both the locations and the order in which new generation capacity should be installed to fully utilize an existing network. The method proposed in this research uses a well-documented operating tool in power engineering, Optimal Power Flow, to optimally allocate new capacity. This section first presents how new generation and connections to external networks are modelled and following on from [25], so that OPF can be utilized as a planning rather than an operating tool for capacity allocation. Then it describes how network constraints are considered during allocation. It concludes with the definition of the objective, which will be optimized during the allocation of new capacity.

2.5.1 Sinks and sources

- New generation capacities are simulated as generators with quadratic benefit functions with negative coefficients:

$$C_g(P_g) = a \cdot P_g^2 + b \cdot P_g + c \quad \text{w.r.t. } a, b, c < 0 \text{ and } P_g > 0 \quad (2.11)$$

where C_g is the operational cost of generator g at output level P_g .

Quadratic functions are used because they can express a great variety of monotonic curves without exacerbating the nonlinear nature of the OPF problem.

These generators are connected to predetermined locations at the grid, termed “Capacity Expansion Locations” or CELs. They are assumed to be the candidate locations (e.g. locations pointed out by the network operator) where new capacity can be installed on the existing network. The term “locations” is used, because a group of generators (e.g. a wind farm) will be simulated with a single source connected to the rest of the grid at predefined locations. The total output of the generators simulates the allocated capacity at each CEL. Different sets of coefficients between benefit functions declare preferences² for the allocation of new capacity between CELs.

- Energy transfers from/to external grids are also simulated as generators with quadratic benefit functions. They will be referred to as Export/Import Points or E/IPs. The coefficients of the benefit functions are negative for exports and positive for imports. The outputs of the generators are negative when they represent exports and positive when they represent imports.

$$C_T(P_T) = a \cdot P_T^2 + b \cdot |P_T| + c \quad (2.12)$$

w.r.t. $a, b, c < 0$ and $P_T < 0$ for exports,

w.r.t. $a, b, c > 0$ and $P_T > 0$ for imports.

where C_T is the operational cost of the generator at output level P_T , simulating the E/IP.

As with CELs, the benefit functions declare preferences for the export/import of power to/from specific E/IPs.

- Existing generation capacities are simulated as generators with constant active power output and given reactive power injection capabilities:

$$\begin{aligned} P_{g,installed} &= const. \\ Q_{g,installed}^{\min} &< Q_{g,installed} < Q_{g,installed}^{\max} \end{aligned} \quad (2.13)$$

- Loads are simulated as sinks of constant active and reactive power:

$$L_d = P_d + jQ_d \quad (2.14)$$

where P_d, Q_d are, respectively, the active and reactive power of load L_d at bus d .

In all the example cases (except where stated otherwise) it will be assumed that loads are equal to their minimum average values. This condition, in conjunction with maximum new generation allocated from the method described in this Section,

² Or the absence of them, if the benefit functions are the same.

usually is a worst-case scenario for generation expansion planners. Of course, the method can be easily expanded to consider other cases that may result in the worst network operating conditions, such as maximum load and minimum generation, maximum load and maximum generation or even a series of cases created with different load values according to a profile.

2.5.2 System Constraints

1. The amount of active and reactive power injected into any system bus k must equal the amount withdrawn from it. The *complex power balance* on the buses is formulated:

$$\sum_t (P_{tk} + jQ_{tk}) + \sum_g (P_{gk} + jQ_{gk}) + \sum_d (P_{dk} + jQ_{dk}) = 0 \quad (2.15)$$

where t =all lines, g =all generators and d =all loads connected to bus k .

P_{tk}, P_{gk}, P_{dk} and Q_{tk}, Q_{gk}, Q_{dk} are, respectively, the active and reactive power they inject to bus k .

If the bus is also an E/IP, then the complex power $P_r + jQ_r$ transferred from/to bus k from/to the external grid must be added (for import) or subtracted (for exports) to the above sum.

2. Proper operation of the power system equipment requires the maintenance of bus voltages close to their rated values:

$$V_b^{\min} < V_b < V_b^{\max}, \text{ for all buses } b \quad (2.16)$$

where V_b^{\min} and V_b^{\max} are the lower and upper bounds of the bus voltage, around the rated value.

3. The installation of new generation capacity is limited by statutory regulations (e.g. Electricity Safety, Quality and Continuity Regulations or ESQCR in the UK [56]), environmental concerns, social policies, technological limitations or system constraints imposed by stability, fault or other security analyses. Here, only those restrictions resulting from statutory regulations and fault analysis are used:

$$LB_g < P_g < UB_g \quad (2.17)$$

where P_g is the generation output at CEL g and LB_g, UB_g are the lower and upper bounds, respectively. The environmental and social impact of the new capacities can be formulated mathematically in the benefit functions described above.

4. When a synchronous generator is connected to an interconnected network, there are practically two ways of controlling its performance. The mechanical power applied on the generator's shaft controls the real power, whereas the field current controls the reactive power injected into the bus and indirectly regulates the terminal voltage. High reactance in the transmission and distribution lines can cause undesirable voltage drops with increased system loading. Big generators are usually committed in terminal voltage regulation (Automatic Voltage Regulation or AVR) using reactive droop compensation. However, if a small generator with AVR control was connected to a utility bus which suffers from a voltage drop, it would have to inject great amounts of reactive power in order to raise the bus voltage. This could result in high field currents and overheating for the generator. For that reason, in most distributed generation applications the generators do not have AVR control. The amount of reactive power they produce, which is connected to voltage regulation, is proportional to the active power. To keep the analysis simple, initially it will be assumed that the CELs accommodate distributed generators. Therefore, they inject power with constant power factors. This assumption also holds for most Distributed Generation (DG) installations that interface to the network through an inverter [57]. This constraint is described by the following equation:

$$p \cdot f_g = \frac{P_g}{\sqrt{P_g^2 + Q_g^2}} = \text{const.} \quad (2.18)$$

Of course, in more general cases, the production of reactive power is controlled or additional reactive power sources (e.g. capacitor banks, FACTS) can be utilized. Then this restriction is relaxed, providing us with higher generation capacities.

5. The thermal tolerance of a line sets a limit to the maximum MVA it can transfer. Therefore, each line has a thermal limit of apparent power (MVA) transfer:

$$S_t < S_t^{\max}, \text{ for all lines } t \quad (2.19)$$

where S_t and S_t^{\max} is the is the apparent and maximum apparent power (thermal limit) of line t , respectively.

6. Each E/IP represents a physical connection to an external network. The capacity of the connection sets a technical limit to the maximum amount of power that can be transferred to and from the external network. However, in cases where the quantity of the exported or imported power is comparable to the size of the external grid, more conservative bounds than the connection capacity must be applied to limit the

voltage rise or drop within the external network. These limits are expressed in (2.20)

$$|P_T| < |P_T^{\max}|, \text{ for all } E/ \text{IPs } T, \quad (2.20)$$

where $P_T > 0$ for imports and $P_T < 0$ for exports.

In addition, the maximum reactive power that the external network can feed into the system or the minimum reactive power requested by the external network must also be provided.

$$Q_T < Q_T^{\max} \text{ or } Q_T < Q_T^{\min}, \text{ for all } E/ \text{IPs } T, \quad (2.21)$$

where $Q_T > 0$ and $Q_T^{\max} > 0$ for import of reactive power

or $Q_T < 0$ and $Q_T^{\min} < 0$ for export of reactive power.

2.5.3 Objective function

The OPF Objective Function OF_{OPF} is the total cost of all simulated generators. It includes the negative cost of generation at CELs and exports at EPs, as well as the cost of imports at IPs. The cost of losses could also be taken into account, but is ignored at this stage of research to keep the model simple for observations.

$$OF_{OPF}(P_g, P_T) = \sum_g C_g(P_g) + \sum_T C_T(P_T) \quad (2.22)$$

2.5.4 OPF target function

The Optimal Power Flow problem reflects the allocation of new generation capacity at CELs and the setting of energy transfers at E/IPs, with respect to the power system constraints. The OPF Target Function TF_{OPF} is the minimum of the objective function OF_{OPF} , with respect to the system constraints described above:

$$TF_{OPF}(P_g, P_T) = \min OF_{OPF}(P_g, P_T) \quad (2.23)$$

2.6 Fault studies

2.6.1 Rationale

Fault studies are an important part of power system analysis. Their target is to predict the system's response under various types of faults, by determining the expected bus voltages and line currents. Usually faults are short circuits at the power lines and buses, caused either by natural phenomena (e.g. broken tree branches) or malfunctioning equipment (e.g. "exhausted" transformers). There are two main categories of faults, depending on whether their impact is symmetric (*balanced*) or not (*unbalanced*) on the three phases of the power system. The unbalanced faults separate into three sub-categories, according to the short circuit loop they create: a) phase-to-ground, b) phase-to-phase and c) two-phases-to-ground. Balanced faults are defined as simultaneous short circuits across all three phases and a possible connection to the ground. Fault study results are used for :

1. The design of the appropriate power system protection.
2. Setting the relays controlling the protection switchgear.
3. The coordination of breaking functions during faults.
4. The selection of protection switchgear ratings.

This research focuses on the last case.

2.6.2 Types of generators and fault studies

There are two broad categories of generators: synchronous and asynchronous (or induction). The short-circuit current is more severe for a synchronous generator suffering from a three-phase fault than a single-phase fault. The opposite is true for an asynchronous generator. However, as more than 90% of the global generation capacity utilises synchronous generation, in order to simplify the analysis in this research it will be assumed that all new generators are synchronous. Therefore, in the following text the term 'generators' refers to synchronous generators, except where indicated otherwise.

2.6.3 Focus on balanced faults

The worst-case scenarios will be considered in our fault studies, in order to validate the installed switchgear. If the switchgear can handle those, all other scenarios will be on the "safe side". Balanced faults are less frequent, but usually far more severe³ than the unbalanced. Thus, this study will focus on balanced faults. In addition, they are the most amenable to calculation. The network remains symmetric, therefore, a solution on a per-phase basis will provide us with the line currents and bus voltages in all three phases (taking

³ Assuming the generated power is mostly fed by synchronous generators.

into account the $\pm 120^\circ$ phase shifts). When the term ‘fault’ is mentioned in the following text it will refer to balanced faults.

2.6.4 Fault system analysis

A fault can be considered as the addition of an impedance⁴ and node in the network, at the point of fault. Therefore, Thevenin’s theorem can be used for the calculation of the new state of the system. *The voltage and current changes throughout the network equal the voltages and currents created in the network, if all sources are zeroed and a voltage source equal to the pre-fault voltage is applied at the point of fault in series with the fault impedance and the internal network impedance seen from that point.* Zeroing of sources means short-circuiting voltage sources and open-circuiting current sources. In order to calculate the final values of the currents and voltages during a fault the changes given by Thevenin’s theorem are superimposed on their pre-fault values. Using basic electric circuit theory, the calculation of the new state of the network simplifies to algebraic equations.

2.6.5 Reactance of synchronous generators during fault

Even though generators do not operate in a steady sinusoidal state during a fault, their response maintains sinusoidal attributes, albeit in a transient nature. Fault currents consist of a sinusoidal component of exponentially decreasing amplitude (up to a constant value) and an exponentially decreasing component of direct current. In terms of electromagnetic machine operation, a) the high initial value is determined by an effective leakage inductance and b) the settled amplitude of the sinusoidal component is determined by the synchronous reactance. The direct current component depends on the time that the fault takes place, so it is different for each phase. Since the time that a fault will occur cannot be predicted, the mathematical approach can be simplified by ignoring this component. Figure 2.1 presents a typical response of a generator’s phase current during a fault, ignoring the direct current component. The current amplitude, I_{\max} , is superimposed on the same figure.

⁴ If the fault impedance is so low, that can be assumed equal to zero; the fault is described with the term ‘solid’ or ‘bolted’.

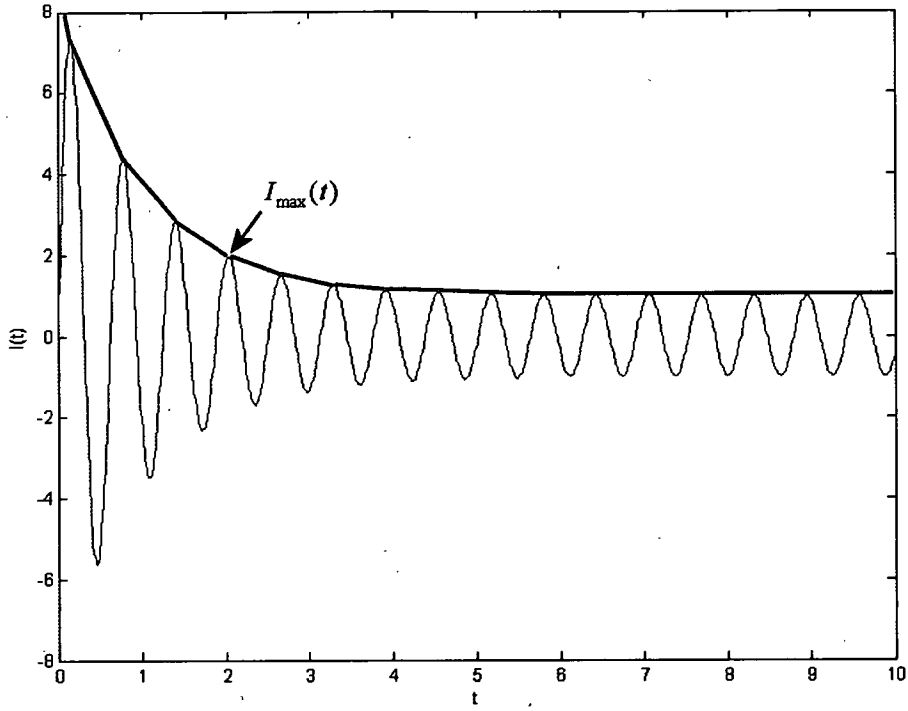


Figure 2.1 Typical current response of a short circuited generator.

Instead, the direct current component is considered empirically during the calculation of the final expected fault currents. The calculated values are multiplied with typical factors, depending on the time instance after the fault and the type of power devices of interest. For example, the higher the switching speed of switchgear, the higher the factor used to determine the fault current which the switchgear must be capable of breaking.

In order to model the transient current response described above, it is assumed that the internal generator reactance X_G is varying through time. The black curve in Figure 2.2 presents how this assumed reactance changes through time. On the same axes, the blue curve represents the RMS value of the fault current :

$$I_{RMS}(t) = \frac{I_{max}(t)}{\sqrt{2}} \quad (2.24)$$

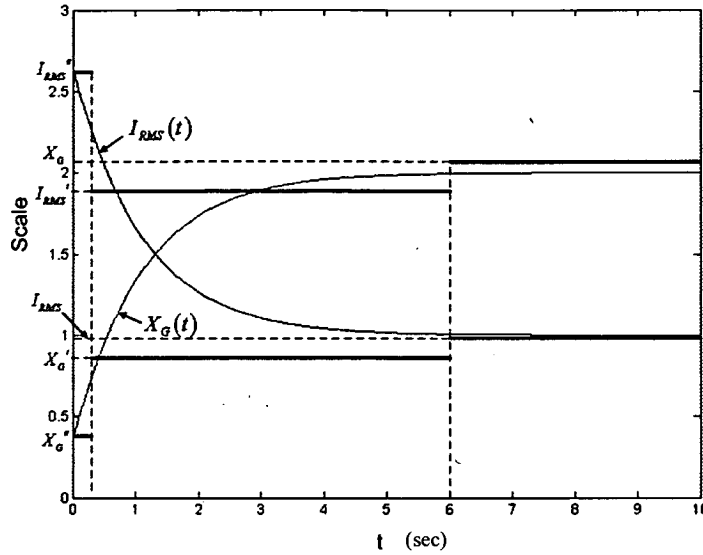


Figure 2.2 Typical variation of generator reactance and RMS fault current response.

For most studies, it is sufficiently precise to approximate the continuously changing reactance with a stepwise function. Three discrete levels of reactance are defined: the subtransient X_G'' , the transient X_G' and the steady state X_G (see Figure 2.2). Respectively, the RMS fault current response is approximated with three discrete levels: the subtransient I_{RMS}'' , the transient I_{RMS}' and the steady state I_{RMS} (see Figure 2.2). For most generators the subtransient period lasts a few tens of milliseconds after the fault occurs. The transient period expands to the next few seconds. The generator enters the steady state when all transient phenomena are extinguished.

The subtransient period is also used in the determination of the MVA switchgear breaking capability and capacity. Therefore, in this research, the subtransient reactance X_G'' will be used for all generators when performing fault analyses. The exact way of calculating the MVA switchgear breaking capability is discussed later.

2.6.6 Generator capacity and subtransient reactance

There is a connection between the capacity of generators and their subtransient reactance, due to fundamental design principles [58]. The subtransient reactance is the sum of two major components: a) the armature leakage reactance and b) a reactance specified by the rotor's amortisseur and field winding. Both components are affected by the rated power the generator must handle. Larger generators typically have subtransient reactances in the range

of 15-20% on the generator reactance base, while smaller gas turbine driven generators may have values of 15% or less.

2.6.7 Example fault analysis

The following example case will help us clarify the above concepts involved in fault studies (Figure 2.3). A synchronous generator of internal sub-transient reactance X_G'' feeds a load of constant impedance Z_L . The impedance of the line connecting the generator bus G with load bus L is Z_{line} . The voltage at bus L is $V_L^{Prefault}$ and the current running through the line is I_L , when a fault occurs on bus L with fault impedance Z_f . Our target is to calculate the fault current running through Z_f , the generation and load contribution to the fault current and the final values of the currents at all branches.

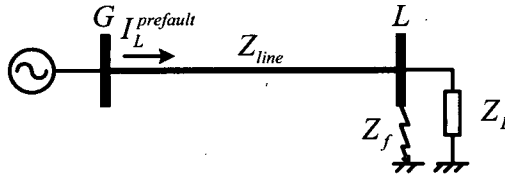


Figure 2.3 Fault analysis example case.

First, the Thevenin equivalent is calculated for the pre-fault circuit with respect to a fault at bus L (Figure 2.4).

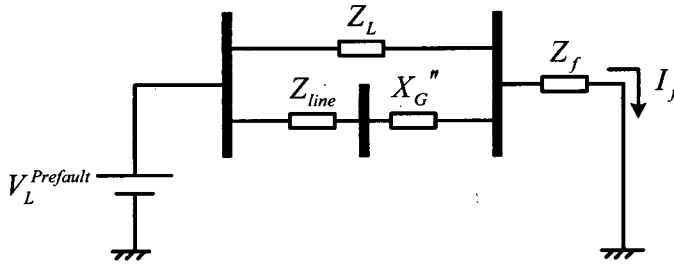


Figure 2.4 Thevenin equivalent of example case.

The fault current is given by the pre-fault voltage at bus L over the total impedance 'seen' from that bus.

$$I_f = \frac{V_L^{Prefault}}{Z_f + \frac{Z_L \cdot (Z_{line} + X_G'')}{Z_L + Z_{line} + X_G''}} \quad (2.25)$$

After calculating the fault current, the currents can be traced backwards to the voltage source in each branch of the circuit. For this specific example, the two branches of the Thevenin circuit are practically a current divider:

$$\frac{I_L^{fault}}{I_G^{fault}} = \frac{X_G'' + Z_{line}}{Z_L} \Leftrightarrow I_L^{fault} = \frac{X_G'' + Z_{line}}{Z_L} I_G^{fault} \quad (2.26)$$

However,

$$I_L^{fault} + I_G^{fault} = I_f \Leftrightarrow I_G^{fault} = I_f - I_L^{fault} \quad (2.27)$$

Therefore, the fault current fed by the generator equals:

$$I_G^{fault} = \frac{Z_L \cdot (Z_{line} + X_G'')}{Z_L + Z_{line} + X_G''} \cdot I_f \quad (2.28)$$

Using (2.26) and (2.28) the fault current due to the load is calculated:

$$I_L^{fault} = \left[1 - \frac{Z_L \cdot (Z_{line} + X_G'')}{Z_L + Z_{line} + X_G''} \right] \cdot I_f \quad (2.29)$$

In order to calculate the final currents during the fault, the pre-fault current I_L is superimposed on the currents feeding the fault:

$$I_G' = I_L - I_G^{fault} \quad (2.30)$$

$$I_L' = I_L - I_L^{fault} \quad (2.31)$$

2.6.8 General formulation of line currents during faults

Generally, the fault current $I_{i,j}^f$ in line i,j for a fault at bus f equals:

$$I_{i,j}^f = \frac{V_i - V_j - (FSF_{i,f} - FSF_{j,f}) \cdot V_f}{\tilde{Z}_{i,j}} \quad (2.32)$$

where $FSF_{k,m}$ is the element at row k and column m of the Fault Sensitivity Factor matrix,

given by the equation : $FSF_{k,m} = \frac{Z_{k,m}}{Z_{m,m} + Z_f}$

where $z_{d,g}$ are the elements at row d and column g of the system's bus impedance matrix $Z_{bus} (= Y_{bus}^{-1})$ and Z_f the fault impedance. V_b is the pre-fault voltage at bus b and $\bar{z}_{q,r}$ is the line impedance of line q,r .

2.6.9 Fault analyses and evaluation of switchgear adequacy

In order to evaluate the adequacy of switchgears under fault conditions, first the expected fault currents must be estimated. Switchgear connects or disconnects one end of a line from a system bus. Therefore, switchgear faces the same fault currents as the lines they are connected to. Using the formulation in Section 2.6.8, the fault currents running through the switchgear are calculated for possible faults at all system buses. Primarily, two specifications determine the adequacy of switchgears during faults: capacity and breaking capability. The analysis differentiates between the two at the point the impact of the direct current component is considered during the calculation of the fault currents.

2.6.9.1 Capacity

As mentioned in Section 2.6.5, the effect of the direct current component is empirically taken into account in the calculation of the fault currents. Specifically, the industrial practice is to create sufficient headroom for peak currents the switchgear must sustain right after the fault by multiplying the expected subtransient RMS current by a factor of 1.6 (ANSI/IEEE Std 242 [59] and Engineering Recommendation G74 [60]). This higher value represents the minimum capacity switchgear must have to be adequate.

2.6.9.2 Breaking capability

The breaking capability of switchgear is specified by the Short Circuit Capacity (SCC⁵, in MVA) of the bus to which it is connected. The SCC is defined as the product of the absolute bus voltage before the fault and the absolute current during the fault:

$$|SCC| = |V_{bus}^{prefault}| |I_{switchgear}^{fault}| \quad (2.33)$$

The prefault bus voltage $V_{bus}^{prefault}$ is an output (state variable) of OPF. $I_{switchgear}^{fault}$ is calculated using the analysis described above. However, in this case the direct current component is considered by increasing the calculated fault current values by a factor of 1.0 to 1.4, depending on the switching speed of the switchgear (Table 2.1). If the calculated SCC is higher than the one described in the switchgear specifications, then the switchgear has inadequate breaking capability.

⁵ The Short Circuit Capacity is also called bus fault level.

Switchgear switching speed	Direct current component factor
8-cycle switchgear or slower	1.0
5-cycle switchgear	1.1
3-cycle switchgear	1.2
2-cycle switchgear	1.4

Table 2.1 Switching speed of switchgear and impact of direct current component.

Note for both capacity and breaking capability:

If the switchgear connects to a generation bus of more than 500 MVA, all the above factors are increased by 0.1.

2.7 Incorporation of Fault Level Constraints in OPF

2.7.1 Why add fault level constraints to OPF?

Currently, engineers allocate new generation capacity in a first-come-first-served manner. This guarantees the future secure operation of the power system, but as it will be demonstrated later, it may not efficiently exploit the capabilities of the existing network. When a new generator requests to be connected to the network, they run a series of power flows in order to determine if there is a need to reinforce the network, so that the future system will not violate any of its operating constraints. In the previous Sections a method for the efficient allocation of new generation capacity was presented, based on OPF as a planning rather than operating tool, which maximally exploits the capabilities of the existing infrastructure.

However, the increase of generation capacity also raises expected fault currents [61]. Heuristically, again this problem is remedied by upgrading the switchgear equipment, which is proven mostly vulnerable after a series of fault analyses for the future system. Alternatively, stressed switchgear is alleviated by manually shifting the system's control variables (generators' outputs, tap settings etc.). Such techniques may work, but there is no guarantee that they result in the global optimum. In particular, in highly meshed systems, finding an acceptable solution may prove to be a highly time-consuming task.

The current OPF optimisation process does not take into account the developing currents during a possible fault. There are no control variables that could limit the possible fault currents to acceptable levels. Therefore, if the plan of the OPF for generation capacity allocation is implemented in the real world as it is, a fault may damage the power system

equipment, if the existing protective equipment is insufficiently rated. Obviously, a method is needed to incorporate the additional constraints in the OPF. If this is achieved, OPF as a planning tool will consider the impact of new generation capacity allocation on expected fault currents and restrict them within the specifications of the existing switchgear equipment.

2.7.2 Fault Level Constrained OPF algorithm

In the following section a generation capacity allocation algorithm is demonstrated, which takes into account the additional constraints imposed by the power system tolerance to fault levels. Besides the control and state variables in OPF, no additional variables are needed. The approach has been termed Fault Level Constrained OPF or FLC OPF. The flowchart of Figure 2.5 demonstrates the general principles of the algorithm.

Analytically:

1. The OPF is constrained by the bounds B for generation capacity. It a) allocates new capacities at CELs and sets import or output levels at E/IPs and b) calculates bus voltages.
2. Fault analysis uses a) the generators' subtransient reactances, determined from the size of the allocated generation capacities at CELs and b) the prefault bus voltages resulting from the OPF.
3. Switchgears with inadequate capacity or breaking capability are determined. If all switchgears are adequate, the current allocation of generation capacity is accepted, the results are printed out and the algorithm stops.
4. An optimisation algorithm, termed Generator Reactance Optimisation Algorithm (GROA), finds the generator subtransient reactances that would limit fault currents within the specifications of the inadequate switchgear of the previous step. The relation between generator capacity and subtransient reactance is used to convert reactances to capacities. The exact operation of this algorithm will be explained in detail in a later Section.
5. The OPF capacity allocation results and the capacities imposed by GROA are compared in order to determine the new bounds B .

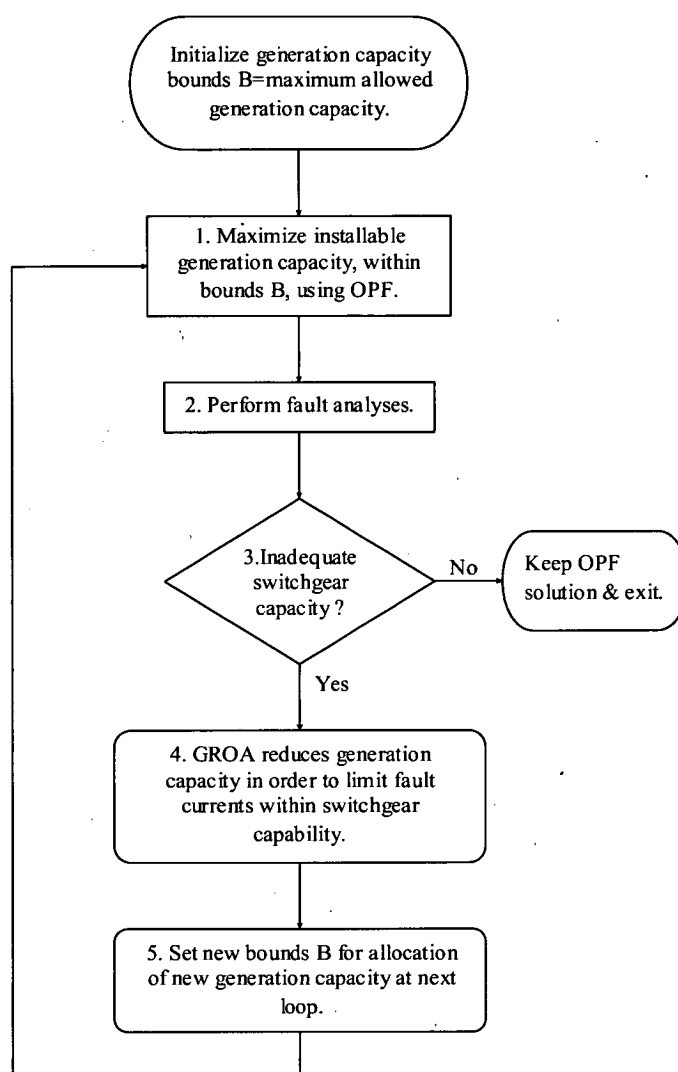


Figure 2.5 Flowchart of Fault Level Constrained OPF algorithm.

Then control is passed back to the 1st step, where OPF reallocates generation capacities using the new B. The basic operations performed within this algorithm are specified in more detail in the next Sections.

2.7.3 Maximization of generation capacity using OPF

According to Section 2.5.1 a generator with a quadratic benefit function is attached to each CEL (see (2.11)) and E/IP (see (2.12)). Existing generation capacities are simulated as generators with constant active power output and given reactive power injection capabilities (see (2.13)). The loads are simulated as sinks of constant active and reactive power (see (2.14)). OPF then allocates the new capacities at CELs and sets the energy transfers at E/IPs,

by solving the target function (see (2.23)) with respect to system constraints (see (2.15)-(2.21)).

2.7.4 Limiting fault currents using Generator Reactance Optimisation Algorithm

According to Section 2.6.4, fault currents are determined by the pre-fault voltage at the point of fault and the network impedances: transmission and distribution lines, transformers' serial impedances, loads' equivalent impedances and generators' internal impedances. It was also noted that the subtransient reactance for big generators is about 15-20% on the generator reactance base, while smaller generators have less than 15%. This relation of p.u. subtransient reactance $X_{p.u.}^{g. ''}$ (on the generator reactance base) to the MVA capacity S^g of the generator can be described using a general function :

$$X_{p.u.}^{g. ''} = f(S^g) \quad (2.34)$$

The p.u. subtransient reactance is then converted from the generator's MVA base S_b^g to the overall system's MVA base S_b :

$$X_{p.u.}^{''} = X_{p.u.}^{g. ''} \frac{S_b}{S_b^g} \Rightarrow X_{p.u.}^{''} = f(S^g) \frac{S_b}{S_b^g} \quad (2.35)$$

However, S_b^g is actually the generator's MVA capacity S^g :

$$S_b^g = S^g \quad (2.36)$$

Therefore, $X_{p.u.}^{''}$ is a function of S^g :

$$X_{p.u.}^{''}(S^g) = f(S^g) \frac{S_b}{S^g} \quad (2.37)$$

To keep the analysis simple it is assumed that $f(S^g)$ is constant, at a value $X_{typical}^{''}$:

$$X_{p.u.}^{g. ''} = f(S^g) = X_{typical}^{''} \quad (2.38)$$

Hence,

$$X_{p.u.}^{''}(S^g) = X_{typical}^{''} \frac{S_b}{S^g} \quad (2.39)$$

In other words, the subtransient reactance $X_{p.u.}^{''}$ for a specific generator capacity S^g can be estimated using function $X_{p.u.}^{''}(S^g)$.

The following curve (Figure 2.6) represents the above function, for $X_{typical}'' = 20\%$ and $S_b = 100 \text{ MVA}$:

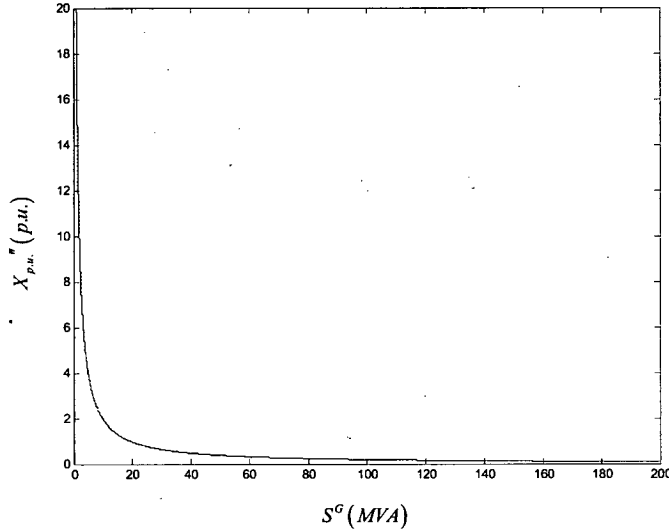


Figure 2.6 Generator reactance (p.u.) vs. generator capacity (MVA).

As such, the size of the new generation capacity determines the sub-transient reactance introduced into the network during a fault (see Section 2.6.5). By changing the size of the generating capacity at a specific location, the magnitude of the resulting currents during a fault can be ‘controlled’. The lower the new generation capacity, the higher the subtransient impedance, resulting in lower fault currents and vice versa.

An optimisation algorithm, called Generator Reactance Optimisation Algorithm (GROA), has been developed to find the optimal reduction of capacity at CELs that will result in fault currents⁶ within the specification of the previously inadequate switchgear. Two target functions have been tested for GROA:

- a) The minimization of the negative total cost at CELs, using the benefit functions supplied at the OPF:

$$TF_{GROA-1}(P_1^{g,GROA}, \dots, P_n^{g,GROA}) = \min \left\{ \sum_{i=1, \dots, n} C_i(P_i^{g,GROA}) \right\} \quad (2.40)$$

*w.r.t. specifications of previously inadequate switchgear
and $P_i^{g,GROA} < B_i^{old}$.*

⁶ Assuming that bus voltages do not change much.

where $C_i(P_i^{g,GROA})$ is the same quadratic cost function with negative coefficients used in OPF (see eq. 1.13) for MW capacity

$$P_i^{g,GROA} = \cos\phi_{g,GROA} \times S_i^{g,GROA} \text{ at CEL } i, \cos\phi_{g,GROA} = \cos\phi_{g,OPF} = \frac{P_i^{g,OPF}}{S_i^{g,OPF}}$$

and B_i^{old} the capacity bounds of the current algorithm loop.

b) The minimization of deviation from the OPF allocation:

$$TF_{GROA-II}(S_i^{g,GROA}, \dots, S_n^{g,GROA}) = \min \left\{ \sum_{i=1, \dots, n} \left| S_i^{g,GROA} - \frac{P_i^{g,OPF}}{\cos\phi_{g,OPF}} \right| \right\} \quad (2.41)$$

w.r.t. specifications of previously inadequate switchgears
and $P_i^{g,GROA} < B_i^{old}$.

The first, generally leads to more efficient capacity allocation when preferences exist for the allocation of new capacity at specific CELs. The second speeds up the convergence of the overall algorithm and results in similar capacity allocation to the first when there are no preferences over CELs.

2.7.5 Changing the bounds of new capacities

Initially, the capacity bounds are determined by the maximum allowed generation capacity at CELs, due to technical, political, environmental or other social reasons. The OPF is solved and the new generation capacity is allocated. The subsequent fault analysis may prove that the current OPF allocation results in higher fault currents than some switchgear can handle. However, as it was already shown, the capacity size is directly connected to the generator subtransient reactance (hence, to fault currents, too) according to the function $X_{p.u.}''(S^g)$. GROA therefore sets new bounds to capacities S^g in order to limit fault currents within switchgear specifications.

The capacity bounds imposed by GROA $(S_i^{g,GROA}, \dots, S_n^{g,GROA})$ are compared with the capacity allocation results of OPF $(S_i^{g,OPF}, \dots, S_n^{g,OPF})$ at each CEL i . The capacity bounds for the next loop change as a function of their difference, from B_i^{old} to B_i^{new} . The function used in this research readjusts the capacity bounds by decreasing the previous overall bounds proportionally to the difference between OPF results and GROA bounds:

$$B_i^{new} = B_i^{old} - Step \cdot (S_i^{g,OPF} - S_i^{g,GROA}) \quad (2.42)$$

where B_i are the overall capacity bounds at CEL i and $Step$ is the proportion factor of $S_i^{g,OPF} - S_i^{g,GROA}$.

There are two reasons for changing bounds gradually, using $Step$, rather than directly to the ones imposed by GROA:

1. Let us assume there is a preference for allocating new capacity at a specific CEL. This can lead the OPF optimisation algorithm to solely allocate new capacity at this CEL, if there is no violation of the OPF constraints. If the fault analysis determines that some switchgear is inadequate, then GROA may determine a much lower capacity bound at this CEL. If the GROA bound directly replaces the overall algorithm bound, i.e. $B_{new} = S_i^{g,GROA}$, then it is possible that the next OPF would not find a feasible solution to cover the existing demand. Except for the capacity bounds the other OPF constraints remain the same. By gradually reducing the bounds for the next OPF, a feasible solution is sought, by progressively 'transferring' capacity between iterations to the other CELs.
2. According to Section 2.6.8, both system impedance and prefault bus voltages determine fault currents. When the capacity bounds are changed in order to limit fault currents, the way the power system is charged is altered and the bus voltage pattern is modified. Therefore, abrupt changes of the capacity bounds would result in very different bus voltage patterns between iterations. Under such conditions, the precision of estimation of the resulting fault currents that can be achieved when changing the generator reactance is compromised. GROA leads the overall algorithm to convergence, because it reduces the capacity bounds to the 'direction' of the optimal solution, enforcing small changes to the voltage patterns.

2.7.6 Algorithm implementation

The implementation of the algorithm is solely programmed in MATLAB [62]. The Sequential Quadratic Programming (SQP) method, part of MATLAB's optimisation toolbox, is used to solve the OPF and run the GROA. A function is also programmed to perform a set of fault analyses, one analysis for a solid fault at each bus.

2.8 Example

In order to demonstrate the effectiveness of the Fault Level Constrained Optimal Power Flow algorithm it was tested on the following test case.

2.8.1 Topology

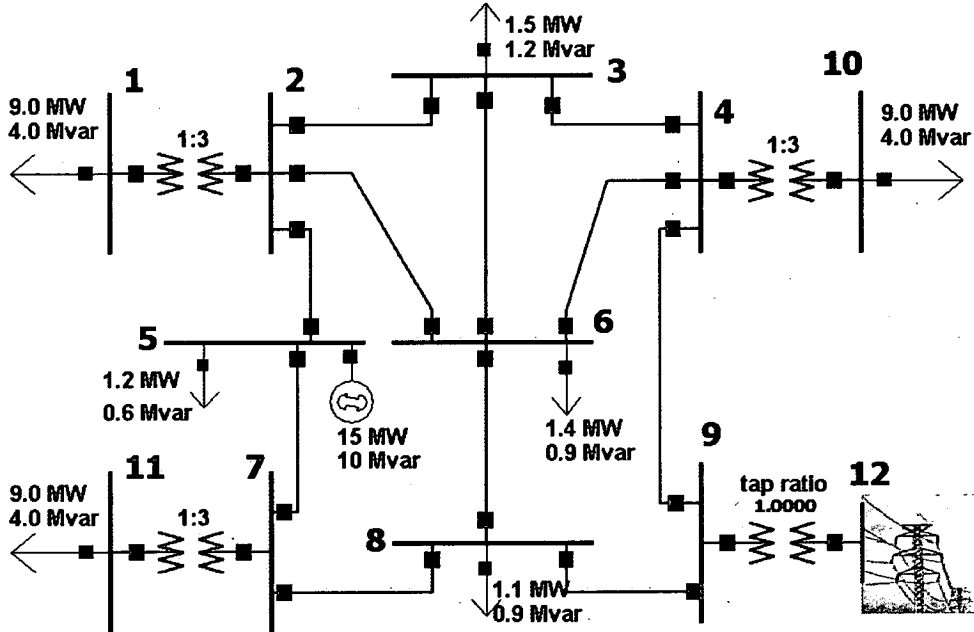


Figure 2.7 The 12-bus 14-line test case.

A 12-bus 15-line network has 3 available CELs at buses 1, 10 and 11 (Figure 2.7). It also has an E/IP to an external network at bus 12. A 15 MW generator is installed on bus 5. It can consume or provide up to 10 MVar of reactive power. The dispatch of its active and reactive power output is assumed to be done centrally with respect to the optimum allocation of new capacity (target function (2.23)). The network has a common rated bus voltage level at 33 kV, except for the CEL buses which have a rated voltage of 11 kV and the E/IP bus at 132 kV. The CEL buses connect to the network through 30MVA transformers with fixed tap ratios 1:3. The E/IP bus connects through a 90MVA transformer with automatic tap changer, which regulates the voltage within a $\pm 2\%$ range of the rated voltage at the low voltage side with a $\pm 10\%$ tap range around the nominal tap ratio (1:4). The data of transformers and lines are presented in Table 2.2. This network was named 'local' and the hypothetical external network connected to it through the E/IP 'external'.

Type	From bus	To bus	R (p.u.)	X (p.u.)	B (p.u.)	MVA
transformer	1	2	0	0.3	0	30
line	2	3	0.48	0.3	0.0008	1000
line	2	5	0.24	0.15	0.0004	14
line	2	6	0.72	0.45	0.001	1000
line	3	4	0.64	0.4	0.001	1000
line	3	6	0.64	0.4	0.001	1000
line	4	6	0.48	0.3	0.0008	1000
line	4	9	0.66	0.35	0.0009	40
transformer	4	10	0	0.3	0	30
line	5	7	0.688	0.43	0.0006	1000
line	6	8	0.768	0.48	0	1000
line	7	8	0.56	0.35	0.0008	1000
transformer	7	11	0	0.3	0	30
line	8	9	0.768	0.48	0	1000
transformer	9	12	0	0.1	0	90

Table 2.2 Line and transformer data.

There are 7 loads connected to buses 1, 3, 5, 6, 8, 10 and 11. Table 2.3 includes the details.

Bus number	P_d (MW)	Q_d (MVar)
1	9	4
3	1.5	1.2
5	1.2	0.6
6	1.4	0.9
8	1.1	0.9
10	9	4
11	9	4

Table 2.3 Demand characteristics.

2.8.2 Constraints

Lines 2-5 and 4-9 are constrained by thermal limits of 14 MVA and 40 MVA, respectively. All other lines are considered to have unlimited capacity (specifies (2.19)). The E/IP is assumed to be able to transfer up to 100 MW from/to the external network without affecting its secure operation (specifies (2.20)). The external network is also capable of providing up to 60 MVar of reactive power to the local network and consuming up to 50 MVar (specifies (2.21)). A hypothetical governmental policy also restricts the maximum allocated capacity to 200 MW at each CEL (specifies (2.17)). Finally, statutory regulations limit bus voltage fluctuations to $\pm 10\%$ around the nominal values (specifies (2.16)). Switchgear is tested only for capacity adequacy, which is 250 MVA at 11 kV, 1000MVA at 33 kV and 3500 MVA at 132 kV (UK standards, [63]).

2.8.3 Assumptions about Capacity Expansion Locations

It is assumed that all new generators connected at CELs produce power at constant 0.9 lagging power factors (specifies (2.18)). It is also assumed that their internal subtransient reactance increases according to their size between $X_{\min}^{g''} = 15\%$ and $X_{\max}^{g''} = 20\%$ on the generator reactance base. Generators are considered to be small when their capacity is well below $S^{smallGen} = 150$ MVA. One simple way of describing the above assumptions is given by (2.43), which is graphically reproduced in Figure 2.8. Equation (2.43) is just one example of how the general function f in (2.34) could be specified. If a better or more accurate function is designed in the future, then it could be easily incorporated into the current formulation just by updating (2.43).

$$\begin{aligned}
 X_{p.u.}^{g''}(S^g) &= X_{\min}^{g''} + (X_{\max}^{g''} - X_{\min}^{g''}) \left(1 - e^{\frac{-S^g}{S^{smallGen}}} \right) \Rightarrow \\
 &\Rightarrow X_{p.u.}^{g''}(S^g) = 0.15 + 0.05 \cdot \left(1 - e^{\frac{-S^g}{150}} \right) \quad (2.43)
 \end{aligned}$$

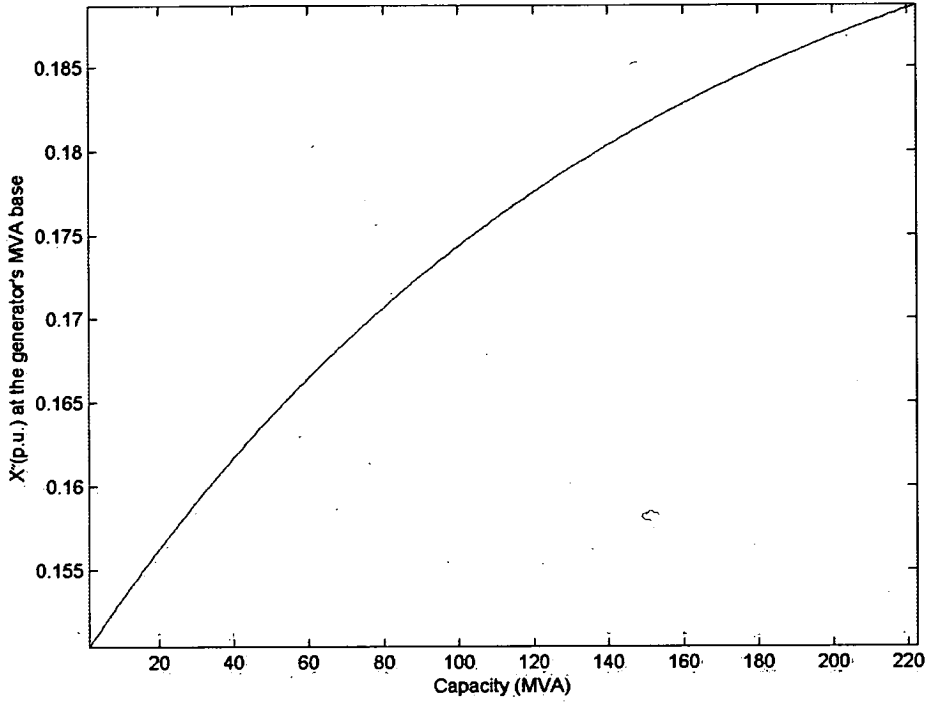


Figure 2.8 New generators' p.u. reactance with respect to their MVA base.

The subtransient reactance from the generator's MVA base S^g is converted to the overall system MVA base $S_b = 100$ MVA using (2.37), in order to get the final $X_{p.u.}''$ p.u. reactance of the new generator with respect to its capacity:

$$X_{p.u.}''(S^g) = X_{p.u.}^g(S^g) \frac{S_b}{S^g} \Rightarrow X_{p.u.}''(S^g) = \frac{15 + 5 \cdot \left(1 - e^{\frac{-S^g}{150}}\right)}{S^g} \quad (2.44)$$

Equation (2.44) was used to produce a graphical representation of the p.u. reactance of new generators, with respect to the system MVA base (Figure 2.9).

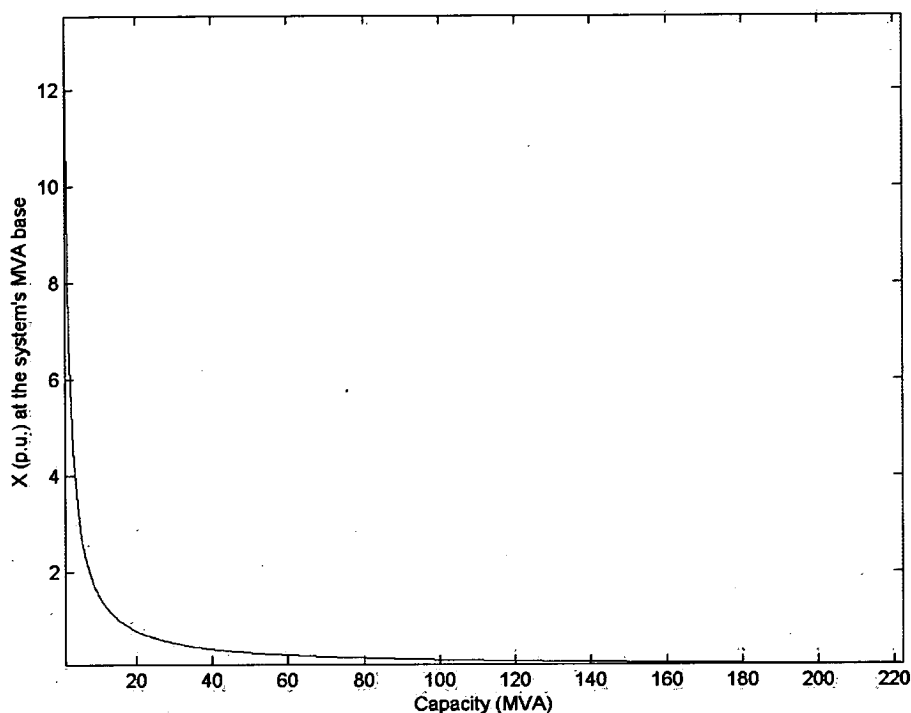


Figure 2.9 New generators' p.u. reactance with respect to the system MVA base.

2.8.4 Algorithm-specific settings

The step used for the update of the capacity bounds on CELs was set to 0.01 (specifies (2.42)). It was found adequately small to produce precise results in a reasonable amount of time (see performance in Sections 2.8.5.1 and 2.8.6.1). So, a step of 0.02 produced final allocations with objective function values 10% lower than the ones achieved in Table 2.14. Steps smaller than 0.005 required several thousands of iterations and a few hours before they finally led the algorithm to converge to the solution that respected both system and network constraints, while very small improvement in efficiency was achieved (0.01% to 0.2% higher objective function).

2.8.5 Test case 1: no preferences for locations

In the first test case, such benefit functions are attached to CELs that no preference is expressed for the allocation of new capacity. The benefit functions have the general form of (2.11), which is repeated here for convenience:

$$C_g(P_g) = a \cdot P_g^2 + b \cdot P_g + c \quad \text{w.r.t. } a, b, c < 0 \text{ and } P_g > 0$$

Table 2.4 contains the benefit function coefficients for each CEL.

CEL bus	a	b	c
1	0	-20	0
10	0	-20	0
11	0	-20	0

Table 2.4 CEL benefit function coefficients.

E/IP benefit functions have the general form of (2.12): $C_T(P_T) = a \cdot P_T^2 + b \cdot |P_T| + c$. Table 2.5 presents the benefit function coefficients for the E/IP at bus 12.

E/IP bus	a	b	c
12	0	-20	0

Table 2.5 E/IP benefit function coefficients.

2.8.5.1 Results

The initial OPF capacity allocation resulted in excess peak fault currents on the transformers connecting buses 1-2 and 4-10. The FLCOPF algorithm reallocated capacity at CELs in order to reduce fault currents within the switchgear specification. Capacity from CELs at buses 1 and 11 was 'shifted' to CEL 10 and a new optimum was reached, which respects both OPF and fault constraints. The algorithm converged in 300 iterations and about 5 minutes on a Pentium 4. The results are presented in Table 2.6, together with the initial OPF capacity allocation.

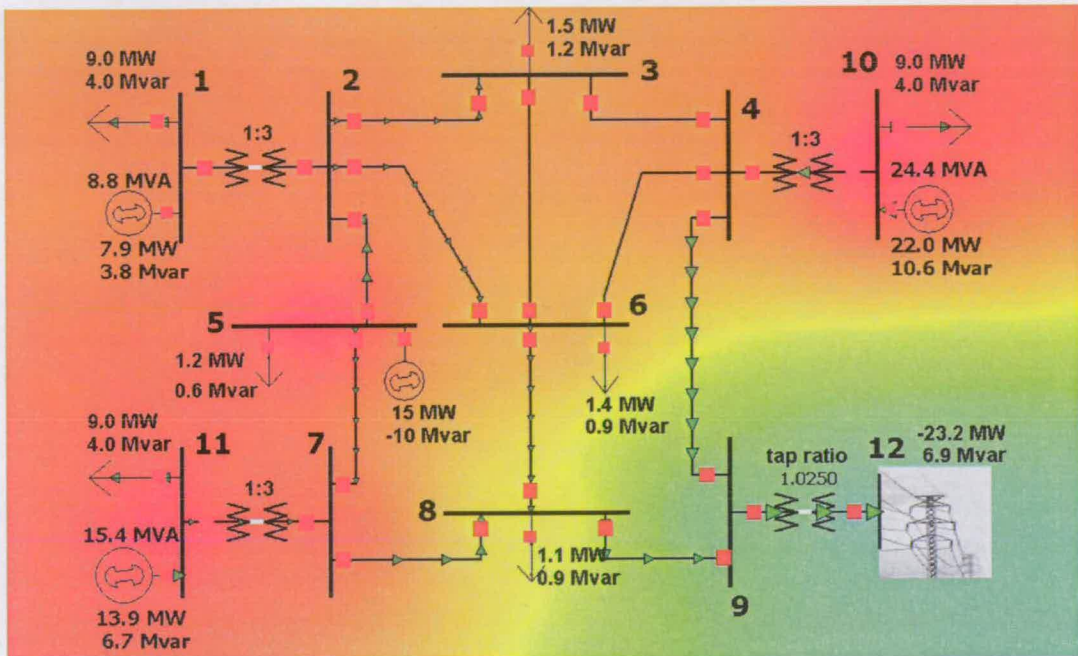
CEL bus	Initial OPF allocation (MVA)	FLCOPF reallocation (MVA)
1	8.83	2.17
10	24.44	30.39
11	15.4	13.06
TOTAL	48.67	45.62

Table 2.6 Allocation of generation capacity at CELs.

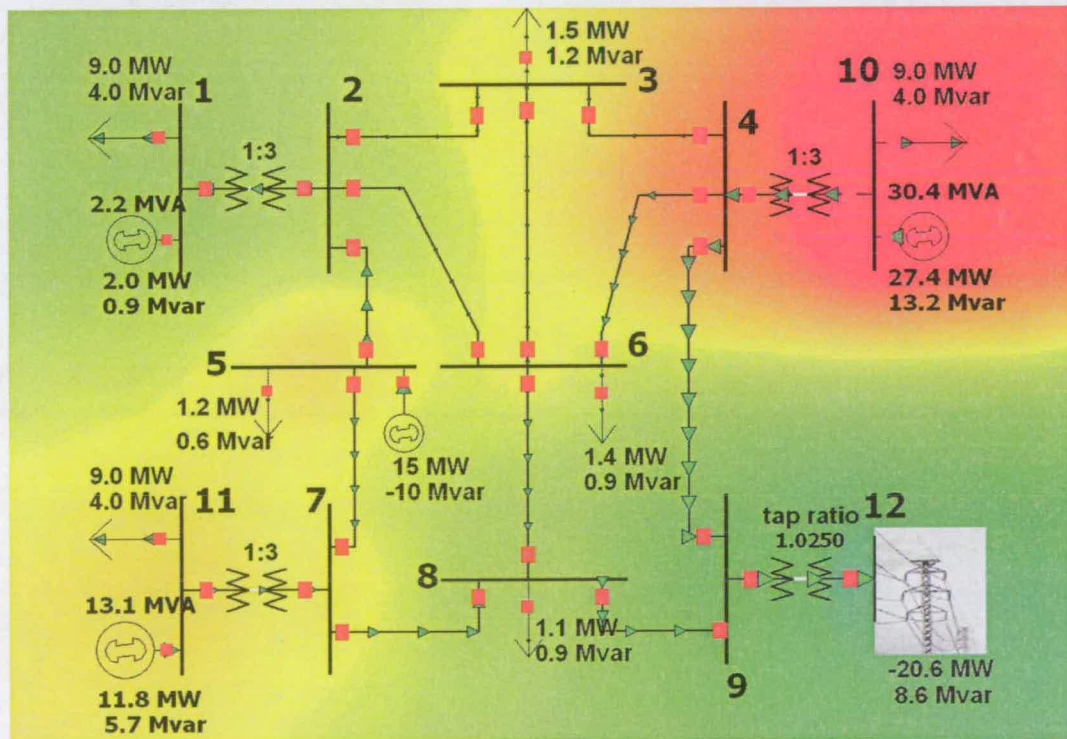
The total new capacity was reduced by only $48.67-45.62=3.05$ MVA after the FLCOPF reallocation. The E/IP was set at an export level of 20.62 MW, while providing the local network with 8.57 MVar of reactive power. Table 2.7 presents the bus voltage patterns of the initial capacity allocation (ignoring fault level constraints) and the FLCOPF reallocation. Figure 2.10 recreates both voltage patterns on contour images superimposed on the test case graph. The power flow data of the simulation results were passed to PowerWorld Simulator [64], which visually recreated the pattern of bus voltage magnitudes. The closer the colour to blue (brighter in b/w prints), the lower the bus voltage and the closer the colour to red (darker in b/w prints), the higher the bus voltage.

Bus number	Voltage (p.u.)	
	initial capacity allocation	FLCOPF reallocation
1	1.087	1.032
2	1.087	1.041
3	1.078	1.050
4	1.082	1.076
5	1.100	1.056
6	1.074	1.049
7	1.093	1.052
8	1.054	1.030
9	0.998	0.996
10	1.100	1.100
11	1.100	1.057
12	0.980	0.980

Table 2.7 Bus voltage pattern of the initial and FLCOPF capacity allocation.



(a)



(b)

Figure 2.10 Voltage pattern contours of the initial allocation (a) and the FLCOPF reallocation (b) of new capacity, superimposed on the test case graph. No locational preferences.

Figure 2.11 contains the MVA capacity reallocation sequence at the CELs (bus 1, 10, 11) vs. the iteration number. Finally, line 2-5 and 4-9 transfer 11.71 MVA and 15.13 MVA respectively, if all new generators operate up to their limits. The tap changer of the transformer between buses 9 and 12 sets the tap ratio to 1.025, in order to maintain the voltage at bus 9 (0.996 p.u.) near to the rated voltage of 1 p.u.

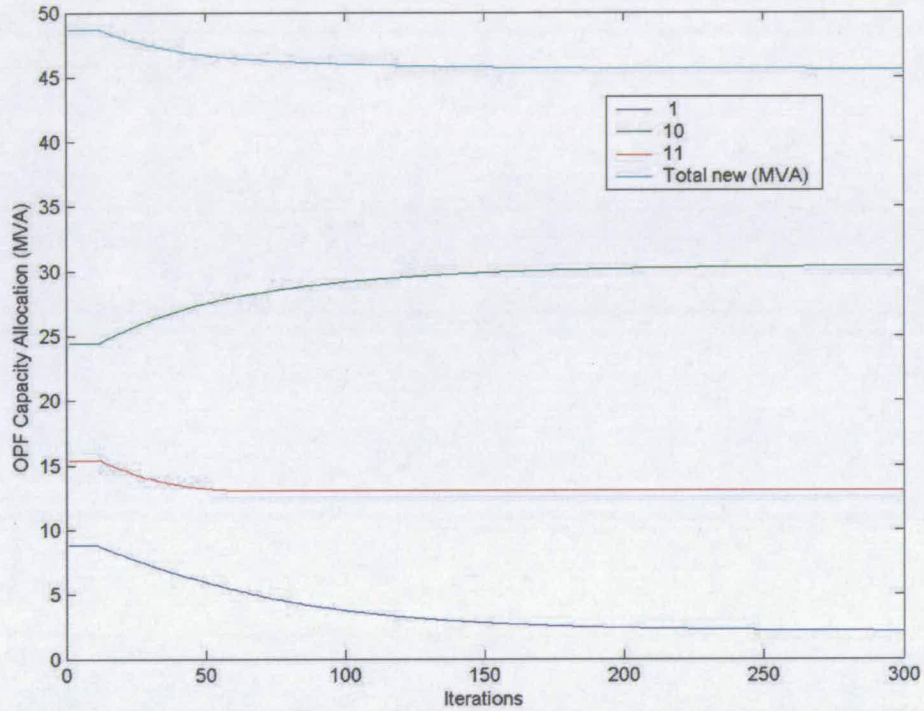


Figure 2.11 Capacity reallocation sequence at the CELs and the E/IP.

Figure 2.12 shows the capacity bounds at each iteration, according to GROA. Figure 2.13 shows how the capacity bounds are updated at the end of each iteration loop.

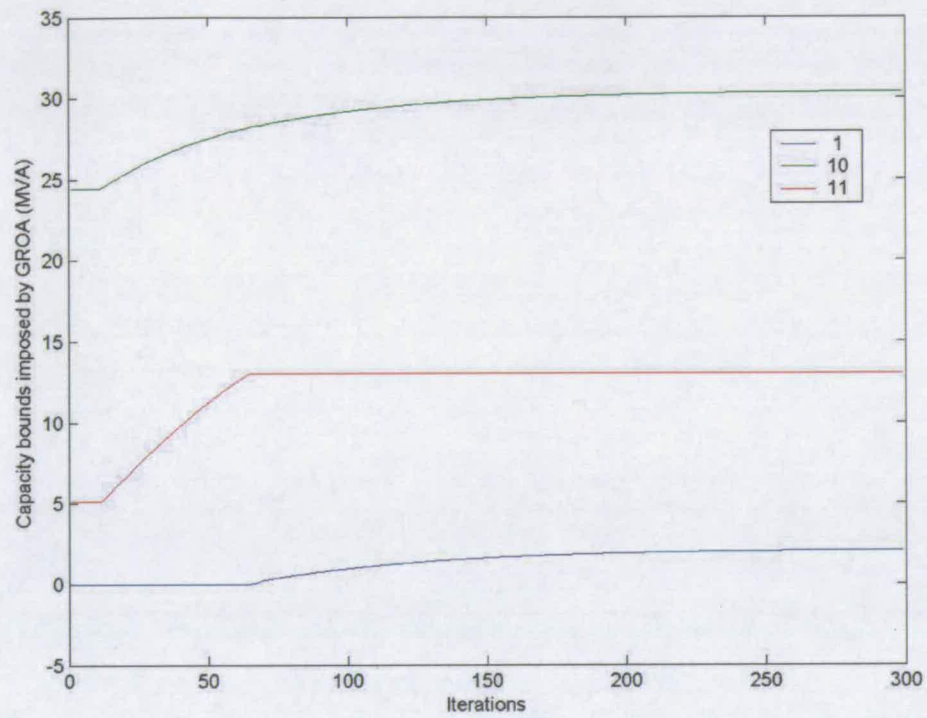


Figure 2.12 Capacity bounds imposed by GROA vs. iteration number.

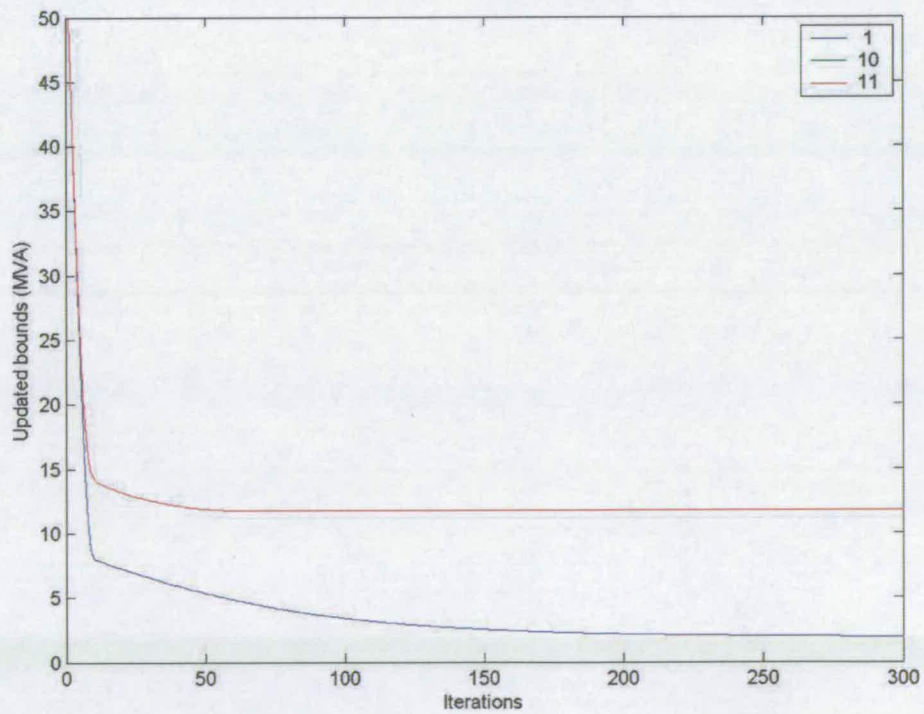


Figure 2.13 Update of bounds at the end of each iteration loop.

2.8.6 Test case 2 : locational preferences

In the second test case, the CEL benefit functions express a preference for the allocation of new capacity at bus 1. Table 2.8 contains the benefit function coefficients for each CEL. Table 2.9 presents the benefit function coefficients for the E/IP at bus 12.

CEL bus	a	b	c
1	0	-30	0
10	0	-20	0
11	0	-20	0

Table 2.8 CEL benefit function coefficients, expressing a preference for bus 1.

E/IP bus	a	b	c
12	0	-20	0

Table 2.9 E/IP benefit function coefficients.

2.8.6.1 Results

The initial OPF capacity allocation resulted again in excess peak fault currents on the transformers connecting buses 1-2 and 4-10. The FLCOPF algorithm reallocated capacity at CELs in order to reduce fault currents within the switchgear specifications. The algorithm converged in 680 iterations and about 12 minutes. The results are presented in Table 2.10, together with the initial OPF capacity allocation.

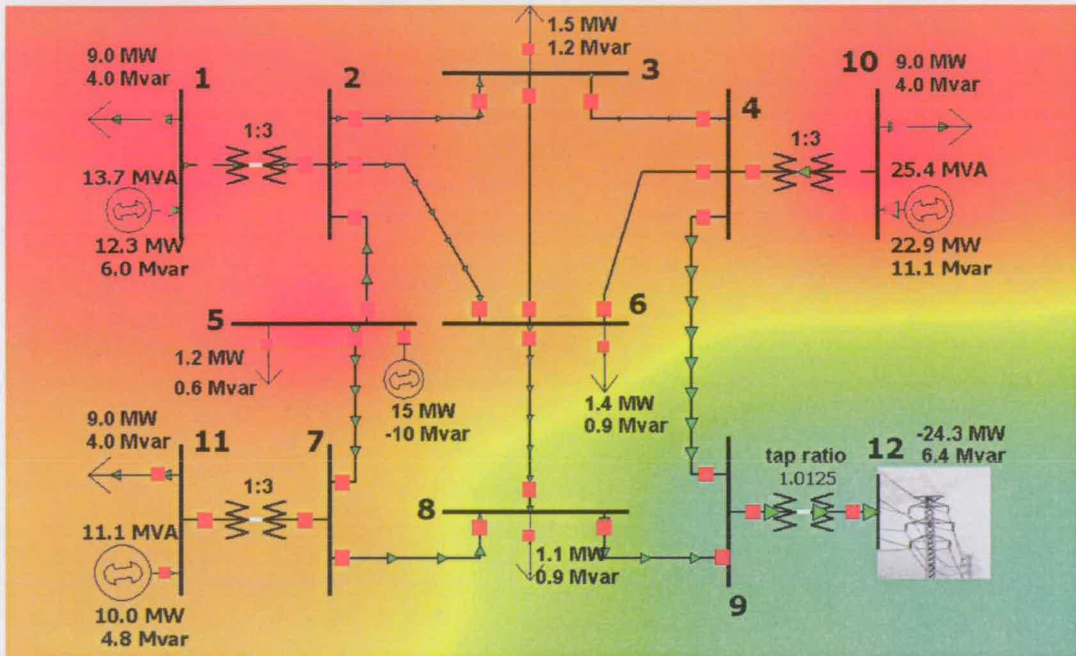
CEL bus	Initial OPF allocation (MVA)	FLCOPF reallocation (MVA)
1	13.66	2.64
10	25.44	30.72
11	11.10	11.66
TOTAL	50.20	45.02

Table 2.10 Allocation of generation capacity at CELs.

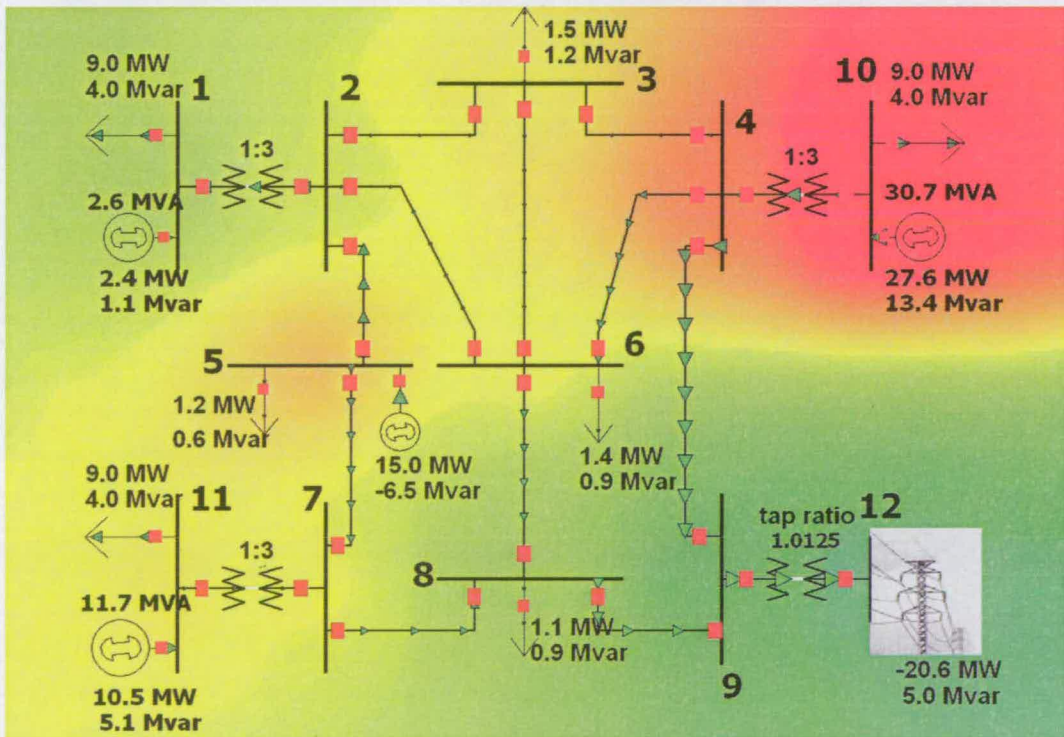
Capacity from CEL at bus 1 and 11 was ‘shifted’ to CEL at bus 10, so the total new capacity was reduced only by $50.20 - 45.02 = 5.18$ MVA. The new optimum respects both OPF and fault constraints. The E/IP was set at an export level of 20.56 MW, while providing the local network with 4.93 MVar of reactive power. Table 2.11 presents the bus voltage patterns of the initial capacity allocation (ignoring fault level constraints) and the FLCOPF reallocation. Figure 2.14 recreates both voltage patterns on contour images superimposed on the test case graph.

Bus number	Voltage (p.u.)	
	initial capacity allocation	FLCOPF reallocation
1	1.100	1.039
2	1.095	1.047
3	1.080	1.053
4	1.081	1.076
5	1.100	1.063
6	1.073	1.051
7	1.072	1.049
8	1.042	1.027
9	0.986	0.987
10	1.100	1.100
11	1.074	1.053
12	0.980	0.980

Table 2.11 Bus voltage pattern of the initial and FLCOPF capacity allocation, when there is a preference for the CEL at bus 1.



(a)



(b)

Figure 2.14 Voltage pattern contours of the initial capacity allocation (a) and the FLCOPF reallocation (b), superimposed on the test case graph. Preference for CEL 1.

Figure 2.15 shows the MVA capacity reallocation sequence at the CELs (bus 1, 10, 11) against the iteration number. Finally, lines 2-5 and 4-9 transfer 10.34 MVA and 15.04 MVA respectively, if all generators operate at full capacity. The tap changer of the transformer between buses 9 and 12 sets the tap ratio to 1.0125, in order to maintain the voltage at bus 9 (0.987 p.u.) near to the rated voltage of 1 p.u.

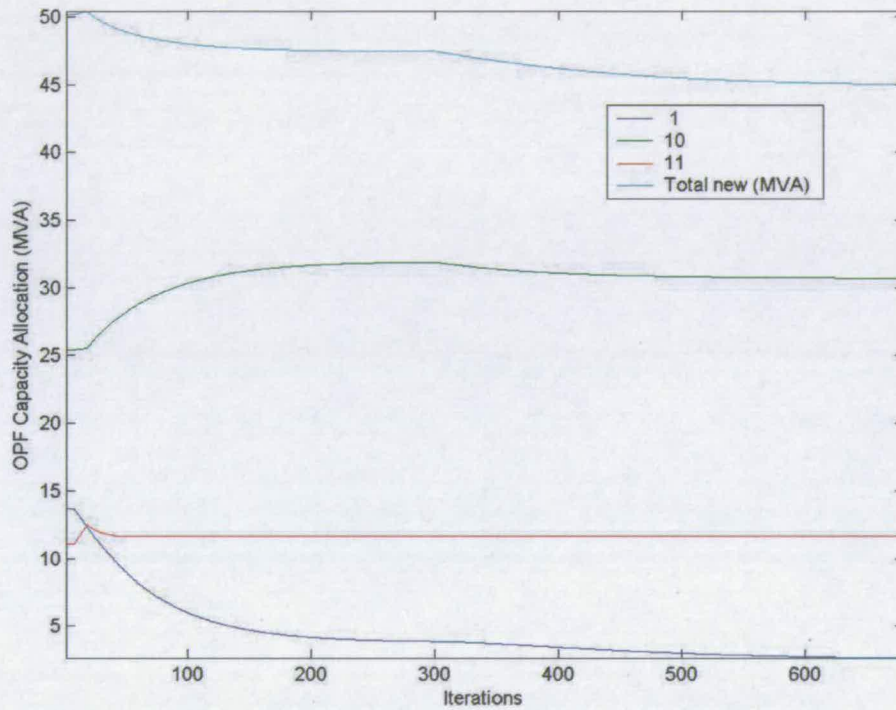


Figure 2.15 Capacity reallocation sequence at the CELs and the E/IP.

Figure 2.16 shows the capacity bounds at each iteration, according to GROA. Figure 2.17 shows how the capacity bounds are updated at the end of each iteration loop.

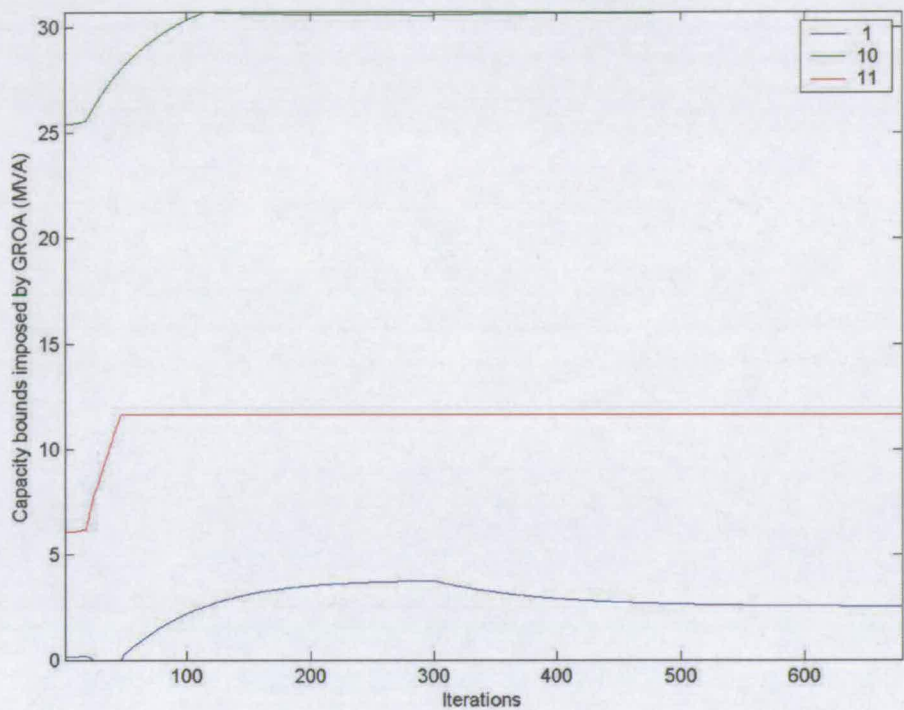


Figure 2.16 Capacity bounds imposed by GROA vs. iteration number.

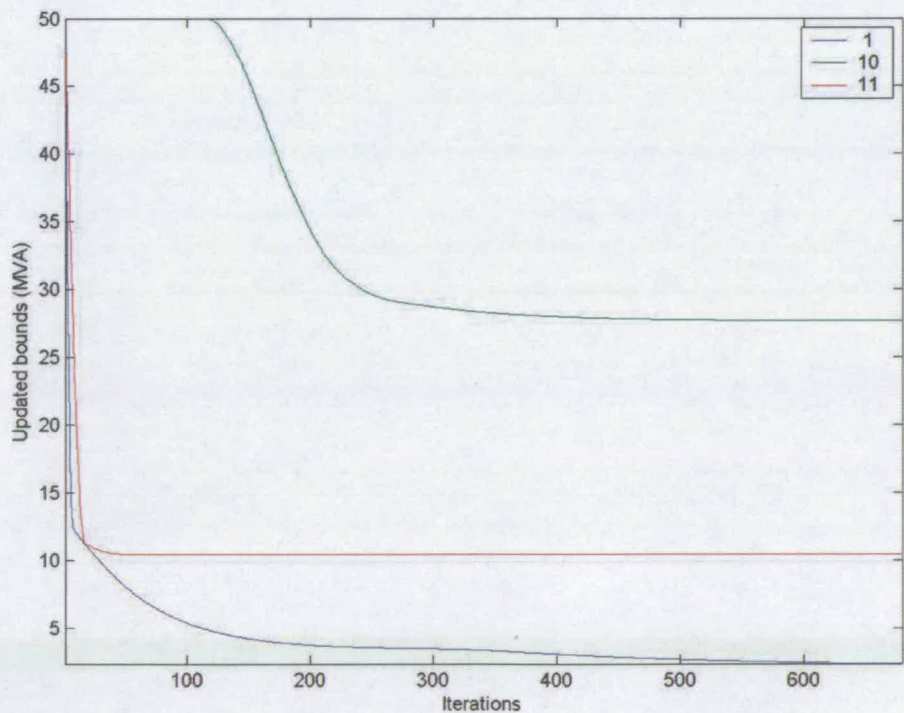


Figure 2.17 Update of bounds at the end of each iteration loop.

2.8.7 Analysis of Results

The benefit functions attached to CELs express capacity allocation preferences. Table 2.12 presents the benefit functions used in test case 1 (no allocation preferences) and test case 2 (allocation preference to CEL at bus 1).

No allocation preferences (test case 1)				Allocation preference to a CEL (test case 2)			
CEL bus	a	b	c	CEL bus	a	b	c
1	0	-20	0	1	0	-30	-0
10	0	-20	0	10	0	-20	0
11	0	-20	0	11	0	-20	0
E/IP bus	a	b	c	E/IP bus	a	b	c
12	0	-20	0	12	0	-20	0

Table 2.12 Benefit functions used in test cases.

Table 2.13 demonstrates how the capacity shifts in the second case from the other CELs to the CEL at bus 1, because it has a benefit function with higher coefficients. It also includes the total capacity allocated in each case and the real power exported to the E/IP at bus 12.

CEL bus	No allocation preferences	Allocation preference to CEL at bus 1
1	2.17 MVA	2.64 MVA
10	30.39 MVA	30.72 MVA
11	13.06 MVA	11.66 MVA
Total	45.62 MVA	45.02 MVA
E/IP at bus 12	20.62 MW	20.56 MW

Table 2.13 Capacity allocation and transfers to E/IP in the two test cases.

When there are no preferences, the allocation mechanism results in the maximum possible total new capacity, so that the overall benefit is maximised. In the second case, the reduction of total new capacity is connected to the effect preferences have on the OPF target function (see (2.23)). Capacity on CEL at bus 1 has higher negative cost (benefit) per MVA than other CELs and exports at E/IP. The second case favours the allocation capacity at the first

CEL and this works against the allocation over the other CELs and the total capacity. In Table 2.14, the total benefits for the two test cases are calculated.

	No allocation preferences			Allocation preference to CEL at bus 1		
CEL bus	MW allocated $P = \cos \varphi \cdot S$	Benefit/MW	Benefit	MW allocated $P = \cos \varphi \cdot S$	Benefit/MW	Benefit
1	1.96	20	39.2	2.38	30	71.4
10	27.35	20	547.0	27.65	20	553.0
11	11.76	20	235.2	10.49	20	209.8
E/IP at bus 12	20.62	20	412.4	20.56	20	411.2
TOTAL	→		1233.8	→		1245.4

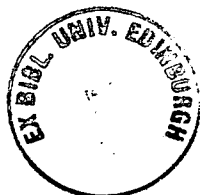
Table 2.14 Calculation of total benefits for both test cases.

Even though the case with allocation preference results in higher total benefit (value of OPF target function), the total capacity is reduced (see Table 2.13). The case with allocation preference results in higher total benefit (value of OPF target function), as expected due to the higher marginal benefit from the allocation at CEL 1. Evidently, when preferences exist there is a trade-off between higher allocation of capacity at the ‘preferred’ CELs and total new capacity.

Exports roughly represent the excess capacity in the local network: the difference between total new capacity and demand. Hence, when total capacity increases exports follow.

2.9 Chapter summary

In this Chapter a method is developed for the incorporation of constraints imposed by switchgear equipment (Fault Level Constraints or FLCs) on the optimal allocation of new generation capacity. The method was termed Fault Level Constrained Optimal Power Flow (FLCOPF), because it uses the OPF as a tool for the optimal allocation of new capacity. OPF is a well-know operating tool in power systems. However, here a method of modelling new generation capacity is presented, so that OPF can also be used to optimally allocate new generation capacity. In other words OPF is used as generation expansion planning, rather than operation planning tool, in the sense that it determines optimal size and location of new generating plants. New generation capacities are simulated as generators with quadratic



benefit functions with negative coefficients. These generators are connected to predetermined locations in the network, with the output of generators simulating the allocated capacity at those locations. Benefit function coefficients represent preferences for the allocation of new capacity between locations.

The method is iterative and contains three discrete steps, which gradually 'shift' the allocation of capacity towards a solution which respects both network and FLCs. In the first step, OPF allocated new capacity ignoring fault levels. Then, fault analyses determined which switchgear would exceed its operational specifications under a possible fault at each system bus. In the second step, a Generation Reduction Optimisation Algorithm (GROA) reduced new capacity at CELs in order to maximize total new generation capacity with respect to the FLCs imposed by that equipment. The subtransient reactance of new generators was estimated as a function of their capacity using an approximate formula (see Section 2.8.3). The lower the new synchronous generation capacity, the higher the subtransient reactance and the lower the fault current. The opposite is also true.

It was assumed that bus voltage patterns do not change much during the optimisation procedure of GROA. Therefore, GROA did not directly set the new upper bounds for capacity in OPF, but pointed the direction which these bounds had to be reduced. So in the third and last step, the new upper capacity bounds at CELs were estimated as a function of the bounds identified by GROA and the last OPF allocation. At the next iteration, the OPF reallocated capacity subject to the new bounds. The iterative process converged to the optimum when there was no significant change of the capacity bounds between iterations and no FLCs were violated.

FLCOPF was tested on a simple 12-bus, meshed, MV network. FLCOPF found the optimal solution for the capacity allocation problem, subject to both network constraints and restrictions imposed by switchgear fault ratings. Furthermore, it was proven that there is a trade-off between higher allocation of capacity at the preferred locations and total new capacity. A comparison between the initial allocation (which ignored FLCs) and the FLCOPF reallocation of capacity (which considers FLCs) demonstrate that FLCs affect the final allocation of capacity at a considerable extend.

Unfortunately, there are two limitations to the approach: FLCOPF needs several hundreds of iterations, even for the small 12-bus network, to converge to the final solution and the iterative nature of this method cannot guarantee global optimality for the final solution.

3. DIRECT INCORPORATION OF FAULT LEVEL CONSTRAINTS IN OPTIMAL POWER FLOW AS A TOOL FOR NETWORK CAPACITY ANALYSIS

3.1 Introduction

Section 2.7 describes how new generation capacity can be modelled and adapted to an Optimal Power Flow (OPF) formulation, so that OPF can be used for the maximisation of total new capacity in an existing network. However, the current formulation does not include the constraints imposed by fault levels in the system constraints. Consequently, the conventional form of OPF as a tool for network capacity analysis also ignores the impact new generation has on fault levels.

In Chapter 2, a three-step iterative process is used so that fault level constraints are considered in the final capacity allocation. First, OPF allocates new capacity ignoring fault levels. Fault analyses determine which switchgear will exceed its operational specifications under a possible fault at each system bus. Then an optimisation algorithm, named Generator Reactance Optimisation Algorithm (GROA), reduces new capacity at the Capacity Expansion Locations (CELs) in order to maximise total new generation capacity with respect to the fault level constraints imposed by that equipment. GROA utilises formula (2.37) in Section 2.7.4 to estimate the p.u. subtransient reactance of new generators with respect to their capacity. Here, it is repeated for convenience:

$$X_{p.u.}''(S^g) = f(S^g) \frac{S_b}{S^g} \quad (3.1)$$

The higher the new capacity S^g , the lower the subtransient reactance $X_{p.u.}''$ and the higher the expected fault currents (see Section 2.7.4 for justification). The opposite is also true. However, it is assumed that bus voltage patterns do not change much during the optimisation procedure of GROA. Therefore, GROA does not directly set the new upper bounds for capacity in OPF, but points the direction which these bounds must be reduced. In the last step, the new upper capacity bounds at CELs are estimated as a function of the bounds identified by GROA and the OPF allocation of the first step. At the next iteration, OPF reallocates capacity subject to the new bounds. The iterative process converges to the optimum when there is no significant change in the capacity bounds between iterations and no fault level constraints are violated.

In this Chapter, a different approach is presented for the direct incorporation of fault level constraints in OPF. A mathematical methodology is developed for the conversion of

constraints imposed by fault levels to simple non-linear (inequality) constraints. No new variables are introduced in the OPF formulation to describe the additional constraints. Most common OPF-solving engines already have the computational capacity to handle numerous non-linear constraints, such as the ones described by the power balance equations (1.10) on buses. Therefore, once fault level constraints are converted to non-linear constraints described by OPF variables, they can be directly introduced to any optimisation process performing the OPF. This new approach was termed Direct Fault Level Constrained OPF (D-FLCOPF). As it will be proven later in this Chapter, grouping fault level constraints together with the rest of the system constraints has several advantages in comparison with the method presented in the previous Chapter which converted them to restrictions on new capacity.

3.2 Defining the problem

Practically, ‘fault level constraints’ refer to the operational limitations of switchgear equipment during a fault. If the specifications of the equipment are not adequate to clear or isolate a fault, then not only the equipment itself will be possibly damaged, but the operation of a broader part of the power system will become insecure. Generally, it is the magnitude of a fault current which is compared with the specifications of the switchgear equipment. For example, in Section 2.6.9 two basic specifications of switchgear were described: capacity and breaking capability. They both set limits to the magnitudes of fault currents that the switchgear can securely break. Therefore, the analysis will be focused on the magnitudes of fault currents, rather than their complex values. The magnitude of the expected fault currents $|I_{i,j}^f|$ must comply with the maximum allowed by the specifications $|I_{spec}|$, such as the one described by the switchgear breaking capability in (1.26):

$$|I_{i,j}^f| < |I_{spec}| \Leftrightarrow |I_{i,j}^f| - |I_{spec}| < 0 \quad (3.2)$$

In order to directly include fault level constraints in OPF, a mathematical expression must be found first which can link the expected fault currents with the OPF variables. These variables are:

$|V_i|$: voltage magnitude of bus i .

\hat{V}_i : voltage angle of bus i .

P^g : real power output of generator G .

Q^g : reactive power output of generator G .

The fault current running through a line with serial impedance $\hat{z}_{i,j}$ between buses i and j for a fault on bus f is given by (1.9), which is repeated here for convenience:

$$I_{i,j}^f = \frac{V_i - V_j - (FSF_{i,f} - FSF_{j,f}) \cdot V_f}{\hat{z}_{i,j}} = \frac{V_i - V_j - FSF_{i,j}^f \cdot V_f}{\hat{z}_{i,j}} \quad (3.3)$$

V_i, V_j, V_f are the voltages of system buses i, j, f . They are explicitly described in magnitude and angle by the OPF variables $|V_k|, \hat{V}_k$, where $k=i, j, f$. On the contrary, $FSF_{i,j}^f = \frac{z_{i,f} - z_{j,f}}{z_{f,f}}$ depends on three elements of the Z_{bus} ($z_{i,f}, z_{j,f}, z_{f,f}$), which are not directly connected with any of the OPF variables. If OPF is used in its conventional form to identify the most economic operating point of generation to cover the demand, then generators have specific impedances and Z_{bus} is constant. However, if the OPF is utilised for the allocation of new capacity, then the generators' size is not specific. The Z_{bus} is a function of the new capacity and so is $FSF_{i,j}^f$ and the expected fault currents. This last case is discussed in the next Section.

3.3 Connecting expected fault currents with new generation size

In D-FLCOPF new generation and export/import point to external networks are modelled exactly the same way as in FLCOPF (see Section 2.5.1). Equation (2.37) estimates the subtransient reactance of new generators according to their capacity. While a change in a generator's reactance linearly affects one element of the Y_{bus} (the one connecting the bus of the generator G with the reference bus: $y_{GG}^{new} = y_{GG}^{old} + y_{GG}^{change}$), it non-linearly alters all elements of the $Z_{bus} = Y_{bus}^{-1}$. If fault level constraints are ignored, changes of the reactances of new generators have no impact in the OPF operation for the allocation of new capacity. In this case OPF uses only the non-diagonal elements of the Y_{bus} to solve the sequence of power flows leading to the optimum. However, the allocation of new capacity changes the Z_{bus} . $FSF_{i,j}^f$ is a function of elements of the Z_{bus} , thus the expected fault currents are also a function of the same elements according to (3.3). Consequently, the problem of direct inclusion of fault level constraints in OPF focuses on the expression of Z_{bus} as a function of new capacity.

Z_{bus}^0 is the impedance matrix of the existing power system (without any new capacity added), built element-by-element or calculated as the inverse of the initial admittance matrix Y_{bus}^0 . The subtransient reactance of a new generator on bus $G1$ affects the diagonal element $y_{G1,G1}$ of the Y_{bus} :

$$y_{G1,G1}^1 = y_{G1,G1}^0 + \frac{1}{jx_{G1}''} \quad (3.4)$$

where jx_{G1}'' is the reactance of the new generator. Equation (3.4) practically describes the modification to an element of the initial matrix Y_{bus}^0 .

The Sherman-Morrison-Woodbury (S-M-W) formula [65], [66] calculates the elements of the new inverse of a matrix after one element is modified, given the inverse of the initial matrix and the modification:

$$B_{r,k} = b_{r,k} - \frac{b_{r,L} b_{S,k} \Delta a_{L,S}}{1 + b_{S,L} \Delta a_{L,S}} \quad (3.5)$$

where B is the new inverse matrix, b is the old inverse matrix, $\Delta a_{L,S}$ the modification of element L, S and a is the initial matrix with $\alpha, b, B \in R^{n \times n}$.

Sherman, Morrison and Woodbury tested their formula on matrixes consisting of real numbers. However, numerical tests with several matrixes consisting of random complex numbers showed that its use can be extended to impedance matrixes, too. Such a simple numerical example with matrixes consisting of random complex numbers is included in Appendix A.1. Therefore, according to (3.5) the elements of the new impedance matrix can be calculated for a new generator on bus $G1$ with subtransient reactance jx_{G1}'' :

$$z_{r,k}^1 = z_{r,k}^0 - \frac{z_{r,G1} z_{G1,k} \frac{1}{jx_{G1}''}}{1 + z_{G1,G1} \frac{1}{jx_{G1}''}} \quad (3.6)$$

Whenever a new generator $(n+1)$ is added on bus $G(n+1)$, similar numerical calculations to (3.6) directly give the impact the new subtransient reactance has on the Z_{bus} , with respect to the modified Z_{bus} from the addition of generator n on bus Gn :

$$z_{r,k}^{n+1} = z_{r,k}^n - \frac{z_{r,G(n+1)} \cdot z_{G(n+1),k} \frac{1}{jx_{G(n+1)}''}}{1 + z_{G(n+1),G(n+1)} \frac{1}{jx_{G(n+1)}''}} \quad (3.7)$$

Subsequently, (3.7) $\xrightarrow{(3.1)}$ $z_{r,k}^{n+1} = z_{r,k}^n - \frac{z_{r,G(n+1)} \cdot z_{G(n+1),k} \frac{1}{jX_{typical}''} \frac{S_b}{S^{n+1}}}{1 + z_{G(n+1),G(n+1)} \frac{1}{jX_{typical}''} \frac{S_b}{S^{n+1}}}$ (3.8)

This way of updating the Z_{bus} , each time OPF allocates new capacity on a bus, shares two important features. Firstly, a serious computational burden is avoided, especially for modern, largely interconnected networks consisting of thousands of buses and tens of thousands of transmission lines. There is no need to invert the new Y_{bus} or build the Z_{bus} element-by-element from scratch each time the capacity allocation is changed and the impact on the expected fault currents has to be re-estimated. Secondly, the S-M-W formula computes any

element of the new impedance matrix with respect to the size of new generation. The mathematical formulation of the impact new capacity has on the Z_{bus} is achieved.

Furthermore, the reactive power capability curves of several types and sizes of generators can be collected from major constructors that will be possibly preferred by the generator investors. From each curve the MVA rating of the generator is extracted and a new curve $S^g(P^g)$ is created, which will connect the MVA rating S^g of new generators with their rated output P^g in MW.

Alternatively, the MVA rating S^g of generators can be estimated from their rated power P^g and rated power factor $p.f.$. The rated $p.f.$ does not change much between different sizes and models (for most synchronous generators the rated $p.f.$ is around 0.8). Therefore, a function of MVA ratings of generators can be created with respect to their rated MW output divided by a constant typical $p.f.$:

$$S^g(P^g) = \frac{P^g}{p.f.} \quad (3.9)$$

$$\text{Consequently, } (3.8) \xrightarrow{(3.9)} z_{r,k}^{n+1} = z_{r,k}^n - \frac{z_{r,G(n+1)} \cdot z_{G(n+1),k} \cdot P^{n+1}}{jX_{\text{typical}}^n \cdot p.f. \cdot S_b + z_{G(n+1),G(n+1)} \cdot P^{n+1}} \quad (3.10)$$

The rated power P^g is also a variable in the OPF when it is used to allocate new generation capacity. In other words, I managed to link $FSF_{i,j}^f$, a function of Z_{bus} elements, to the OPF variables P^g, Q^g (since capacity $Q^g = \sqrt{(S^g)^2 - (P^g)^2}$). Equation (3.3) is now fully defined by the OPF variables. Since fault levels became a function of the OPF variables, they can be directly added to non-linear system constraints:

$$(3.2) \rightarrow \left| I_{i,j}^f \left(|V_1|, \dots, |V_n|, \hat{V}_1, \dots, \hat{V}_n, P^1, \dots, P^k, Q^1, \dots, Q^k \right) \right| - |I_{\text{spec}}| < 0 \quad (3.11)$$

, where n is the number of system buses and k is the number of generators.

3.4 Calculating the derivatives of fault level constraints

The solution of Nonlinear Programming problems is generally achieved in an iterative manner. In each iteration a direction of search towards the global optimum has to be estimated. This means that the derivatives of all non-linear equality and inequality constraints must be calculated with respect to each OPF variable. The derivatives for the traditional non-linear constraints contained in the OPF are calculated in the Appendix A.3. In the next Sections, the calculations of the derivatives for the new nonlinear constraints will be briefly presented. The derivatives are calculated for the magnitude of a current running through a line with impedance $\tilde{z}_{i,j}$ from bus i to bus j for a fault on bus f , with respect to the OPF variables. The detailed calculations are demonstrated in the Appendix A.2.

3.4.1 Derivatives of fault currents with respect to bus voltages

The voltages V_i , V_j , V_f , as well as the $FSF_{i,j}^f$ can be expressed as a sum of a real and an imaginary part:

$$V_i = V_i^x + j \cdot V_i^y \quad (3.12)$$

$$V_j = V_j^x + j \cdot V_j^y \quad (3.13)$$

$$V_f = V_f^x + j \cdot V_f^y \quad (3.14)$$

$$FSF_{i,j}^f = FSF = FSF^x + j \cdot FSF^y \quad (3.15)$$

$$(3.3) \xrightarrow[(3.14),(3.15)]{(3.12),(3.13)} \rightarrow$$

$$I_{i,j}^f = \frac{V_i^x - V_j^x - FSF^x \cdot V_f^x + FSF^y \cdot V_f^y + (V_i^y - V_j^y - FSF^y \cdot V_f^x - FSF^x \cdot V_f^y) \cdot j}{\tilde{z}_{i,j}} \quad (3.16)$$

$$\text{Let } x = V_i^x - V_j^x - FSF^x \cdot V_f^x + FSF^y \cdot V_f^y \quad (3.17)$$

$$\text{and } y = V_i^y - V_j^y - FSF^y \cdot V_f^x - FSF^x \cdot V_f^y \quad (3.18)$$

$$(3.16) \xrightarrow[(3.18)]{(3.17)} I_{i,j}^f = \frac{\sqrt{x^2 + y^2}}{|\tilde{z}_{i,j}|} \quad (3.19)$$

The chain rule can be used to calculate the desired derivatives as a function of two derivatives, which are easier to calculate:

$$\begin{aligned} \frac{d|I_{i,j}^f|}{d|V_i|} &= \frac{d|I_{i,j}^f|}{dV_i^x} \cdot \frac{dV_i^x}{d|V_i|} \\ \frac{d|I_{i,j}^f|}{d|V_j|} &= \frac{d|I_{i,j}^f|}{dV_j^x} \cdot \frac{dV_j^x}{d|V_j|} \\ \frac{d|I_{i,j}^f|}{d|V_f|} &= \frac{d|I_{i,j}^f|}{dV_f^x} \cdot \frac{dV_f^x}{d|V_f|} \end{aligned} \quad (3.20)$$

$$\frac{dV_i^x}{d|V_i|} = \frac{d(|V_i| \cdot \cos \varphi_i)}{d|V_i|} = \cos \varphi_i$$

$$\text{similarly, } \frac{dV_j^x}{d|V_j|} = \cos \varphi_j \quad (3.21)$$

$$\text{and } \frac{dV_f^x}{d|V_f|} = \cos \varphi_f$$

where φ_i , φ_j , φ_f are the voltage angles of buses i, j, f .

$$\begin{aligned} \frac{d|I_{i,j}^f|}{dV_i^x} &\stackrel{(3.19)}{=} \frac{d\left(\frac{\sqrt{x^2 + y^2}}{|\tilde{z}_{i,j}|}\right)}{dV_i^x} = \frac{1}{|I_{i,j}^f| \cdot |\tilde{z}_{i,j}|^2} \left(x \frac{dx}{dV_i^x} + y \frac{dy}{dV_i^x} \right) \\ \text{similarly } \frac{d|I_{i,j}^f|}{dV_j^x} &= \frac{1}{|I_{i,j}^f| \cdot |\tilde{z}_{i,j}|^2} \left(x \frac{dx}{dV_j^x} + y \frac{dy}{dV_j^x} \right) \\ \text{and } \frac{d|I_{i,j}^f|}{dV_f^x} &= \frac{1}{|I_{i,j}^f| \cdot |\tilde{z}_{i,j}|^2} \left(x \frac{dx}{dV_f^x} + y \frac{dy}{dV_f^x} \right) \end{aligned} \quad (3.22)$$

3.4.1.1 If $f \neq i$ and $f \neq j$

- With respect to bus voltage magnitudes:

$$\frac{dx}{dV_i^x} = 1 \quad (3.23)$$

$$\frac{dy}{dV_i^x} = \tan \varphi_i \quad (3.24)$$

$$(3.20) \xrightarrow[(3.23),(3.24)]{(3.21),(3.22)} \frac{d|I_{i,j}^f|}{d|V_i|} = \left[\frac{x + y \cdot \tan \varphi_i}{|I_{i,j}^f| \cdot |\tilde{z}_{i,j}|^2} \right] \cos \varphi_i \quad (3.25)$$

$$\text{Similarly, } \frac{dx}{dV_j^x} = -1 \quad (3.26)$$

$$\text{and } \frac{dy}{dV_j^x} = -\tan \varphi_j \quad (3.27)$$

$$\text{Thus, } (3.20) \xrightarrow[(3.26),(3.27)]{(3.21),(3.22)} \frac{d|I_{i,j}^f|}{d|V_j|} = \left[\frac{-x - y \cdot \tan \varphi_j}{|I_{i,j}^f| \cdot |\tilde{z}_{i,j}|^2} \right] \cos \varphi_j \quad (3.28)$$

$$\text{Similarly, } \frac{dx}{dV_f^x} = -FSF^x + FSF^y \cdot \tan \varphi_f \quad (3.29)$$

$$\text{and } \frac{dy}{dV_f^x} = -FSF^y - FSF^x \cdot \tan \varphi_f \quad (3.30)$$

Thus, $(3.20) \xrightarrow[(3.29),(3.30)]{(3.21),(3.22)}$

$$\frac{d|I_{i,j}^f|}{d|V_f|} = \left[\frac{-x \cdot (-FSF^x + FSF^y \cdot \tan \varphi_f) + y \cdot (-FSF^y - FSF^x \cdot \tan \varphi_f)}{|I_{i,j}^f| \cdot |\tilde{z}_{i,j}|^2} \right] \cos \varphi_f \quad (3.31)$$

- With respect to bus voltage angles:

$$\begin{aligned}\frac{d|I_{i,j}^f|}{d\varphi_i} &= \frac{d|I_{i,j}^f|}{dV_i^x} \cdot \frac{dV_i^x}{d\varphi_i} \\ \frac{d|I_{i,j}^f|}{d\varphi_j} &= \frac{d|I_{i,j}^f|}{dV_j^x} \cdot \frac{dV_j^x}{d\varphi_j} \\ \frac{d|I_{i,j}^f|}{d\varphi_i} &= \frac{d|I_{i,j}^f|}{dV_i^x} \cdot \frac{dV_i^x}{d\varphi_i}\end{aligned}\tag{3.32}$$

$$\begin{aligned}\frac{dV_i^x}{d\varphi_i} &= \frac{d(|V_i| \cos \varphi_i)}{d\varphi_i} = -|V_i| \cdot \sin \varphi_i \\ \text{similarly } \frac{dV_j^x}{d\varphi_j} &= -|V_j| \sin \varphi_j\end{aligned}\tag{3.33}$$

$$\text{and } \frac{dV_f^x}{d\varphi_f} = -|V_f| \sin \varphi_f$$

$$(3.32) \xrightarrow[(3.23),(3.24)]{(3.22),(3.33)} \frac{d|I_{i,j}^f|}{d\varphi_i} = - \left[\frac{x + y \cdot \tan \varphi_i}{|I_{i,j}^f| \cdot |\tilde{z}_{i,j}|^2} \right] \cdot |V_i| \cdot \sin \varphi_i\tag{3.34}$$

$$(3.32) \xrightarrow[(3.26),(3.27)]{(3.22),(3.33)} \frac{d|I_{i,j}^f|}{d\varphi_j} = \left[\frac{x + y \cdot \tan \varphi_j}{|I_{i,j}^f| \cdot |\tilde{z}_{i,j}|^2} \right] \cdot |V_j| \cdot \sin \varphi_j\tag{3.35}$$

$$\begin{aligned}(3.32) \xrightarrow[(3.26),(3.27)]{(3.22),(3.33)} \frac{d|I_{i,j}^f|}{d\varphi_f} &= \dots \\ &= - \left[\frac{x \cdot (-FSF^x + FSF^y \cdot \tan \varphi_f) + y \cdot (-FSF^y - FSF^x \cdot \tan \varphi_f)}{|I_{i,j}^f| \cdot |\tilde{z}_{i,j}|^2} \right] |V_f| \cdot \sin \varphi_f\end{aligned}\tag{3.36}$$

3.4.1.2 If $f = i$

- Calculation of derivatives with respect to voltage magnitudes:

$$\frac{dx}{dV_i^x} = 1 - FSF^x + FSF^y \cdot \tan \varphi_i \quad (3.37)$$

$$\frac{dy}{dV_i^x} = \tan \varphi_i (1 - FSF^x) - FSF^y \quad (3.38)$$

$$(3.20) \xrightarrow[(3.37),(3.38)]{(3.21),(3.22)} \rightarrow$$

$$\frac{d|I_{i,j}^f|}{d|V_i|} = \frac{x \cdot (1 - FSF^x + FSF^y \cdot \tan \varphi_i) + y \cdot (\tan \varphi_i - FSF^y - FSF^x \cdot \tan \varphi_i)}{|I_{i,j}^f| \cdot |\tilde{z}_{i,j}|^2} \cos \varphi_i \quad (3.39)$$

$$\text{similarly, } \frac{dx}{dV_j^x} = -1 \quad (3.40)$$

$$\text{and } \frac{dy}{dV_j^x} = \frac{d(V_i^y - V_j^y \cdot \tan \varphi_j - FSF^y \cdot V_i^x - FSF^x \cdot V_j^y)}{dV_j^x} = -\tan \varphi_j \quad (3.41)$$

$$\text{Thus, } (3.20) \xrightarrow[(3.40),(3.41)]{(3.21),(3.22)} \rightarrow \frac{d|I_{i,j}^f|}{d|V_j|} = \frac{-x - y \cdot \tan \varphi_j}{|I_{i,j}^f| \cdot |\tilde{z}_{i,j}|^2} \cos \varphi_j \quad (3.42)$$

$$\text{Since } f=i: \frac{dx}{dV_f^x} = \frac{dx}{dV_i^x} = 1 - FSF^x + FSF^y \cdot \tan \varphi_f \quad (3.43)$$

$$\text{and } \frac{dy}{dV_f^x} = \frac{dy}{dV_i^x} = \tan \varphi_f \cdot (1 - FSF^x) - FSF^y \quad (3.44)$$

$$\text{Thus, } (3.20) \xrightarrow[(3.43),(3.44)]{(3.21),(3.22)} \rightarrow$$

$$\frac{d|I_{i,j}^f|}{d|V_f|} = \frac{x(1 - FSF^x + FSF^y \cdot \tan \varphi_f) + y(\tan \varphi_f - FSF^y - FSF^x \cdot \tan \varphi_f)}{|I_{i,j}^f| \cdot |\tilde{z}_{i,j}|^2} \cos \varphi_f \quad (3.45)$$

- Calculation of derivatives with respect to voltage angles:

$$\frac{d|I_{i,j}^f|}{d\varphi_i} = \frac{d|I_{i,j}^f|}{dV_i^x} \cdot \frac{dV_i^x}{d\varphi_i} \xrightarrow[(3.37),(3.38)]{(3.22),(3.33)} \rightarrow$$

$$\frac{d|I_{i,j}^f|}{d\varphi_i} = -\frac{x(1 - FSF^x + FSF^y \cdot \tan \varphi_i) + y(\tan \varphi_i (1 - FSF^x) - FSF^y)}{|I_{i,j}^f| \cdot |\tilde{z}_{i,j}|^2} |V_i| \cdot \sin \varphi_i \quad (3.46)$$

$$\frac{d|I_{i,j}^f|}{d\varphi_j} = \frac{d|I_{i,j}^f|}{dV_j^x} \cdot \frac{dV_j^x}{d\varphi_j} \xrightarrow[(3.40),(3.41)]{(3.22),(3.33)} \rightarrow$$

$$\frac{d|I_{i,j}^f|}{d\varphi_j} = \frac{x + y \cdot \tan \varphi_j}{|I_{i,j}^f| \cdot |\tilde{z}_{i,j}|^2} |V_j| \cdot \sin \varphi_j \quad (3.47)$$

$$\begin{aligned} \frac{d|I_{i,j}^f|}{d\varphi_f} &= \frac{d|I_{i,j}^f|}{dV_f^x} \cdot \frac{dV_f^x}{d\varphi_f} \xrightarrow[(3.43),(3.44)]{(3.22),(3.33)} \\ \frac{d|I_{i,j}^f|}{d\varphi_f} &= \frac{x(1 - FSF^x + FSF^y \cdot \tan \varphi_f) + y(\tan \varphi_f(1 - FSF^x) - FSF^y)}{-|I_{i,j}^f| \cdot |\tilde{z}_{i,j}|^2} |V_f| \cdot \sin \varphi_f \end{aligned} \quad (3.48)$$

3.4.1.3 If $f = j$

- Calculation of derivatives with respect to voltage magnitudes:

$$\frac{dx}{dV_j^x} = -1 - FSF^x + FSF^y \cdot \tan \varphi_j \quad (3.49)$$

$$\frac{dy}{dV_j^x} = -\tan \varphi_j (1 + FSF^x) - FSF^y \quad (3.50)$$

$$(3.20) \xrightarrow[(3.49),(3.50)]{(3.21),(3.22)}$$

$$\frac{d|I_{i,j}^f|}{d|V_j|} = \frac{x \cdot (-1 - FSF^x + FSF^y \cdot \tan \varphi_j) - y \cdot (\tan \varphi_j (1 + FSF^x) + FSF^y)}{|I_{i,j}^f| \cdot |\tilde{z}_{i,j}|^2} \cos \varphi_j \quad (3.51)$$

$$\frac{dx}{dV_i^x} = 1 \quad (3.52)$$

$$\frac{dy}{dV_i^x} = \tan \varphi_i \quad (3.53)$$

$$(3.20) \xrightarrow[(3.52),(3.53)]{(3.21),(3.22)} \frac{d|I_{i,j}^f|}{d|V_i|} = \frac{x + y \cdot \tan \varphi_i}{|I_{i,j}^f| \cdot |\tilde{z}_{i,j}|^2} \cos \varphi_i \quad (3.54)$$

$$\text{Since } f=j: \frac{dx}{dV_f^x} = \frac{dx}{dV_j^x} = -1 - FSF^x + FSF^y \cdot \tan \varphi_j \quad (3.55)$$

$$\text{and } \frac{dy}{dV_f^x} = \frac{dy}{dV_j^x} = -\tan \varphi_j - FSF^y - FSF^x \cdot \tan \varphi_j \quad (3.56)$$

$$(3.20) \xrightarrow[(3.55),(3.56)]{(3.21),(3.22)}$$

$$\frac{d|I_{i,j}^f|}{d|V_f|} = \frac{x \cdot (-1 - FSF^x + FSF^y \cdot \tan \varphi_f) - y \cdot (\tan \varphi_f (1 + FSF^x) + FSF^y)}{|I_{i,j}^f| \cdot |\tilde{z}_{i,j}|^2} \cos \varphi_f \quad (3.57)$$

- Calculation of derivatives with respect to voltage angles:

$$\begin{aligned} \frac{d|I_{i,j}^f|}{d\varphi_j} &= \frac{d|I_{i,j}^f|}{dV_j^x} \cdot \frac{dV_j^x}{d\varphi_j} \xrightarrow[(3.49),(3.50)]{(3.22),(3.33)} \\ \frac{d|I_{i,j}^f|}{d\varphi_j} &= - \frac{x(-1 - FFSF^x + FFSF^y \tan \varphi_j) - y(\tan \varphi_j (1 + FFSF^x) + FFSF^y)}{|I_{i,j}^f| \cdot |\tilde{z}_{i,j}|^2} |V_j| \cdot \sin \varphi_j \end{aligned} \quad (3.58)$$

$$\begin{aligned} \frac{d|I_{i,j}^f|}{d\varphi_i} &= \frac{d|I_{i,j}^f|}{dV_i^x} \cdot \frac{dV_i^x}{d\varphi_i} \xrightarrow[(3.52),(3.53)]{(3.22),(3.33)} \\ \frac{d|I_{i,j}^f|}{d\varphi_i} &= - \frac{x + y \cdot \tan \varphi_i}{|I_{i,j}^f| \cdot |\tilde{z}_{i,j}|^2} |V_i| \cdot \sin \varphi_i \end{aligned} \quad (3.59)$$

$$\begin{aligned} \frac{d|I_{i,j}^f|}{d\varphi_f} &= \frac{d|I_{i,j}^f|}{dV_f^x} \cdot \frac{dV_f^x}{d\varphi_f} \xrightarrow[(3.55),(3.56)]{(3.22),(3.33)} \\ \frac{d|I_{i,j}^f|}{d\varphi_f} &= - \frac{x(FFSF^y \cdot \tan \varphi_f - 1 - FFSF^x) - y(\tan \varphi_f (1 + FFSF^x) + FFSF^y)}{-|I_{i,j}^f| \cdot |\tilde{z}_{i,j}|^2} |V_f| \cdot \sin \varphi_f \end{aligned} \quad (3.60)$$

According to (3.3), the derivative of fault currents with respect to buses voltages different than i, j, f is zero. Obviously, the derivative of the magnitude of the fault currents with respect to those voltages is also zero.

3.4.2 Derivatives of fault currents with respect to real and reactive power of generators

If P^G is the real power, Q^G is the reactive power and jY_G the subtransient, transient or steady state admittance of generator G , then:

$$\frac{d|I_{i,j}^f|}{dP^G} = \frac{d|I_{i,j}^f|}{dY_G} \cdot \frac{dY_G}{dS^G} \cdot \frac{dS^G}{dP^G} \quad (3.61)$$

$$\text{and } \frac{d|I_{i,j}^f|}{dQ^G} = \frac{d|I_{i,j}^f|}{dY_G} \cdot \frac{dY_G}{dS^G} \cdot \frac{dS^G}{dP^G} \quad (3.62)$$

$$\frac{d|I_{i,j}^f|}{dY_G} = \dots \text{similar to the calculation of (3.22)} \dots = \frac{1}{|I_{i,j}^f| |\tilde{z}_{i,j}|^2} \left(x \frac{dx}{dY_G} + y \frac{dy}{dY_G} \right) \quad (3.63)$$

$$\frac{dx}{dY_G} = -V_f^x \frac{dFSF^x}{dY_G} + V_f^y \frac{dFSF^y}{dY_G} \quad (3.64)$$

$$\frac{dy}{dY_G} = -V_f^x \frac{dFSF^y}{dY_G} - V_f^y \frac{dFSF^x}{dY_G} \quad (3.65)$$

$$\left\{ \begin{array}{l} \frac{dFSF^x}{dY_G} = R \left(\frac{dFSF}{dY_G} \right) \\ \frac{dFSF^y}{dY_G} = I \left(\frac{dFSF}{dY_G} \right) \end{array} \right. \quad (3.66)$$

$$\left\{ \begin{array}{l} \frac{dFSF^x}{dY_G} = R \left(\frac{dFSF}{dY_G} \right) \\ \frac{dFSF^y}{dY_G} = I \left(\frac{dFSF}{dY_G} \right) \end{array} \right. \quad (3.67)$$

where R and I are the Real and Imaginary parts of a function, respectively, and $\frac{dFSF}{dY_G}$ is unknown and has to be calculated.

A change to generator's admittance $j\Delta Y_G$ is assumed. According to the S-M-W formula, any element κ, λ of the new inverse matrix Z_{bus}' is given by the equation:

$$z_{\kappa,\lambda}' = z_{\kappa,\lambda} - \frac{z_{\kappa,G} \cdot z_{G,\lambda} \cdot j \cdot \Delta Y_G}{1 + z_{G,G} \cdot j \cdot \Delta Y_G} \quad (3.68)$$

$$\text{For } \kappa=i \text{ and } \lambda=f : (3.68) \Rightarrow z_{i,f}' = z_{i,f} - \frac{z_{i,G} \cdot z_{G,f} \cdot j \cdot \Delta Y_G}{1 + z_{G,G} \cdot j \cdot \Delta Y_G} \quad (3.69)$$

$$\text{For } \kappa=j \text{ and } \lambda=f : (3.68) \Rightarrow z_{j,f}' = z_{j,f} - \frac{z_{j,G} \cdot z_{G,f} \cdot j \cdot \Delta Y_G}{1 + z_{G,G} \cdot j \cdot \Delta Y_G} \quad (3.70)$$

$$\text{For } \kappa=f \text{ and } \lambda=f : (3.68) \Rightarrow z_{f,f}' = z_{f,f} - \frac{z_{f,G} \cdot z_{G,f} \cdot j \cdot \Delta Y_G}{1 + z_{G,G} \cdot j \cdot \Delta Y_G} \quad (3.71)$$

If FSF' is the FSF after the change to the generator's admittance, then:

$$FSF' = \frac{z_{i,f}' - z_{j,f}'}{z_{f,f}'} \xrightarrow{(3.69),(3.70),(3.71)} \quad (3.72)$$

$$FSF' = \frac{(A \cdot \mu - k) \cdot \Delta Y_G + A}{(\xi \cdot \mu - \rho) \cdot \Delta Y_G + \xi}$$

where $A = z_{i,f} - z_{j,f}$, $k = (z_{i,G} - z_{j,G}) \cdot z_{G,f} \cdot j$, $\mu = z_{G,G} \cdot j$, $\xi = z_{f,f}$, $\rho = z_{f,G} \cdot z_{G,f} \cdot j$

Using the definition of derivative:

$$\frac{dFSF}{dY_G} = \lim_{\Delta Y_G \rightarrow 0} \frac{FSF' - FSF}{\Delta Y_G} \stackrel{(2.72)}{=} - \frac{k \cdot \xi - A \cdot \rho}{\xi^2} = C \quad (3.73)$$

where κ, ξ, A, ρ are calculated for the current generator set-up (Y_{G1}, Y_{G2}, \dots) , so C is a constant.

$$(3.63) \xrightarrow{(3.64),(3.65)} \xrightarrow{(3.66),(3.67),(3.73)} \quad (3.74)$$

$$\frac{d|I'_{i,j}|}{dY_G} = \frac{x \cdot (-V_f^x \cdot R(C) + V_f^y \cdot I(C)) - y \cdot (V_f^x \cdot I(C) + V_f^y \cdot R(C))}{|I'_{i,j}| \cdot |\tilde{z}_{i,j}|^2}$$

$$Y_G = - \frac{1}{X_G} \stackrel{(3.1)}{=} - \frac{S^G}{f(S^G) \cdot S_b} \quad (3.75)$$

$$\frac{dY_G}{dS^G} \stackrel{(3.75)}{=} \frac{S^G \frac{df(S^G)}{dS^G} - f(S^G)}{S_b [f(S^G)]^2} \quad (3.76)$$

$$\frac{dS^G}{dP^G} = \frac{d(P^G/p.f.)}{dP^G} = \frac{1}{p.f.} \quad (3.77)$$

$$\begin{aligned} \frac{d|I_{i,j}^f|}{dP^G} &\stackrel{(3.1),(3.74)}{=} \stackrel{(3.76),(3.77)}{=} \dots \\ &= \frac{S^G \frac{df(S^G)}{dS^G} - f(S^G)}{S_b [f(S^G)]^2} \frac{x(-V_f^x R(C) + V_f^y I(C)) - y(V_f^x I(C) + V_f^y R(C))}{p.f. |I_{i,j}^f| |\tilde{z}_{i,j}|^2} \end{aligned} \quad (3.78)$$

$$\frac{dS^G}{dQ^G} = \frac{1}{S_b \cdot \sin(\text{acos}(p.f.))} \quad (3.79)$$

$$\begin{aligned} \frac{d|I_{i,j}^f|}{dQ^G} &\stackrel{(3.62),(3.74)}{=} \stackrel{(3.76),(3.79)}{=} \dots \\ &= \frac{S^G \frac{df(S^G)}{dS^G} - f(S^G)}{S_b [f(S^G)]^2} \frac{x(-V_f^x R(C) + V_f^y I(C)) - y(V_f^x I(C) + V_f^y R(C))}{\sin(\text{acos}(p.f.)) |I_{i,j}^f| |\tilde{z}_{i,j}|^2} \end{aligned} \quad (3.80)$$

3.5 Decreasing the number of fault level constraints in capacity allocation

Theoretically, there are as many fault level constraints as the combination of the number of buses which can potentially accommodate a fault and the pairs of fault breaking equipment at the end of each line:

$$n_{FLC} = 2 \cdot n_L \cdot n_B \quad (3.81)$$

where n_{FLC} is the number of fault level constraints, n_B is the number of system buses and n_L is the number of lines. For example, for a small 12-bus-15-line network there are $n_{FLC} = 2 \cdot 12 \cdot 15 = 360$ constraints! In order to reduce the computational burden caused by the large number of additional constraints during the solution of the OPF, a method which identifies the ‘binding’ constraints for the final solution was developed. The number of fault level constraints, which are finally included in the OPF narrows down to a small fraction of its theoretical value. The detailed description of the method follows.

The target is to create a list of ‘active’ fault level constraints, which will contain only the constraints which are binding for the optimum capacity allocation. From all the fault level constraints only the ones in the list will be added in the group of system constraints during the solution of the final OPF. Initially, the list is empty, so a first OPF allocates new capacity

ignoring fault level constraints. Then, a fault level analysis is performed. If no constraints are violated the solution is accepted as the optimum and the method ends. Otherwise, any violated fault level constraints are added to the list of active constraints. OPF reallocates capacity, subject to the list of active constraints and the rest of the system constraints. The process repeats itself until no new fault level constraints are violated. The method was termed Fault Level Constraints Reduction Method (FLCRM). The algorithm is presented in the following flowchart (Figure 3.1).

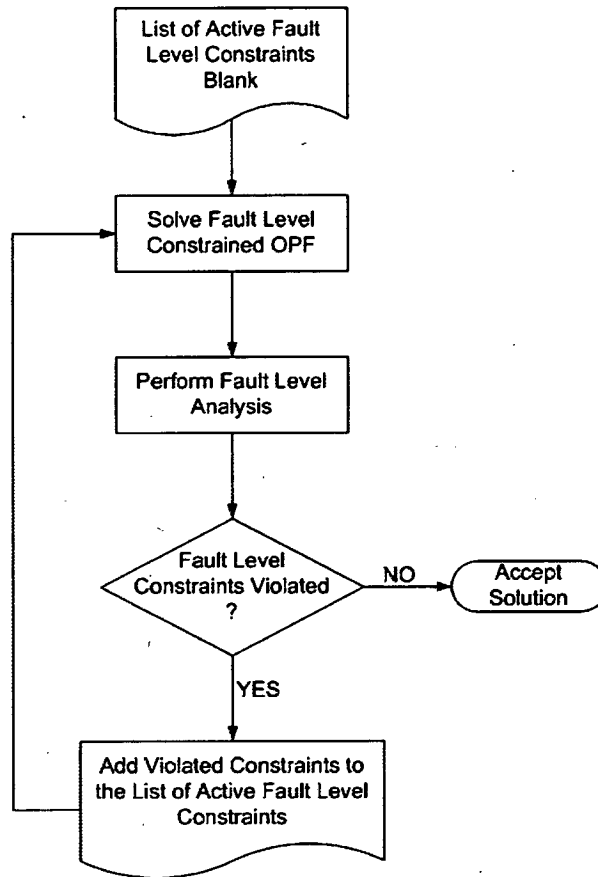


Figure 3.1 Selection of ‘active’ fault level constraints using FLCRM.

3.6 Example

In order to demonstrate the new method (D-FLCOPF) and compare results with the previous approach (FLCOPF) the same test case will be used. New generators and exports/imports to external networks are modelled as in FLCOPF (see Section 2.5.1).

3.6.1 Topology

A 12-bus 15-line network (Figure 3.2) has 3 available CELs at buses 1, 10 and 11. It also has an E/IP to an external network at bus 12. A 15 MW generator is installed on bus 5. It can consume or provide up to 10 MVar of reactive power. The network has a common rated bus voltage level at 33 kV, except for the CEL buses which have a rated voltage of 11 kV and the E/IP bus at 132 kV.

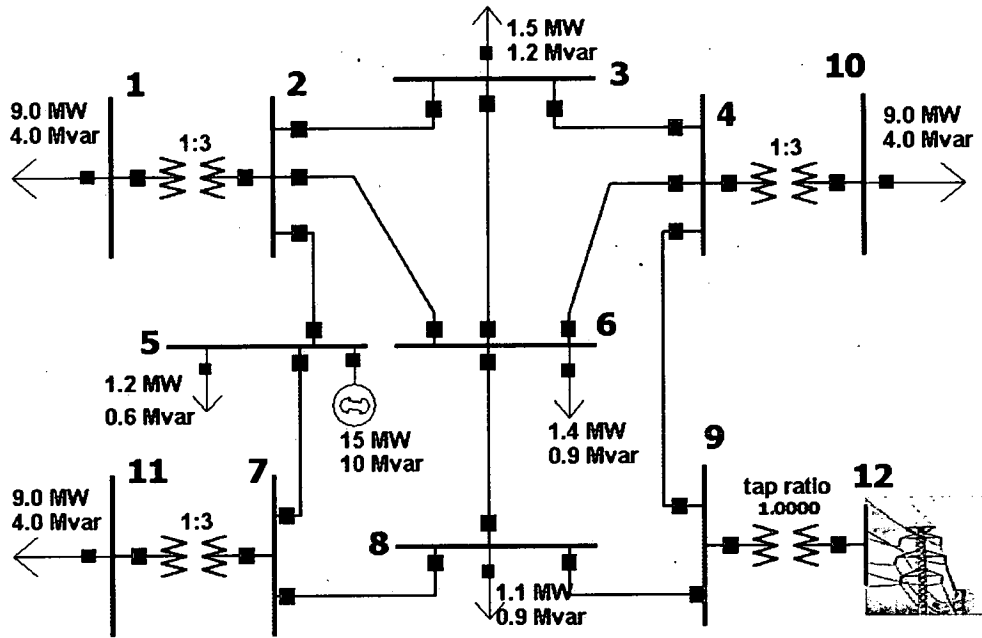


Figure 3.2 The 12-bus 14-line test case.

The CEL buses connect to the network through 30 MVA transformers with fixed taps. The E/IP bus connects through a 90 MVA transformer with automatic tap changer, which regulates the voltage within a $\pm 2\%$ range of the rated voltage at the low voltage side with a $\pm 10\%$ tap range around the nominal tap ratio. The electric characteristics of transformers and lines are presented in Table 3.1.

Type	From bus	To bus	R (p.u.)	X (p.u.)	B (p.u.)	MVA
transformer	1	2	0	0.3	0	30
line	2	3	0.48	0.3	0.0008	unconstrained
line	2	5	0.24	0.15	0.0004	14
line	2	6	0.72	0.45	0.001	unconstrained
line	3	4	0.64	0.4	0.001	unconstrained
line	3	6	0.64	0.4	0.001	unconstrained
line	4	6	0.48	0.3	0.0008	unconstrained
line	4	9	0.66	0.35	0.0009	40
transformer	4	10	0	0.3	0	30
line	5	7	0.688	0.43	0.0006	unconstrained
line	6	8	0.768	0.48	0	unconstrained
line	7	8	0.56	0.35	0.0008	unconstrained
transformer	7	11	0	0.3	0	30
line	8	9	0.768	0.48	0	unconstrained
transformer	9	12	0	0.1	0	90

Table 3.1 Transformer and line characteristics.

Loads consume constant complex power on buses 1, 3, 5, 6, 8, 10 and 11. Table 3.2 demonstrates the electric demand in MW and MVar of the loads.

Bus number	P_d MW	Q_d MVar
1	9	4
3	1.5	1.2
5	1.2	0.6
6	1.4	0.9
8	1.1	0.9
10	9	4
11	9	4

Table 3.2 Demand characteristics.

This network is termed 'local' and the hypothetical network connected through the E/IP as 'external'.

3.6.2 Constraints

Line 2-5 is constrained by a thermal limit of 14 MVA, 4-9 by a thermal limit of 40 MVA, while all other lines are considered to have unlimited capacity. The E/IP is assumed to be capable of exchanging up to 100 MW with the external network without affecting its secure operation. The external network is also capable of providing up to 60 MVar of reactive power to the local network and consuming up to 50 MVar. A hypothetical government policy restricts the maximum allocated capacity to 200 MW at each CEL. Finally, statutory regulations limit bus voltage fluctuations to $\pm 10\%$ around the nominal values. Switchgear is tested only for capacity adequacy, assuming 250 MVA at 11 kV, 1000 MVA at 33 kV and 3500 MVA at 132 kV, which are typical UK ratings.

3.6.3 Assumptions about Capacity Expansion Locations

As in the example used to test FLCOPF, all new generators connected at CELs are assumed to produce power at constant 0.9 lagging power factors. They have an internal subtransient reactance between 15% and 20% on the generator reactance base, so (2.44) gives their p.u. reactance with respect to the size of the new generator. Equation (2.44) is repeated here for convenience:

$$X_{p.u.}''(S^g) = \frac{15 + 5 \cdot \left(1 - e^{\frac{-S^g}{150}}\right)}{S^g} \quad (3.82)$$

3.6.4 Test case 1: no preferences for locations

In the first test case, such cost functions are attached to CELs that no preference is expressed for the allocation of new capacity. This is implemented by applying the same benefit function coefficients (see Table 3.3) for each CEL (specifies (2.11)).

CEL bus	a	b	c
1	0	-20	0
10	0	-20	0
11	0	-20	0

Table 3.3 CEL cost function coefficients when no preferences are expressed.

Table 3.4 presents the cost function coefficients for the E/IP at bus 12 (specifies (2.12)):

E/IP bus	a	b	c
12	0	-20	0

Table 3.4 E/IP cost function coefficients.

3.6.4.1 Results

The FLCRM was performed, in order to add the ‘active’ fault level constraints only in the D-FLCOPF. The initial OPF capacity allocation resulted in excess peak fault currents on the transformers connecting buses 1-2 and 4-10. Only these two fault level constraints were included in the D-FLCOPF algorithm. D-FLCOPF reallocated capacity at CELs in order to reduce fault currents within the switchgear specifications in less than 5 seconds for a 1.7GHz CPU. The new allocation of capacity did not violate any new fault level constraints, so the solution was accepted as final. The results are presented in Table 3.5, together with the initial OPF capacity allocation.

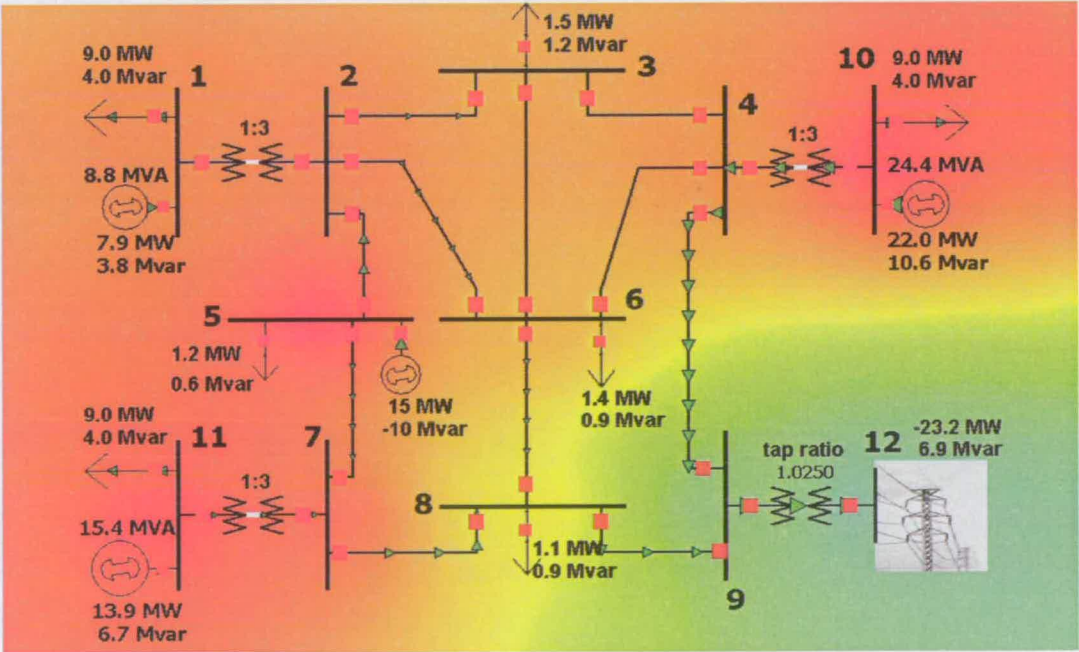
CEL bus	Initial OPF allocation (MVA)	D-FLCOPF reallocation (MVA)
1	8.83	0.00
10	24.44	26.79
11	15.40	19.88
TOTAL	48.68	46.67

Table 3.5 Allocation of generation capacity at CELs.

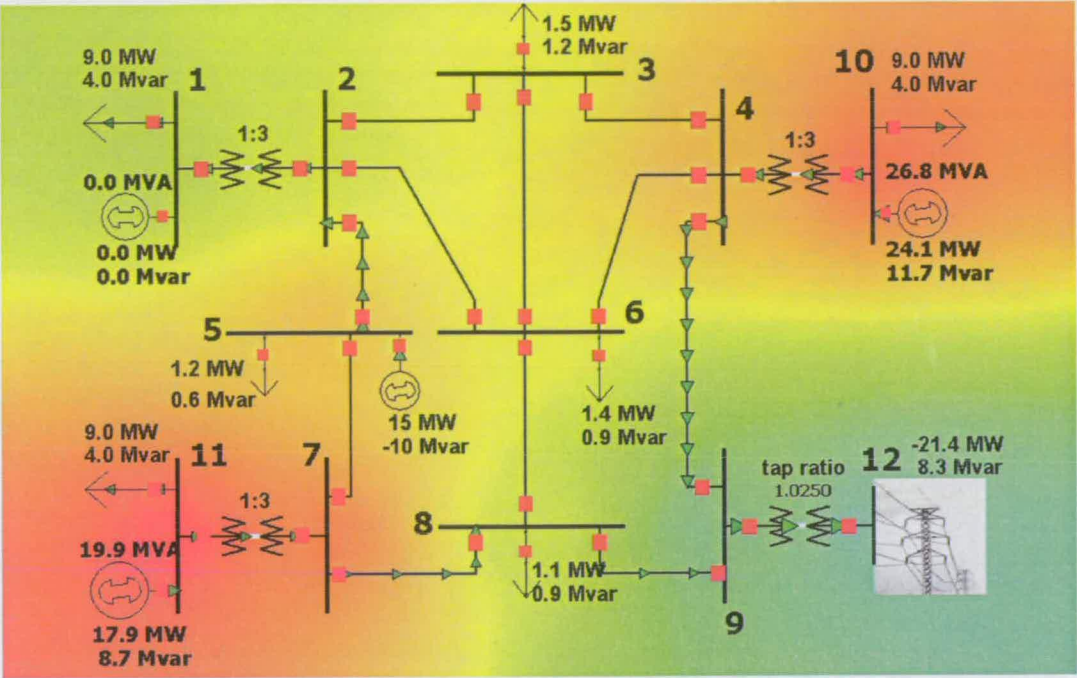
Capacity from CEL at bus 1 was ‘shifted’ to CEL at bus 10 and 11, so the total new capacity was reduced only by $48.68 - 46.67 = 2.01$ MVA. The new optimum respects both OPF and fault constraints. The E/IP was set at an export level of 21.34 MW, while providing the local network with 8.29 MVar of reactive power. Table 3.6 presents the bus voltage patterns of the initial capacity allocation (ignoring fault level constraints) and the D-FLCOPF reallocation. Figure 3.3 recreates both voltage patterns on contour images superimposed on the test case graph.

Bus number	Voltage (p.u.)	
	initial capacity allocation	D-FLCOPF reallocation
1	1.087	1.033
2	1.087	1.045
3	1.078	1.050
4	1.082	1.070
5	1.100	1.067
6	1.074	1.051
7	1.093	1.088
8	1.054	1.045
9	0.998	0.996
10	1.100	1.090
11	1.100	1.100
12	0.980	0.980

Table 3.6 Initial and D-FLCOPF capacity allocation, when there is no preference for any CEL.



(a)



(b)

Figure 3.3 Voltage pattern contours of the initial capacity allocation (a) and the D-FLCOPF reallocation (b), superimposed on the test case graph. No preferences.

Finally, line 2-5 and 4-9 transfer 13.55 MVA and 14.22 MVA, respectively, when all new generators operate at full capacity. The tap changer of the transformer between buses 9 and 12 sets the tap ratio to 1.025, in order to maintain the voltage at bus 9 (0.996 p.u.) near to rated.

3.6.5 Test case 2 : preference for specific CEL

In the second test case, such cost functions are attached to CELs that a preference is expressed for the allocation of new capacity at bus 1. Table 3.7 contains the cost function coefficients for each CEL.

CEL bus	a	b	c
1	0	-30	0
10	0	-20	0
11	0	-20	0

Table 3.7 CEL cost function coefficients, expressing a preference for bus 1.

Table 3.8 presents the cost function coefficients for the E/IP at bus 12.

E/IP bus	a	b	c
12	0	-20	0

Table 3.8 E/IP cost function coefficients.

3.6.5.1 Results

Again, The FLCRM was performed in order to add the ‘active’ fault level constraints in the D-FLCOPF. The initial OPF capacity allocation resulted in excess peak fault currents on the transformers connecting buses 1-2 and 10-4. Only this fault level constraints were included in the D-FLCOPF algorithm. D-FLCOPF reallocated capacity at CELs in order to reduce fault currents within the switchgear specifications in about 6 seconds for a 1.7GHz CPU. The new allocation of capacity did not violate any new fault level constraints, so the solution was accepted as final. The results are presented in Table 3.9, together with the initial OPF capacity allocation.

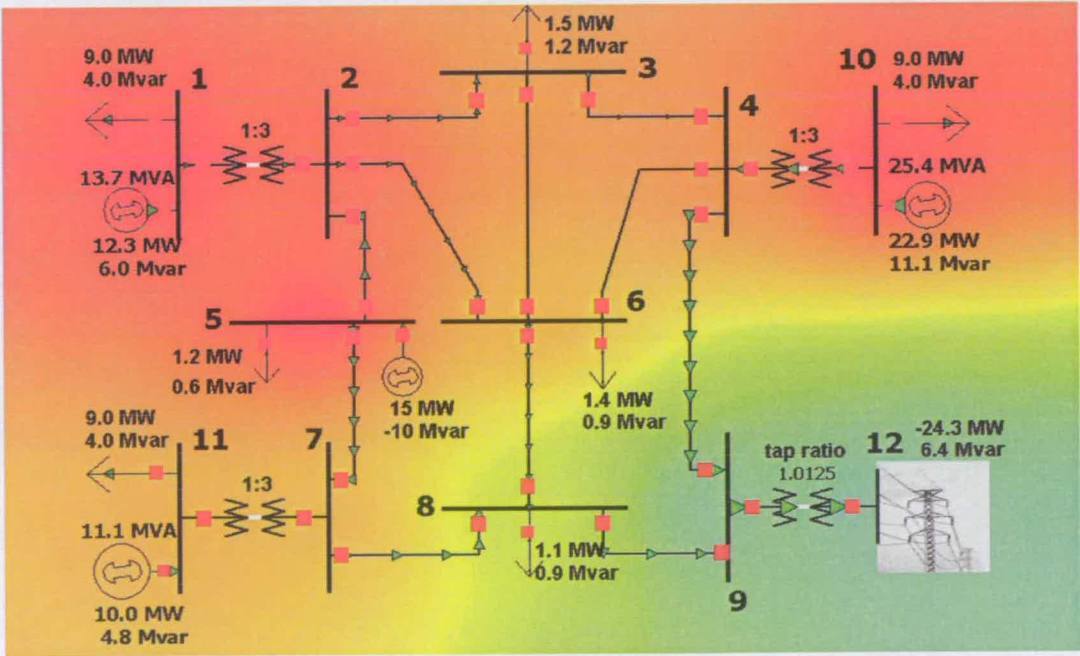
CEL bus	Initial OPF allocation (MVA)	D-FLCOPF reallocation (MVA)
1	13.66	27.00
10	25.44	12.72
11	11.10	0.00
TOTAL	50.20	39.72

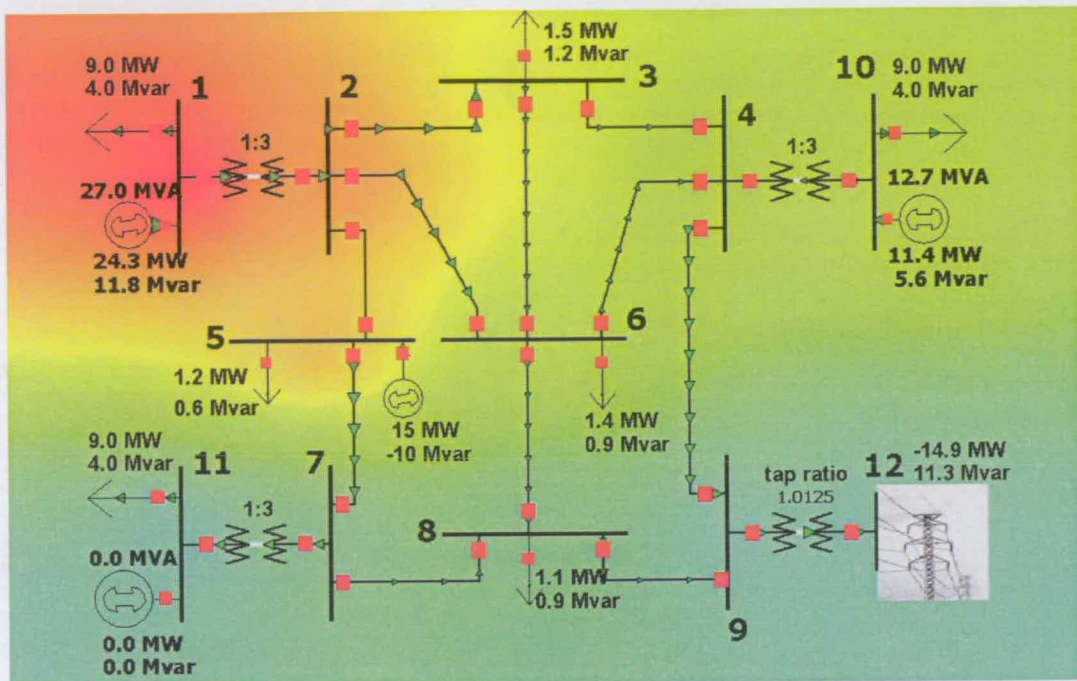
Table 3.9 Allocation of generation capacity at CELs.

Capacity from CEL at bus 10 and 11 was ‘shifted’ to CEL at bus 1, so the total new capacity was reduced by $50.20 - 39.72 = 10.48$ MVA. The new optimum respects both OPF and fault constraints. The E/IP was set at an export level of 14.75 MW, while providing the local network with 11.21 MVar of reactive power. Table 3.10 presents the bus voltage patterns of the initial capacity allocation (ignoring fault level constraints) and the FLCOPF reallocation. Figure 3.4 recreates both voltage patterns on contour images superimposed on the test case graph.

Bus number	Voltage (p.u.)	
	initial capacity allocation	D-FLCOPF reallocation
1	1.100	1.100
2	1.095	1.080
3	1.080	1.046
4	1.081	1.029
5	1.100	1.068
6	1.073	1.034
7	1.072	0.991
8	1.042	0.996
9	0.986	0.981
10	1.100	1.033
11	1.074	0.979
12	0.980	0.980

Table 3.10 Bus voltage pattern of the initial and D-FLCOPF capacity allocation, when there is a preference for the CEL at bus 1.





(b)

Figure 3.4 Voltage pattern contours of the initial capacity allocation (a) and the D-FLCOPF reallocation (b), superimposed on the test case graph. Preference for CEL 1.

Finally, line 2-5 and 4-9 transfer 10.71 MVA and 11.34 MVA respectively, if all new generators operate at full capacity. The tap changer of the transformer between buses 9 and 12 sets the tap ratio to 1.0125, in order to maintain the voltage at bus 9 (0.981 p.u.) near to rated.

3.6.6 Analysis of results

Table 3.11 demonstrates how the capacity shifts in the second case from the other CELs to CEL at bus 1, because it has a cost function with higher coefficients. It also includes the total capacity allocated in each case and the real power exported to the E/IP at bus 12.

CEL bus	No allocation preferences	Allocation preference to CEL at bus 1
1	0.00 MVA	27.00 MVA
10	26.79 MVA	12.72 MVA
11	19.88 MVA	0.00 MVA
Total	46.67 MVA	39.72 MVA
E/IP at bus 12	21.34 MW	14.75 MW

Table 3.11 Capacity allocation and transfers to E/IP in the two test cases.

The inferences drawn from the data above are similar to the ones for FLCOPF in Section 2.8.7. When there are no preferences, the allocation mechanism results in the maximum possible total new capacity in order to maximise the overall benefit. In the second case, the reduction of total new capacity is connected to the effect preferences have on the OPF target function (see eq. 1.25). This case favours the allocation capacity at the first CEL and this works against the allocation over the other CELs and the total capacity. In Table 3.12, the total benefits for the two test cases are calculated.

	No allocation preferences			Allocation preference to CEL at bus 1		
CEL bus	MW allocated $P = \cos \varphi \cdot S$	Benefit/MW	Benefit	MW allocated $P = \cos \varphi \cdot S$	Benefit/MW	Benefit
1	0.00	20	0.0	24.30	30	729.0
10	24.11	20	482.2	11.45	20	229.0
11	17.89	20	357.8	0.00	20	0.0
E/IP at bus 12	21.34	20	426.8	14.75	20	295.0
TOTAL	→		1266.8	→		1253.0

Table 3.12 Calculation of total benefits for both test cases.

Even though, the total new capacity was reduced by $46.67-39.72=6.95$ MVA due to the existence of the allocation preference on CEL 1, the total benefit remained approximately the same. Evidently, when preferences exist there is a trade-off between higher allocation of capacity at the 'preferred' CELs and total new capacity.

3.7 Chapter summary

This Chapter presents a new method (D-FLCOPF) for the incorporation of FLCs in the OPF as a tool for assessing the capacity of a network to absorb new generation. No new variables are introduced in the OPF formulation and FLCs are converted to simple non-linear (inequality) constraints. Most common OPF-solving engines already have the computational capacity to handle numerous non-linear constraints, such as the ones described by the power balance equations on buses. Therefore, once FLCs are converted to non-linear constraints described by OPF variables, they can be directly introduced to any optimisation process performing the OPF.

Finally, the direct incorporation of FLCs in the OPF constraints allows the optimisation procedure to produce shadow costs for those constraints as well. This was not possible with the previous iterative method (see Chapter 3), since the additional constraints were converted to restrictions on new capacity. As it will be shown in a later Chapter (Chapter 7), these shadow costs can be used as economic signals in a reinforcement planning mechanism of a specific network topology.

4. COMPARISON BETWEEN FLCOPF AND D-FLCOPF

4.1 Introduction

Fault Level Constrained Optimal Power Flow (FLCOPF), developed in Chapter 2, is a 3-step iterative allocation procedure of new capacity, which considers fault level constraints in addition to the traditional system constraints. In the first step, new capacity is allocated to the predefined Capacity Expansion Locations (CELs) without considering fault level constraints. In the next two steps, the new capacity is reduced in order to bring expected fault levels within the specifications of the switchgear equipment. The process is repeated until the allocation respects both system and fault level constraints. In Chapter 3, a mathematical methodology was developed to convert constraints imposed by fault levels to simple non-linear (inequality) constraints described by the existing OPF variables. This conversion permitted the direct introduction of the additional constraints in OPF. The new approach was termed Direct Fault Level Constrained Optimal Power Flow (D-FLCOPF). In this Chapter, the different properties, advantages and disadvantages of D-FLCOPF over its predecessor FLCOPF will be investigated. Which method exploits better the potential of the network to accommodate new capacity? Which one results in higher total benefit? Finally, the extent to which preferences affect the above comparison will be examined.

4.2 Connection capacity

Table 2.6, Table 2.10, Table 3.5, Table 3.9 include the results of the capacity allocation using FLCOPF and D-FLCOPF with and without preferences. Table 2.14 and Table 3.12 present the calculation of the overall benefit (equals the target function value) for each allocation. Table 4.1 presents a summary of all four allocations and the calculated benefits.

	No preference		Preference for CEL bus 1	
CEL bus	FLCOPF	D-FLCOPF	FLCOPF	D-FLCOPF
1	2.2 MVA	0.0 MVA	2.6 MVA	27.0 MVA
10	30.4 MVA	26.8 MVA	30.7 MVA	12.7 MVA
11	13.1 MVA	19.9 MVA	11.7 MVA	0.0 MVA
Total	45.7 MVA	46.7 MVA	45.0 MVA	39.7 MVA
Benefit	1233.8	1266.8	1245.4	1253.0

Table 4.1 Calculation of total benefits for both test cases.

As it has already been discussed in Sections 2.8.7 and 3.6.6 (FLCOPF and D-FLCOPF, respectively), they maximise total new capacity when equal allocation preferences over CELs are expressed. According to Table 4.1, D-FLCOPF allocates more total capacity than FLCOPF by 46.7-45.7=1 MVA. The total benefit is also higher by 1266.8-1233.8=33 units. Evidently, for this example case, D-FLCOPF tracks the potential connection capacity better than its iterative predecessor. The underperformance of FLCOPF is possibly based on two factors: a) the iterative update of the capacity bounds, which reduces capacity allocation stepwise, possibly missing the global optimum and b) the assumption that bus voltage patterns do not change much during the capacity optimisation performed by the Generation Reduction Optimisation Algorithm (GROA) is false (see Section 2.7.5 for details).

4.3 Allocation preferences vs. benefit

In Sections 2.8.7 and 3.6.6, a trade-off between total new capacity and preferences was discovered for the two methods. Indeed, according to Table 4.1 FLCOPF allocates 45.7-45.0=0.7 MVA less when a preference was expressed for CEL 1. Similarly, D-FLCOPF allocates 46.7-39.7=7 MVA less for the same preference. Obviously, total capacity has a looser connection to preferences when the allocation is performed by FLCOPF. On the other hand, the total benefit is expected to increase when a preference is expressed, since the attached marginal benefit is higher for the preferred CEL. This is easily proved with equations (4.1): if the same allocation with the one for no preferences is maintained, then the total benefit must be higher (or at least equal when the allocated capacity at the preferred CEL is zero).

$$\begin{aligned}
 TB_{NoPref.} &= x_1 \cdot MB_1 + x_2 \cdot MB_2 \\
 TB_{Pref.} &= x_1 \cdot MB_1' + x_2 \cdot MB_2 = x_1 \cdot (MB_1 + \Delta MB_1) + x_2 \cdot MB_2 = \dots \\
 &\dots = x_1 \cdot MB_1 + x_2 \cdot MB_2 + x_1 \cdot \Delta MB_1 = TB_{NoPref.} + x_1 \cdot \Delta MB_1 > TB_{NoPref.}
 \end{aligned} \tag{4.1}$$

where x_1 and x_2 are the capacity allocations for CEL 1 and 2, MB_1 and MB_2 are the Marginal Benefits of CEL 1 and 2, ΔMB_1 is the Marginal Benefit increment of CEL 1 due to allocation preference and $TB_{NoPref.}$ and $TB_{Pref.}$ are the Total Benefits with and without preferences, respectively.

The preference for CEL 1 increased the total benefit of the FLCOPF allocation by 1245.4-1233.8=11.6 units, in comparison with the case where no preferences were expressed. However, a similar comparison for D-FLCOPF reveals a decrease in benefit by 1266.8-1253.0=13.8 units. The reduction in total benefit for D-FLCOPF, despite the fact that the

marginal benefit of CEL 1 was raised by $30-20=10 \text{ MW}^{-1}$, has a logical explanation which is derived from the details of the capacity allocation.

According to Table 4.1, when there are no preferences D-FLCOPF maximises total benefit for 0 MVA at CEL 1. In other words, the benefit contribution of CEL 1 is zero, irrespective of the common marginal cost/benefit⁷ attached to the CELs. One of the conclusions in Section 3.6.6 was that when there are no preferences ‘the allocation mechanism results in the maximum possible total new capacity in order to maximise the overall benefit’. This means that maximum total new capacity and benefit are achieved when 0 MVA are allocated to CEL 1. Now, when a higher marginal benefit is attached to CEL 1, D-FLCOPF balances out the loss of benefit from the reduced capacity at the rest of the CELs with the extra benefit gained from the increased capacity at that CEL. Table 4.2 contains the loss of total benefit when new capacity is forced to be allocated at CEL 1 in steps of 1 MVA and no preferences are expressed for any of the CELs. Figure 4.1 presents how the total benefit is decreased with respect to the forced new capacity at CEL 1.

CEL 1 (MVA)	0	1	2	3	4	5	6	7	...
CEL 10 (MVA)	26.8	24.8	22.8	21.1	19.4	17.8	16.3	14.9	...
CEL 11 (MVA)	19.9	19.9	19.9	19.8	19.8	19.7	19.6	19.5	...
Total (MVA)	46.7	45.7	44.7	43.9	43.2	42.5	41.9	41.4	...
Benefit	1266.9	1232.8	1202.2	1174.5	1149.6	1127.0	1106.7	1088.3	...
Loss of benefit	0	34.1	64.7	92.4	117.3	139.9	160.2	178.6	...

Table 4.2 Calculation of loss of benefit when new capacity is allocated at CEL 1.

⁷ In the example cases of the FLCOPF and D-FLCOPF 1st order polynomials were used as cost functions attached to CELs. Therefore, the marginal cost for each CEL is given by a single number. When no preferences are expressed, the cost functions are the same for all CELs.

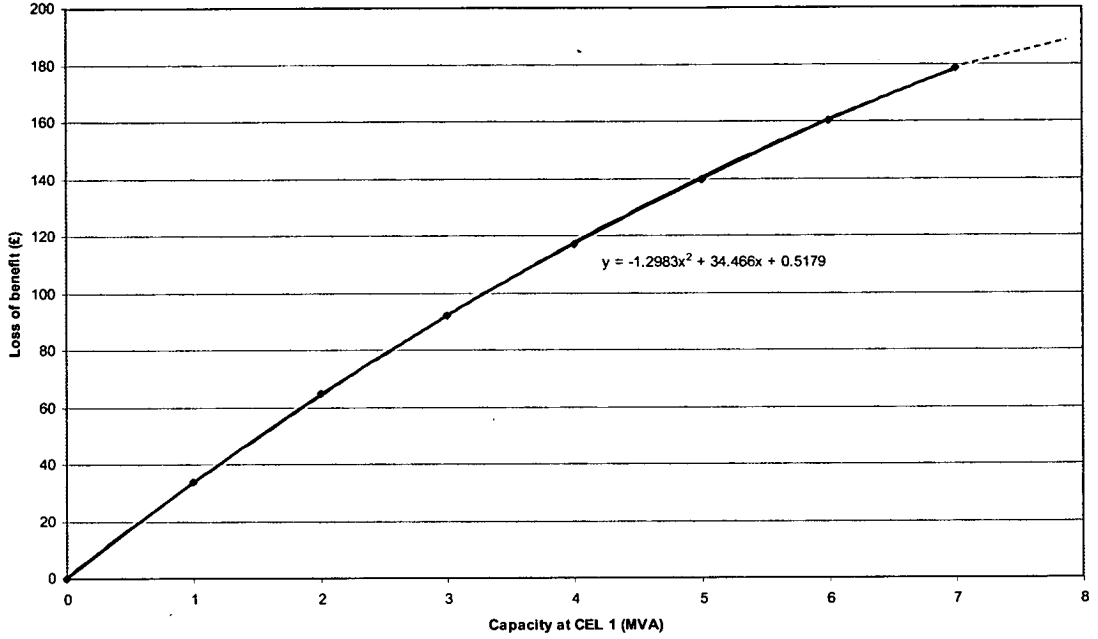


Figure 4.1 Loss of benefit with respect to forced new capacity at CEL 1.

The polynomial trend line approximating the above curve is given by function (4.2).

$$f(x) = -1.2983 \cdot x^2 + 34.466 \cdot x + 0.5179 \quad (4.2)$$

Since $f(26.56) \approx 0$, the loss of benefit is expected to become 0 when approximately 26.56 MVA are allocated to CEL at bus 1. Indeed, D-FLCOPF allocates 27 MVA (see Table 4.1) at CEL 1 to serve the preference for that CEL and satisfy system and fault level constraints.

Besides, even though the total capacity is decreased by $\frac{C_{\text{difference}}}{C_{\text{initial}}} = \frac{7}{46.7} \approx 15\%$ the total benefit remains practically⁸ the same.

4.4 Convergence

Table 4.3 summarises the number of iterations and total time needed from each method to converge (for a 1.7 GHz CPU).

⁸ The benefit decrement of $\frac{\text{Benefit}_{\text{difference}}}{\text{Benefit}_{\text{initial}}} = \frac{13.8}{1266.8} \approx 1\%$ can be interpreted as a precision error, accumulated during the overall D-FLCOPF optimisation procedure.

	No preference		Preference for CEL bus 1	
Attribute	FLCOPF	D-FLCOPF	FLCOPF	D-FLCOPF
Iterations (#)	300	1	680	1
Time (sec)	310	5	720	6

Table 4.3 Summary of convergence attributes of FLCOPF and D-FLCOPF.

Even though, ‘iterations’ serve a different function in each of the two methods (see Figure 4.2) they provide a means of comparison for the speed of convergence. They are independent from the mathematical tools or the computational power used to solve the optimisation problem in each case. However, it must be noticed again that the number of iterations in FLCOPF is strongly influenced by the step used to update the capacity bounds on CELs (see 2.8.4). Conversely, total time in seconds gives a more quantitative scale for the actual convergence time of each algorithm.

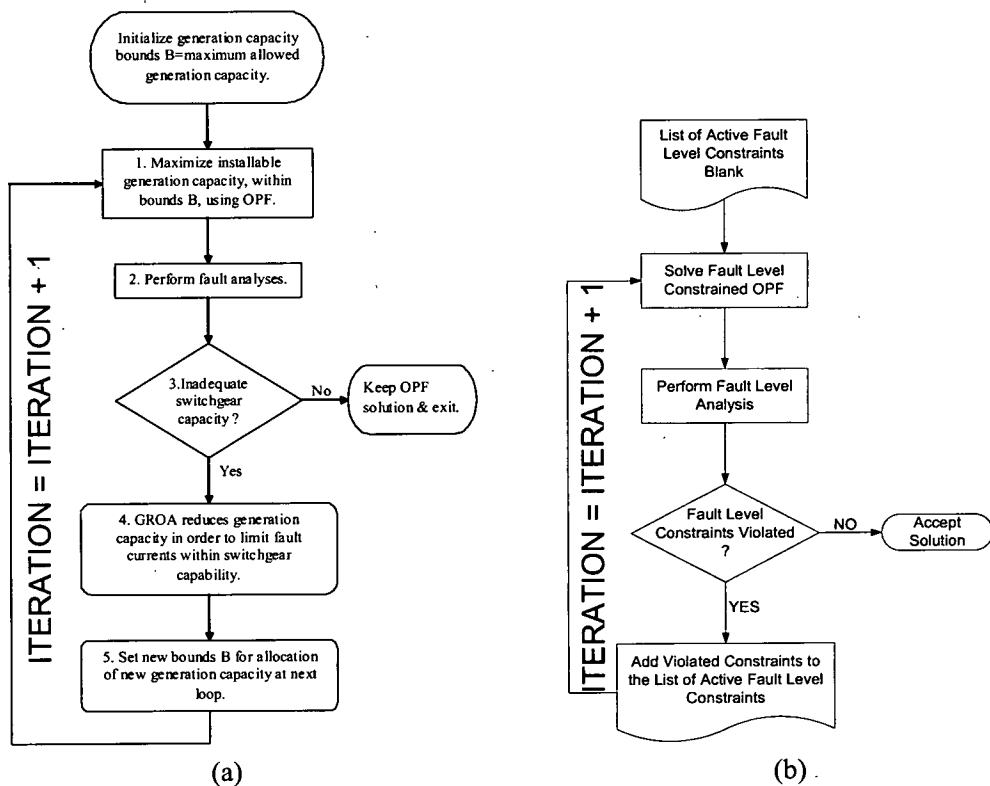


Figure 4.2 ‘Iterations’ of FLCOPF (a) and D-FLCOPF (b).

Obviously, D-FLCOPF converges much faster than FLCOPF in any case. While D-FLCOPF needs only a few seconds and iterations to converge to the final solution, FLCOPF requires several hundreds.

Preferences have a significant impact on the performance of FLCOPF. The allocation preference for CEL 1 doubles the time and the number of iterations. On the contrary, with or without allocation preferences over CELs, D-FLCOPF converges in less than 3 seconds, while the Fault Level Constraints Reduction Method (FLCRM) considers all active fault level constraints in the first iteration.

4.5 Reliability and commercial use

Reliability and creditability are the key features in all successful engineering tools. Practically, any OPF solving engine can be upgraded to D-FLCOPF. The incorporation of fault level constraints is straight forward: they are converted to non-linear inequality constraints and then added to OPF's group of conventional non-linear constraints (e.g. power balance on buses). However, commercially speaking, the outcome is still a new tool, thus difficult to be trusted by engineers, in the beginning at least.

Conversely, the implementation of FLCOPF does not require the redesign of any traditional power engineering tool. Widely available tools can be used to solve the OPF and fault analysis of the capacity allocation process. Engineers have the freedom to choose themselves the implementation of an important part of the overall mechanism. They can choose the software they are more comfortable with or use already.

If non-linear programming, such as Sequential Quadratic Programming, is used to solve the OPF, then the marginal impact of each constraint on the final solution can be graded [67]. This property can be used for the design of an investment planning mechanism. An iterative process would gradually relax the best (for each iteration) value/money investment and OPF would re-allocate capacity. An additional cost should be attached to each marginal constraint relaxation, reflecting the cost of reinforcing the existing infrastructure in reality. Such a mechanism could produce an investment/capacity graph and reinforcement plans of the existing infrastructure. However, D-FLCOPF groups FLCs together with the system constraints. Therefore, the impact of FLCs on capacity allocation is comparable to the one imposed by the rest of the system and network constraints. On the other hand, the iterative process suggested from FLCOPF incorporates FLCs indirectly and investment signals cannot be produced by FLCs, at least at the same scale with system constraints.

4.6 The need for a new capacity planning mechanism

The first-come-first-served policy currently enforced by most Network System Operators (NSOs) in issuing connection permits protects the system from crossing its operating limits, but has no theoretical ground in terms of efficiency of allocation. Inadvertently, it may limit the capability of the network to absorb new generation capacity.

For example, let us assume that three investors request to connect the maximum possible capacity to the CELs at buses 10, 11 and 1 respectively. Their requests are processed on a first-come-first-served basis by the NSO.

This policy was simulated by sequentially relaxing the capacity bounds at the 3 CELs from 0 to 200 MW (as might be dictated by policy). At each turn, D-FLCOPF was used to allocate the maximum possible capacity for the next CEL, simulating the allocated capacity of the previous CELs with “existing generators” operating at those capacities. Of course, since the capacity ‘allocated’ first was fixed for the next allocation, exact values or preferences over locations expressed in the benefit functions attached to the CELs had no impact in the final allocation. The results from this ‘first-come-first-served’ allocation of new capacity are demonstrated in Table 4.4.

Order	CEL bus	Capacity (MVA)
1	10	32.8
2	11	9.9
3	1	0.0
---	Total	42.7

Table 4.4 First-come-first-served capacity allocation.

D-FLCOPF allocates $\frac{46.7-42.7}{42.7}=9.4\%$ more total new capacity (see D-FLCOPF allocation in Table 4.1), than the capacity allocated under the current first-come-first-served NSO policy. Even the less efficient FLCOPF, allocates $\frac{45.7-42.7}{42.7}=7\%$ more capacity than the

one presented in Table 4.4 for the current policy. The above comparisons suggest the following conclusions:

- 1) Manual allocation of capacity is inefficient for networks with more than one candidate location for new capacity. It can undermine the expansion of DG penetration.
- 2) A capacity allocation mechanism is needed to coordinate the installation of new capacity on the network, so that the network operator can harvest the maximum from the capabilities of the existing network to absorb new capacity.

NSOs can use the results of D-FLCOPF or FLCOPF to exploit the potential connection capacity better. For example, the first-come-first-served policy can be replaced with a similar mechanism to the gradual release of capacity for transmission lines (see ‘Annual FTR Auction’ in [68]). Instead of transmission capacity certificates, such a mechanism would gradually release connection certificates for all CELs in parallel. At each round, a certificate represents a fraction of the available capacity at a specific CEL. Financial incentives could direct investment for new capacities (e.g. subsidies) to specific locations, so that certificates for all CELs would be distributed among investors by the end of each round. Of course, the certificates once purchased from the NSO, they could be freely traded between investors. Table 4.5 demonstrates such a release of equal certificates over four rounds.

	Capacity Certificates (in MVA)			
CEL bus	Round 1	Round 2	Round 3	Round 4
1	0	0	0	0
10	6.7	6.7	6.7	6.7
11	5.0	5.0	5.0	5.0
Total released	11.7	23.4	35.1	46.7

Table 4.5 Release of capacity certificates for the D-FLCOPF allocation.

The planning mechanism suggested here is just an oversimplified example of the way a planning mechanism could exploit the D-FLCOPF or FLCOPF results. However, the similarities between transmission capacity release and connection capacity release are interesting: a) they both deal with a ‘scarce good’ in power systems (capacity) and b) buyers are interested in acquiring this good in different locations and time. Thus, the implementation of a mechanism based on transmission capacity release would share similar advantages.

4.7 Chapter summary

When there are no allocation preferences D-FLCOPF exploits the potential connection capacity of the existing network better than FLCOPF. It also delivers capacity allocation plans of higher benefit, than the ones suggested by FLCOPF.

Preferences have a weaker impact on the FLCOPF allocation mechanism. D-FLCOPF favours more the preferred CEL, in return to lower total capacity. On the other hand, in both case preferences do not reduce the total benefit significantly.

Furthermore, FLCOPF needs a significant amount of time to allocate new capacity, even to a small 12-bus-15-line network with only 3 CELs and 1 E/IP. Convergence to the final allocation gets even slower when there is a preference for a specific CEL. Both these elements reduce the commercial viability of the method, when used to allocate new capacity in larger networks with more CELs.

The technical comparison between methodologies in this Chapter suggests that D-FLCOPF is an important improvement for the incorporation of fault level constraints in OPF and the suggested capacity allocation mechanism. However, the iterative procedure of FLCOPF has a significant advantage: the decoupling between OPF from fault levels permits the use of existing professional packages to implement those two basic components. This increases the reliability of the mechanism, but mostly simplifies the implementation of a commercial product. Therefore, FLCOPF probably has as many chances to succeed as the technically superior D-FLCOPF in the market of power engineering tools.

Finally, NSOs can use the allocations of D-FLCOPF or FLCOPF in a capacity planning mechanism that exploits the potential connection capacity better than the current first-come-first-served policy. This Chapter presents such a mechanism, which is similar to the gradual release of transmission capacity through auctioning. Even though, the mechanism suggested here is just an oversimplified example of the way a planning mechanism could exploit the D-FLCOPF or FLCOPF results, the similarities between transmission capacity release and connection capacity release guarantee that they would probably share similar advantages.

5. EXTENSIONS OF THE OPF MODEL FOR CAPACITY ALLOCATION

5.1 Introduction

In the previous Chapters, use of the Optimal Power Flow (OPF) as an allocation tool for new generation capacity was explored. This Chapter examines two extensions of the model used by the OPF in capacity allocation, in order to accommodate generators with intelligent power factor control and reactive power compensation banks.

The new components are again simulated as the output of virtual generators located at the candidate positions at the network. The output of these generators may carry different properties in terms of active and reactive power than the one produced by conventional new capacity, but it still provides us with a measure of their size. Knowing their size, the reactance they add to the existing network can be estimated, hence, their impact on fault levels.

Maintaining the same basic model for these extensions has two major advantages. First, the basic formulation of OPF remains the same and no new variables are added. Second, the common model of virtual generators allows us to convert in a unified manner the size of new investment (whether it is conventional capacity, intelligent generators or capacitor/reactor banks) with the impact it will have on network or Fault Level Constraints (FLCs).

Using the same test case with the previous Chapter, it was shown that the new components can significantly increase the connecting capacity of the network.

5.2 Reactive Power Compensation Banks

Reactive power compensation is usually the most effective way of improving the real power transfer capability of existing networks. Thus, it potentially enhances their capability to supply the increasing demand. To a certain extent, reactive power compensation can be classified as a cheap alternative to new or reinforced transmission lines. A common implementation of reactive power compensation is the installation of shunt capacitors and/or reactors at system buses. High capacitance or reactance is achieved by placing several capacitors in parallel and reactors in series to form Reactive Power Compensation Banks (RPCBs). Capacitors inject reactive power when voltage drops and reactors consume

reactive power when voltage rises, so that bus voltage patterns are regulated within statutory specifications.

The target of the optimisation procedure presented below is to decide the size and location of new RPCBs, so that the network maximises its ability to absorb new generation capacity. A similar approach to the simulation of new generation capacity in OPF has been used to consider the impact of the new devices on power system operation and expected fault currents. Therefore, the final allocation of RPCBs maximises the connecting capacity of the network without violating system constraints or the specifications of switchgear equipment under fault conditions.

5.2.1 Steady-state model

The size (in MVar) of the RPCBs is modelled as the reactive power output of generators with no active power output, located at candidate buses. The size of RPCBs is limited by technical or planning reasons.

$$Q_{\min}^{RPCB} < Q^{RPCB} < Q_{\max}^{RPCB} \quad (5.1)$$

$$P^{RPCB} = 0 \quad (5.2)$$

Positive output represents a capacitor bank, while negative output represents a reactor bank.

5.2.2 Contribution to Fault Levels

The shunt impedance of the new RPCBs decreases the total impedance of the network. Therefore, the bigger the size of the RPCBs the higher the expected fault currents.

The p.u. shunt impedance Z_{RPCB} of a RPCB is calculated as a function of its MVar rating over the system MVA base, simulated in the OPF by the reactive power output Q^{RPCB} of the respective virtual generator and the p.u. voltage V_{RPCB} of the generator's bus:

$$Z_{RPCB} = \frac{|V_{RPCB}|^2}{jQ^{RPCB}} \Leftrightarrow Q^{RPCB} = \frac{|V_{RPCB}|^2}{jZ_{RPCB}} \quad (5.3)$$

Chapter 2 described a detailed expression for fault currents with respect to the bus voltages and the impedance matrix (see (2.25)). According to (5.3), the shunt impedance of a RPCB is a function of the reactive power output of the virtual generator Q^{RPCB} and the magnitude of its terminal voltage $|V_{RPCB}|$. Both are variables in the OPF. Their impact on the expected fault

currents is expressed by the derivatives $\frac{d|I_{i,j}^f|}{dQ^{RPCB}}$ and $\frac{d|I_{i,j}^f|}{d|V_{RPCB}|}$, where $I_{i,j}^f$ is the expected

fault current in line ij for a fault at bus f . The derivatives provide the direction to the optimisation procedure towards the relief of the violated FLCs, with respect to the OPF variables connected with the RPCBs. The calculation of $\frac{d|I_{i,j}^f|}{dQ^{RPCB}}$ is similar to the calculation of $\frac{d|I_{i,j}^f|}{dQ^g}$ for the generators at Capacity Expansion Locations (CELs) in Chapter 3 (see Section 3.4.2):

$$\frac{d|I_{i,j}^f|}{dQ^{RPCB}} = \frac{d|I_{i,j}^f|}{dY^{RPCB}} \cdot \frac{dY^{RPCB}}{dQ^{RPCB}} \quad (5.4)$$

where $jY_{RPCB} = \frac{1}{Z_{RPCB}} \stackrel{(5.3)}{=} \frac{jQ^{RPCB}}{|V_{RPCB}|^2}$ is the shunt admittance of the RPCB.

There is no mathematical distinction between the derivative of the fault current with respect to the shunt admittance of a new generator or RPCB. So, if a RPCB is considered to be located at bus G instead of a generator, then similarly to (2.63):

$$\frac{d|I_{i,j}^f|}{dY_{RPCB}} = \frac{x \cdot (-V_f^x \cdot R(C) + V_f^y \cdot I(C)) - y \cdot (V_f^x \cdot I(C) + V_f^y \cdot R(C))}{|I_{i,j}^f| \cdot |\tilde{z}_{i,j}|^2} \quad (5.5)$$

where $C = -\frac{k \cdot \xi - A \cdot \rho}{\xi^2}$, $A = z_{i,f} - z_{j,f}$ and

$$k = (z_{i,G} - z_{j,G}) \cdot z_{G,f} \cdot j, \mu = z_{G,G} \cdot j, \xi = z_{f,f}, \rho = z_{f,G} \cdot z_{G,f} \cdot j$$

$z_{d,g}$ are the elements at row d and column g of the system's bus impedance matrix $Z_{bus} (= Y_{bus}^{-1})$. $V_i = V_i^x + j \cdot V_i^y$, $V_j = V_j^x + j \cdot V_j^y$ are the bus voltages across line ij with impedance $\tilde{z}_{i,j}$ and $V_f = V_f^x + j \cdot V_f^y$ is the voltage of the faulted bus f analyzed in real and imaginary parts.

$$\frac{dY_{RPCB}}{dQ^{RPCB}} = d \left(\frac{Q^{RPCB}}{|V_{RPCB}|^2} \right) / dQ^{RPCB} = \frac{1}{|V_{RPCB}|^2} \quad (5.6)$$

$$(5.4) \xrightarrow{(5.5)} \xrightarrow{(5.6)} \frac{d|I_{i,j}^f|}{dQ^{RPCB}} = \frac{x \cdot (-V_f^x \cdot R(C) + V_f^y \cdot I(C)) - y \cdot (V_f^x \cdot I(C) + V_f^y \cdot R(C))}{|I_{i,j}^f| \cdot |\tilde{z}_{i,j}|^2 |V_{RPCB}|^2} \quad (5.7)$$

Again, the chain rule will be used to calculate $\frac{d|I_{i,j}^f|}{d|V_{RPCB}|}$:

$$\frac{d|I_{i,j}^f|}{d|V_{RPCB}|} = \frac{d|I_{i,j}^f|}{dQ^{RPCB}} \cdot \frac{dQ^{RPCB}}{d|V_{RPCB}|} \quad (5.8)$$

$$\frac{dQ_{RPCB}}{d|V_{RPCB}|} \stackrel{(5.3)}{=} d \left(\frac{|V_{RPCB}|^2}{jZ_{RPCB}} \right) / d|V_{RPCB}| = \frac{2|V_{RPCB}|}{jZ_{RPCB}} \quad (5.9)$$

$$(5.8) \xrightarrow[(5.9)]{(5.7)} \frac{d|I_{i,j}^f|}{d|V_{RPCB}|} = 2 \frac{x(-V_f^x R(C) + V_f^y I(C)) - y(V_f^x I(C) + V_f^y R(C))}{|I_{i,j}^f| |\tilde{z}_{i,j}|^2 |V_{RPCB}| jZ_{RPCB}} \quad (5.10)$$

Since the connection between new RPCBs and fault currents has been achieved, D-FLCOPF can be expanded to allocate new capacity and RPCBs with respect to both network and FLCs.

5.2.3 Cost model

The cost model allows us to optimise spending on RPCBs. A quadratic cost function is attached to the reactive power output of the virtual generators located at the RPCB candidate location. It simulates the fixed or/and average running cost of an RPCB of respective size Q_{RPCB} , placed at the respective candidate location.

$$C(Q_{RPCB}) = a \cdot (Q_{RPCB})^2 + b \cdot Q_{RPCB} + c \quad (5.11)$$

where $a, b, c > 0$. Different sets of coefficients between cost functions declare preferences for the allocation of new RPCBs capacity between the candidate positions. Preferences could be interpreted as high maintenance cost of some remote candidate locations or civil protests against the expansion of substations in overpopulated urban areas etc.

RPCBs consist of a number of elements (capacitors or reactors), which are combined to provide a high total reactive power. Since they are produced in discrete ratings several sizes need to be combined in order to build a RPCB with a specific total rating. In order to calculate the total cost of an RPCB the sum of costs of its elements has to be calculated. However, each element has a different fixed cost according to each rating. Therefore, the combination of RPCB elements has to be optimised, with the aim of achieving the cheapest possible total fixed cost/MVAr for a specific total rating:

$$C(Q_{RPCB}) = \min \left[\sum_{element} C(Q_{element}) \right] \quad (5.12)$$

The production of the RPCB elements (capacitors or reactors) follows the economy of scale: the higher the rating the lower the fixed cost/MVAr. Thus, an easy way to implement the minimisation procedure of (5.12) is to use as many elements of the highest available⁹ rating as possible and cover the residual RPCB rating by using elements of lower rating. The algorithm below (Figure 5.1) executes this procedure.

i =element rating index.

⁹ Of course lower than the total RPCB rating.

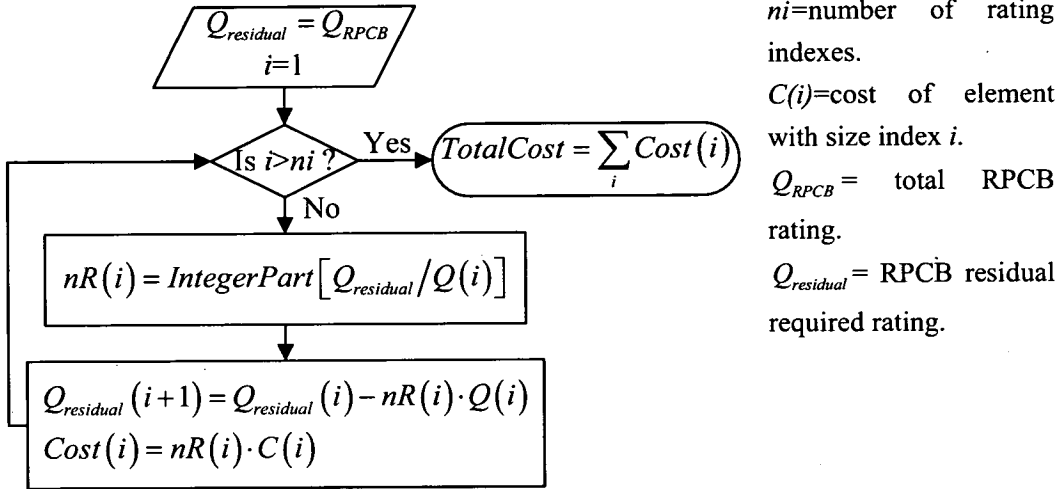


Figure 5.1 Cost optimisation of RPCB elements.

The way the cost functions of the RPCBs are handled determines the preferred investment strategy: a) if the total cost of RPCBs is less than a specific amount, then D-FLCOPF determines the optimal spending of an available budget on new RPCBs in order to increase the potential network capacity and b) if a monetary value is attached to the benefit for the network operator from connecting new generation capacity, then D-FLCOPF maximizes this benefit minus the cost of new RPCBs. So, strategy b) can be used to prepare budgets for regulatory approval.

Strategy a) is implemented as an inequality constraint in the D-FLCOPF formulation:

$$\sum_{RPCB} C(Q^{RPCB}) \leq Budget \quad (5.13)$$

By solving the OPF for different RPCBs budgets a graph presenting new generation capacity over budget amount can be drawn.

Strategy b) is implemented as an additional cost term in the OPF objective function (see Section 2.5.3):

$$(2.22) \xrightarrow{(5.12)} OF_{OPF}(P^g, P^T) = \sum_g C_g(P^g) + \sum_T C_T(P^T) + \sum_{RPCB} C(Q^{RPCB}) \quad (5.14)$$

5.2.4 Example

The same test case with the previous Chapters will be used in order to demonstrate the efficiency of the suggested RPCB allocation method to increase the potential network capacity. Both RPCB investment strategies will be tested: available budget for new RPCBs (strategy A) and b) maximization of the augmented social benefit from new generation

capacity (strategy B). An additional target is to investigate the impact preferences over CELs or RPCBs have on new capacity.

The network is consisted of 12 buses and 15 lines (Figure 5.2). It has 3 available CELs at buses 1, 10 and 11 and an E/IP to an external network at bus 12. A 15 MW generator is installed on bus 5. It can consume or provide up to 10 MVar of reactive power. The network has a common rated bus voltage level at 33 kV, except for the CEL buses which have a rated voltage of 11 kV and the E/IP bus at 132 kV. Candidate locations for new RPCBs are buses 6 and 8. RPCBs are generally not located at generators' buses [69]. For a more detailed description of the network topology, the system and fault level constraints, as well as some assumptions about the CELs please refer to Sections 2.8.1-2.8.3.

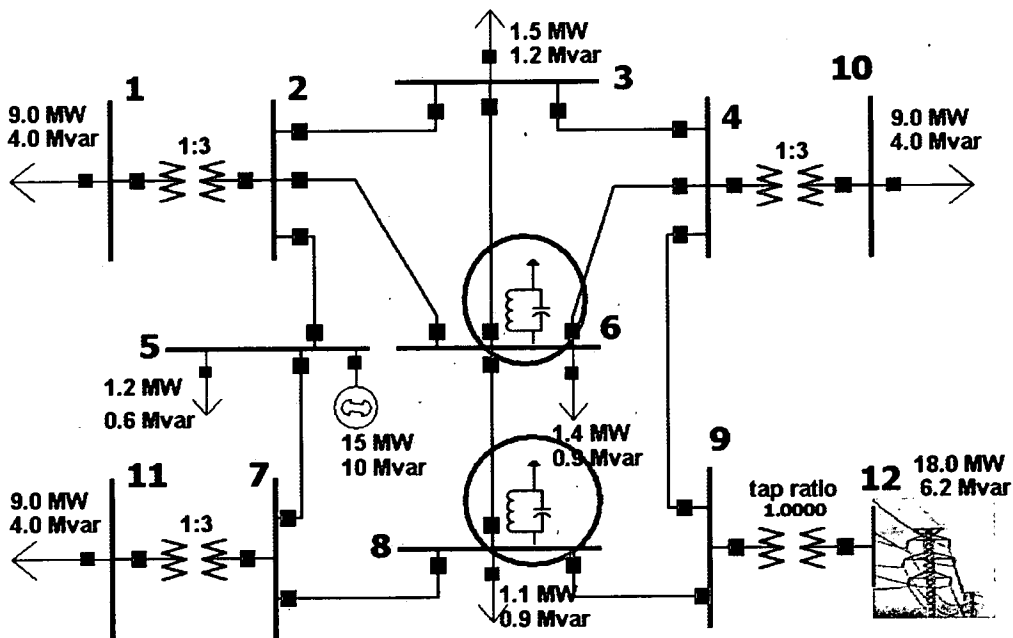


Figure 5.2 The 12-bus 15-line test case with RPCBs at buses 6 and 8.

New generators and exports/imports to external networks are modelled as in FLCOPF (see Section 2.5.1) and D-FLCOPF. New RPCBs are modelled as in Section 5.2.1. Table 5.1 contains the fixed costs of several sizes of MV 3-phase shunt capacitors, provided by a leading supplier [70].

Size (kVar)	150	300	450	600	900	1200
Cost (€)	750	975	1140	1320	1650	2040

Table 5.1 Typical fixed costs of LV capacitors.

The optimisation algorithm described in Figure 5.1 was applied on the collection of capacitors in Table 5.1 to find the minimum cost for capacitor banks of several ratings. The curve in Figure 5.3 describes the connection between the MVar ratings of capacitor banks and their fixed cost. This connection can be approximated by a linear cost of 1700 €/MVar.

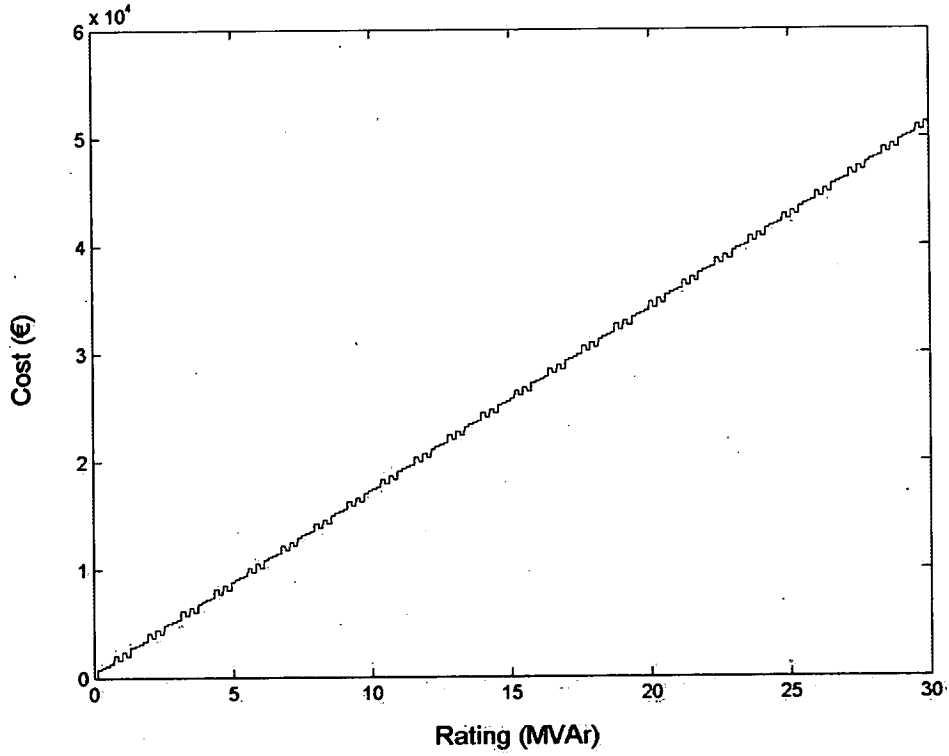


Figure 5.3 Cost of capacitor bank vs. rating, using capacitor costs from Table 5.1.

The cost of inductors is about 3 times higher than the cost of capacitors of the same size (but consuming reactive power) in absolute MVar. Consequently, the inductor banks cost 3 times more. Figure 5.4 presents the cost of RPCBs consisted of capacitors (positive MVar rating) or inductors (negative MVar rating).

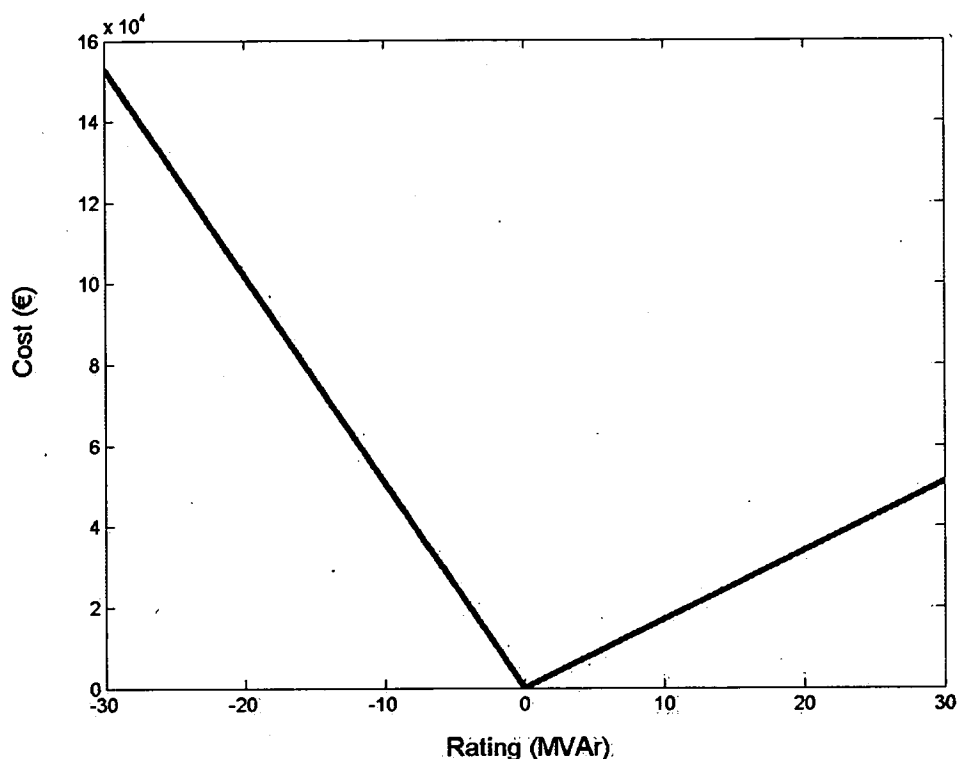


Figure 5.4 Typical cost of LV RPCBs. Positive/negative MVar represent capacitors/reactors.

5.2.4.1 Strategy A

In strategy A, the total cost of RPCBs is restricted by a specific amount, the so-called ‘available budget’. It will be assumed that the cost of the available RPCBs with respect to their MVar rating is given by Figure 5.4. An initial budget of 0 € leads D-FLCOPF to identify the maximum potential connecting capacity of the existing network, without any RPCBs. This is approximately 44 MVA when no preference is expressed for any CEL and 41 MVA when a preference is expressed for the allocation of new capacity at the CEL at bus 1. Generation capacity allocation curves with respect to the size of investment on RPCBs can be produced by increasing the available investment budget in a stepwise manner and letting D-FLCOPF determine the optimum allocation of RPCBs.

If no preference¹⁰ over CELs is expressed, the product is the generation capacity allocation of Figure 5.5 and the RPCBs allocation of Figure 5.6 with respect to an increasing available budget.

¹⁰ Preferences over CELs are expressed by determining the coefficients of the quadratic cost functions attached to the respective CELs, as in Section 2.5.1.

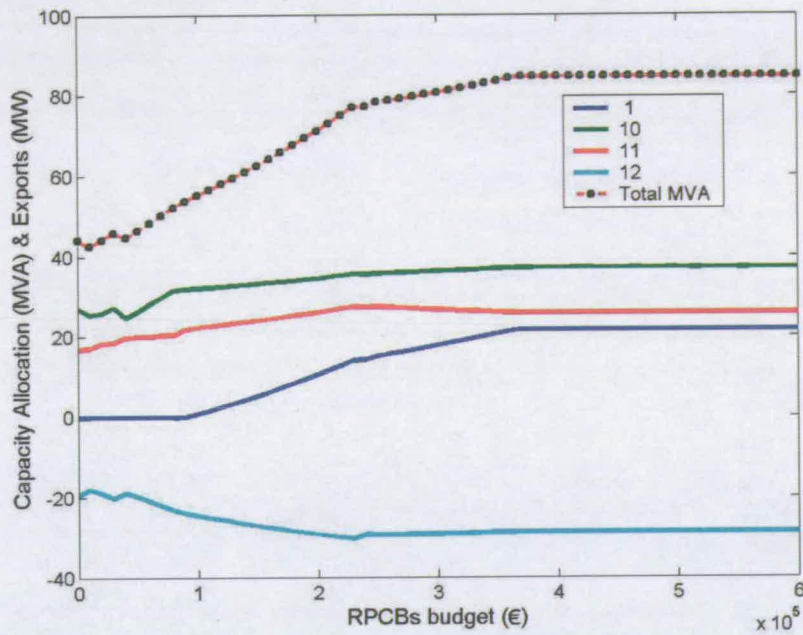


Figure 5.5 Generation capacity allocation at CELs and expected exports at E/IP with respect to the available RPCBs budget. No preferences are expressed over CELs.

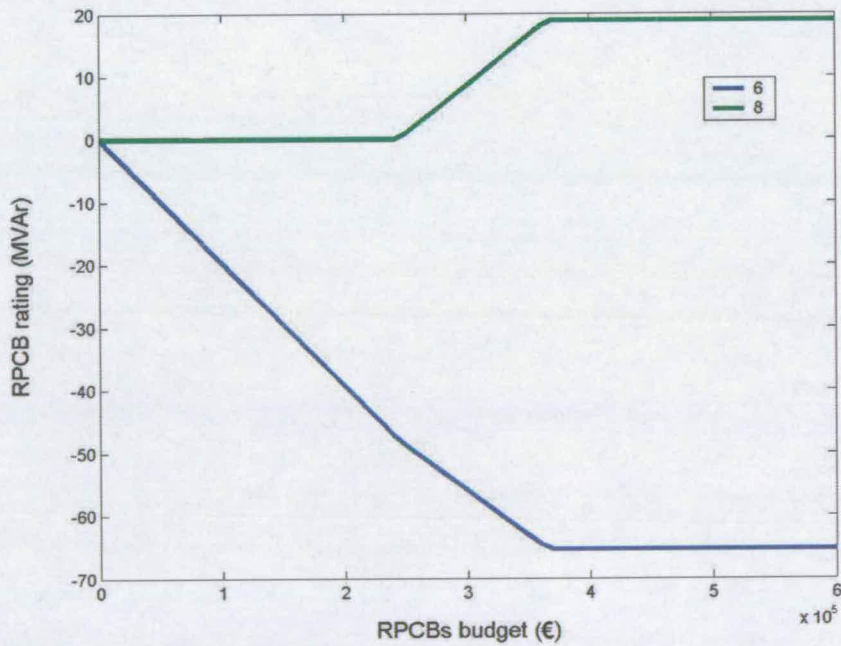


Figure 5.6 RPCBs allocation with respect to the available RPCBs budget. Negative and positive values indicate RPCBs consisted of reactors and capacitors, respectively. No preferences are expressed over CELs.

Similarly, if there is a preference for the CEL at bus 1, then the allocations of new generation capacity and RPCBs are presented in Figure 5.7 and Figure 5.8 respectively.

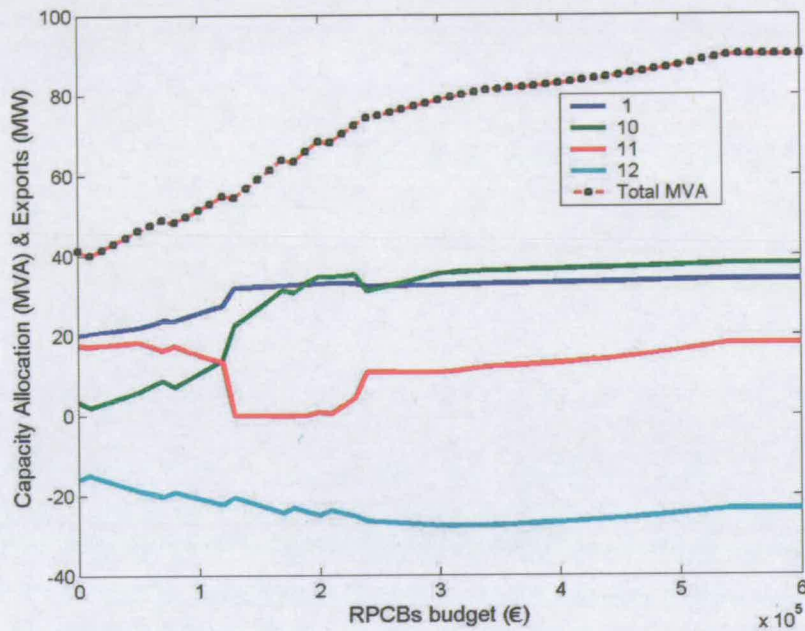


Figure 5.7 Generation capacity allocation at CELs and expected exports at E/IP with respect to the available RPCBs budget. Preference expressed for CEL at bus 1.

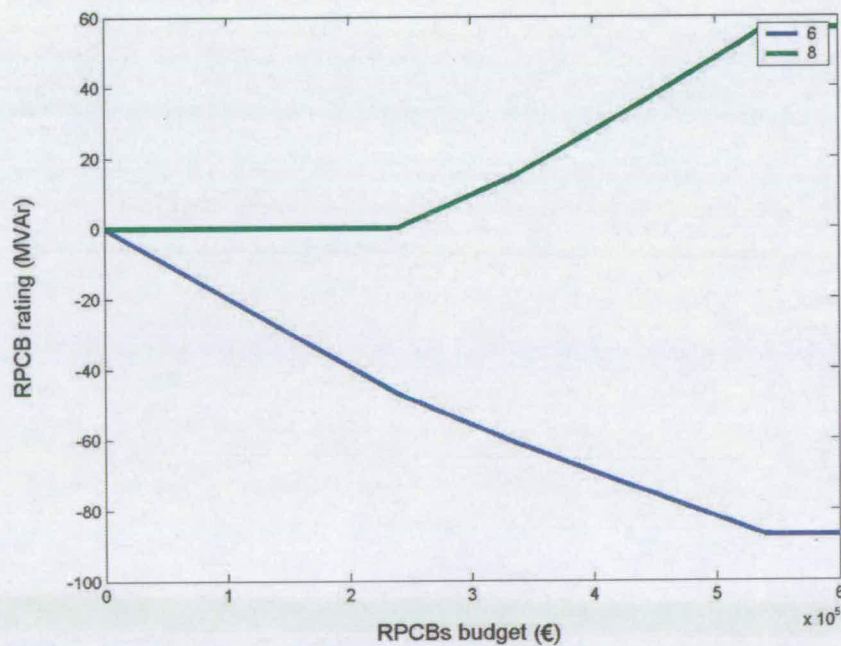


Figure 5.8 RPCBs allocation with respect to the available RPCBs budget. Negative and positive values indicate RPCBs consisted of reactors and capacitors, respectively. Preference expressed for CEL at bus 1.

Figure 5.5 and Figure 5.7 show that there is a maximum generation capacity that can be achieved by investing on RPCBs, approximately 87 MVA with and without preferences for CEL at bus 1. This is due to other network constraints (e.g. line thermal limits) becoming binding at these capacity values, rather than the voltage constraints connected to reactive power balance that RPCBs facilitate.

The small decrements of total capacity at 10,000 €, 30,000 € and 240,000 € when no preferences are expressed and 10,000 €, 80,000 €, 130,000 €, 180,000 € and 210,000 € when preferences are expressed for CEL 1 are results of discrete tap changes of the transformer between buses 9 and 12. Figure 5.9 (no preference) and Figure 5.10 (preference for CEL 1) present the voltage magnitude of the $\pm 2\%$ controlled voltage at bus 9 and the tap ratio of the transformer with respect to the available budget. Clearly, tap changes occur at the budget values for RPCBs mentioned above.

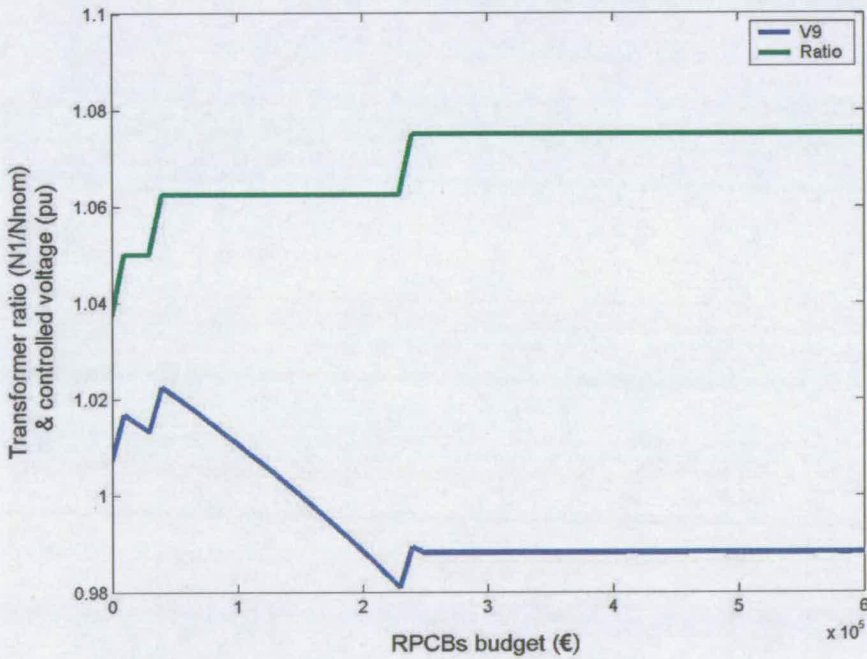


Figure 5.9 Voltage magnitude of the controlled voltage at bus 9 and the tap ratio of the transformer with respect to the available budget. No preferences are expressed over CELs.

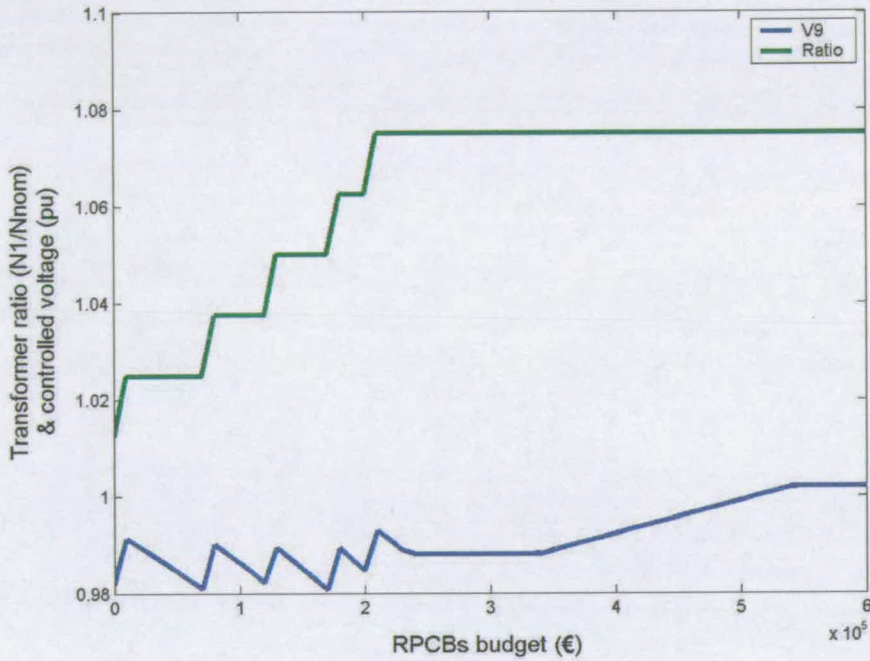


Figure 5.10 Voltage magnitude of the controlled voltage at bus 9 and the tap ratio of the transformer with respect to the available budget. Preference expressed for CEL at bus 1.

5.2.4.2 Strategy B

In strategy B, a monetary value is attached to the benefit for the network operator from connecting new generation capacity. D-FLCOPF maximizes the benefit from new generation capacity minus the cost from new RPCBs. In order to define a monetary value for the benefit from new capacity several assumptions have to be made about the value of new generation for the network operator. For example, electricity regulatory authorities have acknowledged the positive effect of generation connected to distribution networks. Therefore, they have started providing monetary incentives to distribution network operators in order to encourage them to connect small-scale generation to their networks [71]. Here, a monetary benefit of 567 €/year will be arbitrarily assumed for each MW of new generation capacity that the network operator connects to the network.

Now, the connection between the MVar ratings of capacitor banks and their fixed cost (consisted of capacitors with costs as in Table 5.1) can be approximated by a marginal cost of 1700 €/MVar. If capacitors have a life expectancy of 10 years and placement, maintenance and running costs are neglected, the cost averages to 170 €/MVar. Since a marginal equivalent benefit of 20 has been attached to all generators when no preferences are expressed, according to Table 2.4, then a relevant cost to the RPCBs has to be attached equal to:

$$\begin{aligned} 567 \text{ €/MWyear} & \rightarrow 20 \text{ social benefit from new generation capacity} \\ 170 \text{ €/MVAryear} & \rightarrow ? = \frac{170 \cdot 20}{567} \cong 6 \text{ social cost from new capacitor banks} \end{aligned} \quad (5.15)$$

Obviously, having assumed a three times higher fixed cost for reactor banks, their social cost will be 3 times higher.

The efficiency of the RPCB allocation mechanism using strategy B will be examined under several scenarios. Each scenario is determined by the marginal social benefit/cost considered for each CEL/RPCB candidate location. A higher social benefit or lower cost among CELs and RPCBs, respectively, determines preferences. Deviations from the values calculated above as marginal costs (-20 for CELs and 6 for RPCBs) represent the preferences of the network operator over specific locations. For instance, these deviations could be subsidies or taxes for the installation of new capacity at specific locations. In terms of the OPF formulation, the existence or lack of preferences is expressed via the coefficients a, b, c of the quadratic cost functions attached to the respective virtual generators, as it was explained in Sections 2.5.1 and 5.2.1. Table 5.2 presents the scenarios under which strategy B will be tested:

	Scenario 1			Scenario 2			Scenario 3			Scenario 4			Scenario 5			Scenario 6		
type/bus	a	b	c	a	b	c	a	b	c	a	b	c	a	b	c	a	b	c
CEL/1	0	-20	0	0	-20	0	0	-20	0	0	-35	0	0	-35	0	0	-35	0
CEL/10	0	-20	0	0	-20	0	0	-20	0	0	-20	0	0	-20	0	0	-20	0
CEL/11	0	-20	0	0	-20	0	0	-20	0	0	-20	0	0	-20	0	0	-20	0
EIP/12	0	-20	0	0	-20	0	0	-20	0	0	-20	0	0	-20	0	0	-20	0
RPCB/6	0	6	0	0	4	0	0	6	0	0	6	0	0	4	0	0	6	0
RPCB/8	0	6	0	0	6	0	0	4	0	0	6	0	0	6	0	0	4	0

Table 5.2 Scenarios of preferences under which Strategy B will be tested.

Scenario 1 describes the case where no preferences are expressed for either CELs or RPCB candidate locations. Scenarios 2-3 describe cases where there is no preference expressed for any CEL, but there is a preference for the allocation of higher RPCB ratings at either bus 6 or bus 8. In scenario 4, a preference is expressed for the allocation of new generation capacity at bus 1. Scenarios 5-6 describe cases where there are preferences expressed for both new capacity at CEL 1 and the allocation of higher RPCB ratings at either bus 6 or bus 8. The allocation results of D-FLCOPF for each scenario are presented in Table 5.3.

type/bus	Scenario 1	Scenario 2	Scenario 3	Scenario 4	Scenario 5	Scenario 6
CEL/1	0	14.8 MVA	0	33.0 MVA	33.0 MVA	33.2 MVA
CEL/10	31.4 MVA	35.6 MVA	31.6 MVA	35.2 MVA	35.2 MVA	34.4 MVA
CEL/11	17.8 MVA	27.6 MVA	19.9 MVA	5.4 MVA	5.4 MVA	0
EIP/12	-23.0 MW	-29.4 MW	-24.2 MW	-25.8 MW	-25.8 MW	-22.9 MW
RPCB/6	-3.1 MVar	-47.9 MVar	0	-45.9 MVar	-45.9 MVar	-29.5 MVar
RPCB/8	0	0	-7.7 MVar	0 MVar	0 MVar	-15.2 MVar
Total new capacity	49.2 MVA	78.0 MVA	51.5 MVA	73.6 MVA	73.6 MVA	67.6 MVA

Table 5.3 D-FLCOPF allocation results for the RPCBs test case.

Scenarios 2, 3, 5, 6, which describe cases where there are preferences for one of the RPCB candidate locations, result in a higher RPCB rating at these locations in comparison with scenarios 1 and 4. Scenarios 4 and 5 result in the same allocation of new capacity and RPCBs. This means that the preference for higher RPCB rating at bus 6 has no impact on the final solution. The reason is that the preference for the allocation of new capacity at bus 1 dominates and results in the highest possible rating of the RPCB at bus 6. Therefore, whether there is a preference for that RPCB candidate location or not does not affect the solution.

5.2.5 Limitations

At this point, it is important to be noted that there is no provision in the objective function of the above optimizations for the minimization of losses or handling of reactive power. The only objective is the MW maximization of generation capacity. Therefore, it is possible that the solutions actually reflect a competition between RPCBs and new generators as sources or sinks of reactive power. The result is great amounts of reactive power produced at one point and consumed at another, which may be rather distant. In other words, the current method is probably inefficient in terms of reactive power management, which is one of the fundamental targets of network planners. Further research is needed towards the incorporation of those factors in order to complete the suggested approach as a more realistic application.

5.3 Alternative voltage control of distributed generators

Distribution Network Operators (DNOs) are generally reluctant to allow any operation by independent generators, which could potentially disrupt the passive role of the distribution network to supply demand. Specifically, Distributed Generators (DGs) are not permitted to perform Automatic Voltage Regulation (AVR), an inherent feature of synchronous generators to regulate the terminal bus voltage by adjusting their reactive power output, as it may destabilize the automatic load tap changers of distribution transformers. However, Section 2.5.2 illustrated an additional technical reason why DGs do not operate in AVR mode. If a small generator with AVR control is connected to a utility bus which suffers from voltage drops, it has to inject great amounts of reactive power in order to raise the bus voltage. This may result in high field currents and overheating for the generator, which would trigger protection and disconnect the generator from the network. For those reasons, in most distributed generation applications the generators do not have AVR control.

DGs usually operate in Power Factor Control (PFC) mode. They produce proportional amounts of active and reactive power in order to maintain constant Power Factor (PF) at all

times. PFC results in much lower field currents than AVR under voltage drops, therefore reduces thermal stresses on the generator [72].

Unfortunately, PFC has an adverse effect on the generator's terminal bus voltage. The terminal p.u. voltage change ΔV of a radial feeder is approximated by the equation:

$$\Delta V = R \cdot P + X \cdot Q \quad (5.16)$$

where $R+jX$ is the line impedance and P, Q the active and reactive power produced by the DG. When P increases V rises. In PFC mode P/Q is maintained constant, so when P increases Q follows and V increases even further! Conversely, when P decreases, Q decreases as well, leading to further voltage drop. Reference [3] has identified the rise of voltages as one of the major impacts of the connection of new DGs on the network. This statement was confirmed with the results of the test cases in Chapters 2 and 3, where new generators have been assumed to operate in PFC mode. The amount of new capacity at some CELs was practically restricted by the amount of reactive power the generator could inject into the bus without violating the maximum permitted voltage (1.1 p.u.), just to maintain constant PF.

In equation (5.16), if Q was allowed to compensate for the voltage rise or drop P creates to the feeder by adjusting to the opposite direction (with P), then V could be maintained within statutory limits, even for higher P values. Of course, such a method presupposes that the DNOs will have to relax their directions to DGs for strict PFC.

5.3.1 Automatic Voltage / Power Factor Control

Reference [73] suggests a voltage control method for DGs, which assumes a more flexible directive from DNOs for the voltage control by DGs. The authors' target was to develop a voltage control method capable of keeping the DGs online during light load or heavy load conditions by combining the advantages of AVR and PFC. The method was termed Automatic Voltage / Power Factor Control (AVPFC) and it relaxes the PFC when voltage approaches the statutory limits. When voltage approaches the statutory limits V_{\min} or V_{\max} the PFC is deactivated and the DG adjusts the production of reactive power to support voltage. The generator decreases the P/Q ratio when voltage drops at a critical level V_{\min}^{PFC} and increases P/Q ratio when voltage reaches a threshold V_{\max}^{PFC} . Obviously, when the ratio P/Q changes, the PF changes and has to be restricted between the minimum and maximum operating power factors PF_{\min} and PF_{\max} respectively. Figure 5.11 presents the voltage control region of the AVPFC. The generator operates on the thick, dashed line.

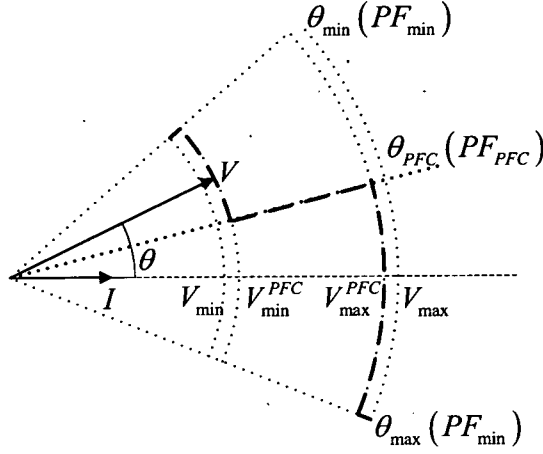


Figure 5.11 AVPFC response.

5.3.2 Central Voltage Control

Theoretically, voltage control of the LV system buses can be achieved centrally, in a similar manner to the HV grid, through active and reactive power dispatch of the generators. The technology in telecommunications is mature enough to provide cheap, but reliable solutions for the remote control of small-scale generation. Two possible central voltage control methods have been identified, according to the level of administration the DNO may decide to enforce over DGs:

1. Central Voltage Control (CVC), where the DNO has absolute control of the real and reactive power output of the DG at all times. DGs which operate under this control scheme were termed CVC-Gens.
2. Emergency Central Voltage Control (ECVC), where the DNO takes over the control of real and reactive power output of the DG when its voltage output rises above or below a critical value. During normal operation DGs perform PFC. DGs which operate under this control scheme were termed ECVC-Gens.

5.3.3 Steady-state behaviour

DG capacity is simulated with the real power output P^g of virtual generators placed at the CELs. The size of DGs may be limited by the available technology, environmental or political reasons to P_{\max}^g :

$$0 \leq P^g \leq P_{\max}^g \quad (5.17)$$

In order to examine the impact each voltage control scheme has on network capacity using the OPF, the behavior of DGs implementing those schemes during steady-state operation has to be estimated.

The main difference in the OPF formulation between DGs operated under the current voltage control scheme (PFC) and Intelli-Gens or CVC-Gens/ECVC-Gens is that the PF constraint (1.20) is relaxed when the voltage drops or rises beyond a critical value. Since the focus is on capacity planning it is logical to expect that new capacity will only raise voltage levels. Thus, in order to simplify analysis it will be assumed that the PF constraint is relaxed only when the generator's voltage V_G rises to a critical value $V_{threshold}$. In addition, in order to consider leading and lagging PFs the angle $\theta_G = \text{sign}(PF) \cdot \cos^{-1}(PF)$ will be constrained instead of directly restricting the PF, where $\text{sign}(PF)$ is positive for lagging and negative for leading PF.

Finally, the minimum PF_{\min} and maximum PF_{\max} operating PFs are roughly the same for various sizes of DGs. Therefore, it can be presumed that PF_{\min} , θ_{\min} , PF_{\max} , θ_{\max} are common for all new DGs. Furthermore, PF_{\max} is usually the rated¹¹ PF, so it is usually the target PF_{PFC} of PFC. Both these assumptions can be described in the OPF formulation by the following constraints for the virtual generators at the CELs:

$$\begin{aligned} PF_{\min} < PF_G < PF_{\max} &\Rightarrow \theta_{\min} < \theta_G < \theta_{\max} \\ \text{and } PF_{\max} = PF_{PFC} &\Rightarrow \theta_{\max} = \theta_{PFC} \end{aligned} \quad (5.18)$$

5.3.3.1 Intelli-Gens

The voltage control strategy of Intelli-Gens is described by the curve in the θ_G vs. V_G graph in Figure 5.12. In practice, a hysteresis loop is designed around $V_{threshold}$ in the control circuit of the generator's field, with the task of prohibiting oscillations between θ_{PFC} and θ_{\min} . However, the effect of hysteresis in steady-state operation is insignificant, so the mathematical description of the strategy can be approximated with a single curve.

¹¹ The DG produces rated power at this PF.

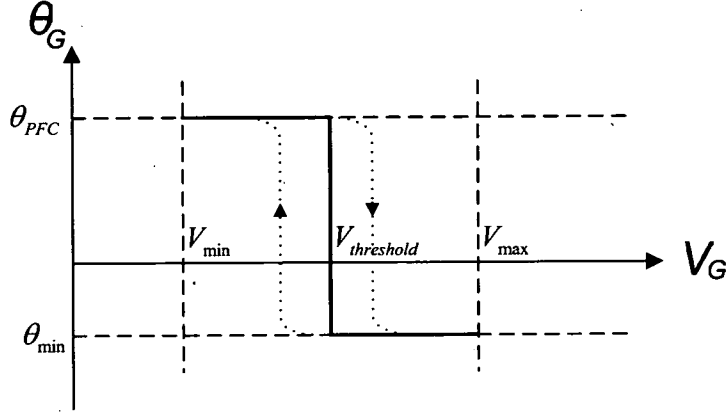


Figure 5.12 Voltage control strategy of Intelli-Gens.

Equation (5.19) describes this control strategy mathematically:

$$\begin{aligned} \theta_G &= \theta_{PFC} & \text{when } V_{\min} \leq V_G < V_{\text{threshold}} \\ \theta_{\min} < \theta_G < \theta_{PFC} & \text{when } V_G = V_{\text{threshold}} \\ \theta_G &= \theta_{\min} & \text{when } V_G > V_{\text{threshold}} \end{aligned} \quad (5.19)$$

In order to avoid the optimisation burden that discrete transitions create (5.19) is approximated with the equality constraint below:

$$\theta_G = \theta_{eq} \Rightarrow \tan^{-1}(Q^G / P^G) = A + K \cdot \tan^{-1}(B \cdot V_G + C) \quad (5.20)$$

where $K = K_{\text{steep}} \frac{\theta_{PFC} - \theta_{\min}}{\pi}$,

$$A = \theta_{\min} + K \frac{\tan^{-1}[(V_{\max} - V_{\min}) \cdot \eta\mu_{\text{threshold}}^{\min} \cdot \sigma\nu_{\max}^{\min} + (V_{\min} - V_{\text{threshold}}) \cdot \eta\mu_{\max}^{\min} \cdot \sigma\nu_{\text{threshold}}^{\min}]}{(V_{\max} - V_{\text{threshold}}) \cdot \eta\mu_{\text{threshold}}^{\min} \cdot \eta\mu_{\max}^{\min}}$$

where $\eta\mu_y^x = \sin\left(\frac{\theta_x - \theta_y}{K}\right)$ and $\sigma\nu_y^x = \cos\left(\frac{\theta_x - \theta_y}{K}\right)$

$$B = \frac{\tan\left(\frac{\theta_{\text{threshold}} - A}{K}\right) - \tan\left(\frac{\theta_{\max} - A}{K}\right)}{V_{\text{threshold}} - V_{\max}} \quad \text{and} \quad C = \tan\left(\frac{\theta_{\max} - A}{K}\right) - B \cdot V_{\max}.$$

K_{steep} is a real number marginally over 1, which defines the steepness of \tan^{-1} . The higher the value, the smoother the transition from θ_{PFC} to θ_{\min} . A value of 1.01 for K_{steep} produces a quite smooth function without significant loss in precision. A detailed analysis of the way the above set of constraints was calculated can be found in the Appendix. This approximation creates a 'smooth' transition around $V_{\text{threshold}}$ for θ_G with respect to V_G (Figure 5.13).

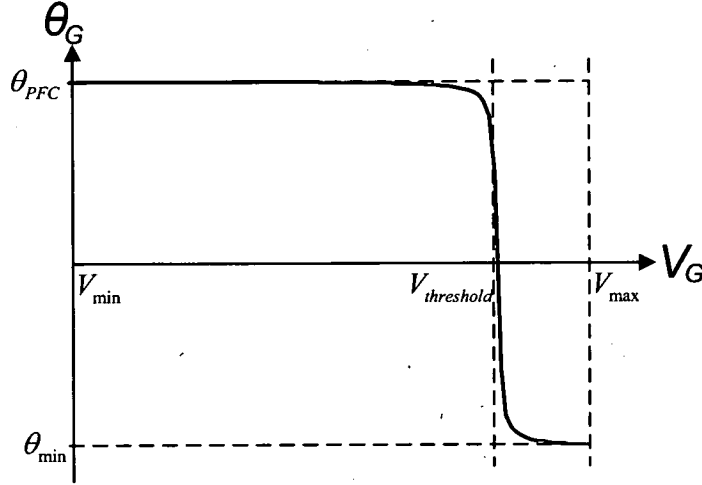


Figure 5.13 ‘Smoothing’ of control strategy transition for Intelli-Gens.

The derivatives of the PF constraints provide the direction to the optimisation procedure towards the relief of the violated PF constraints, with respect to the OPF variables.

$$\frac{d\theta_{eq.}}{dP^G} = \frac{Q^G}{(P^G)^2} \cdot \frac{1}{\left[1 + \left(\frac{Q^G}{P^G}\right)^2\right]} \quad (5.21)$$

$$\frac{d\theta_{eq.}}{dQ^G} = -\frac{1}{P^G} \cdot \frac{1}{\left[1 + \left(\frac{Q^G}{P^G}\right)^2\right]} \quad (5.22)$$

$$\frac{d\theta_{eq.}}{dV_G} = \frac{K \cdot B}{1 + (B \cdot V_G + C)^2} \quad (5.23)$$

Obviously, the derivatives with respect to the OPF variables which are not involved in the constraints are equal to zero. A detailed calculation of the PF constraints with respect to the OPF variables can be found in the Appendix.

5.3.3.2 CVC-Gens

When DGs are centrally dispatched, their voltage control region is restricted only by:

- a. their operating limits

$$PF_{min} < PF < PF_{max} \Rightarrow \theta_{min} < \theta_G < \theta_{max} \quad (5.24)$$

- b. The statutory voltage regulations

$$V_{min} \leq V_G < V_{max} \quad (5.25)$$

Constraints (5.24) and (5.25) are presented graphically in Figure 5.14.

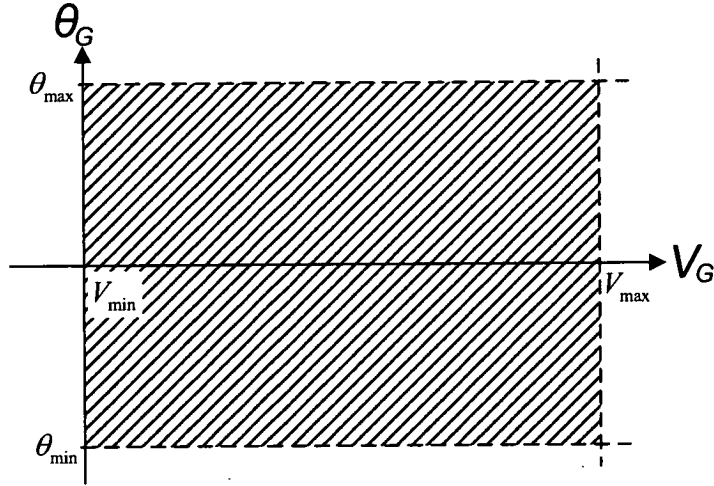


Figure 5.14 Central voltage control region of DGs.

5.3.3.3 ECVC-Gens

When the DGs operate under the ECVC scheme, voltage control passes to the DNO when the voltage of the generator reaches a critical value $V_{threshold}$. Below $V_{threshold}$ the DGs produces active and reactive power under PFC.

Equation (5.19) describes the same control strategy mathematically:

$$\begin{aligned} \theta_G &= \theta_{PFC} & \text{when } V_{min} \leq V_G \leq V_{threshold} \\ \theta_{min} \leq \theta_G < \theta_{PFC} & \text{when } V_{threshold} < V_G \leq V_{max} \end{aligned} \quad (5.26)$$

In order to avoid the optimisation burden the discrete change of the control scheme creates at $V_{threshold}$ (5.26) is approximated with the set of PF constraints below:

$$\begin{aligned} L_C \leq \theta_G \leq U_C, \text{ where } \theta_G &= \tan^{-1}(Q^G / P^G), \\ L_C &= A + K \cdot \tan^{-1}(B \cdot V_G + C) \text{ and } U_C = \theta_{PFC} \end{aligned} \quad (5.27)$$

where A , B , C and K are the same with the ones defined for Intelli-Gens in Section 5.3.3.1. A detailed analysis of the way the above set of constraints was calculated can be found in the Appendix. This approximation creates a 'smooth' transition for θ_G with respect to V_G , which is shown in Figure 5.15.

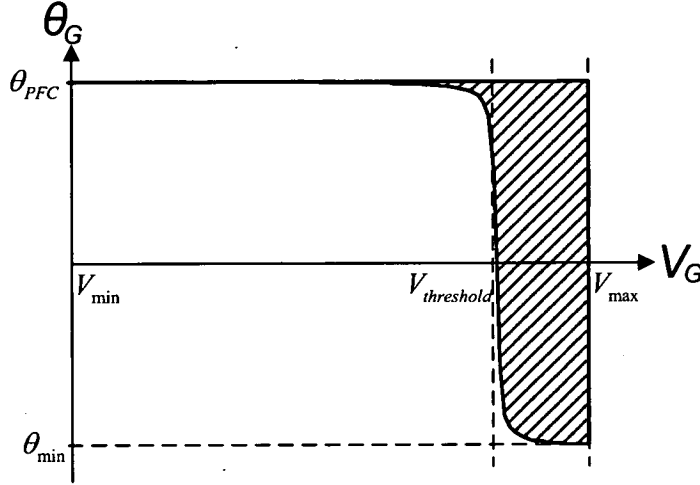


Figure 5.15 ‘Smoothing’ of control strategy transition from PFC to CVC when the DNO performs ECVC.

The derivatives of the PF constraints provide the direction to the optimisation procedure towards the relief of the violated PF constraints, with respect to the OPF variables.

$$\frac{dC_L}{dP^G} = \frac{Q^G}{(P^G)^2} \cdot \frac{1}{\left[1 + \left(\frac{Q^G}{P^G}\right)^2\right]} \quad (5.28)$$

$$\frac{dC_L}{dQ^G} = -\frac{1}{P^G} \cdot \frac{1}{\left[1 + \left(\frac{Q^G}{P^G}\right)^2\right]} \quad (5.29)$$

$$\frac{dC_L}{dV_G} = \frac{K \cdot B}{1 + (B \cdot V_G + C)^2} \quad (5.30)$$

$$\frac{dC_U}{dP^G} = -\frac{Q^G}{(P^G)^2} \cdot \frac{1}{\left[1 + \left(\frac{Q^G}{P^G}\right)^2\right]} \quad (5.31)$$

$$\frac{dC_U}{dQ^G} = \frac{1}{P^G} \cdot \frac{1}{\left[1 + \left(\frac{Q^G}{P^G}\right)^2\right]} \quad (5.32)$$

Derivatives with respect to OPF variables which are not involved in the constraints are equal to zero. A detailed calculation of the PF constraints with respect to the OPF variables can be found in the Appendix.

5.3.4 Contribution to fault levels

The impact of DGs on fault levels as a function of their impedance and voltage output is given by the derivatives calculated in 3.4.2 and 3.4.1, respectively. However, the impedance they add to the impedance matrix is given as a function of their MVA capacity S^G by (2.1), which is indifferent to the voltage control policy enforced by the DNO. (S^G can be calculated from the OPF variable P^G using the methods described at the end of Section 3.3). In addition, the voltage output of DGs is described by the same variable V_G in the OPF formulation, no matter if it describes the result of PFC, AVPFC or CVC/ECVC. Therefore, the mathematical description of the contribution of DGs to fault levels is common for all voltage control schemes.

5.3.5 Cost model

The cost model used in Chapters 2 and 3 assumes that the negative cost (benefit) C_g from new generation capacity is connected only to the size of new generators P_g :

$$C_g(P_g) = a \cdot P_g^2 + b \cdot P_g + c \quad (5.33)$$

w.r.t. $a, b, c < 0$ and $P_g > 0$, where C_g is the operational cost of generator g at output level P_g . If the voltage control scheme enforced by the DNO affects the allocated size of DGs at the CELs, then its impact will be reflected in the OPF objective function. Therefore, the existing cost model is capable of encapsulating the effects of different voltage control schemes.

5.3.6 Example

The same test case with the same constraints and assumptions will be used as in Section 5.2.4, except that the CELs at buses 1, 10 and 11 this time will accommodate in turn PFC-Gens, Intelli-Gens, CVC-Gens and ECVC-Gens. The voltage control strategy of Intelli-Gens and ECVC-Gens has a common $V_{threshold} = 1.05$ p.u. (see Section 5.3.3) for the relaxation of the PFC from a PF of 0.9 lagging. When the generators' voltage reaches $V_{threshold}$ they are permitted to operate at any PF between 0.9 lagging and 0.9 leading. CVC-Gens are controlled by the DNO to operate between 0.9 lagging and 0.9 leading PFs for any bus voltage within the statutory voltage regulations. The impact of each voltage control strategy on network capacity will be examined assuming that there is no preference for the allocation of new generation capacity at any specific CEL. The initial capacity allocation (FLCs ignored) from D-FLCOPF is presented in Table 5.4. The new MVA capacity at each CEL is

achieved for the PF written next to the MVA value. The positive sign stands for lagging PF, while the negative sign stands for leading PF.

	PFC	Intelli-Gens	CVC-Gens	ECVC-Gens
CEL bus 1	9.2 MVA / +0.90	28.3 MVA / -0.96	31.2 MVA / -0.90	25.3 MVA / -0.94
CEL bus 10	25.9 MVA / +0.90	24.8 MVA /+0.99	28.9 MVA /+0.90	28.7 MVA /+0.99
CEL bus 11	15.3 MVA / +0.90	33.0 MVA / -0.96	35.0 MVA / -0.97	31.3 MVA / -0.96
E/IP	-25.2 MW	-38.1 MW	-39.9 MW	-39.0 MW
Total capacity	50.4 MVA	86.1 MVA	95.1 MVA	85.3 MVA
Losses	4.0 MW	29.2 MW	31.8 MW	27.0 MW
Objective Fun.	-1411.5	-2424.2	-2557.7	-2425.1
Transf. ratio	1.0125	1.075	1.075	1.075

Table 5.4 Initial capacity allocation (FLCs ignored).

If FLCs are ignored, PFC results in the lowest total new capacity and exports. Obviously, the broader the voltage operating region of the generators (see Figure 5.13, Figure 5.15 and Figure 5.16) the broader the solution space for the OPF. Consequently, the OPF objective function has a value which increases in each case that PF control is relaxed further: in turn PFC, Intelli-Gens, ECVC-Gens, CVC-Gens.

The initial capacity allocation violates the breaking capacity of the switchgear connected to buses 1 and 10. Table 5.5 presents the reallocation of capacity for each method using D-FLCOPF when FLCs are included in the set of network constraints.

	PFC	Intelli-Gens	CVC-Gens	ECVC-Gens
CEL bus 1	0.0	36.6 MVA / -0.98	33.7 MVA / -0.90	36.6 MVA / -0.98
CEL bus 10	31.4 MVA / +0.90	7.0 MVA / +0.90	20.8 MVA / +0.95	7.1 MVA / +0.90
CEL bus 11	17.2 MVA / +0.90	35.2 MVA / -0.97	35.5 MVA / -0.98	35.2 MVA / -0.97
E/IP	-23.6 MW	-29.7 MW	-34.0 MW	-29.7 MW
Total capacity	48.6 MVA	78.8 MVA	90.0 MVA	78.9 MVA
Losses	3.9 MW	30.7 MW	34.7 MW	30.7 MW
Objective Fun.	-1347.0	-2123.8	-2377.7	-2124.4
Transf. ratio	1.0125	1.075	1.0875	1.075

Table 5.5 Reallocation of capacity considering FLCs.

In all cases, D-FLCOPF reallocated capacity from the CEL at bus 1 to the other CELs in order to relieve the FLCs. Even though the additional constraints (FLCs) reduce total capacity in all cases, the highest reduction is noticed for the case with new generators operating in PFC. Furthermore, total new capacity achieved with generators operating under one of the relaxed voltage control schemes is almost double than the one achieved with PFC.

An interesting effect of the introduction of FLCs is that the allocations of Intelli-Gens and ECVC-Gens become identical! The explanation can be easily derived from the voltage/PF profiles (Figure 5.15) of the generators before and after the introductions of the FLCs. The blue dashed lines on the figures below (Figure 5.16) show the shifting of the Voltage/PF operating points of each new generator at CEL x before ($x:1$) and after ($x:2$) the introduction of FLCs. On the same figures the following lines are superimposed a) the minimum and maximum operating PFs (expressed with signed angles θ) as parallel lines to the voltage axis and b) the response of AVPFC at $V_{threshold} = 1.05$ p.u. as a reference boundary for the PFC relaxation of Intelli-Gens (equality constraint (5.20)) and ECVC-Gens (inequality constraints (5.27)).

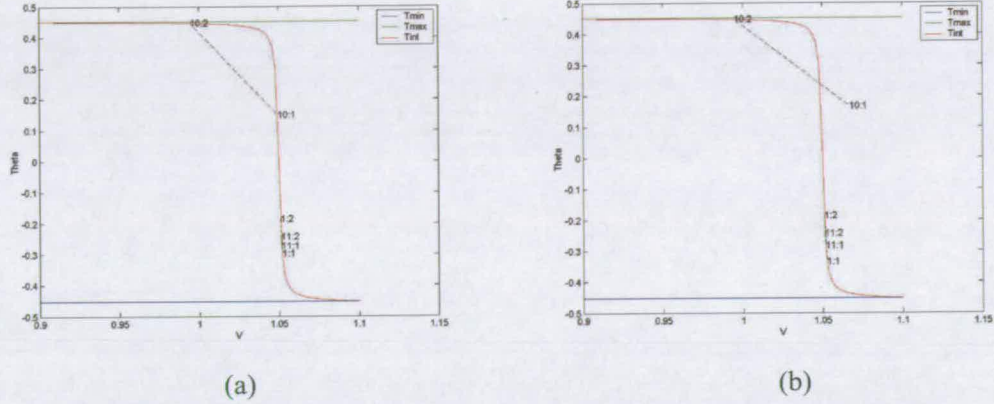


Figure 5.16 Shifting of Voltage/PF operating points of new generators operating under a) AVPFC and b) ECVC for $V_{threshold} = 1.05$ p.u. due to the introduction of FLCs.

According to equation (2.3), expected fault currents for the switchgear are proportional to the voltage of the switchgear bus. FLCs force ECVC-Gens to decrease their voltage output, so that expected fault currents of switchgear connected to the generators' buses are reduced. The AVPFC curve sets a lower bound to the voltage reduction of ECVC-Gens. Similar behaviour was noticed for ECVC-Gens when $V_{threshold}$ was decreased to 1.035 p.u. (Figure 5.17) and increased to 1.065 p.u. (Figure 5.18): when FLCs are included in the set of system constraints the allocation of Intelli-Gens and ECVC-Gens becomes the same.

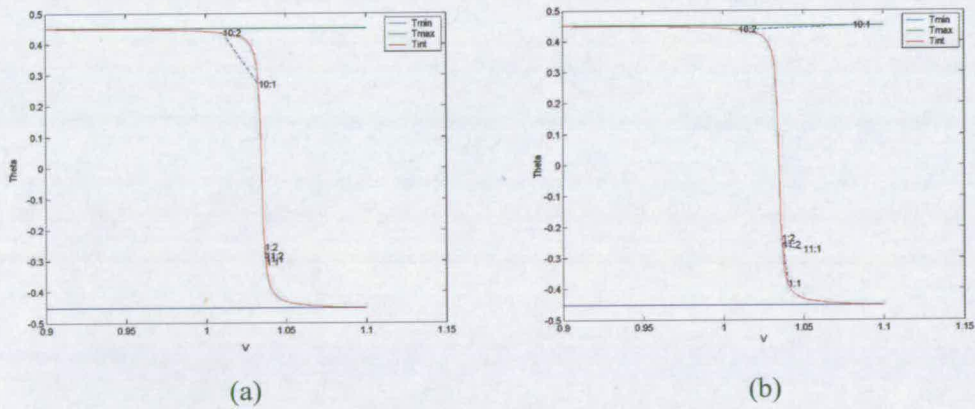


Figure 5.17 Shifting of Voltage/PF operating points of new generators operating under a) AVPFC and b) ECVC for $V_{threshold} = 1.035$ p.u. due to the introduction of FLCs.

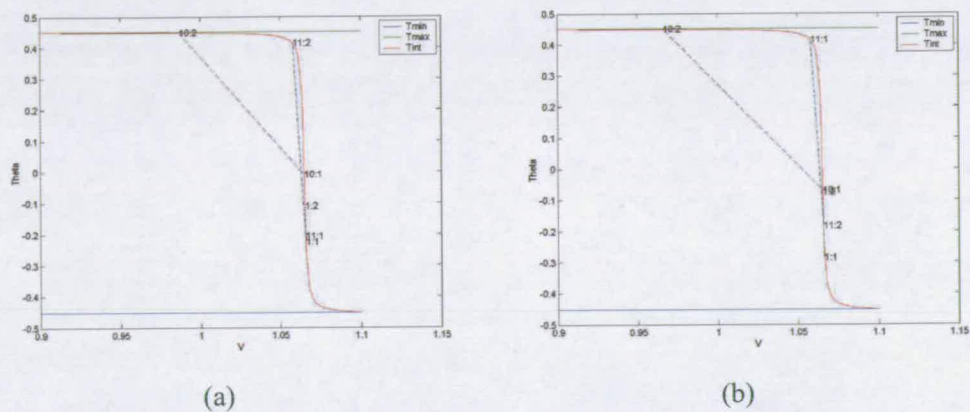


Figure 5.18 Shifting of Voltage/PF operating points of new generators operating under a) AVPFC and b) ECVC for $V_{threshold}=1.065$ p.u. due to the introduction of FLCs.

5.3.7 Transmission losses

However, the impressive total capacity achieved from the methods with relaxed PF comes at a cost: high losses (see row ‘losses’ in Table 5.5). This is due to the fact that most of the reactive power consumed by Intelli-Gens, CVC-Gens and ECVC-Gens during their attempt to maintain acceptable terminal voltage, is provided from the distant E/IP at bus 12. Reactive power travelling for long distances through a network raises losses. That is why even though more capacity of Intelli-Gens than ECVC-Gens can be installed at the same network, the allocation of ECVC-Gens results in higher exports and OPF objective function (see rows ‘E/IP’ and ‘ObjectiveFun.’).

Currently, losses are not considered by the DNO during capacity planning, mostly because they are kept within a reasonable level under PFC. However, if the DNO is to relax the strict PFC policy on new generators using one of the more flexible decentralised (Intelli-Gens) or centralised (ECVC-Gens or CVC-Gens) voltage control schemes, transmission losses become a significant proportion of new capacity. Table 5.6 presents the transmission losses according to the voltage control strategy selected by the DNO as a percentage of the total new capacity. Total new capacity is converted from MVA to MW using the PFs presented in the same table.

	PFC	Intelli-Gens	CVC-Gens	ECVC-Gens
Total capacity	43.7 MW	76.3 MW	84.9 MW	76.4 MW
Losses	8.9 %	40.2 %	40.9 %	40.2 %

Table 5.6 Transmission losses as a percentage of the total new capacity.

According to the above table, a big part of new capacity is effectively...lost on the way!

5.3.8 Limitations

Similarly to the limitations of the method allocating new RPCBs there is no provision in the objective function of the above optimizations for the minimization of losses or handling of reactive power. The objective function only provides benefit for the network operator from new generation capacity, which is indifferent of the voltage control policy implemented. There is no cost directly attached to the reactive power production or consumption of new generators or their contribution to losses. For example, even if there may be no great difference between two cases, where nearly the same amount of total new MW capacity is allocated, there may be a significant difference in reactive power required to support the respective systems. It may be the case that the solutions actually reflect a competition between new generators as sources or sinks of reactive power. The result is great amounts of reactive power produced at one point and consumed at a distant other, which obviously increases losses. In other words, the current method is probably inefficient in terms of reactive power management and losses, which is one of the fundamental targets of network planners. Further research is needed towards the incorporation of those factors in order to complete the suggested approach as a more realistic application.

5.4 Chapter summary

This Chapter examined two extensions of the model used by the OPF in capacity allocation, in order to accommodate alternative generators voltage control policies and reactive power compensation banks.

In the first part of this Chapter, an extension of the OPF as a tool for network capacity analysis was presented, so that it can support the optimal placement of RPCBs. This tool can be proven particularly useful to network operators. It can facilitate a) the optimal investment of an available budget for new RPCBs (strategy A) or b) the maximization of revenue from additional capacity re-leased by new RPCBs (strategy B). The method was applied to a typical LV network with several CELs and an EIP. The capacity analysis of this network demonstrated that the operator can practically double the connecting capacity of the existing network by a small investment on RPCBs. This means that existing networks can accommodate more generation capacity than initially estimated, minimizing the tremendous cost of their expansion for the operator.

However, the impressive total capacity achieved from the methods with relaxed PF comes at a cost: high transmission losses (see row 'losses' in Table 5.5). The high losses are explained by two facts. Firstly, most of the reactive power consumed by Intelli-Gens, CVC-Gens and ECVC-Gens during their attempt to maintain acceptable terminal voltage, is provided from a distant Export/Import Point (E/IP). Secondly, in the same table it can be noticed that Intelli-Gens, CVC-Gens and ECVC-Gens located at Capacity Expansion Locations (CELs) 1 and 11 operate in leading PFs, while those located at CEL 10 operate in lagging PF (see rows with CELs in Table 5.5). The operating points of the virtual generators located at CELs are roughly the operating points that new generators should adopt so that the existing network is capable of accommodating such high penetration of new capacity. Since load is assumed constant, this means that the reactive power produced (lagging PF) by one group of generators is consumed (leading PF) by another in an effort to keep the overall bus voltage pattern within statutory regulations. This creates a 'push-pull' effect of reactive power on the network, which is also known as 'hunting'. Whichever of the two is the decisive factor; reactive power travelling for long distances through a network raises losses.

The main conclusion of the second part of this Chapter is that the relaxation of DNOs' strict PFC policies, specifically, through widespread application of intelligent automatic voltage/power factor control schemes allow the connecting capacity of the existing network to be better exploited. Furthermore, the allocation of new Intelli-Gens and ECVC-Gens becomes identical and not very different than CVC-Gens when FLCs are considered. Therefore, Intelli-Gens should be preferred due to the simplicity of their control (locally), but efficient exploitation of the existing network.

Concluding, these two new applications of OPF, allocation of RPCBs and incorporation of voltage control strategies in allocation of new generation capacity raise a new challenge for the power systems engineer: further research is needed, so that the capabilities of OPF as a planning rather than operating tool can be fully exploited.

6. CONSIDERING THE IMPACT OF NEW CAPACITY ON LOSSES

6.1 Introduction

Chapter 5 investigated the impact of a possible relaxation of the current DNO voltage control policy on the capability of an existing network to absorb new capacity. Several possible alternative voltage control methods have been suggested as a replacement of the current strict Power Factor Control (PFC) method imposed by the DNO.

‘Intelli-Gens’, are assumed to be generators equipped with a voltage controller based on work by Kiprakis et al [73]. This method of voltage control is distributed in the sense that generators support voltage only by collecting data from their terminal bus.

Two more voltage control methods have been envisaged according to the level of central administration that the DNO may decide to enforce in the future. Centrally Voltage Controlled Generators or CVC-Gens are generators which have their reactive power production centrally controlled by the DNO in all cases. Emergency Centrally Voltage Controlled Generators or ECVC-Gens are generators operating in PFC mode, but operate exactly like CVC-Gens when their terminal bus voltage exceeds some ‘emergency’ boundaries.

A 12-bus test case has been used in the assessment of network capability to absorb new capacity when the alternative voltage control methods are used instead of PFC. It was found that any of the alternative methods would practically double total new capacity that can be installed on the existing network (see row ‘Total capacity’ in Table 5.5). However, the impressive total capacity achieved from the methods with relaxed PF comes at a cost: high transmission losses (see **Error! Reference source not found.** Table 5.5).

Currently, losses are not considered by the DNO during capacity planning, mostly because they are kept within a reasonable level under PFC. However, if the DNO is to relax the strict PFC policy on new generators using one of the more flexible decentralised (Intelli-Gens) or centralised (ECVC-Gens or CVC-Gens) voltage control schemes, transmission losses become a significant proportion of new capacity. According to **Error! Reference source not found.**, practically a big part of new capacity is ...lost on the way! Of course, such a result would be completely unacceptable in terms of efficiency. Therefore, if the DNO ever decides

to relax the current voltage control strategy, it will most probably consider revising the capacity planning policy to take into account expected losses.

This Chapter presents a methodology for the incorporation of losses in the optimisation algorithm for the allocation of new capacity analysed so far. As it is justified later on, the methodology is indifferent to the voltage control method imposed by the DNO on new generation capacity. The same example with Chapter 5 is used to examine if the consideration of losses affects the final capacity allocation and at which extend for each voltage control method used by the DNO.

6.2 Calculation of losses

If the Π equivalent of a transmission line connecting bus i with bus m has p.u. resistance of $R_{k,m}$ and the p.u. voltages at buses k and m are V_k and V_m respectively, then the transmission losses $P_{k,m}^{losses}$ on that line are equal to:

$$P_{k,m}^{losses} = \frac{|V_k - V_m|^2}{R_{k,m}} \quad (6.1)$$

The resistance of transmission line k,m is expressed as a function of the admittance matrix Y_{bus} :

$$\text{Real}(Y_{bus}(k,m)) = \frac{1}{R_{k,m}}, \text{ where Real is the real part of a complex matrix.} \quad (6.2)$$

Bus voltages V_i, V_j can be analysed to their magnitudes $|V_k|, |V_m|$ and angles θ_k, θ_m :

$$\begin{aligned} V_k &= |V_k| \cdot \cos \theta_k + j \cdot |V_k| \cdot \sin \theta_k \\ V_m &= |V_m| \cdot \cos \theta_m + j \cdot |V_m| \cdot \sin \theta_m \end{aligned} \quad (6.3)$$

Therefore,

$$\begin{aligned} V_k - V_m &\stackrel{(6.3)}{=} |V_k| \cdot \cos \theta_k - |V_m| \cdot \cos \theta_m + j \cdot (|V_k| \cdot \sin \theta_k - |V_m| \cdot \sin \theta_m) \Rightarrow \\ |V_k - V_m| &= \sqrt{(|V_k| \cdot \cos \theta_k - |V_m| \cdot \cos \theta_m)^2 + (|V_k| \cdot \sin \theta_k - |V_m| \cdot \sin \theta_m)^2} \end{aligned}$$

$$\begin{aligned} \text{Thus, } |V_k - V_m|^2 &= (|V_k| \cdot \cos \theta_k - |V_m| \cdot \cos \theta_m)^2 + (|V_k| \cdot \sin \theta_k - |V_m| \cdot \sin \theta_m)^2 \Rightarrow \\ &\Rightarrow |V_k - V_m|^2 = |V_k|^2 + |V_m|^2 - 2 \cdot |V_k| \cdot |V_m| \cos(\theta_k - \theta_m) \end{aligned} \quad (6.4)$$

By substitution of (6.2) and (6.4) in (6.1):

$$P_{k,m}^{losses} = \left[|V_k|^2 + |V_m|^2 - 2 \cdot |V_k| \cdot |V_m| \cos(\theta_k - \theta_m) \right] \cdot \text{Real}(Y_{bus}(k,m)) \quad (6.5)$$

6.3 Expressing losses as a function of OPF variables

In order to incorporate losses in the optimisation procedure of OPF as a tool for capacity allocation, first they must be expressed as function of the OPF variables. Bus voltages $|V_k|, |V_m|$ and the respective angles θ_k, θ_m in (6.5) are actually OPF variables, while the Y_{bus} expresses the passive elements of the network, so it is not connected with any of the OPF variables. Therefore, $P_{k,m}^{losses}$ in (6.5) is a function of those OPF variables:

$P_{k,m}^{losses}(|V_k|, |V_m|, \theta_k, \theta_m)$. The total network losses are equal to the sum of losses of each line:

$$P_{lines}^{losses}(|V_1|, \dots, |V_b|, \theta_1, \dots, \theta_b) = \sum_{k=1 \dots b} \left(\sum_{m=k \dots b} P_{k,m}^{losses} \right), \text{ where } b = \text{number of buses.} \quad (6.6)$$

The internal summation of line losses $\left(\sum_{m=k \dots b} P_{k,m}^{losses} \right)$ is calculated for $m=k \dots b$, so that losses at each line are considered only once in the total losses.

6.4 Considering losses during allocation of new capacity

Losses are considered during the allocation of new capacity by including them as a penalty in the objective function (1.24) of the OPF as a tool for capacity allocation:

$$OF_{OPF}(P_g, P_T, |V_b|, \theta_b) = \sum_g C_g(P_g) + \sum_T C_T(P_T) - W_L \cdot P_{lines}^{losses}(|V_k|, \theta_k) \quad (6.7)$$

where g are the CEL buses and T are the buses connected to external networks (as described in Section 2.5.1) and k are all the system buses. W_L is a penalty weight for losses and determines how much the network operator values losses. For example, if the operator values losses as much as the benefit from new capacity, then W_L should be set to 1 so that any marginal increment of the benefit (due to new capacity on the network) must not increase total losses more than the increment itself. If $W_L=0$ then the impact of new capacity on losses is ignored.

6.5 Finding the direction to optimum allocation

The solution of Nonlinear Programming problems, like the OPF, is generally achieved in an iterative manner. In each iteration a direction of search towards the global optimum has to be estimated. Therefore, the derivatives of the augmented objective function (6.7) need to be calculated with respect to the OPF variables in order to determine the direction towards the optimum capacity allocation considering losses. Nevertheless, the variables contained in the term of the objective function, which captures the benefit for the network operator from new capacity (P_g, P_T) are not included in the term which depicts the deficiency of the solution due to losses $W_L \cdot P_{lines}^{losses}(|V_k|, \theta_k)$ (where k is any of the system buses) and vice versa. Therefore, only the partial derivatives of losses with respect to the OPF variables $|V_k|, \theta_k$ need to be calculated and these will be the derivatives of the overall objective function with respect to these variables.

$$\frac{dOF_{OPF}(P_g, P_T, |V_b|, \theta_b)}{d|V_k|} = W_L \cdot \frac{dP_{lines}^{losses}(|V_k|, \theta_k)}{d|V_k|} = W_L \cdot 2 \sum_{d=1 \dots b} [|V_k| - |V_d| \cos(\theta_k - \theta_d)] \quad (6.8)$$

$$\frac{dOF_{OPF}(P_g, P_T, |V_b|, \theta_b)}{d\theta_k} = W_L \cdot \frac{dP_{lines}^{losses}(|V_k|, \theta_k)}{d\theta_k} = W_L \cdot 2 \sum_{d=1 \dots b} [|V_k| |V_d| \sin(\theta_k - \theta_d)] \quad (6.9)$$

where b = the number of buses.

The derivatives of the objective function with respect to the rest of the OPF variables (P_g, P_T) remain unchanged.

6.6 Example

The test case of Section 5.3.6 will be used, with the same constraints and assumptions. However, CELs at buses 1, 10 and 11 will now accommodate in turn PFC-Gens, Intelli-Gens, CVC-Gens and ECVC-Gens. The voltage control strategy of Intelli-Gens and ECVC-Gens has a common $V_{threshold} = 1.05$ p.u. (see Section 5.3.3) for the relaxation of the PFC from a PF of 0.9 lagging. When the generators' voltage reaches $V_{threshold}$ they are permitted to operate at any PF between 0.9 lagging and 0.9 leading. CVC-Gens are controlled by the DNO to operate between 0.9 lagging and 0.9 leading PFs for any bus voltage within the statutory voltage regulations. Again, the impact of each voltage control strategy on network capacity will be examined, but this time losses will also be considered during capacity allocation.

It will be presupposed that the generation expansion planner has no preference for the allocation of new generation capacity at any specific CEL i.e. all CELs have a marginal cost of -20. Exports of power are valued as much as new capacity i.e. the E/IP has a marginal cost of -20, too. Finally, in order to consider the impact of the capacity allocation on losses $W_L=20$ (see Section 6.4), i.e. equal to the negative value of the marginal benefit from new capacity. This means that during the optimisation of the objective function (6.7) any marginal increment of capacity on the network must not increase total losses more than the increment itself:

The initial capacity allocation (FLCs ignored) under strict PFC with and without considering losses in the objective function is presented in Table 6.1.

Considering losses	PFC	
	$W_L=0$	$W_L=20$
CEL bus 1	9.2 MVA / +0.90	9.2 MVA / +0.90
CEL bus 10	25.9 MVA / +0.90	25.9 MVA / +0.90
CEL bus 11	15.3 MVA / +0.90	15.3 MVA / +0.90
E/IP	-25.2 MW	-25.2 MW
Total capacity	50.4 MVA	50.4 MVA
Losses	4.0 MW	4.0 MW
Objective Fun.	-1411.5	-1332.6
Transf. ratio	1.0125	1.0125

Table 6.1 Initial capacity allocation (FLCs ignored) under strict PFC.

The reduction of the objective function is equal to the cost of losses:

$$1411.5-1332.6=78.9 \cong 4(MW) \times 20(units/MW) \quad (6.10)$$

Therefore, under strict PFC losses do not have any effect on capacity allocation. Besides, only a small fraction (less than 9% according to **Error! Reference source not found.**) of the new capacity is wasted on losses anyway.

The problem of high losses arises when the strict PFC policy is relaxed by the DNO. Table 6.2 presents the capacity allocation of new Intelli-Gens, ECVC-Gens and CVC-Gens when FLCs are ignored. The new MVA capacity allocated to each CEL is achieved for the PF written next to the MVA value. The positive sign stands for lagging PF, while the negative sign stands for leading PF. PFs of +1 and -1 mean that they approach unity from lagging and leading values, respectively. In all three cases of relaxed PFC policy, capacity is shifted from CELs at bus 1 (mostly) and bus 11 to the CEL at bus 10 once losses are considered. The new optimal allocations of Intelli-Gens, CVC-Gens and ECVC-Gens decrease losses by 29.2-20.4=8.8 MW, 31.8-21.0=10.8 MW and 27.0-21.0=6 MW, respectively. They also increase exports, even if total new capacity is reduced. This means that less power is wasted 'on the way', since loads always consume the same amount of power. In addition, the difference between the objective function values resulting from the three relaxed voltage control strategies is also reduced. Actually, when losses are considered CVC-Gens and ECVC-Gens allocations become almost identical.

Considering losses	Intelli-Gens		CVC-Gens		ECVC-Gens	
	$W_L=0$	$W_L=20$	$W_L=0$	$W_L=20$	$W_L=0$	$W_L=20$
CEL bus 1	28.3 MVA / -0.96	10.9 MVA / -0.92	31.2 MVA / -0.90	15.4 MVA / -0.90	25.3 MVA / -0.95	15.4 MVA / -0.91
CEL bus 10	24.8 MVA / +0.99	37.5 MVA / -1	28.9 MVA / +0.90	39.4 MVA / +0.99	28.7 MVA / +0.99	39.4 MVA / +0.99
CEL bus 11	33.0 MVA / -0.96	30.3 MVA / -0.95	35.0 MVA / -0.97	27.3 MVA / -0.98	31.3 MVA / -0.96	27.0 MVA / -0.97
E/IP	-38.1 MW	-39.8 MW	-39.9 MW	-42.2 MW	-39.0 MW	-42.1 MW
Total capacity	86.1 MVA	78.8 MVA	95.1 MVA	82.0 MVA	85.3 MVA	81.8 MVA
Losses	29.2 MW	20.4 MW	31.8 MW	21.0 MW	27.0 MW	21.0 MW
Objective Fun.	-2424.2	-1915.4	-2557.7	-2012.1	-2425.1	-2008.6
Transf.ratio	1.075	1.0625	1.075	1.0625	1.075	1.0625

Table 6.2 Allocation of new Intelli-Gens, CVC-Gens and ECVC-Gens when FLCs are ignored.

The initial capacity allocation raises fault levels beyond the breaking capacity of the switchgear connected to buses 1 and 10. If FLCs are included in the set of network constraints and capacity is reallocated for each method the results presented in Table 6.3 (strict PFC) and Table 6.4 (Intelli-Gens, ECVC-Gens and CVC-Gens) are produced.

	PFC	
Considering losses	$W_L=0$	$W_L=20$
CEL bus 1	0.0	0.0
CEL bus 10	31.4 MVA / +0.90	31.4 MVA / +0.90
CEL bus 11	17.2 MVA / +0.90	17.2 MVA / +0.90
E/IP	-23.6 MW	-23.6 MW
Total capacity	48.6 MVA	48.6 MVA
Losses	3.9 MW	3.9 MW
Objective Fun.	-1347.0	-1268.2
Transf. ratio	1.0125	1.0125

Table 6.3 Reallocation of capacity under strict PFC due to FLCs.

	Intelli-Gens		CVC-Gens		ECVC-Gens	
Considering losses	$W_L=0$	$W_L=20$	$W_L=0$	$W_L=20$	$W_L=0$	$W_L=20$
CEL bus 1	36.6 MVA / -0.98	0.2 MVA / +0.90	33.7 MVA / -0.90	11.9 MVA / -0.90	36.6 MVA / -0.98	0.2 MVA / +0.90
CEL bus 10	7.1 MVA / +0.90	37.0 MVA / -1	20.8 MVA / +0.95	37.9 MVA / -1	7.1 MVA / +0.90	37.0 MVA / -1
CEL bus 11	35.2 MVA / -0.97	18.8 MVA / +1	35.5 MVA / -0.98	25.0 MVA / -0.96	35.2 MVA / -0.97	18.8 MVA / +1
E/IP	-29.7 MW	-29.6 MW	-34.0 MW	-35.1 MW	-29.7 MW	-29.6 MW
Total capacity	78.9 MVA	56.0 MVA	90.0 MVA	74.8 MVA	78.9 MVA	56.0 MVA
Losses	30.7 MW	10.1 MW	34.7 MW	21.2 MW	30.7 MW	10.1 MW
Objective Fun.	-2123.6	-1508.4	-2377.7	-1728.0	-2123.6	-1508.3
Transf.ratio	1.075	1.0625	1.0875	1.075	1.075	1.0625

Table 6.4 Reallocation of new Intelli-Gens, CVC-Gens and ECVC-Gens due to FLCs.

Again, under strict PFC losses do not have a significant effect on capacity allocation. In all cases with relaxed PFC, capacity was shifted from the CELs at bus 1 and 11 to the CEL at bus 10 in order to relieve the violated FLCs and reduce total losses. Intelli-Gens and ECVC-Gens allocations, which became identical when FLCs were introduced to the optimisation process, remain identical after losses are considered.

The greatest decrement in losses is noticed for Intelli-Gens and ECVC-Gens (both by 30.7-10.1=20.6 MW), while losses are decreased less for CVC-Gens (34.7-21.2=13.5 MW). Table 6.5 presents the transmission losses of Table 6.4 as a percentage of the total new capacity with respect to the voltage control strategy implemented by the DNO. Total new capacity is converted from MVA to MW using the PFs presented in Table 6.4. A comparison with the respective decrements in losses from Table 6.2, where FLCs were ignored, makes it clear that FLCs reduce losses more for Intelli-Gens than other more relaxed voltage control strategies.

	PFC		Intelli-Gens		CVC-Gens		ECVC-Gens	
FLCs	Ignored	Considered	Ignored	Considered	Ignored	Considered	Ignored	Considered
Total capacity	43.7 MW	43.7 MW	76.3 MW	56.0 MW	84.9 MW	72.6 MW	76.4 MW	56.0 MW
Losses	8.9 %	8.9 %	40.2 %	18.0 %	40.9 %	29.2 %	40.2 %	18.0 %

Table 6.5 Transmission losses as a percentage of total new capacity when losses are considered during capacity allocation.

6.7 Chapter summary

In this Chapter, a method for the consideration of losses during allocation of new capacity to an existing network was discussed. A common example with the previous Chapter was used, where the impact of allocation on losses was ignored, in order to assess the magnitude of losses under different voltage control strategies implemented by the DNO.

The discussed method of incorporating losses in the optimisation procedure had two major effects on the allocation of new capacity:

- Expected exports increased, even though total new capacity decreased. In other words, less power was lost 'on the way' to the demand.

- b) The consideration of losses on top of FLCs further decreases the difference between the total capacities achieved with decentralized (Intelli-Gens) and centralized (CVC-Gens and ECVC-Gens) voltage control. This is probably a consequence of the more efficient (total new capacity over losses) allocation achieved under the decentralized voltage control scheme.

Clearly, if the current strict PFC policy is to be relaxed in order to allow more capacity to connect to the existing network, losses have to be taken into account. Otherwise, a great amount of power will be lost in transmission due to transfer of large amounts of reactive power over long distances.

7. REINFORCEMENT PLANNING MECHANISM

7.1 Introduction

Electricity networks are called on to accommodate more and more generation capacity in order to supply the increasing demand. Social, planning and environmental reasons hinder the expansion of the existing infrastructure, whereas lack of investment prohibits its reinforcement. Therefore, the efficient utilisation of the existing network is not only suggested for economy, but also imposed by need. The previous Chapters examined a novel method that facilitates assessment of the potential capabilities of the existing network to accommodate new generation capacity. The method modelled new capacity and energy transfers to external networks as the output of virtual generator placed on predetermined Capacity Expansion Locations (CELs) and Export/Import Points (E/IPs) respectively. Then the Optimal Power Flow (OPF), a well-documented tool in efficient power system operation, was used to specify the size of new capacity at CELs so that total new capacity and exports to the E/IPs are maximised.

The installation of new generation capacity brings the network closer to its operational limits. Sooner or later investment is needed to increase those limits, so that generation can supply the continuous demand growth. Investment on network infrastructure bears a very high cost for network operators, thus, a planning mechanism is needed to expand the capabilities of the network in the most efficient way. Since generation and network expansion is so closely linked, it is logical to seek the overall optimum in a combined approach.

In order to solve the OPF, Sequential Quadratic Programming (SQP) is used. The LaGrange multipliers, sensitivity by-products of SQP attached to each constraint explicitly described in the OPF, can be used to facilitate network planning decisions. Later in this Chapter, it will be proven that in most practical cases they indicate which line, transformer or other equipment would improve the capacity of the network to absorb new generation; if upgraded first. Finally, based on the signals from those multipliers, an investment planning mechanism for the reinforcement of the existing infrastructure is built. The target of the mechanism is to plan the expenditure of an available budget on reinforcing the network, so that it can absorb as much new generation capacity as possible.

7.2 Sequential Quadratic Programming

SQP is used for the solution of OPF, because it outperforms every other tested Nonlinear Programming method in terms of efficiency, accuracy, and percentage of successful solutions, over a large number of test problems [41]. The solution of Nonlinear Programming problems generally requires an iterative procedure to establish a direction of search at each major iteration. Basically, SQP sequentially forms a Quadratic Programming (QP) problem at each iteration based on the quadratic approximation of the Lagrangian function. The Lagrangian function is practically the objective function $f(x)$ to be minimized, augmented with the constraint functions $g_i(x)$ penalized by parameters λ_i (called LaGrange multipliers):

$$L(x, \lambda) = f(x) + \sum_{i=1}^m \lambda_i \cdot g_i(x) \quad (7.1)$$

where $i=1, \dots, m$ and m the number of constraints.

QP concerns the minimization of a linearly constrained quadratic objective function; the LaGrangian in this case. Thus, the nonlinear constraints described in Section 2.4 are linearised in the beginning of each iteration. The QP part of the iterative process consists of two stages: a) it finds a feasible starting point, if the initial point given in the SQP problem is not feasible and b) calculates an iterative sequence of feasible points. The sequence of feasible points finally converges to the solution of the subproblem, as it attempts to satisfy the Kuhn-Tucker equations.

The solution to the QP subproblem produces a vector d_k , which is used to form a new iterate $x_{k+1} = x_k + a \cdot d_k$. The step length parameter a is determined by an optimisation procedure, which targets to determine a x_{k+1} that minimises a merit function, such as the one stated in [74]:

$$M(x) = f(x) + \sum_{i=1}^{m_k} [r_i g_i(x)] + \sum_{i=m_k+1}^m [r_i \cdot \max\{0, g_i(x)\}] \quad (7.2)$$

where r_i is a penalty parameter for constraint i . [6] recommends setting the penalty parameter of the next iteration equal to:

$$(r_{k+1})_i = \max_i \left\{ \lambda_i, \frac{1}{2} [(r_k)_i + \lambda_i] \right\} \quad (7.3)$$

The next QP subproblem is formed with x_{k+1} as the new feasible starting point and a new approximation of the LaGrange function is calculated around this point. The overall process converges to the optimum when d_k gets sufficiently small.

7.3 Meaning of LaGrange multipliers in the OPF solution

As it is already mentioned, the solution of the QP subproblem at each major iteration of the SQP complies with the Kuhn-Tucker equations. The Kuhn-Tucker equations are necessary conditions for optimality of a constrained optimisation problem:

$$\nabla f(x) + \sum_{i=1}^m \lambda_i \cdot \nabla g_i(x) = 0 \quad (7.4)$$

$$\lambda_i \cdot g_i(x) = 0 \quad (7.5)$$

$$\lambda_i \geq 0 \quad (7.6)$$

Equation (7.4) describes a cancelling of the gradients between the objective function $f(x)$ and the constraints $g(x)$ at the solution point. For the gradients to be cancelled, the LaGrange multipliers are necessary to balance the deviations in magnitude of the objective function and constraint gradients. Generally, the magnitudes of gradients represent the effect marginal changes of function variables have on the function value. Therefore, each multiplier reflects the impact of a marginal relaxation of the respective constraint on the objective function value.

A constraint is considered 'active' when the solution lies on the constraint boundaries. Only active constraints are included in this cancelling operation. Constraints that are not active must not be included in this operation and so are given LaGrange multipliers equal to zero. This is stated implicitly in equations (7.5) and (7.6).

During the final iteration of SQP, the QP subproblem produces the LaGrange multipliers connecting the overall optimum of the objective function with the constraints. When SQP is used to solve the OPF, not only does it optimally allocate new generation capacity at CELs and set the energy transfers at E/IPs, but it also calculates the LaGrange multipliers for all the active system constraints. An examination of the multipliers can facilitate decisions about which constraint, if marginally relaxed, would result in the greatest increase of the objective function.

When OPF is utilised for generation capacity allocation a higher value of the objective function means higher total new generation capacity. Subsequently, when OPF allocates new generation capacity the LaGrange multipliers indicate which system constraint would result in even higher total generation capacity, if it was marginally relaxed.

7.4 Network reinforcement planning mechanism based on LaGrange multipliers

At this point, the fact that LaGrange multipliers reflect only the impact of marginal changes of the constraints on total new generation has to be stressed. They do not directly specify how much these constraints should be relaxed and in which order, to optimally increase the potential connection capacity. This is because reinforcements are usually lumpy, while LaGrange multipliers specify the benefit due to a unit relaxation of a constraint (e.g. by 1 MVA for lines thermal limits). Benefits due to relaxation of a particular constraint may be highly non-linear, so any linearisation-based calculation may lead to large errors when the upgrade size is substantial. Therefore, the signals received by the multipliers cannot lead us directly to the optimum investment plan. In this Section an iterative Reinforcement Planning Mechanism (RPM) is developed, which uses the multipliers to identify the most cost effective equipment, marginally upgrade it and reallocate capacities at each iteration. In other words, the multipliers are used as sensitivities connecting the active constraints set by equipment that reach their operating limits and the current capacity allocation given by the OPF. In the following text the RPM is examined in more detail by analysing it into specific steps.

7.4.1 Step 1: Creating a list of realistic investments

The RPM aims to produce an investment plan for the reinforcement of the existing infrastructure, in order to increase the potential of the existing network to accommodate new generation capacity. In terms of power system analysis, this is done by selectively alleviating active constraints which limit the ability of the network to absorb new capacity. Nevertheless, not all constraints can be relaxed in real world power systems. For instance, some transmission lines can be upgraded and their thermal limit increased, but none of the bus voltage limits can be relaxed as they are imposed by statutory regulations. This narrows down the number of constraints considered during network reinforcement planning. The constraints which are susceptible to improvement in real-world power systems are called 'feasible'. The investments in the equipment which technically create these constraints will be termed 'feasible investments' from this point on.

In addition, social, political or other non-technical reasons may prevent the investors (e.g. network operator) from reinforcing parts of the network, even if an investment is feasible and would result in maximum return on investment. For example, local authorities or citizens could oppose the expansion of a substation in a highly populated area. Feasible investments which is not possible to attract non-technical risks, like the ones mentioned above, will be termed 'realistic' from this point on.

Obviously, the RPM has to assess only those investments which are considered to be realistic. In this first step of the mechanism, the RPM segregates network constraints to feasible and

non-feasible. Then, according to the subjective and case-specific data provided by the user, it filters out those constraints where an investment would not be realistic.

7.4.2 Step 2: Allocating new generation capacity with the OPF

New generation capacity is allocated to the network, which is reinforced by the investment plan up to the current *step*. To achieve this, a method based on the OPF formulation was developed in Chapter 3 (D-FLCOPF). The method produces:

- An assessment of the network capacity to absorb new generation, with respect to system, network and fault level constraints.
- The LaGrange multipliers for the system's constrained equipment (e.g. congested transmission lines, switchgear expected to break fault currents close to specifications etc.).

7.4.3 Step 3: 'Discretising' marginal reinforcement

Section 7.3 concluded that when OPF is used as a tool for capacity allocation and it is solved with SQP the LaGrange multipliers attached to constraint equipment define the benefit increment for the network operator from additional generation capacity, if the constraint equipment is marginally upgraded. Nevertheless, 'marginal change' is a mathematical concept only. Practically, numerical processes (like the solution of the OPF) simulate 'marginal changes' on quantities with 'discrete changes in very small steps'. Thus, whatever decision engine the planning mechanism may contain, it certainly has to upgrade the specifications of equipment in small discrete steps in order to preserve the meaning of the LaGrangian signals.

The upgrading of equipment in small steps in terms of power system analysis can be interpreted as small improvements of the specification of the existing equipment. The objective function increment Δf can be approximated using the LaGrange multiplier λ_e attached to the discretely upgraded specifications Δs_e of equipment e :

$$\frac{df}{ds_e} = \lambda_e \Rightarrow \Delta f = \lambda_e \cdot \Delta s_e \quad (7.7)$$

This approximation is depicted in Figure 7.1.

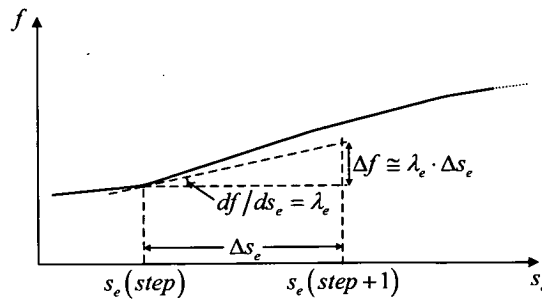


Figure 7.1 Estimation of objective function increase due to investment.

If $step$ determines how many times this specific equipment has been selected by RPM as an optimum investment, thus $\Delta s_e = s_e(step+1) - s_e(step)$.

In some cases of investment the upgrade of equipment does not affect only the set of constraints during allocation of capacity. It also affects the physical characteristics of the network. The network characteristics have to be updated together with such investments before D-FLCOPF allocates new capacity.

For example, the upgrade of transmission or distribution lines in order to increase their thermal limit alters the impedance of the network. The new line resistance R_{new} and reactance X_{new} has to be calculated as a function of the old resistance R_{old} and reactance X_{old} . Generally, the thermal limit S is given as the product of the rated voltage V_{rated} and current I_{rated} of the line:

$$S = |V_{rated}| \cdot |I_{rated}| \Rightarrow |V_{rated}| = \frac{S}{|I_{rated}|} \quad (7.8)$$

Since the rated voltage of a line remains unchanged after a minor reinforcement, according to (7.8) the ratio of the thermal limit over the rated current before (S_{old}) and after (S_{new}) the reinforcement remains unchanged and equal to approximately 1 p.u.:

$$S_{new} = |I_{rated,new}| p.u. \text{ and } S_{old} = |I_{rated,old}| p.u. \quad (7.9)$$

Let us assume that the upgrade of a line by $S_{step} = S_{new} - S_{old}$, decreases transmission losses by:

$$L_{step} = L_{new} - L_{old} = -S_{step} \cdot L_{perc.} \quad (7.10)$$

where $L_{perc.}$ expresses losses as a percentage of S_{step} .

However, the losses before and after the upgrade are equal to:

$$\begin{aligned} L_{old} &= |I_{rated,old}|^2 \cdot R_{old} \\ L_{new} &= |I_{rated,new}|^2 \cdot R_{new} \end{aligned} \quad (7.11)$$

(7.10) is recalculated using (7.9) and (7.11):

$$\begin{aligned} L_{step} &= S_{new}^2 \cdot R_{new} - S_{old}^2 \cdot R_{old} \Rightarrow \\ R_{new} &= \frac{S_{old}^2 \cdot R_{old} + L_{step}}{S_{new}^2} \end{aligned} \quad (7.12)$$

If the thermal limit before and after the upgrade is expressed as a function of the rated voltage and line impedance:

$$S_{new} = \frac{|V_{rated}|^2}{|Z_{new}|} \Rightarrow S_{new} = \frac{|V_{rated}|^2}{|R_{new} + jX_{new}|} \quad (7.13)$$

$$S_{old} = \frac{|V_{rated}|^2}{|Z_{old}|} \Rightarrow S_{old} = \frac{|V_{rated}|^2}{|R_{old} + jX_{old}|} \quad (7.14)$$

Both terms of (7.13) are divided by (7.14) and solved with respect to X_{new} :

$$\frac{S_{new}}{S_{old}} = \frac{|R_{old} + jX_{old}|}{|R_{new} + jX_{new}|} \Rightarrow$$

$$X_{new} = \sqrt{\left(R_{old}^2 + X_{old}^2\right) \frac{S_{old}^2}{S_{new}^2} - R_{new}^2} \quad (7.15)$$

In real life, the effect of upgrade on thermal limits may be more complicated. Here is just an example of simplified analysis, which may be updated to consider more realistic situations.

7.4.4 Step 4: Defining the cost of investment

One of the most important parameters used during the evaluation of candidate investments is their costs. The RPM framework includes as candidate investments the network equipment which could potentially replace parts of existing infrastructure in order to increase the capacity of the network to absorb new generation. The cost of network equipment is practically defined by its specifications: rating, reliability, life expectancy etc. Therefore, it is important to know the specifications of the equipment that represent possible options during reinforcement planning.

According to Section 7.4.3, the RPM plans the upgrading of equipment in small, discrete steps at each investment iteration, in order to preserve the economic meaning of the LaGrange multipliers (see Section 7.3). Since the cost of equipment is a function of specifications, the cost of upgrading specific equipment e by a small step will be a function of its specifications at the current step $step$: $C_{e,incrm.}(s_e(step))$. $Step$ determines how many times this specific equipment has been selected by RPM as an optimum investment. An example of how this cost could be mathematically described is a quadratic cost function with respect to $step$:

$$C_{e,incrm.}(s_e(step)) = a \cdot step^2 + b \cdot step + c \quad (7.16)$$

where $a, b, c, step \geq 0$ and $a, b, c \in \mathbb{R}$ and $step \in \mathbb{N}$

When e is not planned for upgrading in one of the previous investment iterations (i.e. $step=0$) it carries a replacement (or starting) cost $C_{e,start}$. For example, if in a real-life situation the switchgear in a substation had to be upgraded even by a few MVA of breaking capacity, then the whole switchgear would be replaced. Of course, in this case the replacement cost would be much higher than the cost induced by the improved specifications. Therefore, the replacement cost should also be considered during the calculation of the cost of investment C_e on equipment e for $step$ times:

$$C_e(step) = C_{e,start}(step) + C_{e,incrm.}(s_e(step)) \quad (7.17)$$

where $C_{e,start}(step) = C_{e,start}$ for $step = 0$ or $C_{e,start}(step) = 0$ for $step > 0$

A graphical representation of C_e is depicted in Figure 7.2.

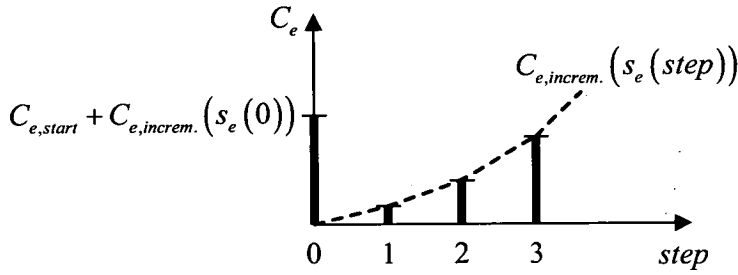


Figure 7.2 Cost of upgrading equipment in discrete steps.

Prices of equipment for a range of specifications can be gathered from network equipment suppliers. They depend on the category the equipment belongs (e.g. MV or HV transmission line etc.), which also determines a minimum investment cost, and the characteristics of the application. For example, MV switchgear may start from a retail price of 15,000 €, but it can reach 150,000 depending on the breaking capacity and capability required. If the RPM is to prepare a short-term investment plan, these prices directly define the cost of new equipment with respect to its specification. If the planning is extended for longer time frames, then more complicated factors have to be considered during the mathematical formulation of the cost of equipment. For example, inflation, reduction of prices in the future due to expected technological progress and other time-connected factors must be taken into account.

During this step of each RPM investment iteration, the costs of ‘marginally’ upgrading (i.e. by a small step) network equipment which comprise realistic investment options are calculated.

7.4.5 Step 5: Optimum investment

If among all realistic investments it is decided by the RPM to marginally upgrade the equipment with the highest LaGrange multiplier, then the investor will have the highest possible return for his investment: for example, if the investor is the network operator, he will achieve the maximum possible increment of benefit from additional generation. However, this is not sufficient to qualify an investment as optimum. For example, if the investment is on equipment which is very expensive to upgrade (e.g. transmission line), then it may result in the maximum possible return, but it will also have a very high cost. Therefore, it is logical to define as optimum the investment which results in the highest ‘net profit’, which is the subtraction of the investment cost from the return.

Consequently, the investment cost has to be converted to a comparable quantity with the benefit from new generation in order to calculate the expected net profit from each possible investment. The investment cost $C_e(s)$ of a new equipment e is a function of its

specifications s (see Section 7.4.4). The division of the cost with the life expectancy of the new equipment provides the average yearly cost of investment.

In order to simplify the analysis it will be assumed that only the marginal coefficients of the quadratic cost functions attached to CELs are non-zero and they are all equal to r . In other words, 1 MW of new generation capacity increases the objective function by r . Let us assume that the benefit r from new capacity has an equivalent monetary value of R for the network operator.

Now, let us also assume that the upgrade of the specifications s_e of a network equipment e by Δs_e is expected to increase the objective function by Δf . The rise of the objective function would have a monetary value ΔR_e equal to:

$$\begin{aligned} \text{Increment of obj.fun. by } r &\Rightarrow \text{Increment of operator's revenue by } R \\ \text{Increment of obj.fun. by } \Delta f &\Rightarrow \text{Increment of operators revenue by } \Delta R_e = \Delta f \frac{R}{r} \end{aligned} \quad (7.18)$$

R and r are constant, so ΔR_e is proportional to Δf :

$$\Delta R_e = k \cdot \Delta f, \text{ where } k = \frac{R}{r} = \text{const.} \quad (7.19)$$

By substituting (7.7) in (7.19) the increment of the benefit function Δf is connected with the equipment upgrade Δs_e :

$$\Delta R_e = k \cdot \lambda_e \cdot \Delta s_e \quad (7.20)$$

where λ_e is the LaGrange multiplier attached to the OPF constraint related to equipment e .

If the upgrade Δs_e of a network equipment e costs $C_e(s_e)$ and is expected to increase the monetary benefit by ΔR_e , then the net return on the investment is equal to:

$$NetR_e = \Delta R_e - C_e(\text{step}) = k \cdot \lambda_e \cdot \Delta s_e - C_e(\text{step}) \quad (7.21)$$

The RPM considers an investment on equipment $e_{opt.}$ optimal when it has the highest net return $NetR_e$ among all realistic investments:

$$e_{opt.} = e \{ \max(NetR_e) \} \quad (7.22)$$

7.4.6 Step 6: Updating investment plan and cost

In this step, RPM adds the investment, which was selected as optimum in the previous step, to the end of the list of investments from previous iterations. The list of investments determines the order with which the investments must be implemented in order to maximise the benefit of the network operator from new generation at each iteration of investment. However, upgrading equipment in small steps is not realistic, not to mention the installation burden

from which the cost was neglected. Thus, the investment on the same equipment, but different iterations, can be accumulated as one investment at the iteration that this investment was selected as optimum for the first time. Finally, the cost of the optimum investment in this iteration is added to the total cost of investment up to this iteration. The total cost of investment can also be added to a list of expected investment costs. Each row of this list would signify the cost of implementing the investment plan up to the respective row in the list of investments.

7.5 Planning loop

After the investment plan is updated in Step 6, the control of the algorithm is passed back to Step 2, where the future network is assessed. Steps 3-5 are repeated, so that the new optimum investment is identified, Step 6 updates the investment plan; control is passed back to Step 2 and so on. The algorithm iterates until the capacity allocation violates only constraints which are not realistic investments or the network operator's budget roof is reached. Figure 7.3 shows the flowchart of the iterative algorithm implementing the RPM.

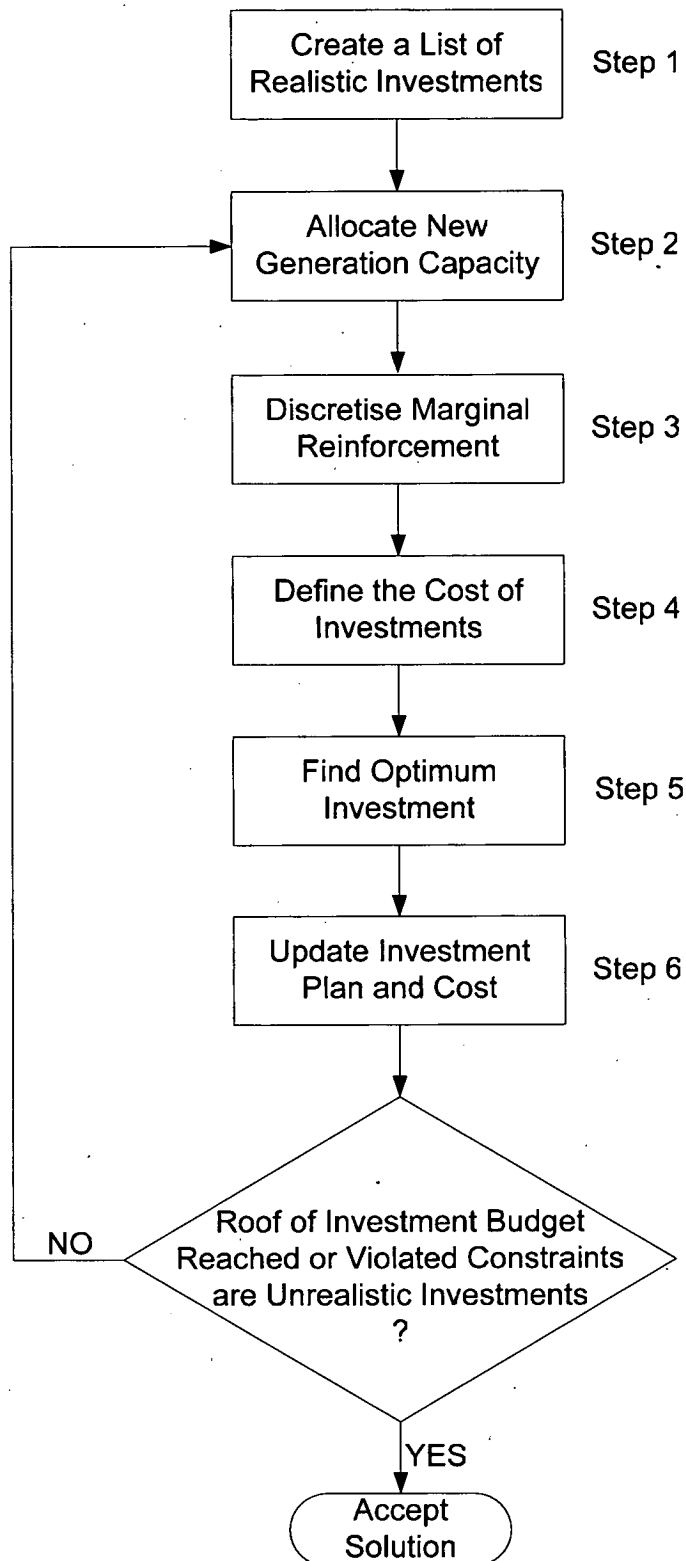


Figure 7.3 Flowchart of the iterative algorithm implementing the RPM.

7.6 Considering long-term load forecasts

In the previous Chapters, the change of demand/load through time was neglected, because the target was to assess the capacity of the network to absorb new generation at the present time or a specific time in the future. However, this Chapter focuses on reinforcement planning, a process which affects the characteristics of the network over a long period of time. During this time, expected demand changes (mostly increases), affecting the flow of power through the network. Consequently, the change of demand can affect both the amount and location of equipment which constrain the capacity of the network to absorb new generation. This Section develops a methodology in order to consider the effect of load change through time on reinforcement planning.

Let us assume that there is a constant increase $d_i\%$ every time unit (e.g. year) for load L_i . 'Load forecast' is defined as the size of L_i at time unit t :

$$L_i(t) = (d_i)^t \cdot L_i(0) \quad (7.23)$$

where $t=0,1,\dots$ with $t=0$ the present time.

Using the above methodology, investment plans that consider future demand growth could be created. In this case, loads would be considered equal to their forecasts. The forecasted values are calculated before the execution of step 1 in RPM, which assesses the capacity of the network to absorb new generation. The analysis can be simplified if loads are assumed to have constant power factors through time. Thus, if $L_i(t)$ is the real power demand of load i in time t , then a proportional reactive power demand $k \cdot L_i(t)$ is assumed for the same time.

7.7 Considering the retirement of generators

Electricity generation plants have a limited life expectancy. Sometimes this is supposed to be reached when basic equipment of the plant become unreliable due to age and spare parts are not produced any longer. In other cases, the production technology of the plant is outdated and its operation is no longer profitable. In any case, all generation plants eventually go out of service at some point in the future. This is called retirement.

When a big generator permanently disconnects from the grid power flow and voltage patterns change. New constraints may become binding for the future operation of the power system. The exact time of retirement is not always predictable (e.g. because it is not known when a new, more competitive production technology may be established), but when it is it has to be considered during network reinforcement planning.

In Section 2.5.1, existing generation capacity was modelled with fixed sources of real power equal to the capacity (in MW). When RPM reaches the point in time (see Section 7.6) that the retirement of a generator is expected, the respective source could be simply removed from the

power system model. Thus, the optimum investment on the network infrastructure would be decided according to the expected drop in power production.

7.8 Example

The RPM will be tested on the 12-bus network that has been used up to now as an example network. A detailed description of the network topology is presented in Section 3.6.1. It will be investigated if the different voltage control policies presented in Chapter 5 (PFC, Intelli-Gens, CVC-Gens and ECVC-Gens) have any impact on the optimum investment plan produced by the RPM. Transmission losses will also be taken into account during allocation optimisation, according to the methodology presented in Chapter 6. $W_L=20$ (see Section 6.4), i.e. value of losses per MW equal to the negative value of the marginal benefit from new capacity.

7.8.1 Investment economics

It will be assumed that the only realistic investments are the ones on thermal limits of transformers and transmission lines and the breaking capacity of switchgear (see 2.6.2). Transformers and lines have a common initial cost of upgrade $C_{line,start} = 50,000$ €. For each upgrade of the thermal limit by 5 MVA a flat cost (indifferent of line length, initial capacity etc.) equal to $C_{line,incrm.} = 5,000$ € will be assumed. Similarly, the replacement cost of switchgear will be set to $C_{switchgear,start} = 15,000$ € and the incremental cost for 50 MVA of additional breaking capacity will be equal to $C_{switchgear,incrm.} = 610.5$ €.

The above assumptions for the cost of investment are calculated according to average costs¹² of transmission lines, given by the British Network Operator, whereas ABB provided the typical prices for MV switchgear of several breaking capacities. The hypothetical investment budget available for this specific network is equal to 200,000 €. Inflation, fluctuations of equipment prices and technological advances will be ignored.

In Section 5.2.4.2 the network operator receives a subsidy of 567 €/year for each additional MW of generation capacity connected to the network. If a marginal equivalent benefit of 20 is attached to all Capacity Expansion Locations (CELs) as in the previous Chapters, then each additional MW of generation capacity will increase the OPF objective function by $r=20$. According to (7.19) the marginal relaxation Δs_e of system constraint e will increase the monetary benefit of the network operator by $\Delta R_e = k \cdot \lambda_e \cdot \Delta s_e$, where λ_e is the LaGrange multiplier of e and $k = \frac{R}{r} = \frac{567}{20} = 28.35$ €/MWyear. In our example, the growth of monetary

¹² Acquired with personal communications during CIRED 2005 conference in Turin.

benefit ΔR_e from the upgrade of lines/transformers and switchgear minus their cost (see beginning of Section), according to (7.21), gives the expected net profit from each investment. Equation (7.22) compares those net profits and defines the optimum investment, which would result in the maximum possible net profit for the network operator.

7.8.2 Results

Using the above parameters for the economics and triggering of investments a series of simulations was completed, which implemented the RPM for the 12-bus network of the example. For all the figures produced from the RPM the same notation was used to signify investments. The green squares along the plot of total capacity represent investment iterations i.e. small upgrades of network equipment. Tags next to the squares show the exact iteration that the investment is planned for. The notation used for the tags is the following:

→ *iteration, investment*

where *iteration* is the RPM iteration that *investment* is planned for. Iteration 0 represents the current network status. Thus, no investment is planned for this iteration in any case. An investment is defined by a) 'Tf-t' for an investment on transmission line f-t and b) 'Sm>n' for an investment on switchgear at bus m, which breaks fault currents in transmission line m-n. For example, '→2,T1-2' means that the RPM has planned in the second iteration an investment for the upgrade of transmission line connecting buses 1 and 2.

7.8.2.1 Investment plan under strict power factor control

First, RPM created an investment plan under strict Power Factor Control (PFC) for new generators. More details of how this assumption is formulated in the OPF for capacity allocation can be found in Chapter 2. The allocation of new capacity to the three CELs (buses 1, 10 and 11), the E/IP (bus 12) and total new capacity with respect to the cost of investment is given in Figure 7.4. Figure 7.4 shows that RPM plans first the reinforcement of S1>2 and then S10>4 with 50 MVA higher breaking capacity. Figure 7.4 also gives us the information that if this investment plan is implemented, then total new capacity¹³ will reach 51 MVA, 2 MVA more than the connecting capacity of the current network, which is 49 MVA (see Table 6.4). After 2 iterations planning stops. This is because there is no realistic investment available for RPM. Other constraints (e.g. statutory voltage level) become binding, which cannot be alleviated with any of the available investment options.

Figure 7.5 presents the progress of benefit from the new capacity for the network operator. Planned investments increase benefit for the network operator from new capacity from 36,140 €/year to 38,027 €/year, an increment of 1,887 €/year. According to the x-axis of Figure 7.4, the total cost of investment is 30,000 €. If these investments are assumed to be implemented

¹³In comparison with the existing capacity

quickly (e.g. in a few years), then a good estimation of the time needed for the investment return to equalise the cost is about $30,000/1,887=15.9$ years.

Finally, Figure 7.6 presents the expected tap ratio and regulated voltage at bus 12 of the transformer with automatic tap changer throughout the planning period. The tap changer does not respond, because the voltage at the regulated bus lies within the desired bandwidth (1 ± 0.2 p.u.).

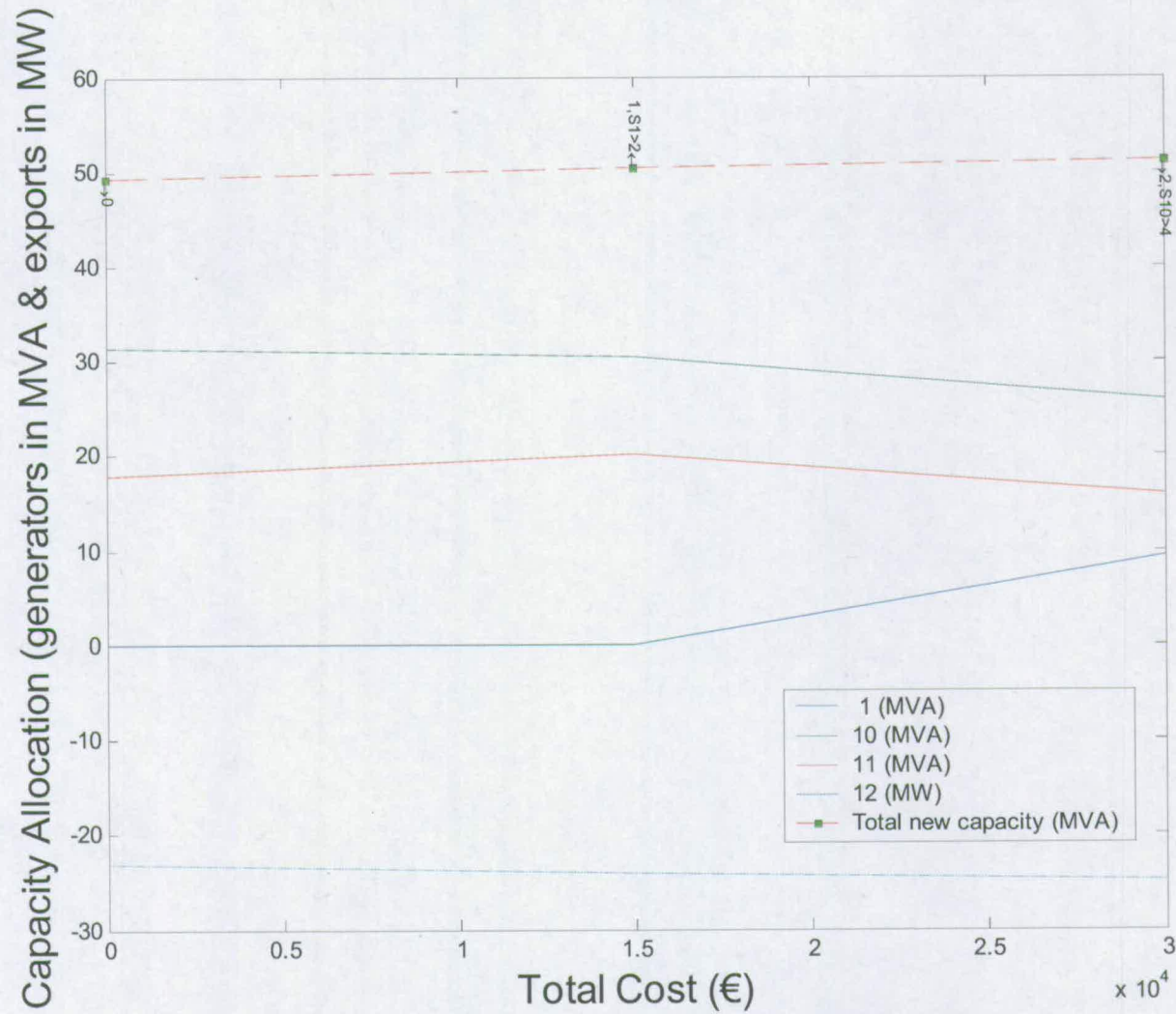


Figure 7.4 Investment plan created by the RPM assuming strict PFC for new generators.

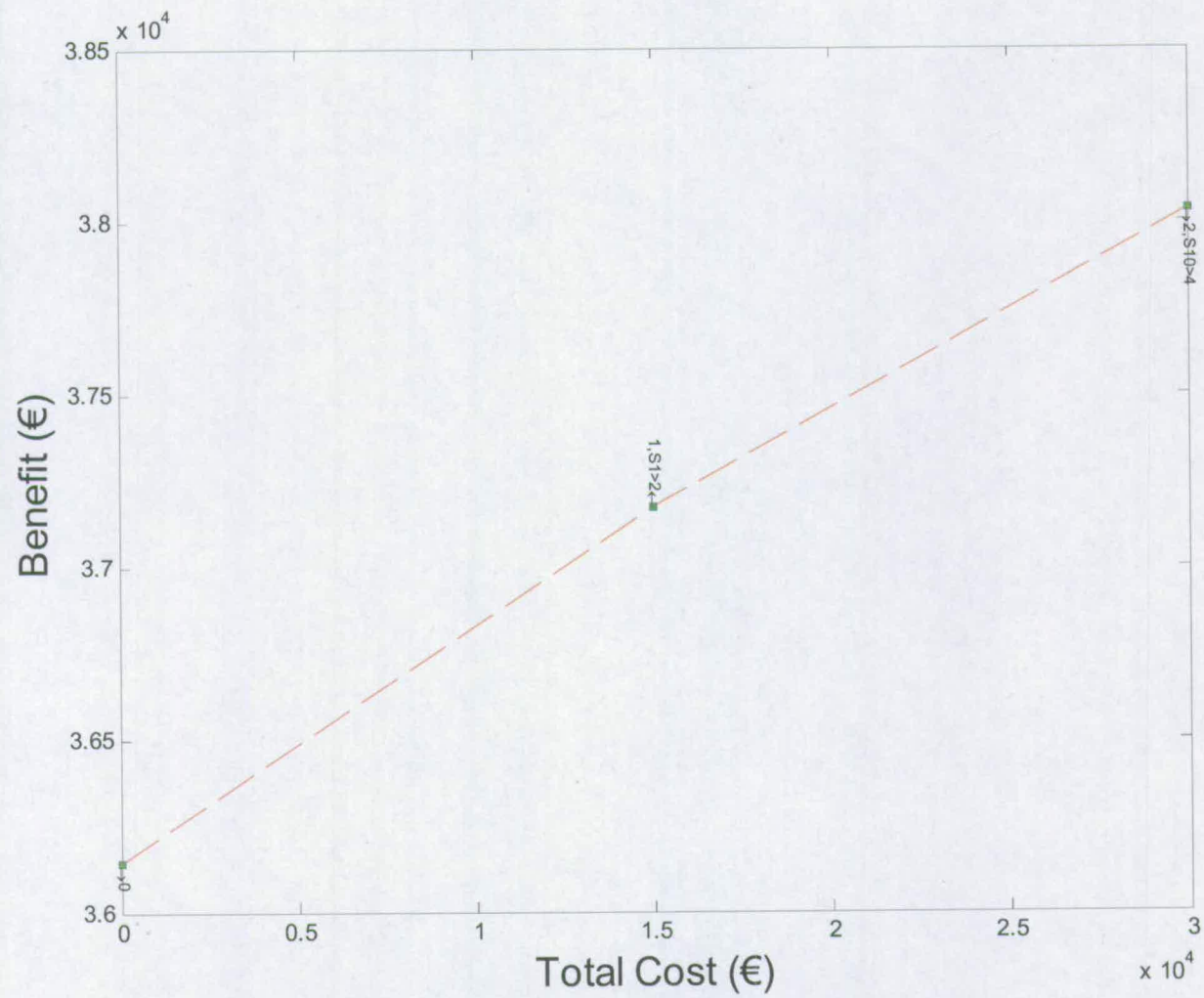


Figure 7.5 Benefit for the network operator vs. cost of investment.

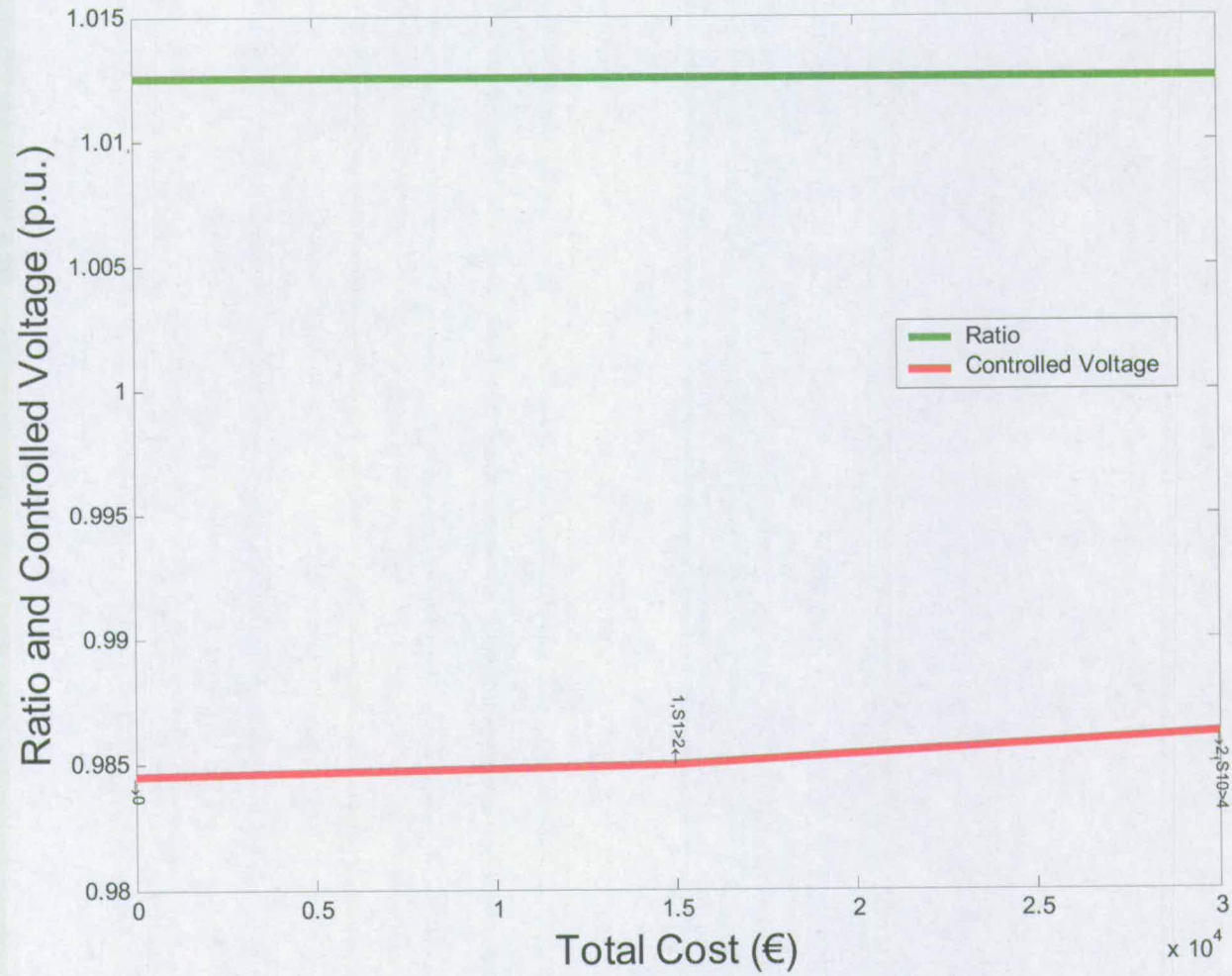


Figure 7.6 Expected tap ratio and regulated voltage of the transformer with automatic tap changer vs. cost of investment.

7.8.2.2 Investment plan under widespread use of Intelli-Gens

In this case RPM created an investment plan assuming that all new generators will be Intelli-Gens. More details of how this assumption is formulated in the OPF for capacity allocation can be found in Chapter 5. The allocation of new capacity to CELs, the E/IP and total new capacity with respect to the cost of investment is given in Figure 7.7. The RPM plans the reinforcement of transmission lines T4-9 and T4-10 by 30 and 45 MVA, respectively. It also plans the replacement of S1>2 and S10>4 by switchgear with 50 and 350 MVA higher breaking capacity, respectively. The investment plan stops after 23 iterations when the reinforcement plan reaches the limitations of the available budget. The planning horizon is short enough for illustration purposes. However, planning investments much further into the future wouldn't have much meaning in most practical cases. Probably other investments will be done on the network by the time the above plan will be completed, e.g. new transmission lines between buses or even new buses, which would practically change the study case. According to the same figure, at the end of the investment plan total new capacity reaches 106 MVA. This is 50 MVA more than the connecting capacity of the current network, which is 56 MVA (see Table 6.4), if all new generators are Intelli-Gens!

Figure 7.8 shows the benefit from new capacity for the network operator with respect to the cost of investment. Planned investments increase benefit from new capacity from 43,130 €/year to 92,818 €/year, an increment of 49,688 €/year. According to the x-axis of Figure 7.8, the total cost of investment is 198,663 €/year. Each investment on the network starts paying back from the time it is implemented. Things become confusing if the fact is considered that after a few investments it is difficult to allocate the increase of capacity to specific investments. Each investment represents the relaxation of a constraint, which may or may not become binding in different points in time. Therefore, the calculation of return from planned investments scattered all over the planning horizon (as in this case) is quite a complicated process. Here, a very conservative estimation of the pay-back time will be calculated by dividing the total cost of investment with the profit for the network operator from the additional capacity due to investment. This is equivalent to assuming that all investments start to pay back at the end of the planning horizon, which gives a much longer time than reality. Such an approximate calculation gives a pay-back time of $198,663/49,688=4$ years for this case.

This high investment return can be explained by the fact that once an investment is included in the plan and the high initial cost is paid, then each further upgrade costs very little in comparison with the benefit it will bring for the network operator. For example, the first planned investment on T4-9 costs 50,000 € and increases benefit by $61,850-54,900=9,950$ €/year (Figure 7.9a). Therefore, the first investment on T4-9 will pay back in about $50,000/9,950=5.03$ years. The next investment on the same line costs 5,000 € and increases

benefit by $68,300 - 62,300 = 6,000$ € (Figure 7.9b). Therefore, the later investment will pay back in about $5,000 / 6,000 = 0.83$ years, which is less than 6 times lower than in the first case!

Figure 7.10 presents the response of the tap changer with respect to the total cost of investment.

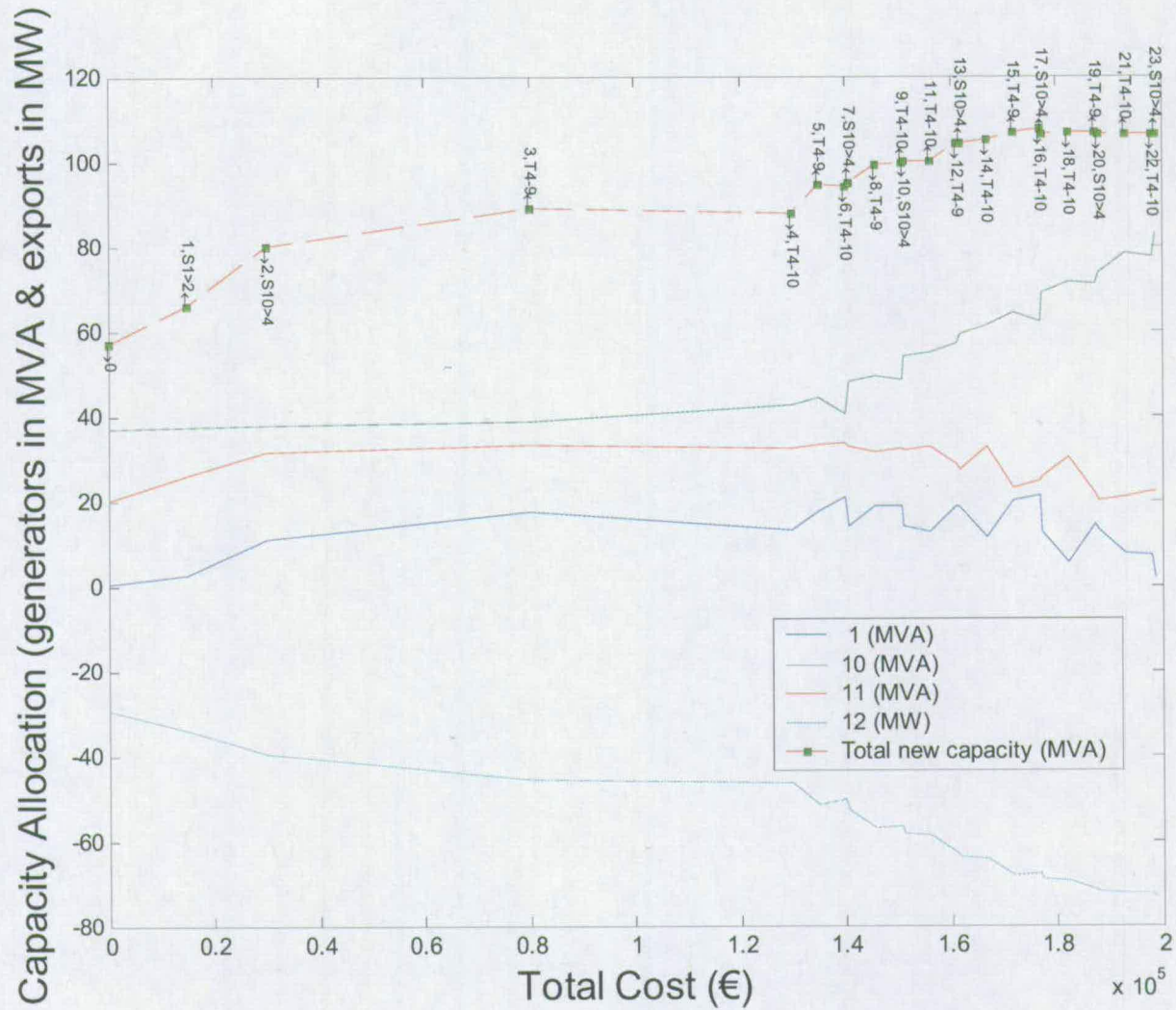


Figure 7.7 Investment plan created by the RPM assuming widespread deployment of Intelli-Gens.

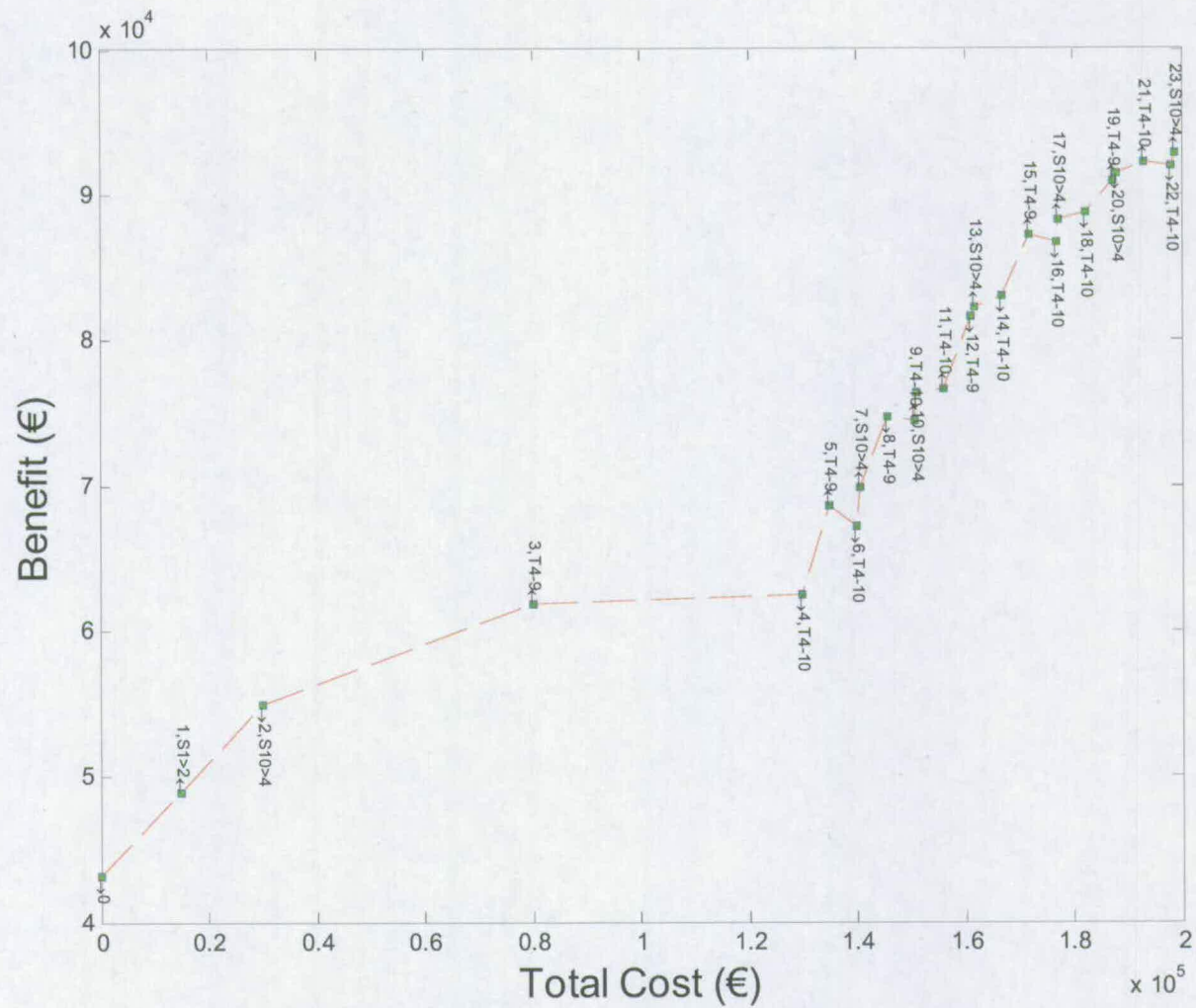


Figure 7.8 Benefit for the network operator vs. cost of investment.

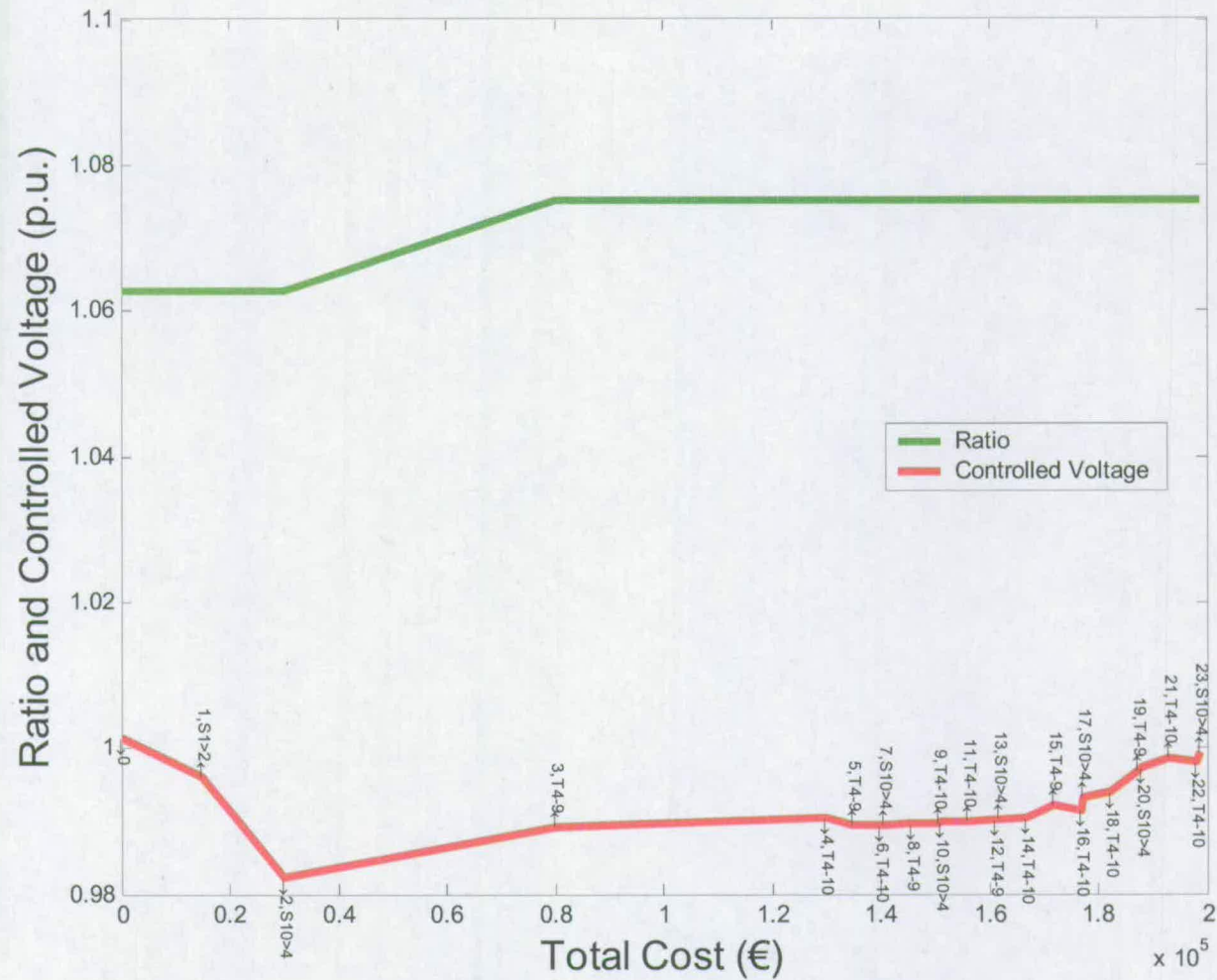


Figure 7.10 Expected tap ratio and regulated voltage of the transformer with automatic tap changer vs. cost of investment.

7.8.2.3 Investment plan under widespread use of ECVC-Gens

In this case RPM created an investment plan assuming that all new generators will be ECVC-Gens. More details of how this assumption is formulated in the OPF for capacity allocation can be found in Chapter 5. The allocation of new capacity to CELs and the E/IP, as well as the total new capacity with respect to the cost of investment is given in Figure 7.11. The RPM plans the reinforcement of T4-9, T4-10 by 35, 40 MVA each. It also plans the replacement of S1>2 and S10>4 by switchgear with 50 and 400 MVA higher breaking capacity, respectively. The plan stops after 25 investment iterations, when the reinforcement plan reaches the limitations of the available budget. However, the plan is so extensive that it wouldn't have much meaning to continue further. Figure 7.11 also show that in 24 iterations total new capacity can reach 114 MVA, if this reinforcement plan is to be used. This is 58 MVA more than the 56 MVA (see Table 6.4) connecting capacity of the current network if all new generators are ECVC-Gens.

Figure 7.12 presents the benefit from new capacity for the network operator with respect to investment cost. Planned investments increase benefit from 43,129 €/year to 97,989 €/year from the additional capacity due to investment on the network infrastructure, an increment of 54,860 €/year. According to the x-axis of Figure 7.12, the total cost of investment is 199,274 €. An approximate calculation (as in 6.9.3.2) gives a pay-back time of $199,274/54,860=3.6$ years for this case.

Figure 7.13 presents the response of the tap changer with respect to the total cost of investment.

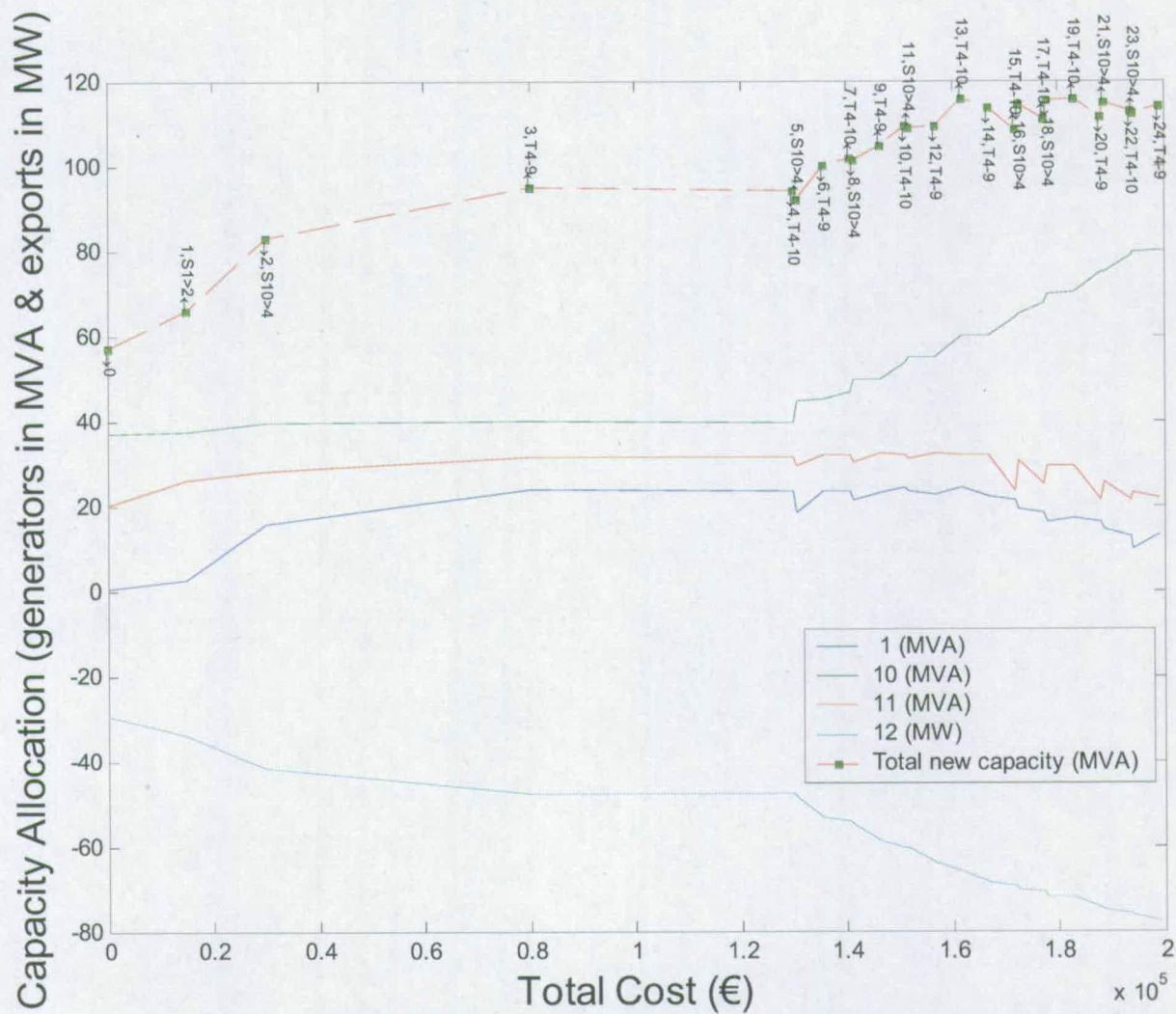


Figure 7.11 Investment plan created by the RPM assuming widespread deployment of ECVG-Gens.

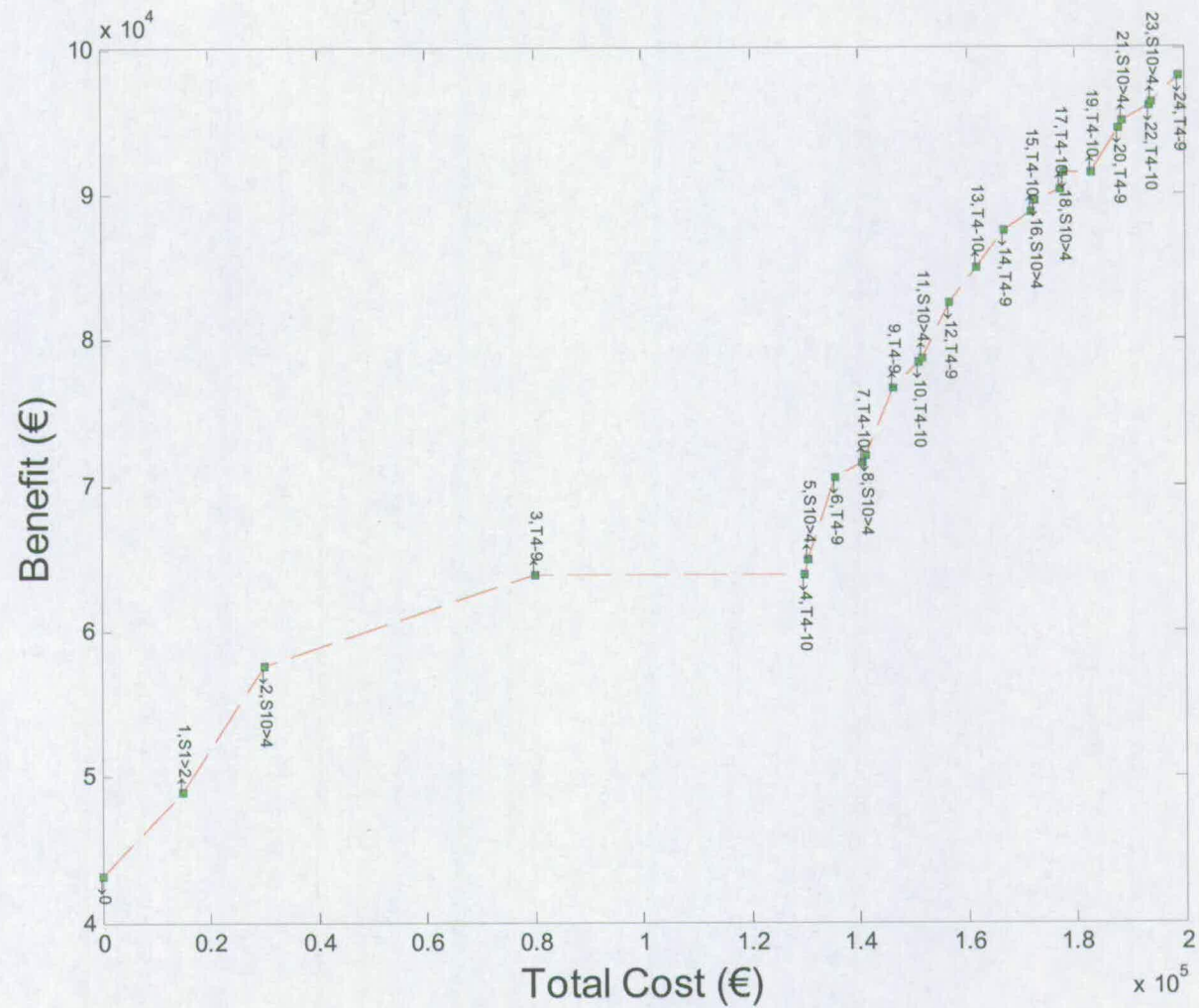


Figure 7.12 Benefit for the network operator vs. cost of investment.

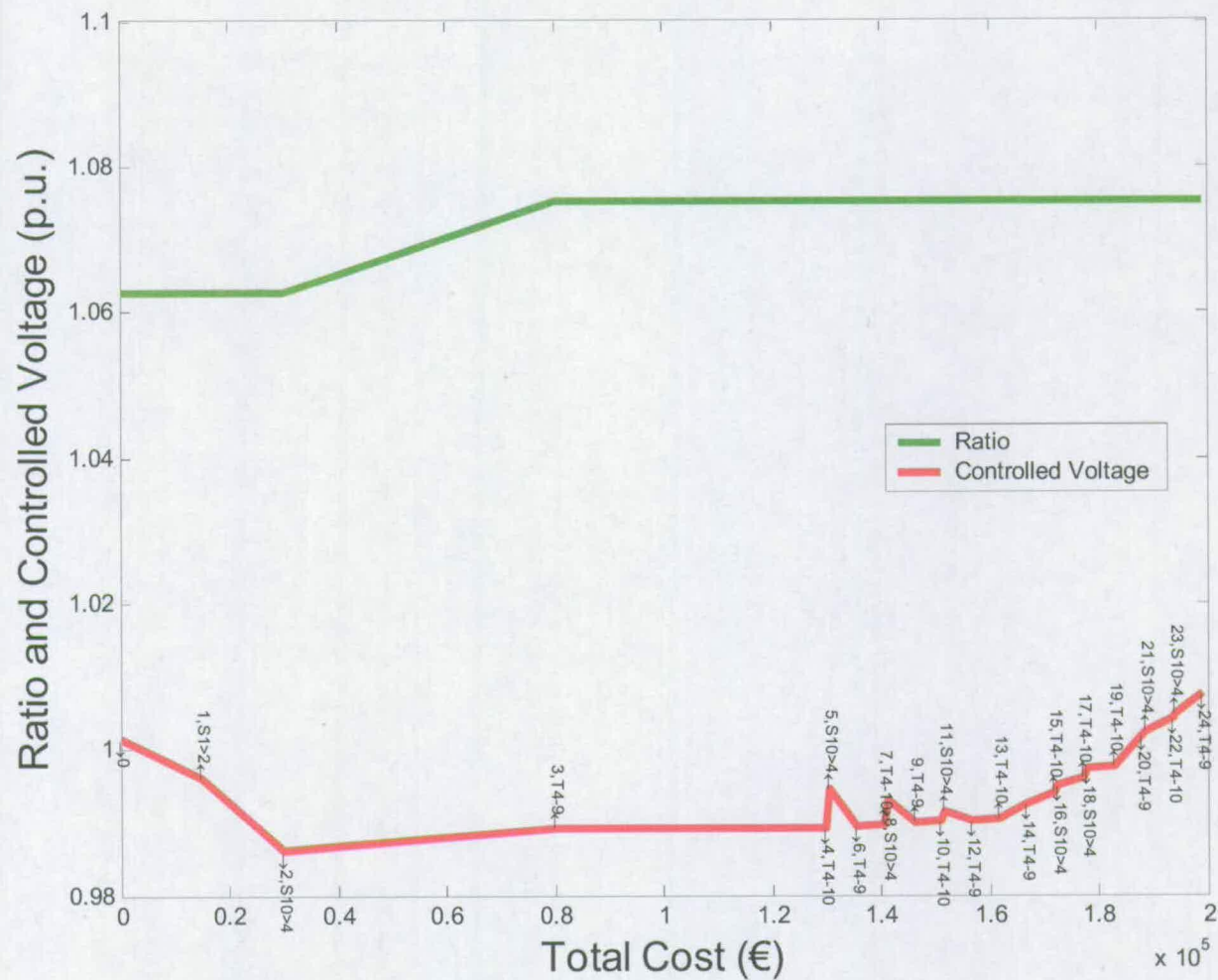


Figure 7.13 Expected tap ratio and regulated voltage of the transformer with automatic tap changer vs. cost of investment.

7.8.2.4 Investment plan under widespread use of CVC-Gens

Finally, RPM created an investment plan assuming that all new generators will be CVC-Gens. More details of how this assumption is formulated in the OPF for capacity allocation can be found in Chapter 5. The allocation of new capacity to CELs and the E/IP, as well as the total new capacity with respect to the cost of investment is given in Figure 7.14. The RPM plans the reinforcement of T4-9 and T4-10 by 35 and 40 MVA, respectively. It also plans the replacement of S1>2 and S10>4 by switchgear with 50 and 400 MVA higher breaking capacity, respectively. The investment plan stops after 24 iterations, when the RPM invests the entire available budget. At the end of the reinforcement plan total new capacity could reach 114 MVA. This is 39 MVA more than the connecting capacity of the current network, which is 75 MVA (see Table 6.4) if all new generators are CVC-Gens.

Figure 7.15 shows the benefit from new capacity for the network operator with respect to investment cost. Planned investments increase benefit from new capacity for the network operator from 49,480 €/year to 98,011 €/year, an increment of 48,531 €/year. The total cost of investment is 199,274 €. An approximate calculation (as in 6.9.3.2 and 6.9.3.3) gives an investment pay-back time of $199,274/48,531 = 4.3$ years for this case.

Figure 7.16 presents the expected tap ratio and regulated voltage at bus 12 of the transformer with automatic tap changer throughout the planning period.

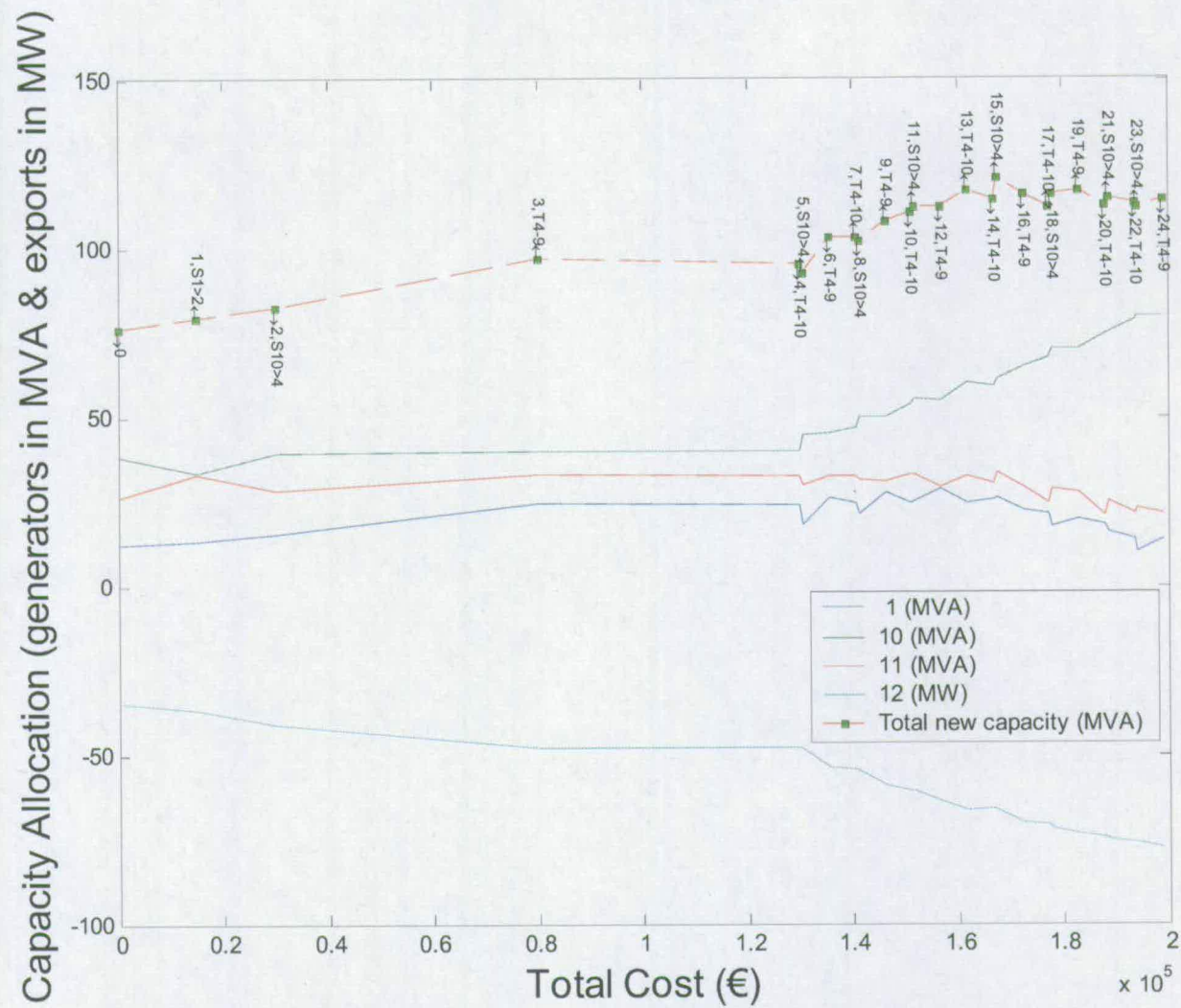


Figure 7.14 Investment plan created by the RPM assuming widespread deployment of CVC-Gens.

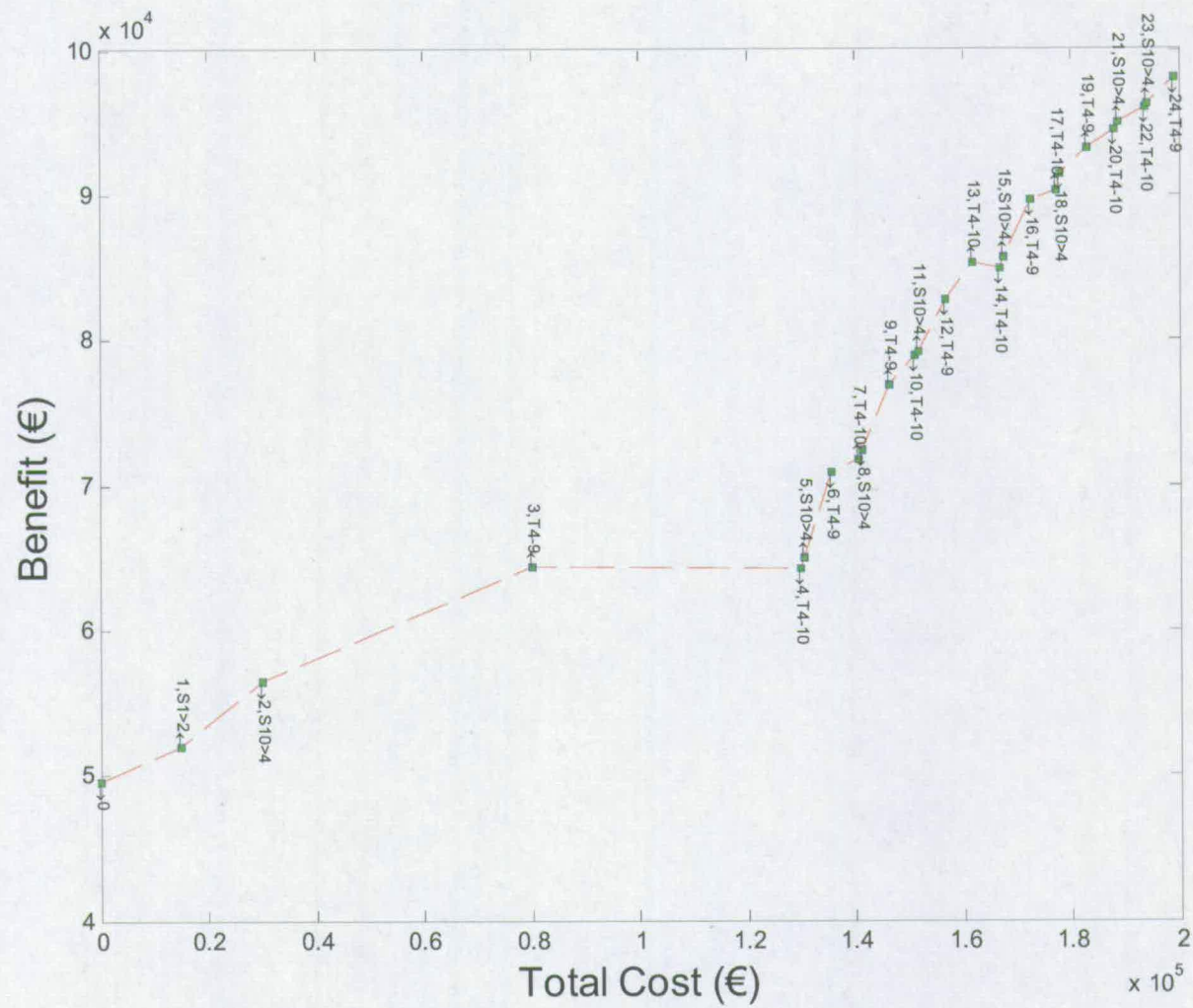


Figure 7.15 Benefit for the network operator vs. cost of investment.

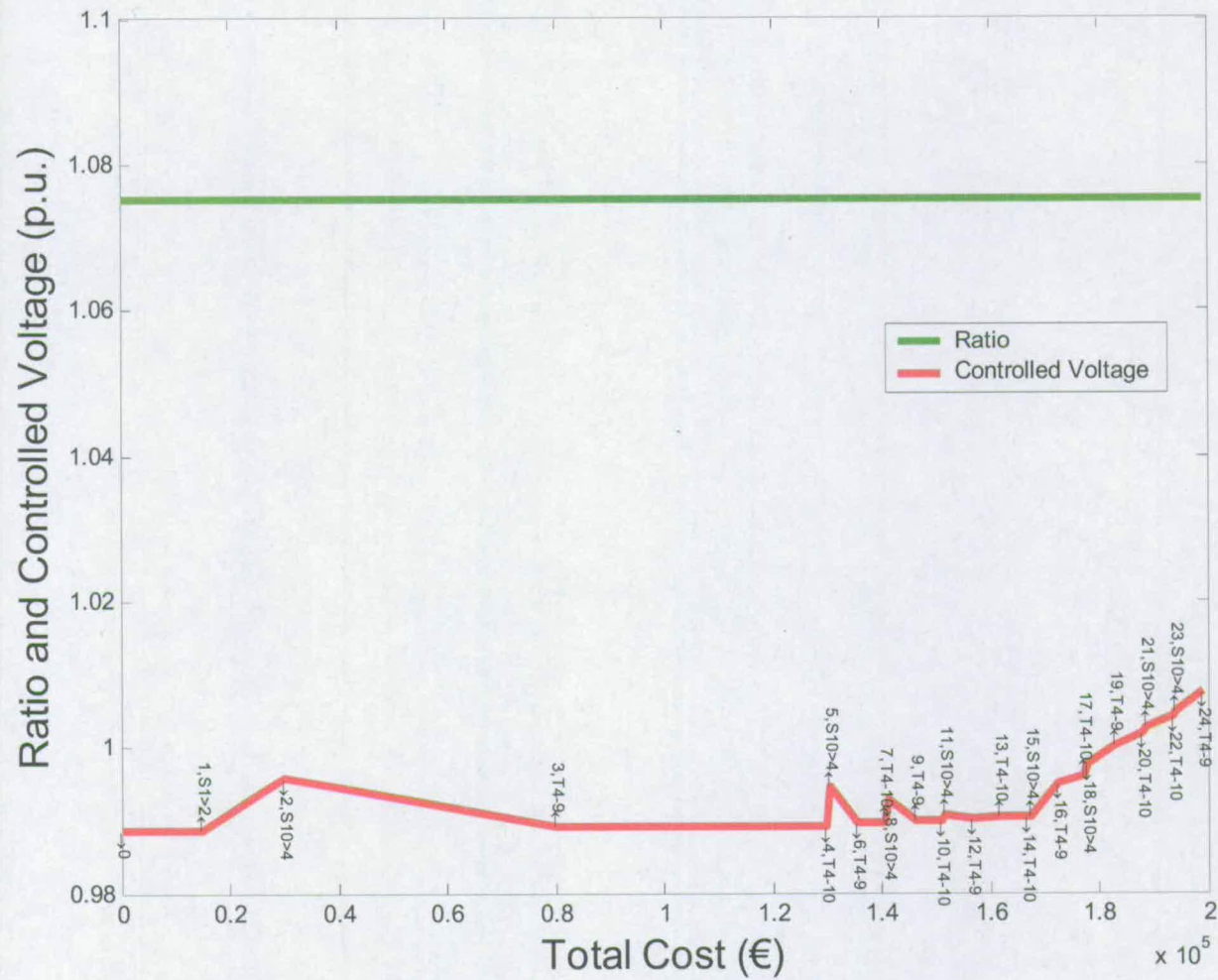


Figure 7.16 Expected tap ratio and regulated voltage of the transformer with automatic tap changer vs. cost of investment.

7.8.3 Comparison of results

Table 7.1 presents a summary of the reinforcement plans produced by RPM for the four voltage control policies.

	PFC	Intelli-Gens	ECVC-Gens	CVC-Gens
Initial capacity (MVA)	49	56	56	75
Final capacity (MVA)	51	106	114	114
Capacity increase (MVA)	2	49	57	38
Planning Horizon (RPM iterations)	2	23	24	24
Investments (MVA)	S1>2 : 50 S10>4 : 50	T4-9 : 30 T4-10 : 45 S1>2 : 50 S10>4 : 350	T4-9 : 35 T4-10 : 40 S1>2 : 50 S10>4 : 400	T4-9 : 35 T4-10 : 40 S1>2 : 50 S10>4 : 400
Approximate pay-back time (years)	15.9	4	3.6	4.3

Table 7.1 Comparative analysis of reinforcement plans.

As it was demonstrated in detail in Chapter 5, the introduction of Fault Level Constraints (FLCs) forces Intelli-Gens and ECVC-Gens to have similar behaviour in voltage control. The consideration of the impact of new capacity on losses during optimisation of allocation in Chapter 6 did not change this fact. That is why total capacity before and after investment on the network has similar values, with a slight advantage towards the more relaxed ECVC policy (see row ‘capacity increase’ in Table 7.1).

The row of ‘investments’ in Table 7.1 clearly shows that in the case of non-PFC voltage control policies the RPM plans investments on some common equipment between policies: a) the transmission line 4-9 (T4-9), b) the transformer between buses 4 and 10 (T4-10), c) the switchgear at buses 1 and 10 breaking the primary circuit of the transformers between buses 1, 2 (S1>2) and 10, 4 (S10>4), respectively. Therefore, even if the future preferred voltage control policy is not clear at present, the network operator can still plan the upgrade of this equipment, anyway.

The reinforcement of network infrastructure improves the capability of the power system to absorb new generation capacity. Consequently, voltages at generator buses rise and the

emergency voltage control mode of ECVC-Gens is activated. Therefore, the more the network is reinforced the more possible it becomes for ECVC-Gens to operate as CVC-Gens. This is proven by the comparative results for initial and final generation capacity for each voltage control policy in Table 7.1. Even if $75-56=19$ MVA more CVC-Gens capacity can be installed on the current network, the allocation plan converges with the one for ECVC-Gens at the end of the reinforcement plan (both achieve 114 MVA of new capacity). Figure 7.17, where the total capacity with respect to investment cost for each case is superimposed on the same graph, demonstrates this convergence between the two policies. Generally, total capacity is much higher for relaxed PFC policies than strict PFC after the implementation of the investment plans. The difference between total capacities achieved for PFC, Intelli-Gens and CVC-Gens/ECVC-Gens increases as the cost of investment increases. A similar tendency exists for the benefits from new capacity in each case for the network operator with respect to investment cost (Figure 7.18).

The last row of Table 7.1 presents the approximate pay-back time of the investment plan for each voltage control policy. For all cases, the relevantly low pay-back time can be explained by an economic practice included in the RPM. Once an investment is included in the plan and the high initial cost is paid, then each further upgrade costs very little in comparison with the benefit it will bring for the network operator. Let us not forget that this approximate 'pay-back time' is a very conservative estimation of the actual pay-back time. The total cost of investment was divided by the profit for the network operator from the additional capacity due to investment. This is equivalent to assuming that all investments start to pay back at the end of the planning! Of course investments on the network start to pay back immediately after they are implemented, thus, actual pay-back time is expected to be even shorter in reality.

The two investments done under PFC do not release much additional generation capacity. As a consequence, the respective investment pay-back time is much higher than for the other 'flexible' policies (see last row of Table 7.1). The reason for this is founded upon a fundamental disadvantage of PFC. There is practically no control over voltage rise due to new generation capacity, so statutory voltage limits soon become the unresolved constraints for generation expansion. On the contrary, the other more relaxed voltage control policies seem to favour investment on the network, delivering a much lower pay-back time (see last row of Table 7.1). If the results are examined in more detail, then the disadvantage of the current voltage control policy (PFC) with respect to efficiency is demonstrated once more: the pay-back time of investments under PFC is one order higher than the other more relaxed policies. Especially, if a central voltage control policy is implemented (CVC-Gens or ECVC-Gens) pay-back time is around 4 times less than under PFC.

The implementation of CVC or ECVC generator voltage control practically requires the development of an extensive and highly sophisticated communication system. This system must be able to receive information from all generators about local voltage patterns and transmit control signals for their reactive power output ... in real time! Such a sophisticated

communication system may require significant investment from network operators and creates a serious technical challenge for engineers.

Summarising the comparative analysis, Intelli-Gens perform very competitively in comparison with the centralised CVC-Gens or ECVC-Gens. They combine a low pay-back time for investment on the network with the applicability and simplicity of a decentralised voltage control policy. The 'intelligent' voltage control algorithm is integrated into the generators' field control, so the investor on generation bears the additional, but small cost. Therefore, even if CVC-Gens and ECVC-Gens exploit the enhanced capabilities of the reinforced network slightly better, the high cost for the network operator of a centralised voltage control system may be a serious drawback for its establishment.

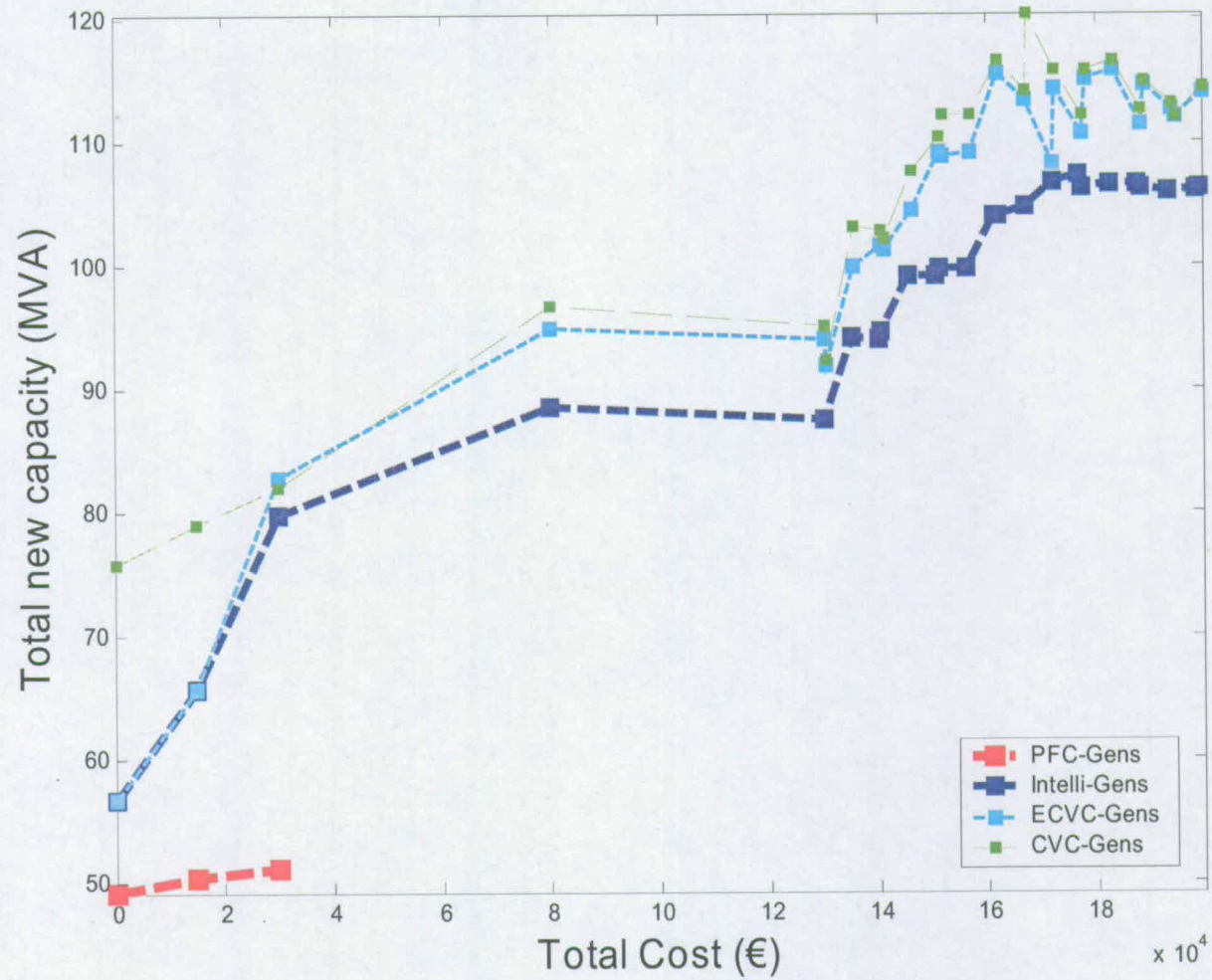


Figure 7.17 Total new capacity vs. cost of investment under different voltage control policies.

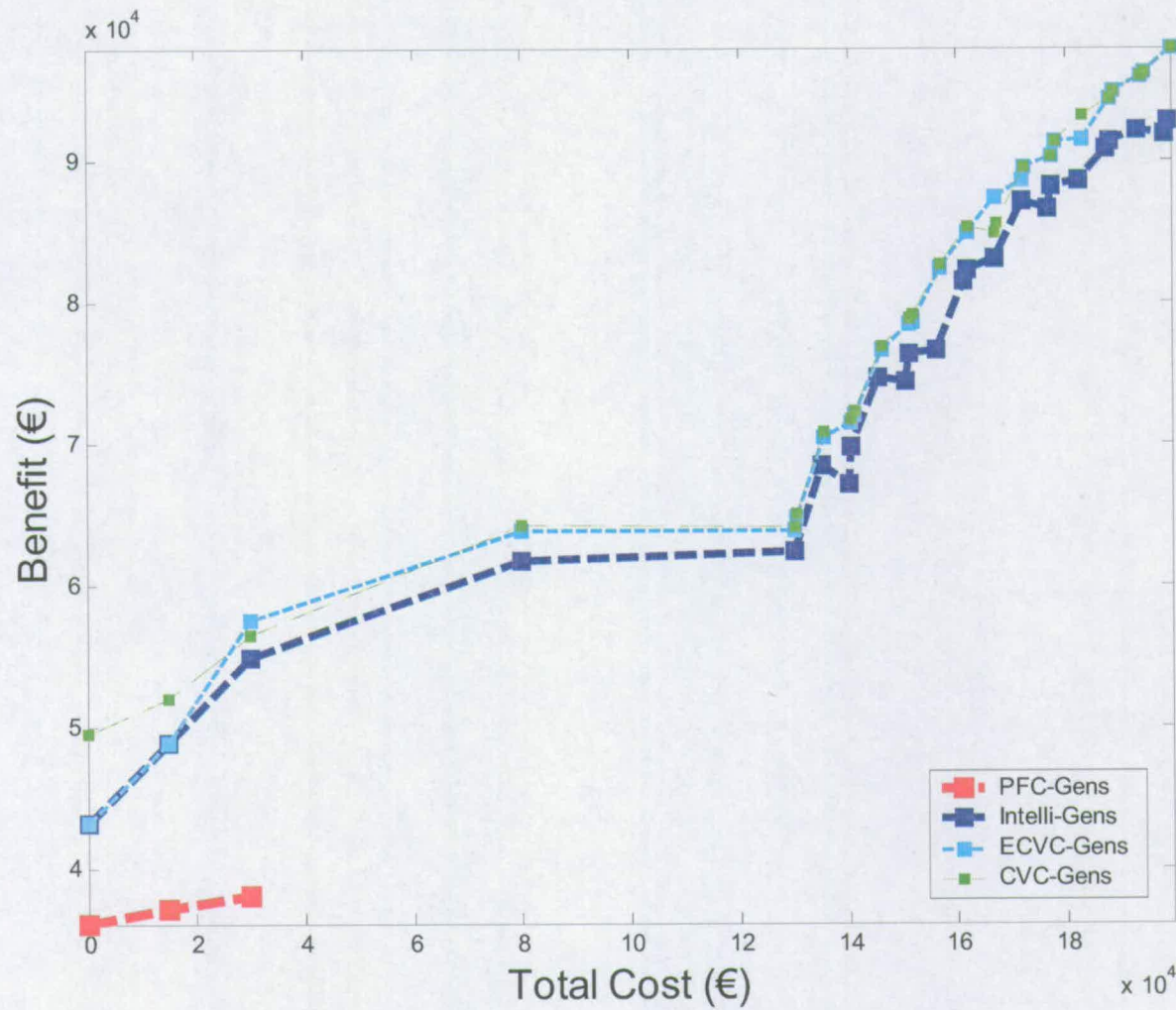


Figure 7.18 Benefit for the network operator vs. cost of investment under different voltage control policies.

7.9 Chapter summary

This Chapter examines a Reinforcement Planning Mechanism (RPM), as it was termed, of existing networks. 'Existing' in the sense that network equipment can only be upgraded/replaced, so that the network topology is maintained throughout planning. The target of the mechanism is to expand the capability of the network to absorb new generation capacity so that the system will always be able to serve the increasing demand. This is done in the most economic way for the network operator. The economic signals produced for constraint equipment from the OPF during the allocation of new capacity are used to define the most profitable investment at each point in time. The final product of RPM is an investment plan, which can be used by the network operator or other potential investors as a guide for when and which equipment to upgrade.

The formulation developed in Chapter 5 was used to incorporate different voltage control algorithms for new generators. A technique presented in Chapter 6 was also used to consider the impact of the allocation of new capacity on losses; because in that Chapter it was shown that a big part of new generation may be consumed on transmission (especially for the more 'relaxed' voltage control policies).

The RPM was tested on the same 12-bus, LV, meshed network; a typical topology for urban/suburban networks. It was demonstrated that the current strict PFC policy, followed by most network operators, may not only limit the capability of the existing network to absorb new generation capacity (as it was shown in Chapter 5 as well), but also reduce the positive effects of investment on the network in comparison with the other 'relaxed' voltage control policies. Finally, the decentralised (Intelli-Gens), partially centralised (ECVC-Gens) or centralised (CVC-Gens) control of the reactive power output of new generators, drastically decreases the pay-back time of investment with the latter giving the most impressive results. However, the slightly higher allocation efficiency of a centralised voltage control system in comparison with 'intelligent' decentralised control probably does not justify the high capital and maintenance cost it bears for the network operator. Therefore, intelligent voltage control algorithms should be considered as a competitive alternative to the current trend towards central management. Of course, further research is needed to clarify the technical and economic advantages of each approach before any specific inferences are announced. The certain thing is that under any of the more 'relaxed' voltage control policies, centralised or decentralised, network infrastructure becomes an attractive investment option.

8. THE IMPACT OF FAULT LEVELS ON THE ECONOMIC OPERATION OF POWER SYSTEMS

8.1 Introduction

In the previous Chapters Optimal Power Flow (OPF) was considered as a tool for network capacity analysis. However, the original version of OPF is a well-known tool in power engineering. It defines the optimal operating point of generators to cover the demand with respect to system constraints, for instance voltage levels on buses, lines thermal limits and the active and reactive power capability of the generators. Traditionally, protection was designed to meet the security needs of a vertically integrated power system, where expected fault levels were more or less predictable under all scenarios. Therefore, it was rather improbable for the specifications of the switchgear equipment to restrict any OPF solution.

Indeed, fault current breaking devices usually do not constitute a constraint for the economic operation of well planned power systems under normal conditions (e.g. UK and most European and North-American power systems). Nevertheless, in great disasters even these power systems are called to operate under completely unpredicted conditions. Surviving switchgear, which is designed for an entirely different mode of operation may even exacerbate, rather than remedy, the problem by malfunctioning.

Furthermore, the competitive environment of the modern electricity markets reduces the system's security margins, while parts of networks and their maintenance pass to private operators. Generation and network patterns appear that were not considered in the original planning of the protection. Similarly, in some developing countries, power companies compromise security investment with the urgent need for new generation. Thus, there may be cases nowadays that OPF solutions may result in fault currents exceeding the breaking capability or capacity of the existing switchgear during a possible fault, leaving the system practically unprotected. A preliminary study carried out by the Power Systems Engineering Research Center in the U.S. acknowledged *'the potential economic impact arising from the increase of fault current due to the interconnection of new merchant plants'* and that *'the generation of the merchant plants under the fault current limitation may result in higher cost of operation than the operation without this constraint'* [75].

Therefore, a methodology is needed to regulate the operation of such 'non-conventional' power systems with respect to the limitations posed by existing switchgear. If some economy could be achieved towards this fundamental aim, then it would be more than desirable. This

Chapter presents the formulation of an enhanced OPF with these additional constraints. No new variables are introduced and they can be directly introduced to any optimisation process performing the OPF. Tests on a simple 12-bus network verified the significant impact of fault levels on the economic operation of power systems that operate under extreme conditions.

Approximate fault current calculations, which are a standard in the industry, assume fixed values of voltages (e.g. 1 p.u. or 1.05 p.u.) and therefore do not reflect the influence of pre-fault load current. The idea behind the approach described in this work is to make calculations more precise by calculating fault currents as a function of actual, rather than assumed, values of pre-fault voltages. The OPF can change the values of the pre-fault voltages, thus, adjust the expected values of fault currents.

8.2 Incorporation of FLCs in OPF as an operating tool

Fault Level Constraints (FLCs) refer to the operational limitations of switchgear equipment during a fault. If the specifications of the switchgear equipment are not adequate to clear or isolate a fault, then not only the equipment itself will be possibly damaged, but the operation of a broader part of the power system will become insecure. Generally, it is the magnitude of a fault current which is compared with the specifications of the switchgear equipment. Two basic specifications of switchgear are capacity and breaking capability. They both set limits to the magnitudes of fault currents that the switchgear can securely break. Therefore, this analysis will focus on the magnitudes of fault currents, rather than their complex values.

The magnitude of the expected fault currents $|I_{i,j}^f|$ between buses i and j for a fault at bus f must comply with the maximum allowed by the specifications $|I_{spec}|$:

$$|I_{i,j}^f| < |I_{spec}| \Leftrightarrow |I_{i,j}^f| - |I_{spec}| < 0 \quad (8.1)$$

In order to include FLCs in OPF, the first task is to find a mathematical expression linking the expected fault currents with the OPF variables. These variables are the voltage magnitude $|V_i|$ and angle φ_i of any bus i and the real P^g and reactive Q^g power of any generator g . In Chapters 2 and 3 a detailed analysis of how this can be done for OPF as a planning tool for the allocation of new generation capacity has been presented. The difference between that analysis and our current target is practically the convenience that in OPF as an operating tool the impedance matrix, the basic element of fault analysis, is constant for a given network, generators' reactance and fault type/location. In the formulation of OPF as a planning tool this matrix was defined as a function of new capacity, since the serial reactances of new generators were expressed as a function of their size.

The fault current flowing through a line with series impedance $\tilde{z}_{i,j}$ for a fault on bus f is given by the equation (see Section 2.6.8):

$$I_{i,j}^f = (V_i - V_j - FSF_{i,j}^f \cdot V_f) / \tilde{z}_{i,j} \quad (8.2)$$

where V_i, V_j, V_f are the voltages of buses i, j, f . They are described in magnitude and angle by the OPF variables $|V_k|, \varphi_k$, where $k=i, j, f$. $FSF_{i,j}^f = (z_{i,f} - z_{j,f}) / z_{f,f}$ where $z_{i,f}, z_{j,f}$ and $z_{f,f}$ are the elements of the impedance matrix. This matrix is constant, as it was explained in the previous Section. Therefore, equation (8.2) shows that FLCs are effectively constraints on the complex nodal voltages.

The solution of Nonlinear Programming problems, such as OPF, generally requires an iterative procedure to establish a direction of search at each step towards the global optimum. This requires the calculation of the derivatives of all non-linear equality and inequality constraints with respect to each OPF variable. This section briefly presents the derivatives for the new constraints.

The analysis differentiates according to the fault location.

- If $f \neq i$ and $f \neq j$ then:

$$\frac{d|I_{i,j}^f|}{d|V_i|} = \frac{x + y \tan \varphi_i}{|I_{i,j}^f| |\tilde{z}_{i,j}|^2} \cos \varphi_i, \quad \frac{d|I_{i,j}^f|}{d\varphi_i} = -\frac{x + y \tan \varphi_i}{|I_{i,j}^f| |\tilde{z}_{i,j}|^2} |V_i| \sin \varphi_i \quad (8.3)$$

- If $f = i$ then:

$$\frac{d|I_{i,j}^f|}{d|V_i|} = \frac{x A + y B}{|I_{i,j}^f| |\tilde{z}_{i,j}|^2} \cos \varphi_i, \quad \frac{d|I_{i,j}^f|}{d\varphi_i} = -\frac{x A + y B}{|I_{i,j}^f| |\tilde{z}_{i,j}|^2} |V_i| \sin \varphi_i \quad (8.4)$$

- If $f = j$ then:

$$\frac{d|I_{i,j}^f|}{d|V_i|} = \frac{x + y \tan \varphi_i}{|I_{i,j}^f| |\tilde{z}_{i,j}|^2} \cos \varphi_i, \quad \frac{d|I_{i,j}^f|}{d\varphi_i} = \frac{x + y \tan \varphi_i}{-|I_{i,j}^f| |\tilde{z}_{i,j}|^2} |V_i| \sin \varphi_i \quad (8.5)$$

Similarly, $\frac{d|I_{i,j}^f|}{d|V_j|}, \frac{d|I_{i,j}^f|}{d\varphi_j}$ and $\frac{d|I_{i,j}^f|}{d|V_f|}, \frac{d|I_{i,j}^f|}{d\varphi_f}$ can be calculated.

According to (8.2), fault currents are connected only with the OPF variables describing the voltages across the line under consideration and the faulted bus. Therefore :

$$\frac{d|I_{i,j}^f|}{d|V_s|} = \frac{d|I_{i,j}^f|}{d\varphi_s} = 0 \quad \forall \text{ bus } s \neq i, j, f \quad (8.6)$$

The only difference between the above set of derivatives and the one calculated in Chapter 3

for OPF as a planning tool is that $\frac{d|I'_{i,j}|}{dP^g} = \frac{d|I'_{i,j}|}{dQ^g} = 0 \quad \forall \text{ generator } g$. This is because here

the outputs of the generators represent their actual real and reactive output, not their capacity. The generators have a fixed size, their impedances are constant, and so their real or reactive output does not define their series reactance, as with OPF for capacity allocation. Fault currents are determined practically by the system voltage pattern (see (8.5) and (8.6)).

Finally, the number of FLCs included in the OPF during optimisation can be reduced using the Fault Level Constraints Reduction Algorithm (FLCRA) developed in Chapter 3. This algorithm identifies those FLCs which are binding for the OPF and includes them in the set of non-linear constraints.

8.3 Example

The simple LV 12-bus/15-line network that was used in all the previous Chapters will be used here, too, to demonstrate the impact of fault level constraints on the solution of the OPF. For a detailed description of the passive elements of the network please refer to Chapter 2. The production cost functions are shown on Figure 8.1 next to the respective generators. The average values of loads, in terms of active and reactive power consumption, are also shown in the same figure next to the respective loads. The internal subtransient reactance of generators is 15% on the generators' reactance base. The adequacy of the switchgear will only be assessed in terms of breaking capacity. The capacity of the switchgear installed at the ends of each transmission line and transformer complies with the UK standards: 250 MVA at 11 kV and 1000 MVA at 33 kV.

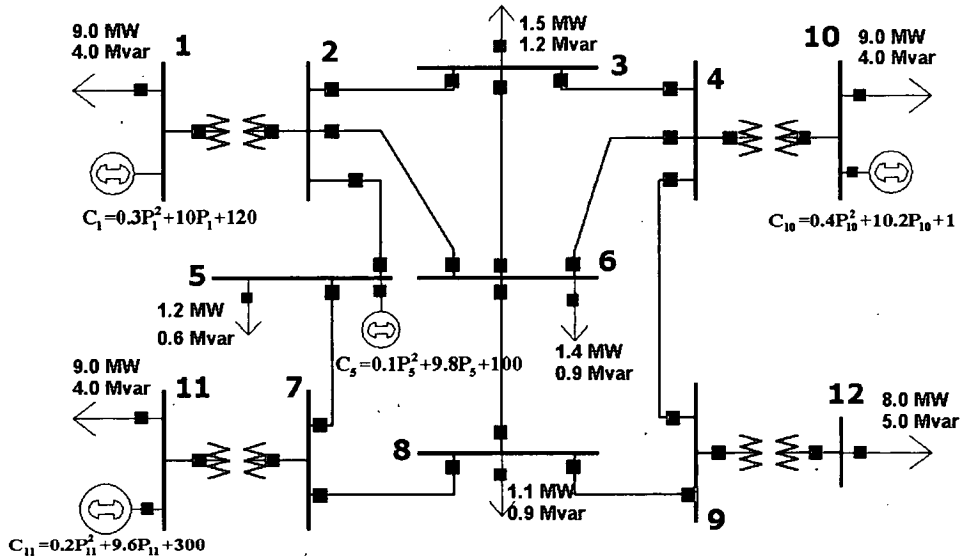


Figure 8.1 The 12-bus test case network.

In order to examine the impact of FLCs on the economic operation of the test case system, the OPF was solved under different operating scenarios. For each scenario the operating point of each generator and the overall system production cost before and after considering FLCs was recorded. The solutions ignoring FLCs were termed as ‘initial’, while the solutions which considered them were termed as ‘final’. The OPF which has the additional capability to consider FLCs was implemented in MATLAB with Sequential Quadratic Programming.

8.3.1 Average load (1st scenario)

First, the case that loads consume power equal to their average values was considered (presented in Figure 8.1). The operating point of generators and the total production cost of the initial solution are presented in Table 8.1. This solution violated the capacity of the switchgear connected to the primaries of transformers 1-2 and 10-4 by approximately 6% and 3%, respectively. The final solution is presented in the same table.

	Property	Initial	Final	Change (%)
Generator at bus 1	Real power (MW)	7.23	6.83	-5.53
	Reactive Power (MVar)	5.27	6.36	20.68
	Voltage (p.u.)	1.08	1.05	-2.78
Generator at bus 5	Real power (MW)	5.69	5.42	-4.75
	Reactive Power (MVar)	0.89	0.89	0.00
	Voltage (p.u.)	1.09	1.09	0.00
Generator at bus 10	Real power (MW)	12.27	12.52	2.04
	Reactive Power (MVar)	9.03	8.55	-5.32
	Voltage (p.u.)	1.08	1.05	-2.78
Generator at bus 11	Real power (MW)	15.60	16.06	2.95
	Reactive Power (MVar)	5.23	6.11	16.83
	Voltage (p.u.)	1.10	1.07	-2.73
Total production	Cost (€/h)	1051.73	1055.51	0.36

Table 8.1 Initial and final solutions of first scenario.

The last column of Table 8.1 presents the impact of FLCs as a percent change of the initial solution properties. FLCs increased the total production cost by 0.36 % and had an impact on the operating points of all generators. OPF shifted power production from the generators at buses 1 and 5 to generators at buses 10 and 11 in order to alleviate expected fault currents at the constraint switchgear.

8.3.2 Light load (2nd scenario)

In the second scenario, all loads are scaled down by 40 % (preserving their power factor). Such a scenario would result from light load conditions e.g. overnight. The initial and final solutions of this scenario are presented in

Table 8.2, in a similar manner to the results of the first scenario in Table 8.1. The initial solution violated the capacity of the switchgear connected to the primary of transformer 1-2 by 6 %. FLCs increased the total production cost only by 0.16 %, but still had an impact on the operating points of all generators. Significant power production shifted again from generators located at buses 1 and 5 to generators at 10 and 11.

	Property	Initial	Final	Change (%)
Generator at bus 1	Real power (MW)	3.11	2.99	-3.86
	Reactive Power (MVar)	3.05	3.58	17.38
	Voltage (p.u.)	1.08	1.05	-2.78
Generator at bus 5	Real power (MW)	4.50	4.30	-4.44
	Reactive Power (MVar)	0.49	-0.17	-134.69
	Voltage (p.u.)	1.09	1.06	-2.75
Generator at bus 10	Real power (MW)	5.68	5.91	4.05
	Reactive Power (MVar)	5.14	4.91	-4.47
	Voltage (p.u.)	1.08	1.04	-3.70
Generator at bus 11	Real power (MW)	11.13	11.24	0.99
	Reactive Power (MVar)	3.17	3.60	13.56
	Voltage (p.u.)	1.10	1.07	-2.73
Total production	Cost (€/h)	803.64	804.94	0.16

Table 8.2 Initial and final solutions of second scenario.

8.3.3 Heavy load (3rd scenario)

The third scenario simulates a case of heavy demand e.g. winter evening. All loads are scaled up by 40% (preserving their power factor). The initial and final solutions of this scenario are presented in Table 8.3, in a similar manner to the results of the first scenario and second scenario. The initial solution violated the capacity of the switchgear connected to the primaries of transformers 1-2 and 10-4 by approximately 7% and 6%, respectively.

	Property	Initial	Final	Change (%)
Generator at bus 1	Real power (MW)	11.39	10.51	-7.73
	Reactive Power (MVar)	7.53	9.54	26.69
	Voltage (p.u.)	1.09	1.06	-2.75
Generator at bus 5	Real power (MW)	6.90	6.53	-5.36
	Reactive Power (MVar)	1.38	-1.15	-183.33
	Voltage (p.u.)	1.09	1.06	-2.75
Generator at bus 10	Real power (MW)	19.08	19.37	1.52
	Reactive Power (MVar)	13.21	12.32	-6.74
	Voltage (p.u.)	1.09	1.05	-3.67
Generator at bus 11	Real power (MW)	19.95	21.00	5.26
	Reactive Power (MVar)	7.06	8.70	23.23
	Voltage (p.u.)	1.10	1.08	-1.82
Total production	Cost (€/h)	1357.35	1364.96	0.56

Table 8.3 Initial and final solutions of third scenario.

FLCs increased the total production cost by 0.56 % and had a major impact on the operating points of all generators. Generators at buses 1, 5 and 11 had to change their real power output more than 6% on average due to the additional constraints imposed by fault levels.

8.3.4 Planned network maintenance (4th scenario)

In the fourth scenario line 4-9 goes off-line due to planned maintenance. Loads are assumed to consume power equal to their average values. The initial and final solutions of this scenario are presented in Table 8.4. The initial solution violated the capacity of the switchgear connected to the primary of transformer 1-2 by approximately 6%.

	Property	Initial	Final	Change (%)
Generator at bus 1	Real power (MW)	7.96	6.45	-18.97
	Reactive Power (MVar)	6.15	9.25	50.41
	Voltage (p.u.)	1.09	1.06	-2.75
Generator at bus 5	Real power (MW)	5.90	5.56	-5.76
	Reactive Power (MVar)	1.44	-2.48	-272.22
	Voltage (p.u.)	1.09	1.06	-2.75
Generator at bus 10	Real power (MW)	9.49	9.60	1.16
	Reactive Power (MVar)	6.42	5.13	-20.09
	Voltage (p.u.)	1.08	1.04	-3.70
Generator at bus 11	Real power (MW)	18.26	20.16	10.41
	Reactive Power (MVar)	7.11	9.58	34.74
	Voltage (p.u.)	1.10	1.09	-0.91
Total production	Cost (€/h)	1055.80	1065.27	0.90

Table 8.4 Initial and final solutions of fourth scenario.

FLCs increased the total production cost by nearly 1% and had a major impact on the operating points of all generators. Especially the generators connected to buses 1 and 11 had to change their real power output by approx. 19% and 10%, respectively.

8.3.5 Constrained remote switchgear (5th scenario)

In the 5th scenario the ability of the enhanced OPF to alleviate constrained protection equipment, located remotely from generation units, is investigated. The breaking capacity of all switchgear connected on bus 6 was downgraded almost 10 times (11% of UK standard),

until it became binding for the OPF. The initial solution violated the capacity of the switchgear connected with lines 2-6, 4-6 and 6-8 by an average value of 25%. The initial and final solutions of this scenario are presented in Table 8.5.

The remote FLCs increased total production cost by more than 3.3%, the highest of all previous scenarios. Even if the downgrading of switchgear is not a practical situation, this scenario demonstrates the importance of distance between generation units and constrained protection equipment. The curve in Figure 8.2 depicts the strong link between breaking capacity of the downgraded switchgear and total production cost.

	Property	Initial	Final	Change (%)
Generator at bus 1	Real power (MW)	7.23	8.80	21.72
	Reactive Power (MVar)	5.27	5.64	7.02
	Voltage (p.u.)	1.08	0.99	-8.33
Generator at bus 5	Real power (MW)	5.69	5.07	-10.90
	Reactive Power (MVar)	0.89	0.59	-33.71
	Voltage (p.u.)	1.09	1.01	-7.34
Generator at bus 10	Real power (MW)	12.27	3.75	-69.44
	Reactive Power (MVar)	9.03	3.44	-61.90
	Voltage (p.u.)	1.08	0.93	-13.89
Generator at bus 11	Real power (MW)	15.60	24.68	58.21
	Reactive Power (MVar)	5.23	12.62	141.30
	Voltage (p.u.)	1.10	1.07	-2.73
Total production	Cost (€/h)	1051.73	1087.06	3.36

Table 8.5 Initial and final solutions of fifth scenario.

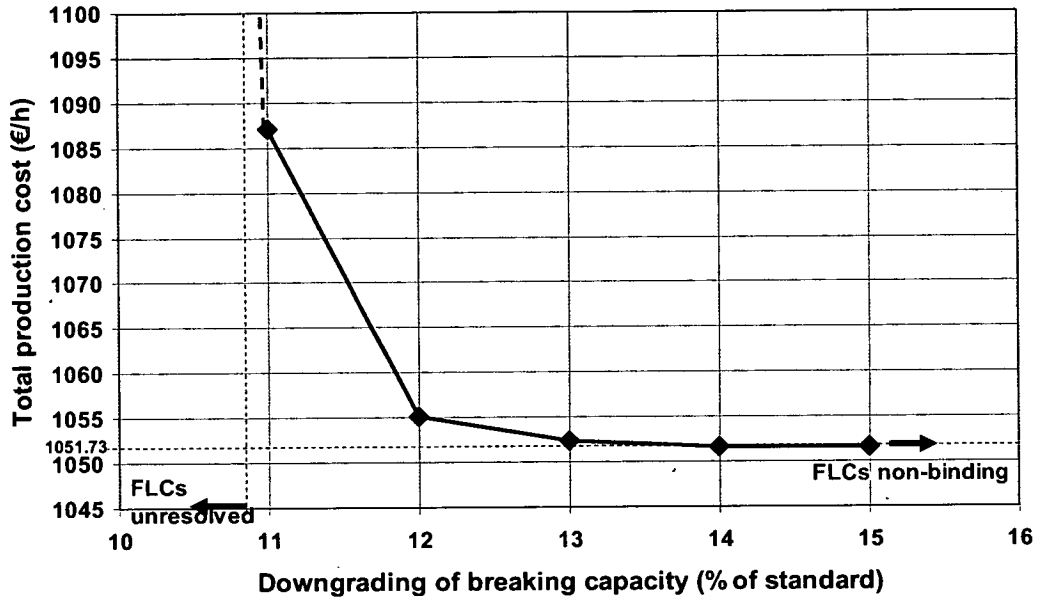
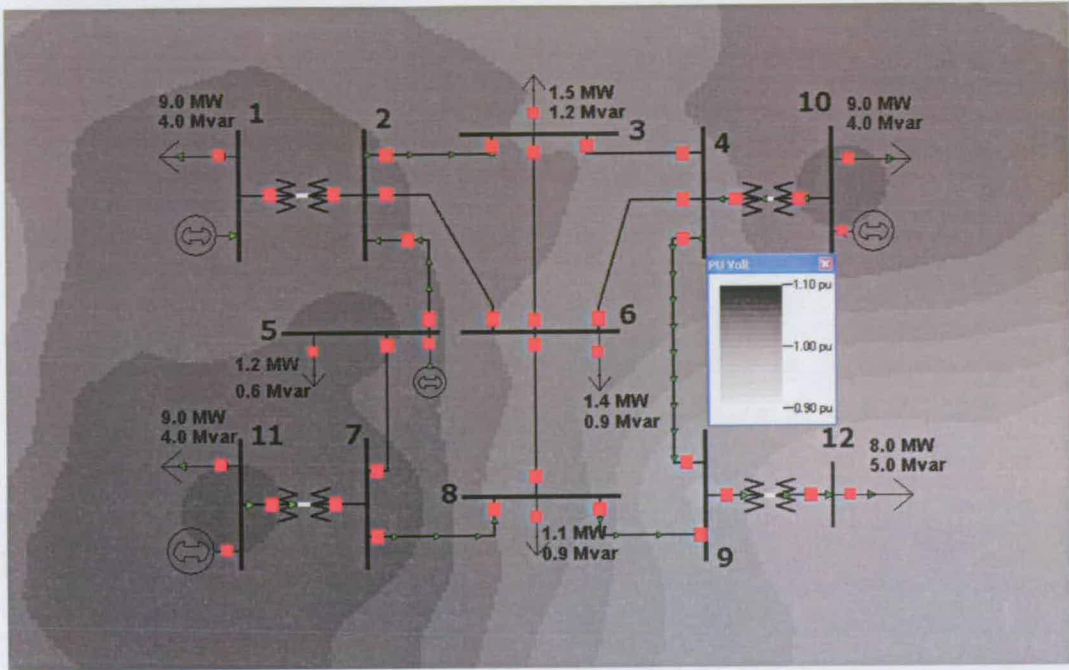


Figure 8.2 Production cost vs. breaking capacity of switchgear connected to remote bus 6.

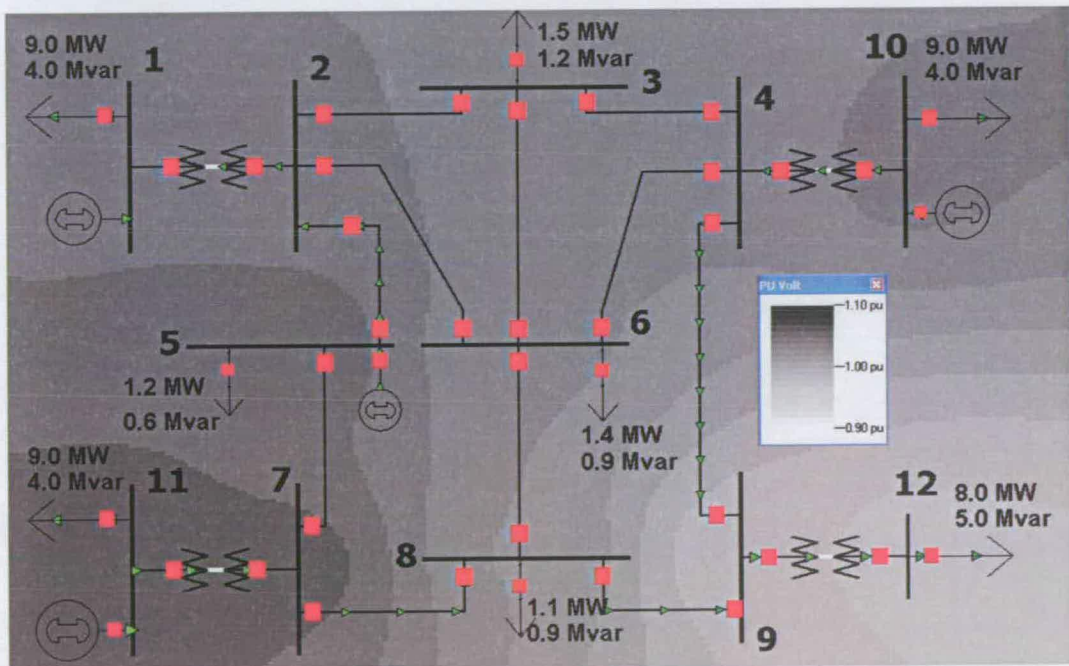
8.4 Effect of FLCs on OPF bus voltage pattern

According to the results of the test case, FLCs do not seem to affect significantly the total production cost under normal conditions (first two scenarios). The deviation from the initial solution increases when the system faces a higher demand (3rd and 4th scenarios), where the total production cost rises up to 1% (see last row of Table 8.3 and Table 8.4). A greater deviation is noticed when the binding FLCs correspond to protection equipment located away from generators (5th scenario).

On the contrary, FLCs have a major impact on the bus voltage pattern. The following contours depict the initial and final bus voltage pattern for each scenario that has been studied above. Figure 8.3, Figure 8.4, Figure 8.5, Figure 8.6 and Figure 8.7 are the p.u. voltage patterns of the system operating under the 1st, 2nd, 3rd, 4th and 5th scenario, respectively. Clearly, the introduction of FLCs seriously alters voltage patterns, especially around the lines and transformers where the constraint switchgear is connected. These are transformers 1-2, 10-4 for the 1st, 3rd scenarios, transformer 1-2 for the 2nd, 4th scenarios, lines 2-6, 4-6, 6-8 for the 5th scenario. Such a ‘manipulation’ of the voltage pattern is an expected function of the enhanced OPF during the alleviation of the violated FLCs. According to (8.2), the terminal bus voltages across the line where the constraint switchgear is connected determine the expected fault currents.

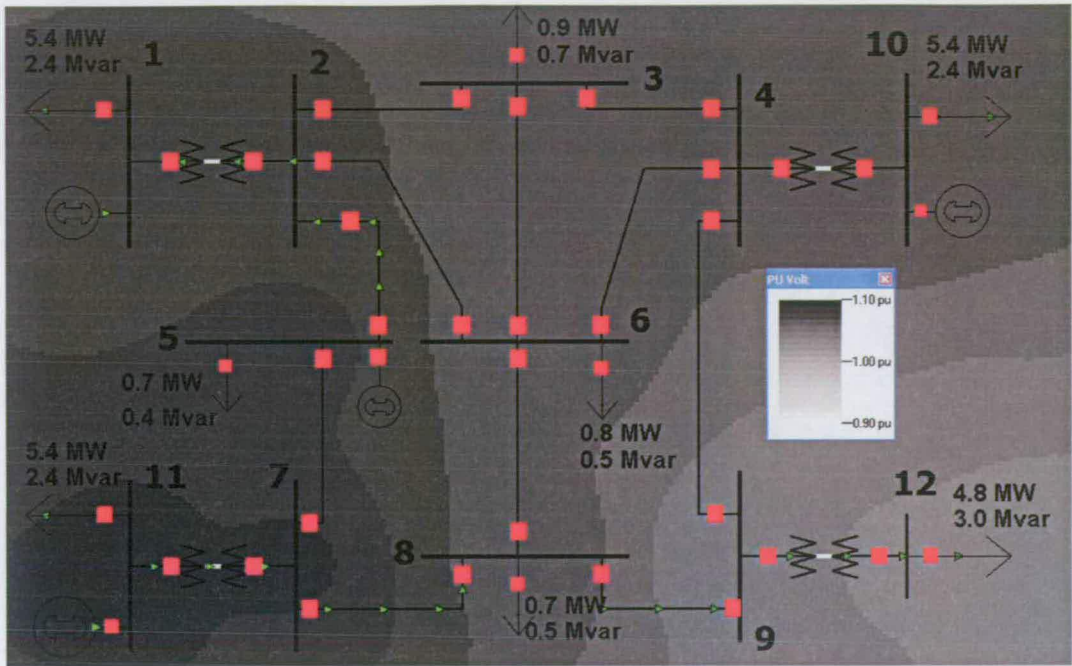


(a)

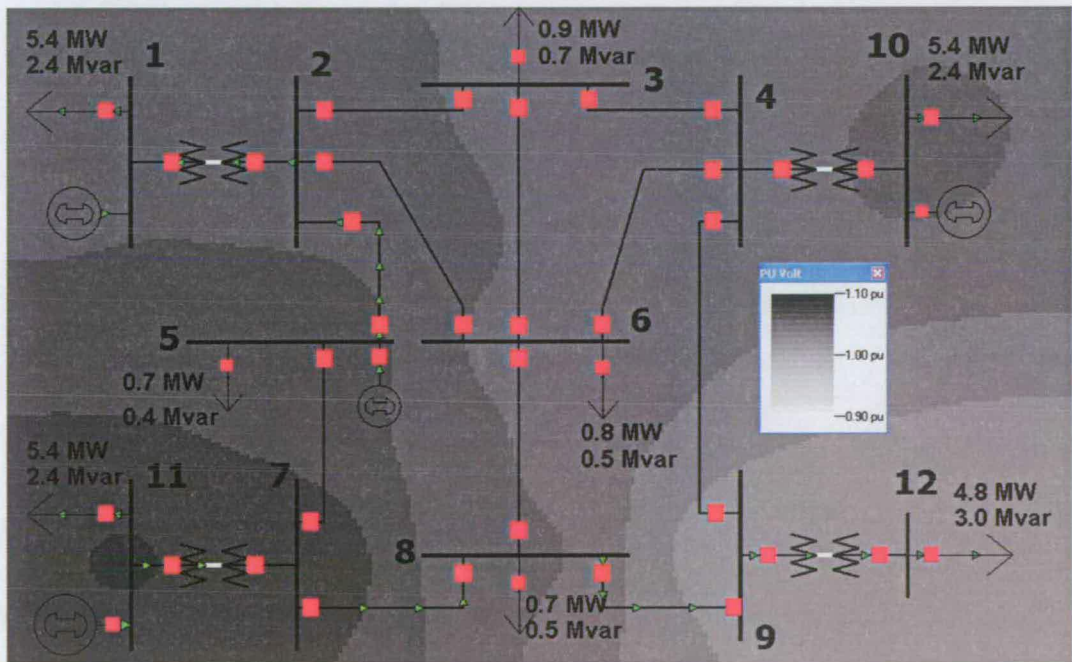


(b)

Figure 8.3 Initial (a) and final (b) bus voltage pattern for the 1st scenario (average load).

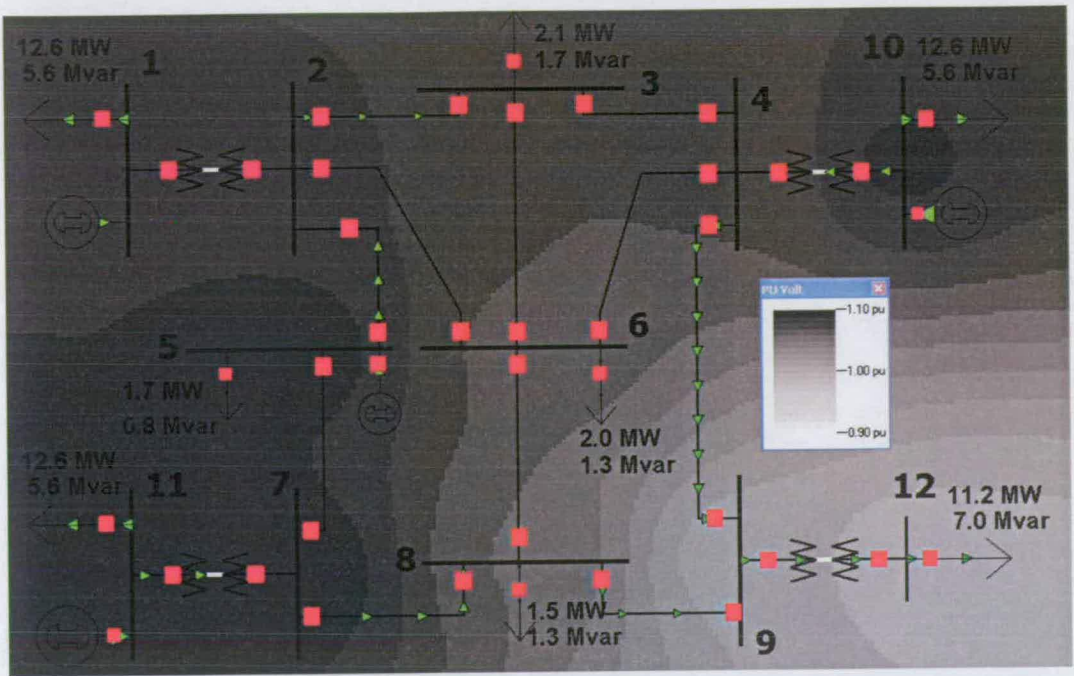


(a)

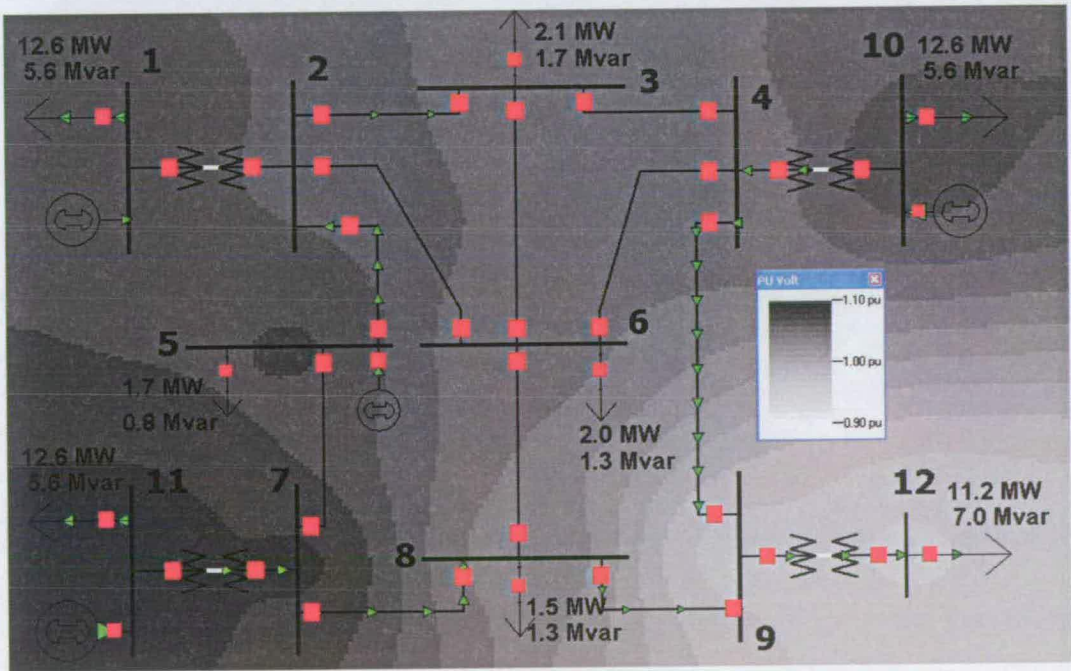


(b)

Figure 8.4 Initial (a) and final (b) bus voltage pattern for the 2nd scenario (light load).

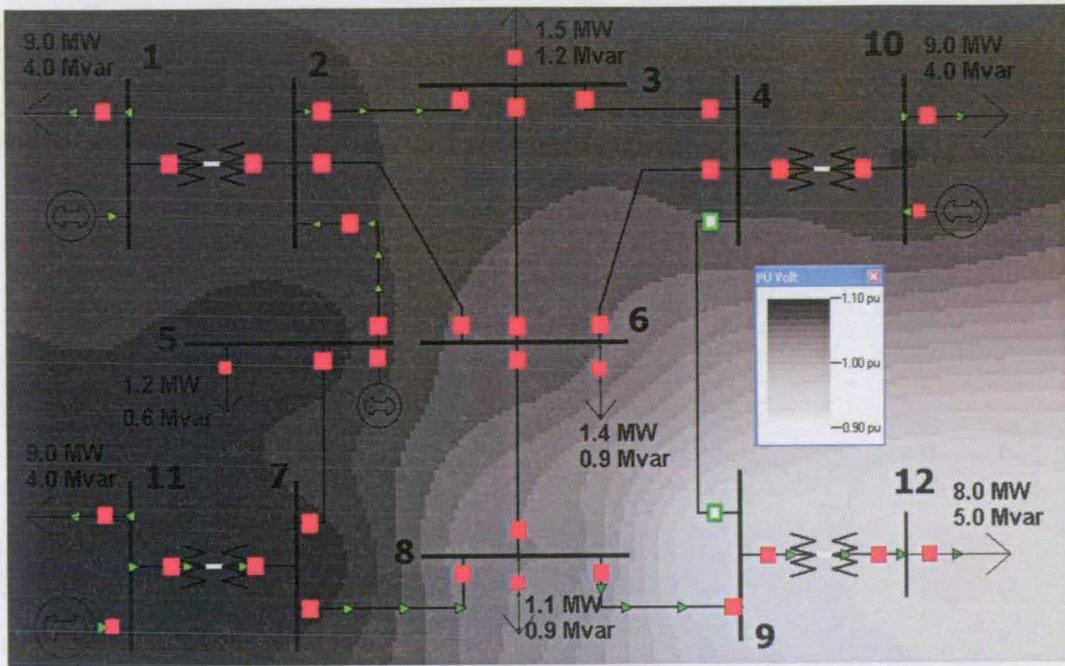


(a)

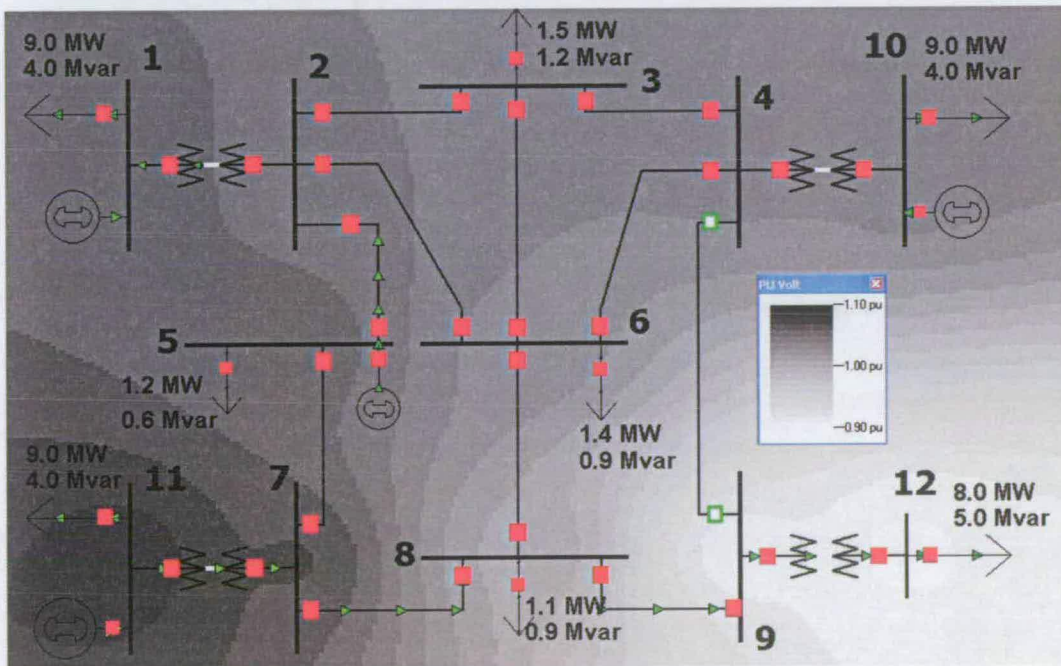


(b)

Figure 8.5 Initial (a) and final (b) bus voltage pattern for the 3rd scenario (high load).

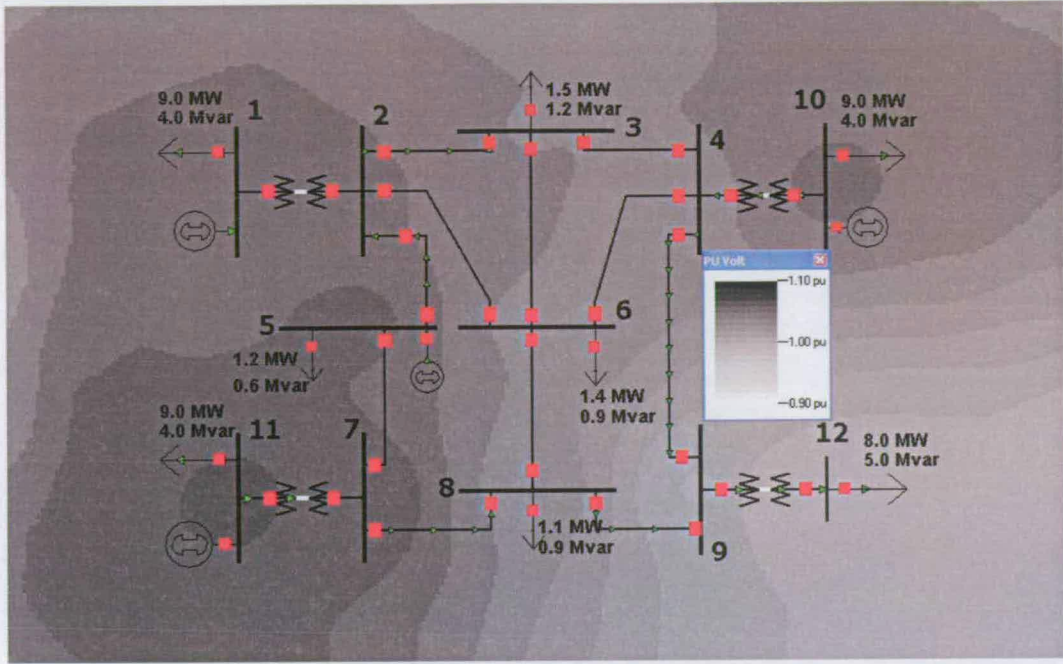


(a)

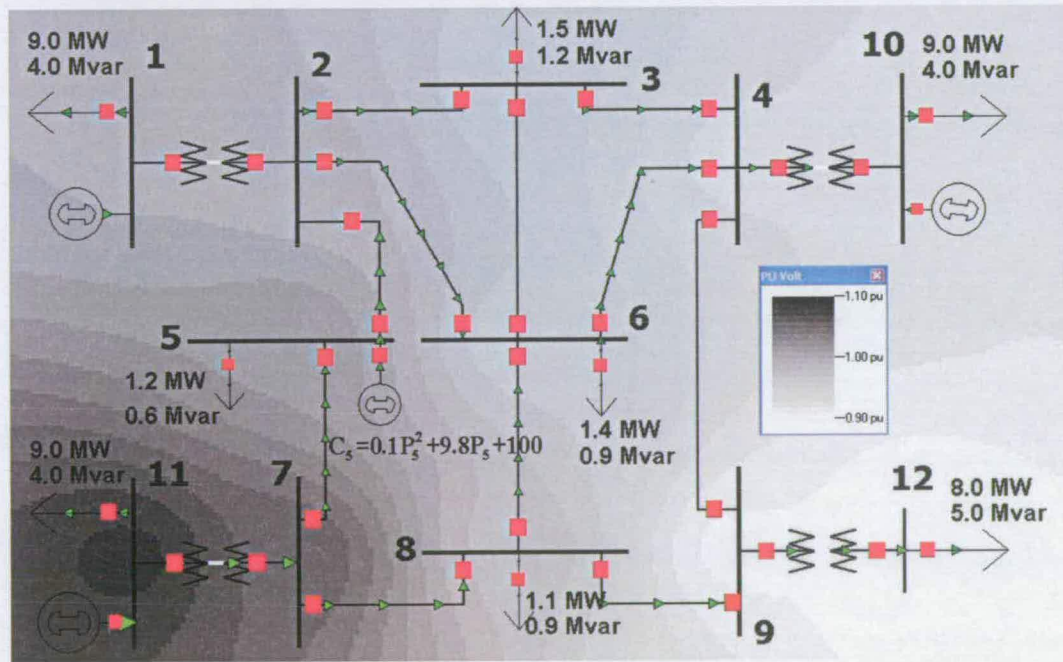


(b)

Figure 8.6 Initial (a) and final (b) bus voltage pattern for the 4th scenario (planned network maintenance).



(a)



(b)

Figure 8.7 Initial (a) and final (b) bus voltage pattern for the 5th scenario (constrained remote switchgear).

8.5 Performance of OPF with FLCs

The FLCRA reduced the number of FLCs from 360 to 2 or 1 (depending on the scenario), so the impact of FLCs on computational time was insignificant. It took less than 3 s for a 1.7 GHz CPU to solve any of the OPFs, whether FLC were considered or not.

One iteration was enough for FLCRA to trace the binding FLCs, which means that the violated FLCs from the initial solutions were the ones binding for the final solutions as well. Therefore, even though FLCRA is based on an iterative procedure it does not require many iterations to identify the additional constraints from fault levels.

8.6 Chapter summary

The aim of this Chapter was to demonstrate that fault levels may have a significant impact on the economic operation of modern power systems. First, a simple method was presented for the incorporation of fault level constraints in the Optimal Power Flow (OPF), the main optimisation tool for the economic operation of power systems. The constraints imposed by fault levels are converted to simple non-linear (inequality) constraints, described by variables of the conventional OPF. Most common OPF-solving engines already have the computational capacity to handle numerous non-linear constraints, such as the ones described by the power balance equations on buses. Therefore, once Fault Level Constraints (FLCs) are converted to non-linear constraints described by OPF variables, they can be directly introduced to any optimisation process performing the OPF. This enhanced OPF was applied on a simple 12-bus network under several operating scenarios. The results verified the significant impact fault levels have on the optimum operating point of the power system. Obviously, this method can facilitate the economic operation of heavily loaded or constrained networks. The simulation results demonstrate that the system operator has to take evasive action even under anticipated system conditions (e.g. heavy demand or planned maintenance), in order to alter the bus voltage pattern and avoid possible switchgear overstress. Such actions include slight changes of the real and reactive power output of generators, which in turn incur a divergence from the original OPF solution. The magnitude of these changes increases with the distance between constrained fault breaking devices and generation. In any case, the new method guarantees that this is done in the most cost-efficient way.

9. CONCLUSIONS

9.1 Introduction

In this final Chapter, the main conclusions of this work are summarised. The thesis statement is answered and potential extensions are discussed.

9.2 Optimal capacity allocation

In the first stage of this research, a method for the allocation of maximum new capacity on existing networks was developed. The key point was in the modelling of new generators and interconnections to external grids as the outputs of virtual generators connected at respective points on the network. OPF can then determine their output, which represents size of new capacity or volume of imports/exports, by optimising an objective function. The objective function is the summation of benefit functions attached to each virtual generator and determines the benefit (monetary, communal etc.) for the network operator from expected energy exports and the ability of the network to absorb new generation capacity. Here OPF is used as a planning tool, but like in the OPF for operating purposes, the optimisation is done subject to network constraints. This guarantees that the final allocation will not result in power flows or voltage patterns violating network constraints or statutory regulations. Preferences for the allocation of new capacity can be determined at specific locations or exports can be directed to specific interconnections by tuning the benefit function parameters of the respective virtual generators. If all benefit functions of virtual generators are the same, then OPF finds the network headroom: the allocation that results in the maximum possible total new capacity for a given network.

9.3 Incorporation of fault level constraints

The next stage of this research focused on developing a methodology for the incorporation of constraints imposed by the specifications of existing network switchgear equipment on new generation capacity. The new constraints were termed Fault Level Constraints (FLCs).

Initially, an iterative approach was suggested, which included FLCs indirectly in the optimisation procedure of capacity allocation. FLCs were converted to upper bounds on new capacity. During each iteration a fault analysis was performed and the results directed the

bounds towards an OPF allocation that respected both network and FLCs. However, the solution provided from the iterative approach has no theoretical link to global optimality. Therefore, a new method was developed for the integration of FLCs in the group of OPF constraints. FLCs were converted to simple non-linear (inequality) constraints and no new variables were introduced in the OPF formulation. Most common OPF-solving engines already have the computational capacity to handle numerous non-linear constraints, such as the ones described by the power balance equations on buses. Therefore, once FLCs are converted to non-linear constraints described by OPF variables, they can be directly introduced to any optimisation process performing the OPF. The enhanced OPF directly allocates capacity with respect to both network and FLCs.

The performance of the two methods was tested on a typical distribution network. The one-step optimisation method demonstrated much better capacity allocation properties than its iterative counterpart when tested on the same example case. However, the iterative method has a significant advantage: The decoupling between OPF from fault levels permits the use of existing professional packages to implement those two basic components. This increases the reliability of the mechanism, but mostly simplifies the implementation of a commercial product.

Finally, a capacity planning mechanism was developed so that Network Operators (NOs) can use the allocations of the two methods to exploit the potential connection capacity better than the current first-come-first-served policy. The mechanism is based on the gradual release of transmission capacity through auctioning. It is just an oversimplified example of the way a planning mechanism could exploit the results of the suggested capacity allocation methods. Nonetheless, the similarities between transmission capacity release and connection capacity release guarantee that they would probably share similar advantages

9.4 Studying the impact of reactive power injections on the allocation of new capacity

The model of OPF for capacity allocation was extended, in order to accommodate two basic forms of reactive power manipulation: Reactive Power Compensation Banks (RPCBs) and generators' voltage control policies.

Reactor or capacitor banks were simulated with the reactive power outputs of virtual generators with zero active power output. Simulations on a simple distribution network proved that NOs can practically double the connecting capacity of the existing network by a small investment on RPCBs. This means that existing networks can accommodate more generation capacity than initially estimated, minimizing the significant cost of their expansion for the operator.

Alternative generator voltage control policies were converted to voltage/reactive power constraints for the virtual generators representing new generation capacity. Analysis of capacity allocations to a specific example network under different policies indicated that widespread application of intelligent automatic voltage/power factor control schemes allow the connecting capacity of the existing network to be better exploited.

However, the impressive total capacity achieved from some of the voltage control policies comes at a cost: high transmission losses. To tackle this deficiency, the OPF formulation was extended further so that the optimisation algorithm considers losses during the allocation of new capacity. The extension concerning losses is indifferent to the voltage control policy used. Allocations of capacity were performed on the same test case, with and without considering losses. When losses were considered expected exports were higher than the case that losses were not considered, even though total new capacity was lower. In other words, less power was lost 'on the way' to the demand. Currently, losses are not considered by NOs during generation capacity planning. Therefore, if the NOs are to change their voltage control policy in order to increase the connecting capacity of their networks, they have to consider the impact of new capacity on losses. The extended OPF as a tool for capacity allocation is a tool which can assist the NO to complete this task efficiently.

The exciting results of the extensions of OPF for capacity allocation state one more fact: further research is needed, so that the capabilities of OPF as a planning rather than operating tool can be fully exploited.

9.5 Network reinforcement planning mechanism

Throughout this research Sequential Quadratic Programming (SQP) was used for the solution of OPF. The LaGrange multipliers, sensitivity by-products of SQP attached to each constraint explicitly described in the OPF, can be used to facilitate network planning decisions. Based on the signals from those multipliers, an investment planning mechanism was designed for the efficient reinforcement of the existing infrastructure. The final product of the mechanism is an investment plan, which can be used from the network operator or other potential investors as a guide for when and which equipment to upgrade.

It was proven that the current generators' voltage control policy (for Power Factor Control see Chapter 5) followed by most network operators not only limits the capability of the existing network to absorb new generation capacity, but also reduces the positive effects of investment on the network in comparison with alternative voltage control policies. Simulation results proved that any of the suggested decentralised, partially centralised or centralised control methods of the reactive power output of new DGs drastically increases

the pay-back time of investment. The efficient plans provided by the above mechanism indicate that distribution network infrastructure is still a profitable investment.

9.6 Impact of FLCs in the economic operation of power systems

With a minor simplification of the OPF formulation for capacity allocation (generators have a specific capacity) it became possible to investigate the effect of FLCs on the economic operation of power systems. It was shown that the system operator may have to take evasive action even under anticipated system conditions (e.g. heavy demand or planned maintenance), in order to alter the bus voltage pattern and avoid possible switchgear overstress. These actions cause a divergence from the solutions provided by conventional OPF methods (methods which ignore FLCs) and increase operating cost to ensure reliability of protection. The new method guarantees that they are done in the most cost-efficient way.

9.7 Thesis limitations, conclusions and future work

As the power industry moves towards a more competitive environment, additional constraints become binding for power system operation [76]. Notably, fault levels and system stability are two constraints that should also be considered during OPF solution. Stability analysis involves the solution of many non-linear differential equations describing the dynamic oscillation of the machines in the power system. The solution of such equations requires numerical methods, thus, the incorporation of system stability as an additional constraint to OPF is not a straight forward process. Several suggestions have been published already in this field [77]-[78]. The importance of stability as a restricting factor for the installation of new generation is acknowledged, however one of the purposes of this research is to stress that fault levels should also not be ignored. System stability constraints will be the target of future research.

In addition, throughout this research it was assumed that all new generators are traditional synchronous machines, while new renewable power plants may often be inverter interfaced. However, this assumption does not reduce the value of our analysis. The high speed current control and over-current shut-down inherent in inverter interfaced DG results in very low fault current contribution (less than 200% of the rated current) [57]. This could be taken into account in the calculation of expected fault currents by doubling the pre-fault rated current of those DGs and using this fault value during switchgear adequacy control. Finally, it is assumed that new capacity consisted only of synchronous generators, because they have much higher fault current contribution, describing a 'worst-case scenario'.

Furthermore, the optimisation method suggested in this research for network reinforcement has an important limitation. It is based on an iterative process which traces the next optimum investment with respect to the network attained from the previous investment. However, there may be cases that if one of the previous less efficient investment options was completed, then it would lead to a set of much more efficient investment options in the next iteration. Therefore, there is a possibility that the suggested approach may not directly lead to the optimum investment plan for the total planning horizon.

A way to circumnavigate this problem would be to create a hybrid method, which would trace the best combinations of investments in two consecutive iterations, rather than for the next iteration only. First, all possible investment options would be implemented in turn and in each of them the net benefit for the network operator would be calculated. Then, again for each of the investment option, the best investment for the next iteration would be traced using the method explained in Section 7.4.5. This process would create couples of investments for the current iteration and estimated best consecutive investments. The net benefit from each couple would be summed and the investment of the current iteration that corresponds to the couple with the higher sum would be added to the reinforcement plan. The method could be possibly extended to cover more iterations into the future with combinations of investments, but an elaborate research is needed to explain how exactly this can be done.

The main conclusion of this thesis is that OPF can also be used as a powerful planning tool, besides being a widely-used operating tool. A methodology was developed for the incorporation of FLCs in OPF. Certainly, several other constraints should be included while assessing the ability of a network to absorb new capacity, such as those imposed by stability. The scope of this research extends far beyond the results achieved in this thesis. The final objective is the creation of a unified modelling approach for all 'side effects' of booming DG in distribution networks. Furthermore, further research is needed towards the improvement of the reinforcement planning method, so that the optimal long-term investment plan can be guaranteed. The encouraging conclusions of this thesis justify the pursuing of this target using OPF, as a starting point at least.

10. REFERENCES

- [1] R. E. Brown, P. Jiuping, F. Xiaorning, and K. Koutlev, "Siting distributed generation to defer T&D expansion," in *Transmission and Distribution Conference and Exposition*, vol. 2, 2001, pp. 622-627.
- [2] UCTE, "Declaration of UCTE concerning the challenges and risks of integrating booming wind power in a reliable electricity system of continental europe," Union for the Coordination of Transmission of Electricity, May 2005.
- [3] C. L. Masters, "Voltage rise: the big issue when connecting embedded generation to long 11 kV overhead lines," *Power Engineering Journal*, vol. 16, pp. 5-12, 2002.
- [4] G. P. Harrison and A. R. Wallace, "Maximizing Distributed Generation Capacity in Deregulated Markets," in *IEEE/PES Transmission & Distribution Conference & Exposition*. Dallas, USA, September 2003.
- [5] N. J. Balu, R. Adapa, G. Cauley, M. Lauby, and D. J. Maratukulam, "Review of expert systems in bulk power system planning and operation," *Proceedings of the IEEE*, vol. 80, pp. 727-731, 1992.
- [6] S. A. Farghal, M. S. Kandil, and M. R. Abdel-Aziz, "Generation expansion planning: an expert system approach," *Generation, Transmission and Distribution [see also IEE Proceedings-Generation, Transmission and Distribution]*, *IEE Proceedings C*, vol. 135, pp. 261-267, 1988.
- [7] F. D. Galiana, D. T. McGillis, and M. A. Marin, "Expert systems in transmission planning," *Proceedings of the IEEE*, vol. 80, pp. 712-726, 1992.
- [8] M. S. Kandil, S. M. El-Debeiky, and N. E. Hasanien, "Rule-based system for determining unit locations of a developed generation expansion plan for transmission planning," *IEE Proceedings on Generation, Transmission and Distribution*, vol. 147, pp. 62-68, 2000.
- [9] A. K. David and R. Zhao, "An expert system with fuzzy sets for optimal planning [of power system expansion]," *IEEE Transactions on Power Systems*, vol. 6, pp. 59-65, 1991.
- [10] S. Ching-Tzong, L. Guor-Rurng, and C. Jiann-Jung, "Long-term generation expansion planning employing dynamic programming and fuzzy techniques," *Proceedings of IEEE International Conference on Industrial Technology*, vol. 1, pp. 644-649 vol.2, 2000.

- [11] S. Dhar, "Power system long-range decision analysis under fuzzy environment," *IEEE Trans. Power Appar. Syst.*, vol. PAS-98, pp. 713-718, March/April 1979.
- [12] H. Satoh and Y. Serizawa, "Fuzzy decision-making on electric energy strategy for long-term generation expansion planning," in *IFAC power systems and power plant control*. Seoul, Korea, 1989.
- [13] R. Tanabe, K. Yasuda, and R. Yokoyama, "An algorithm for linguistic risk assessment of uncertain factors in generation planning," *Electrical Engineering in Japan*, vol. 115, pp. 112-118, 1995.
- [14] A. Keane and M. O'Malley, "Optimal Allocation of Embedded Generation on Distribution Networks," *Power Systems, IEEE Transactions on*, vol. 20, pp. 1640-1646, 2005.
- [15] K. Nara, Y. Hayashi, K. Ikeda, and T. Ashizawa, "Application of tabu search to optimal placement of distributed generators," presented at IEEE Power Engineering Society Winter Meeting, 2001.
- [16] W. Kit Po and W. Yin Wa, "Combined genetic algorithm/simulated annealing/fuzzy set approach to short-term generation scheduling with take-or-pay fuel contract," *Power Systems, IEEE Transactions on*, vol. 11, pp. 128-136, 1996.
- [17] S. Kannan, S. M. R. Slochanal, and N. P. Padhy, "Application of evolutionary computation techniques for generation expansion planning," in *Transmission and Distribution Conference and Exposition, 2003 IEEE PES*, vol. 1, 2003, pp. 120-125 Vol.1.
- [18] H. Sasaki, J. Kubokawa, M. Watanabe, R. Yokoyama, and R. Tanabe, "A solution of generation expansion problem by means of neural network," presented at First international forum on applications of neural networks to power systems, Seattle, 1991.
- [19] J. Zhu and M. Chow, "A review of emerging techniques on generation expansion planning," *IEEE Transactions on Power Systems*, vol. 12, pp. 1722-1728, November 1997.
- [20] S. Kannan, S. M. R. Slochanal, and N. P. Padhy, "Application and comparison of metaheuristic techniques to generation expansion planning problem," *Power Systems, IEEE Transactions on*, vol. 20, pp. 466-475, 2005.
- [21] B. Kuri, M. Redfern, and F. Li, "Optimization of rating and positioning of dispersed generation with minimum network disruption," presented at IEEE Power Eng. Soc. Gen. Meeting, Denver, CO, 2004.
- [22] Y. Fukuyama and C. Hsiao-Dong, "A parallel genetic algorithm for generation

- expansion planning," *IEEE Transactions on Power Systems*, vol. 11, pp. 955-961, 1996.
- [23] P. Jong-Bae, P. Young-Moon, W. Jong-Ryul, and K. Y. Lee, "An improved genetic algorithm for generation expansion planning," *Power Systems, IEEE Transactions on*, vol. 15, pp. 916-922, 2000.
 - [24] A. R. Wallace and G. P. Harrison, "Planning for optimal accommodation of dispersed generation in distribution networks," presented at CIRED 17th Int. Conf. Electr. Distrib., Barcelona, Spain, May 2003.
 - [25] G. P. Harrison and A. R. Wallace, "Optimal power flow evaluation of distribution network capacity for the connection of distributed generation," *Generation, Transmission and Distribution, IEE Proceedings*, vol. 152, pp. 115-122, 2005.
 - [26] A. Ramos, I. J. Perez-Arriaga, and J. Bogas, "A nonlinear programming approach to optimal static generation expansion planning," *Power Systems, IEEE Transactions on*, vol. 4, pp. 1140-1146, 1989.
 - [27] S. Mary Raja Slochanal, S. Kannan, and R. Rengaraj, "Generation expansion planning in the competitive environment," in *International Conference on Power System Technology, 2004*, vol. 2, 2004, pp. 1546-1549 Vol.2.
 - [28] P. Jong-Bae, K. Jin-Ho, and K. Y. Lee, "Generation expansion planning in a competitive environment using a genetic algorithm," *Power Engineering Society Summer Meeting, IEEE*, vol. 3, pp. 1169-1172, 2002.
 - [29] E. Gnansounou, J. Dong, S. Pierre, and A. Quintero, "Market oriented planning of power generation expansion using agent-based model," in *Power Systems Conference and Exposition, IEEE PES, 2004*, pp. 1306-1311 vol.3.
 - [30] P. Bresesti, M. Gallanti, and D. Lucarella, "Market-based generation and transmission expansions in the competitive market," in *Power Engineering Society General Meeting, IEEE 2003*, vol. 1, pp. 459-462.
 - [31] J. Carpienter, "Contribution e l'etude do dispatching economique," *Bulletin society Francaise electriciens*, vol. 3, August 1962.
 - [32] J. Carpienter, "Optimal Power Flows," *International Journal of Electric Power and Energy Systems*, vol. 1, pp. 3-15, April 1979.
 - [33] H. W. Dommel and W. F. Tinney, "Optimal power flow solutions," *IEEE Trans. Power Appar. Syst.*, vol. PAS-87, pp. 1866-1876, 1968.
 - [34] M. Huneault and F. Galiana, "A survey of the optimal power flows literature," *IEEE Transactions on Power Systems*, vol. 6, pp. 762-770, May 1991.
 - [35] D. Sun, B. Ashley, B. Brewer, A. Hughes, and W. Tinney, "Optimal power flow by

- Newton Approach," *IEEE Transactions on Power Apparatus and Systems*, vol. PAS-103, pp. 2864-2880, October 1984.
- [36] O. Alsac, J. Bright, M. Prais, and B. Stott, "Further developments in LP-based optimal power flow," *IEEE Transactions on Power Systems*, vol. 5, pp. 697-711, August 1990.
 - [37] S. K. Mukherjee, A. Recio, and C. Douligieris, "Optimal power flow by linear programming based optimization," presented at Southeastcon, Birmingham, AL, USA, April 1992.
 - [38] N. Karmarkar, "A new polynomial-time algorithm for linear programming," *IEEE Transactions on Power Systems*, vol. 4, pp. 373-395, 1984.
 - [39] L. Vargas, V. Quintana, and A. Vannelli, "Tutorial description of an interior point method and its applications to security-constrained economic dispatch," *IEEE Transactions on Power Systems*, vol. 8, pp. 1315-1325, August 1993.
 - [40] K. Iba, "Reactive power optimization by genetic algorithm," *IEEE Transactions on Power Systems*, vol. 9, pp. 685-692, 1994.
 - [41] W. Hock and K. Schittkowski, "A Comparative Performance Evaluation of 27 Nonlinear Programming Codes," *Computing*, vol. 30, pp. 335, 1983.
 - [42] G. W. Ault and J. R. McDonald, "Planning for distributed generation within distribution networks in restructured electricity markets," *Power Engineering Review, IEEE*, vol. 20, pp. 52-54, 2000.
 - [43] M. S. Kandil, S. M. El-Debeiky, and N. E. Hasanien, "Hybrid mathematical and rule-based system for transmission network planning in open access schemes," *Generation, Transmission and Distribution, IEE Proceedings*, vol. 148, pp. 455-462, 2001.
 - [44] P. M. S. Carvalho and L. A. F. M. Ferreira, "Planning large-scale distribution networks for robust expansion under deregulation," in *Power Engineering Society Summer Meeting, IEEE 2000*, vol. 3, pp. 1305-1310.
 - [45] D. Zhong, J. Wu, and D. Kong, "Enhanced genetic algorithm in electric network planning," in *Proceedings of the 3rd World Congress on Intelligent Control and Automation, 2000*, vol. 1, pp. 53-57.
 - [46] H. Mori and Y. Iimura, "An improved tabu search approach to distribution network expansion planning under new environment," in *International Conference on Power System Technology, 2004. PowerCon 2004*, vol. 1, pp. 981-986.
 - [47] A. Orths, "Power network planning for high penetration of dispersed energy resources. Optimal multi-criteria planning method," in *Transmission and*

- Distribution Conference and Exposition, IEEE PES 2003*, vol. 1, pp. 393-398.
- [48] V. A. Levi and M. S. Calovic, "Linear-programming-based decomposition method for optimal planning of transmission network investments," *Generation, Transmission and Distribution [see also IEE Proceedings-Generation, Transmission and Distribution]*, *IEE Proceedings C*, vol. 140, pp. 516-522, 1993.
 - [49] S. H. M. Hashimoto, R. Romero, and J. R. S. Mantovani, "Efficient linear programming algorithm for the transmission network expansion planning problem," *Generation, Transmission and Distribution, IEE Proceedings-*, vol. 150, pp. 536-542, 2003.
 - [50] S. Haffner, A. Monticelli, A. Garcia, and R. Romero, "Specialised branch-and-bound algorithm for transmission network expansion planning," *Generation, Transmission and Distribution, IEE Proceedings-*, vol. 148, pp. 482-488, 2001.
 - [51] S. N. Siddiqi and M. L. Baughman, "Value-based transmission planning and the effects of network models," *Power Systems, IEEE Transactions on*, vol. 10, pp. 1835-1842, 1995.
 - [52] R. Romero, A. Monticelli, A. Garcia, and S. Haffner, "Test systems and mathematical models for transmission network expansion planning," *Generation, Transmission and Distribution, IEE Proceedings-*, vol. 149, pp. 27-36, 2002.
 - [53] G. Giannakopoulos, *Analysi systimaton elektrikis energias - Monimi katastasi litourgias*: Patras university press, 2000.
 - [54] A. Wood and B. Wollenberg, *Power generation, operation and control*. New York: John Wiley & Sons, 1996.
 - [55] J. Grainger and W. Stevenson, *Power System Analysis*. New York: McGraw-Hill, inc., 1994.
 - [56] "Guidance on the Electricity Safety, Quality and Continuity Regulations ": Department of Trade and Industry (UK), 2005.
 - [57] S. R. Wall, "Performance of inverter interfaced distributed generation," in *IEEE/PES Transmission & Distribution Conference & Exposition*, vol. 2, 2001, pp. 945-950.
 - [58] J. M. Fogarty, "Connections between generator specifications and fundamental design principles," presented at IEEE International Electric Machines and Drives Conference IEMDC 2001, Cambridge, USA, 2001.
 - [59] "IEEE recommended practice for protection and coordination of industrial and commercial power systems," ANSI/IEEE Std 242, 1986.
 - [60] "Engineering Recommendation G74 - Procedure to meet the requirements on IEC 909 for the calculation of short-circuit currents in three-phase AC power systems,"

- Electricity Association (UK), 1992.
- [61] T. Ackermann and V. Knyazkin, "Interaction between distributed generation and the distribution network: operation aspects," presented at Transmission and Distribution Conference and Exhibition 2002: Asia Pacific. IEEE/PES, 2002.
- [62] P. Venkataraman, *Applied Optimization with Matlab Programming* John Wiley & Sons, 2002.
- [63] B. M. Weedy and B. J. Cory, *Electric Power Systems*, 4th ed. New York: Wiley, 1998.
- [64] "PowerWorld Simulation," Version 10.0 ed. Champaign, IL 61820: PowerWorld Corporation, 2005.
- [65] J. Sherman and W. J. Morrison, "Adjustment of an inverse matrix corresponding to changes in the elements of a given column or a given row of the original matrix," *Ann. Math. Statist.*, vol. 20, pp. 621, 1949.
- [66] M. A. Woodbury, "Inverting modified matrices," Princeton Univ., Princeton, N.J. 1950.
- [67] P. N. Vovos, J. W. Bialek, and G. P. Harrison, "Optimal generation capacity allocation and network expansion signalling using OPF," presented at 39th International Universities Power Engineering Conference, Bristol, UK, 2004.
- [68] Pennsylvania, Maryland, Delaware, and N. J. ISO, "Manual 6, Financial Transmission Rights," Section 6: FTR Auctions, 2004, pp. 31.
- [69] Z. Elrazaz and A. A. Al-Ohaly, "Optimal coordination of shunt recators to enhance system performance at light load operation.," *IEE Proceedings on Generation, Transmission and Distribution*, vol. 140, pp. 293-298, July 1993.
- [70] Y. Baghzouz and S. Ertem, "Shunt capacitor sizing for radial distribution feeders with distorted substation voltages," *IEEE Transactions on Power Delivery*, vol. 5, April 1990.
- [71] Ofgem, "Electricity distribution price control review," Office of Gas and Electricity Markets, March 2004.
- [72] T. W. Eberly and R. C. Schaefer, "Voltage versus VAr/power-factor regulation on synchronous generators," *IEEE Trans. Ind. Apps.*, vol. 38, pp. 1682-1687, 2002.
- [73] A. E. Kiprakis and A. R. Wallace, "Maximising Energy Capture from Distributed Generation in Weak Networks," *IEE Proceedings on Generation, Transmission and Distribution*, vol. 151, pp. 611-618, 2004.
- [74] M. J. D. Powell, "A Fast Algorithm for Nonlinearly Constrained Optimization Calculations, Numerical Analysis," in *Lecture Notes in Mathematics*, vol. 630, G. A.

- Watson, Ed.: Springer Verlag, 1978.
- [75] N. Nimpitiwan and G. T. Heydt, "Consequences of Fault Currents Contributed by Distributed Generation," Intermediate report for the PSERC project 'New implications of power system fault current limits' publication 04-34, November 2004.
- [76] J. A. Momoh, R. J. Koessler, B. S. M. S. Bond, D. Sun, A. Pa-palexopoulos, and P. Ristanovic, "Challenges to optimal power flow," *IEEE Trans. Power Systems*, vol. 12, pp. 444-455, 1997.
- [77] D. Gan, R. J. Thomas, and R. D. Zimmerman, "Stability-constrained optimal power flow," *IEEE Transactions on Power Delivery*, vol. 15, pp. 535-540, 2000.
- [78] Y. Sun, Y. Xinlin, and H. F. Wang, "Approach for optimal power flow with transient stability constraints," *IEE Proceedings on Generation, Transmission and Distribution*, vol. 151, pp. 8-18, 2004.

A. APPENDIX

A.1 The Sherman-Morrison-Woodbury formula extension to matrixes of complex numbers

The Sherman-Morrison-Woodbury formula gives the inverse of a matrix modified by one element, given the inverse of the initial matrix and the modification.

$$B_{r,k} = b_{r,k} - \frac{b_{r,L} b_{S,k} \Delta a_{L,S}}{1 + b_{S,L} \Delta a_{L,S}} \quad (\text{A.1})$$

where B is the new inverse matrix, b is the old inverse matrix, $\Delta a_{L,S}$ the modification of element L, S and α is the initial matrix with $\alpha, b, B \in R^{n \times n}$.

The formula was verified using numerical examples of matrixes with real numbers. Here, an example with a modified impedance matrix Z_{bus} of a random network (i.e. random complex numbers) will be presented.

$$\text{If } Z_{bus} = \begin{bmatrix} 0.0003 + 0.415i & 0.0002 + 0.0315i \\ 0.0002 + 0.0315i & 0.0002 + 0.1507i \end{bmatrix}$$

$$\text{and } Y_{bus} = Z_{bus}^{-1} = \begin{bmatrix} 0.1653 - 28.6522i & -0.0000 + 5.9988i \\ -0.0000 + 5.9988i & 0.0000 - 7.8927i \end{bmatrix}$$

Then if the top left element of the Z_{bus} is modified, so that $Z'_{bus}(1,1) = Z_{bus}(1,1) + 0.1i$, then

$$\text{the new inverse matrix } Y'_{bus} = Z'^{-1}_{bus} = \begin{bmatrix} 0.0111 - 7.4129i & 0.0066 + 1.5520i \\ 0.0066 + 1.5520i & 0.0040 - 6.9617i \end{bmatrix}.$$

If (A.1) is applied to the modified matrix for $b = Z_{bus}$ is the old inverse matrix, $\Delta a_{L,S} = 0.1i$ the modification of element $Z_{bus}(1,1)$ and $\alpha = Z_{bus}$ is the initial matrix, then the new inverse is

$$\text{calculated as } Y'_{bus} = \begin{bmatrix} 0.0111 - 7.4129i & 0.0066 + 1.5520i \\ 0.0066 + 1.5520i & 0.0040 - 6.9617i \end{bmatrix}.$$

The results are identical. Therefore, the S-M-W formula works with matrixes consisted of complex numbers and can be applied to the Z_{bus} matrix.

A.2 Calculation of the derivatives of fault level constraints

The fault current in line i - j for a solid fault on bus f is:

$$I_{ij}^f = \frac{V_i - V_j - FSF_{i,j}^f \cdot V_f}{\tilde{Z}_{i,j}} \quad (A.2)$$

where V_i prefault voltage of bus i , V_j the pre fault voltage of bus j , V_f the pre fault voltage of the faulted bus f , $FSF_{ij}^f = \frac{z_{i,f} - z_{j,f}}{z_{f,f}}$ (where $z_{k,\lambda}$ elements of Z_{bus}) and $\tilde{z}_{i,j}$ the serial line impedance of line ij .

The voltages V_i , V_j , V_f , as well as the $FSF_{i,j}^f$ can be expressed as a sum of a real and an imaginary part:

$$V_i = \text{Real}(V_i) + j \cdot \text{Imag}(V_i) = V_i^x + j \cdot V_i^y \quad (A.3)$$

$$V_j = \text{Real}(V_j) + j \cdot \text{Imag}(V_j) = V_j^x + j \cdot V_j^y \quad (A.4)$$

$$V_f = \text{Real}(V_f) + j \cdot \text{Imag}(V_f) = V_f^x + j \cdot V_f^y \quad (A.5)$$

$$FSF_{i,j}^f = FSF = \text{Real}(FSF) + j \cdot \text{Imag}(FSF) = FSF^x + j \cdot FSF^y \quad (A.6)$$

$$\begin{aligned} (A.1) \xrightarrow{(A.2)(A.3)} I_{i,j}^f &= \frac{V_i^x + j \cdot V_i^y - V_j^x - j \cdot V_j^y - (FSF^x + j \cdot FSF^y) \cdot (V_f^x + j \cdot V_f^y)}{\tilde{Z}_{i,j}} \Rightarrow \\ \Rightarrow I_{i,j}^f &= \frac{V_i^x - V_j^x - FSF^x \cdot V_f^x + FSF^y \cdot V_f^y + (V_i^y - V_j^y - FSF^y \cdot V_f^y - FSF^x \cdot V_f^x) \cdot j}{\tilde{Z}_{i,j}} \end{aligned} \quad (A.7)$$

$$\text{Let} \quad x = V_i^x - V_j^x - FSF^x \cdot V_f^x + FSF^y \cdot V_f^y \quad (A.8)$$

$$\text{and} \quad y = V_i^y - V_j^y - FSF^y \cdot V_f^y - FSF^x \cdot V_f^x \quad (A.9)$$

$$(A.6) \xrightarrow{(A.7)} I_{i,j}^f = \frac{x + j \cdot y}{\tilde{Z}_{i,j}} \Rightarrow |I_{i,j}^f| = \left| \frac{x + j \cdot y}{\tilde{Z}_{i,j}} \right| = \frac{|x + j \cdot y|}{|\tilde{Z}_{i,j}|} \Leftrightarrow |I_{i,j}^f| = \frac{\sqrt{x^2 + y^2}}{|\tilde{Z}_{i,j}|} \quad (A.10)$$

A.2.1 Derivatives of fault currents with respect to voltage magnitudes and angles

According to (A.2), the derivative of fault currents with respect to buses voltages different than i , j , f is zero. Obviously, the derivative of the magnitude of the fault currents with respect to those voltages is also zero. The chain rule will be used in order to calculate the desired derivatives as a function of two derivatives, which are easier to calculate:

$$\begin{aligned} \frac{d|I_{i,j}^f|}{d|V_i|} &= \frac{d|I_{i,j}^f|}{dV_i^x} \cdot \frac{dV_i^x}{d|V_i|} \\ \text{similarly, } \frac{d|I_{i,j}^f|}{d|V_j|} &= \frac{d|I_{i,j}^f|}{dV_j^x} \cdot \frac{dV_j^x}{d|V_j|} \\ \text{and, } \frac{d|I_{i,j}^f|}{d|V_f|} &= \frac{d|I_{i,j}^f|}{dV_f^x} \cdot \frac{dV_f^x}{d|V_f|} \end{aligned} \quad (\text{A.11})$$

$$\begin{aligned} \frac{dV_i^x}{d|V_i|} &= \frac{d(|V_i| \cdot \cos \varphi_i)}{d|V_i|} = \cos \varphi_i \\ \text{similarly, } \frac{dV_j^x}{d|V_j|} &= \cos \varphi_j \\ \text{and } \frac{dV_f^x}{d|V_f|} &= \cos \varphi_f \end{aligned} \quad (\text{A.12})$$

where $\varphi_i, \varphi_j, \varphi_f$ are the voltage angles of buses i, j, f .

$$\begin{aligned} \frac{d|I_{i,j}^f|}{dV_i^x} &= \frac{d\left(\frac{\sqrt{x^2+y^2}}{|\tilde{z}_{i,j}|}\right)}{dV_i^x} = \frac{1}{|\tilde{z}_{i,j}|} \frac{d\sqrt{x^2+y^2}}{dV_i^x} = \frac{1}{|\tilde{z}_{i,j}| \cdot 2 \cdot \sqrt{x^2+y^2}} \cdot \frac{d(x^2+y^2)}{dV_i^x} = \dots \\ &= \frac{1}{2 \cdot |\tilde{z}_{i,j}| \cdot |I_{i,j}^f| \cdot |\tilde{z}_{i,j}|} \cdot 2 \cdot \left(x \frac{dx}{dV_i^x} + y \frac{dy}{dV_i^x}\right) = \frac{1}{|I_{i,j}^f| \cdot |\tilde{z}_{i,j}|^2} \left(x \frac{dx}{dV_i^x} + y \frac{dy}{dV_i^x}\right) \\ \text{similarly } \frac{d|I_{i,j}^f|}{dV_j^x} &= \frac{1}{|I_{i,j}^f| \cdot |\tilde{z}_{i,j}|^2} \left(x \frac{dx}{dV_j^x} + y \frac{dy}{dV_j^x}\right) \\ \text{and } \frac{d|I_{i,j}^f|}{dV_f^x} &= \frac{1}{|I_{i,j}^f| \cdot |\tilde{z}_{i,j}|^2} \left(x \frac{dx}{dV_f^x} + y \frac{dy}{dV_f^x}\right) \end{aligned} \quad (\text{A.13})$$

A. If $f \neq i$ and $f \neq j$

- Calculation of derivatives with respect to voltage magnitudes:

$$\text{Then, } \frac{dx}{dV_i^x} = \frac{d(V_i^x - V_j^x - FSF^x \cdot V_f^x + FSF^y \cdot V_f^y)}{dV_i^x} = 1 \quad (\text{A.14})$$

$$\begin{aligned} \frac{dy}{dV_i^x} &= \frac{d(V_i^y - V_j^y - FSF^y \cdot V_f^x - FSF^x \cdot V_f^y)}{dV_i^x} = \dots \\ &= \frac{d(V_i^x \cdot \tan \varphi_i - V_j^y - FSF^y \cdot V_f^x - FSF^x \cdot V_f^y)}{dV_i^x} = \tan \varphi_i \end{aligned} \quad (\text{A.15})$$

$$(A.10) \xrightarrow[(A.13),(A.14)]{(A.11),(A.12)} \rightarrow \frac{d|I_{i,j}^f|}{d|V_i|} = \left[\frac{x + y \cdot \tan \varphi_i}{|I_{i,j}^f| \cdot |\tilde{z}_{i,j}|^2} \right] \cos \varphi_i \quad (A.16)$$

$$\text{Similarly, } \frac{dx}{dV_j^x} = \frac{d(V_i^x - V_j^x - FSF^x \cdot V_f^x + FSF^y \cdot V_f^y)}{dV_j^x} = -1 \quad (A.17)$$

$$\begin{aligned} \text{and } \frac{dy}{dV_j^x} &= \frac{d(V_i^y - V_j^y - FSF^y \cdot V_f^x - FSF^x \cdot V_f^y)}{dV_j^x} = \dots \\ &= \frac{d(V_i^y - V_j^x \cdot \tan \varphi_j - FSF^y \cdot V_f^x - FSF^x \cdot V_f^y)}{dV_j^x} = -\tan \varphi_j \end{aligned} \quad (A.18)$$

$$\text{Thus, } (A.10) \xrightarrow[(A.16),(A.17)]{(A.11),(A.12)} \rightarrow \frac{d|I_{i,j}^f|}{d|V_j|} = \left[\frac{-x - y \cdot \tan \varphi_j}{|I_{i,j}^f| \cdot |\tilde{z}_{i,j}|^2} \right] \cos \varphi_j \quad (A.19)$$

$$\begin{aligned} \text{Similarly, } \frac{dx}{dV_f^x} &= \frac{d(V_i^x - V_j^x - FSF^x \cdot V_f^x + FSF^y \cdot V_f^y)}{dV_f^x} = \dots \\ &= \frac{d(V_i^x - V_j^x - FSF^x \cdot V_f^x + FSF^y \cdot V_f^x \cdot \tan \varphi_f)}{dV_f^x} = -FSF^x + FSF^y \cdot \tan \varphi_f \end{aligned} \quad (A.20)$$

$$\begin{aligned} \text{and } \frac{dy}{dV_f^x} &= \frac{d(V_i^y - V_j^y - FSF^y \cdot V_f^x - FSF^x \cdot V_f^y)}{dV_f^x} = \dots \\ &= \frac{d(V_i^y - V_j^y - FSF^y \cdot V_f^x - FSF^x \cdot V_f^x \cdot \tan \varphi_f)}{dV_f^x} = -FSF^y - FSF^x \cdot \tan \varphi_f \end{aligned} \quad (A.21)$$

$$\begin{aligned} &\text{Thus, } (A.10) \xrightarrow[(A.19),(A.20)]{(A.11),(A.12)} \rightarrow \\ \frac{d|I_{i,j}^f|}{d|V_f|} &= \left[\frac{-x \cdot (-FSF^x + FSF^y \cdot \tan \varphi_f) + y \cdot (-FSF^y - FSF^x \cdot \tan \varphi_f)}{|I_{i,j}^f| \cdot |\tilde{z}_{i,j}|^2} \right] \cos \varphi_f \end{aligned} \quad (A.22)$$

- Calculation of derivatives with respect to voltage angles:

$$\begin{aligned} \frac{d|I_{i,j}^f|}{d\varphi_i} &= \frac{d|I_{i,j}^f|}{dV_i^x} \cdot \frac{dV_i^x}{d\varphi_i} \\ \text{similarly } \frac{d|I_{i,j}^f|}{d\varphi_j} &= \frac{d|I_{i,j}^f|}{dV_j^x} \cdot \frac{dV_j^x}{d\varphi_j} \\ \text{and } \frac{d|I_{i,j}^f|}{d\varphi_i} &= \frac{d|I_{i,j}^f|}{dV_i^x} \cdot \frac{dV_i^x}{d\varphi_i} \end{aligned} \quad (\text{A.23})$$

$$\begin{aligned} \frac{dV_i^x}{d\varphi_i} &= \frac{d(|V_i| \cos \varphi_i)}{d\varphi_i} = -|V_i| \cdot \sin \varphi_i \\ \text{similarly } \frac{dV_j^x}{d\varphi_j} &= -|V_j| \sin \varphi_j \\ \text{and } \frac{dV_f^x}{d\varphi_f} &= -|V_f| \sin \varphi_f \end{aligned} \quad (\text{A.24})$$

$$(A.22) \xrightarrow[(A.13),(A.14)]{(A.12),(A.23)} \frac{d|I_{i,j}^f|}{d\varphi_i} = - \left[\frac{x + y \cdot \tan \varphi_i}{|I_{i,j}^f| \cdot |\tilde{z}_{i,j}|^2} \right] \cdot |V_i| \cdot \sin \varphi_i \quad (\text{A.25})$$

$$(A.22) \xrightarrow[(A.16),(A.17)]{(A.12),(A.23)} \frac{d|I_{i,j}^f|}{d\varphi_j} = \left[\frac{x + y \cdot \tan \varphi_j}{|I_{i,j}^f| \cdot |\tilde{z}_{i,j}|^2} \right] \cdot |V_j| \cdot \sin \varphi_j \quad (\text{A.26})$$

$$\begin{aligned} (A.22) \xrightarrow[(A.16),(A.17)]{(A.12),(A.23)} \frac{d|I_{i,j}^f|}{d\varphi_f} &= \dots \\ &= - \left[\frac{x \cdot (-FSF^x + FSF^y \cdot \tan \varphi_f) + y \cdot (-FSF^y - FSF^x \cdot \tan \varphi_f)}{|I_{i,j}^f| \cdot |\tilde{z}_{i,j}|^2} \right] |V_f| \cdot \sin \varphi_f \end{aligned} \quad (\text{A.27})$$

B. If $f=i$

- Calculation of derivatives with respect to voltage magnitudes:

$$\begin{aligned} \frac{dx}{dV_i^x} &= \frac{d(V_i^x - V_j^x - FSF^x \cdot V_i^x + FSF^y \cdot V_i^y)}{dV_i^x} = \dots \\ &= \frac{d(V_i^x - V_j^x - FSF^x \cdot V_i^x + FSF^y \cdot V_i^x \cdot \tan \varphi_i)}{dV_i^x} = 1 - FSF^x + FSF^y \cdot \tan \varphi_i \end{aligned} \quad (\text{A.28})$$

$$\begin{aligned} \frac{dy}{dV_i^x} &= \frac{d(V_i^y - V_j^y - FSF^y \cdot V_i^x - FSF^x \cdot V_i^y)}{dV_i^x} = \dots \\ &= \frac{d(V_i^x \cdot \tan \varphi_i - V_j^y - FSF^y \cdot V_i^x - FSF^x \cdot V_i^x \cdot \tan \varphi_i)}{dV_i^x} = \dots \\ &= \tan \varphi_i (1 - FSF^x) - FSF^y \end{aligned} \quad (\text{A.29})$$

$$(A.10) \xrightarrow[(A.27),(A.28)]{(A.11),(A.12)}$$

$$\frac{d|I_{i,j}^f|}{d|V_i|} = \frac{x \cdot (1 - FSF^x + FSF^y \cdot \tan \varphi_i) + y \cdot (\tan \varphi_i - FSF^y - FSF^x \cdot \tan \varphi_i)}{|I_{i,j}^f| \cdot |\tilde{z}_{i,j}|^2} \cos \varphi_i \quad (A.30)$$

$$\text{similarly, } \frac{dx}{dV_j^x} = \frac{d(V_i^x - V_j^x - FSF^x \cdot V_i^x + FSF^y \cdot V_i^y)}{dV_j^x} = -1 \quad (A.31)$$

$$\begin{aligned} \text{and } \frac{dy}{dV_j^x} &= \frac{d(V_i^y - V_j^y - FSF^y \cdot V_i^x - FSF^x \cdot V_i^y)}{dV_j^x} = \dots \\ &= \frac{d(V_i^y - V_j^y \cdot \tan \varphi_j - FSF^y \cdot V_i^x - FSF^x \cdot V_i^y)}{dV_j^x} = -\tan \varphi_j \end{aligned} \quad (A.32)$$

$$\text{Thus, } (A.10) \xrightarrow[(A.30),(A.31)]{(A.11),(A.12)} \frac{d|I_{i,j}^f|}{d|V_j|} = \frac{-x - y \cdot \tan \varphi_j}{|I_{i,j}^f| \cdot |\tilde{z}_{i,j}|^2} \cos \varphi_j \quad (A.33)$$

$$\text{Since } f=i: \frac{dx}{dV_f^x} = \frac{dx}{dV_i^x} = 1 - FSF^x + FSF^y \cdot \tan \varphi_f \quad (A.34)$$

$$\text{and } \frac{dy}{dV_f^x} = \frac{dy}{dV_i^x} = \tan \varphi_f \cdot (1 - FSF^x) - FSF^y \quad (A.35)$$

$$\text{Thus, } (A.10) \xrightarrow[(A.33),(A.34)]{(A.11),(A.12)}$$

$$\frac{d|I_{i,j}^f|}{d|V_f|} = \frac{x(1 - FSF^x + FSF^y \cdot \tan \varphi_f) + y(\tan \varphi_f - FSF^y - FSF^x \cdot \tan \varphi_f)}{|I_{i,j}^f| \cdot |\tilde{z}_{i,j}|^2} \cos \varphi_f \quad (A.36)$$

- Calculation of derivatives with respect to voltage angles:

$$\begin{aligned} \frac{d|I_{i,j}^f|}{d\varphi_i} &= \frac{d|I_{i,j}^f|}{dV_i^x} \cdot \frac{dV_i^x}{d\varphi_i} \xrightarrow[(A.27),(A.28)]{(A.12),(A.23)} \\ \frac{d|I_{i,j}^f|}{d\varphi_i} &= -\frac{x(1 - FSF^x + FSF^y \cdot \tan \varphi_i) + y(\tan \varphi_i(1 - FSF^x) - FSF^y)}{|I_{i,j}^f| \cdot |\tilde{z}_{i,j}|^2} |V_i| \cdot \sin \varphi_i \end{aligned} \quad (A.37)$$

$$\begin{aligned} \frac{d|I_{i,j}^f|}{d\varphi_j} &= \frac{d|I_{i,j}^f|}{dV_j^x} \cdot \frac{dV_j^x}{d\varphi_j} \xrightarrow[(A.30),(A.31)]{(A.12),(A.23)} \\ \frac{d|I_{i,j}^f|}{d\varphi_j} &= \frac{x + y \cdot \tan \varphi_j}{|I_{i,j}^f| \cdot |\tilde{z}_{i,j}|^2} |V_j| \cdot \sin \varphi_j \end{aligned} \quad (A.38)$$

$$\begin{aligned} \frac{d|I_{i,j}^f|}{d\varphi_f} &= \frac{d|I_{i,j}^f|}{dV_f^x} \cdot \frac{dV_f^x}{d\varphi_f} \xrightarrow[(A.33),(A.34)]{(A.12),(A.23)} \\ \frac{d|I_{i,j}^f|}{d\varphi_f} &= \frac{x(1 - FSF^x + FSF^y \cdot \tan \varphi_f) + y(\tan \varphi_f(1 - FSF^x) - FSF^y)}{-|I_{i,j}^f| \cdot |\tilde{z}_{i,j}|^2} |V_f| \cdot \sin \varphi_f \end{aligned} \quad (A.39)$$

C. If $f=j$

- Calculation of derivatives with respect to voltage magnitudes:

$$\begin{aligned} \frac{dx}{dV_j^x} &= \frac{d(V_i^x - V_j^x - FSF^x \cdot V_j^x + FSF^y \cdot V_j^y)}{dV_j^x} = \dots \\ &= \frac{d(V_i^x - V_j^x - FSF^x V_j^x + FSF^y \cdot V_j^x \cdot \tan \varphi_j)}{dV_j^x} = -1 - FSF^x + FSF^y \cdot \tan \varphi_j \end{aligned} \quad (A.40)$$

$$\begin{aligned} \frac{dy}{dV_j^x} &= \frac{d(V_i^y - V_j^y - FSF^y \cdot V_j^x - FSF^x \cdot V_j^y)}{dV_j^x} = \dots \\ &= \frac{d(V_i^y - FSF^y \cdot V_j^x - (1 + FSF^x) \cdot V_j^x \cdot \tan \varphi_j)}{dV_j^x} = -\tan \varphi_j (1 + FSF^x) - FSF^y \end{aligned} \quad (A.41)$$

$$(A.10) \xrightarrow{(A.11),(A.12) \atop (A.39),(A.40)}$$

$$\frac{d|I_{i,j}^f|}{d|V_j|} = \frac{x \cdot (-1 - FSF^x + FSF^y \cdot \tan \varphi_j) - y \cdot (\tan \varphi_j (1 + FSF^x) + FSF^y)}{|I_{i,j}^f| \cdot |\tilde{z}_{i,j}|^2} \cos \varphi_j \quad (A.42)$$

$$\frac{dx}{dV_i^x} = \frac{d(V_i^x - V_j^x - FSF^x \cdot V_j^x + FSF^y \cdot V_j^y)}{dV_i^x} = 1 \quad (A.43)$$

$$\begin{aligned} \frac{dy}{dV_i^x} &= \frac{d(V_i^y - V_j^y - FSF^y \cdot V_j^x - FSF^x \cdot V_j^y)}{dV_i^x} = \dots \\ &= \frac{d(V_i^x \cdot \tan \varphi_i - V_j^y - FSF^y \cdot V_j^x - FSF^x \cdot V_j^y)}{dV_i^x} = \tan \varphi_i \end{aligned} \quad (A.44)$$

$$(A.10) \xrightarrow{(A.11),(A.12) \atop (A.42),(A.43)} \frac{d|I_{i,j}^f|}{d|V_i|} = \frac{x + y \cdot \tan \varphi_i}{|I_{i,j}^f| \cdot |\tilde{z}_{i,j}|^2} \cos \varphi_i \quad (A.45)$$

$$\text{Since } f=i : \frac{dx}{dV_f^x} = \frac{dx}{dV_j^x} = -1 - FSF^x + FSF^y \cdot \tan \varphi_f \quad (A.46)$$

$$\text{and } \frac{dy}{dV_f^x} = \frac{dy}{dV_j^x} = -\tan \varphi_f - FSF^y - FSF^x \cdot \tan \varphi_f \quad (A.47)$$

$$(A.10) \xrightarrow{(A.11),(A.12) \atop (A.45),(A.46)}$$

$$\frac{d|I_{i,j}^f|}{d|V_f|} = \frac{x \cdot (-1 - FSF^x + FSF^y \cdot \tan \varphi_f) - y \cdot (\tan \varphi_f (1 + FSF^x) + FSF^y)}{|I_{i,j}^f| \cdot |\tilde{z}_{i,j}|^2} \cos \varphi_f \quad (A.48)$$

- Calculation of derivatives with respect to voltage angles:

$$\frac{d|I'_{i,j}|}{d\varphi_j} = \frac{d|I'_{i,j}|}{dV_j^x} \cdot \frac{dV_j^x}{d\varphi_j} \xrightarrow[(A.39),(A.40)]{(A.12),(A.23)}$$

$$\frac{d|I'_{i,j}|}{d\varphi_j} = - \frac{x(-1 - FFSF^x + FFSF^y \tan \varphi_j) - y(\tan \varphi_j(1 + FFSF^x) + FFSF^y)}{|I'_{i,j}| \cdot |\tilde{z}_{i,j}|^2} |V_j| \cdot \sin \varphi_j \quad (A.49)$$

$$\frac{d|I'_{i,j}|}{d\varphi_i} = \frac{d|I'_{i,j}|}{dV_i^x} \cdot \frac{dV_i^x}{d\varphi_i} \xrightarrow[(A.42),(A.43)]{(A.12),(A.23)}$$

$$\frac{d|I'_{i,j}|}{d\varphi_i} = - \frac{x + y \cdot \tan \varphi_i}{|I'_{i,j}| \cdot |\tilde{z}_{i,j}|^2} |V_i| \cdot \sin \varphi_i \quad (A.50)$$

$$\frac{d|I'_{i,j}|}{d\varphi_f} = \frac{d|I'_{i,j}|}{dV_f^x} \cdot \frac{dV_f^x}{d\varphi_f} \xrightarrow[(A.45),(A.46)]{(A.12),(A.23)}$$

$$\frac{d|I'_{i,j}|}{d\varphi_f} = \frac{x(FFSF^y \tan \varphi_f - 1 - FFSF^x) - y(\tan \varphi_f(1 + FFSF^x) + FFSF^y)}{-|I'_{i,j}| \cdot |\tilde{z}_{i,j}|^2} |V_f| \cdot \sin \varphi_f \quad (A.51)$$

A.2.2 Derivatives of fault currents with respect to real and reactive power of generators

If P^G is the real power, Q^G is the reactive power and jY_G the subtransient, transient or steady state admittance of generator G , then:

$$\frac{d|I'_{i,j}|}{dP^G} = \frac{d|I'_{i,j}|}{dY_G} \cdot \frac{dY_G}{dP^G} \quad (A.52)$$

$$\text{and } \frac{d|I'_{i,j}|}{dQ^G} = \frac{d|I'_{i,j}|}{dY_G} \cdot \frac{dY_G}{dQ^G} \quad (A.53)$$

$$\frac{d|I'_{i,j}|}{dY_G} \stackrel{(A.9)}{=} \frac{d\left(\frac{\sqrt{x^2 + y^2}}{|\tilde{z}_{i,j}|}\right)}{dY_G} = \dots \text{similar to the calculation of (A.12)} \dots$$

$$\dots = \frac{1}{|I'_{i,j}| \cdot |\tilde{z}_{i,j}|^2} \left(x \frac{dx}{dY_G} + y \frac{dy}{dY_G} \right) \quad (A.54)$$

$$\frac{dx}{dY_G} = \frac{d(V_i^x - V_j^x - FFSF^x \cdot V_f^x + FFSF^y \cdot V_f^y)}{dY_G} = -V_f^x \frac{dFFSF^x}{dY_G} + V_f^y \frac{dFFSF^y}{dY_G} \quad (A.55)$$

$$\frac{dy}{dY_G} = \frac{d(V_i^y - V_j^y - FFSF^y \cdot V_f^x + FFSF^x \cdot V_f^y)}{dY_G} = -V_f^y \frac{dFFSF^y}{dY_G} - V_f^x \frac{dFFSF^x}{dY_G} \quad (A.56)$$

$$\text{Attention: } F_{SF} = F_{SF}^x + jF_{SF}^y \Rightarrow \frac{dF_{SF}}{dY_G} = \frac{dF_{SF}^x}{dY_G} + j \cdot \frac{dF_{SF}^y}{dY_G}$$

Therefore

$$\frac{dF_{SF}^x}{dY_G} = \text{real} \left(\frac{dF_{SF}}{dY_G} \right) \quad (\text{A.57})$$

$$\frac{dF_{SF}^y}{dY_G} = \text{imag} \left(\frac{dF_{SF}}{dY_G} \right) \quad (\text{A.58})$$

$\frac{dF_{SF}}{dY_G}$ is unknown and has to be calculated.

However, $Z_{bus} = Y_{bus}^{-1}$. If a change to generator's admittance is assumed to be $j\Delta Y_G$, then ΔY_G is added to the diagonal element y_{GG} of the admittance matrix. According to the Sherman-Morrison-Woodbury formula, any element κ, λ of the new inverse matrix Z_{bus}' is given by the equation:

$$z_{\kappa,\lambda}' = z_{\kappa,\lambda} - \frac{z_{\kappa,G} \cdot z_{G,\lambda} \cdot j \cdot \Delta Y_G}{1 + z_{G,G} \cdot j \cdot \Delta Y_G} \quad (\text{A.59})$$

$$\text{For } \kappa=i \text{ and } \lambda=f : (\text{A.58}) \Rightarrow z_{i,f}' = z_{i,f} - \frac{z_{i,G} \cdot z_{G,f} \cdot j \cdot \Delta Y_G}{1 + z_{G,G} \cdot j \cdot \Delta Y_G} \quad (\text{A.60})$$

$$\text{For } \kappa=j \text{ and } \lambda=f : (\text{A.58}) \Rightarrow z_{j,f}' = z_{j,f} - \frac{z_{j,G} \cdot z_{G,f} \cdot j \cdot \Delta Y_G}{1 + z_{G,G} \cdot j \cdot \Delta Y_G} \quad (\text{A.61})$$

$$\text{For } \kappa=f \text{ and } \lambda=f : (\text{A.58}) \Rightarrow z_{f,f}' = z_{f,f} - \frac{z_{f,G} \cdot z_{G,f} \cdot j \cdot \Delta Y_G}{1 + z_{G,G} \cdot j \cdot \Delta Y_G} \quad (\text{A.62})$$

If F_{SF}' is the F_{SF} after the change to the generator's admittance, then:

$$\begin{aligned} F_{SF}' &= \frac{z_{i,f}' - z_{j,f}'}{z_{f,f}'} \xrightarrow{(\text{A.59}), (\text{A.60}), (\text{A.61})} \\ F_{SF}' &= \frac{z_{i,f} - \frac{z_{i,G} \cdot z_{G,f} \cdot j \cdot \Delta Y_G}{1 + z_{G,G} \cdot j \cdot \Delta Y_G} - z_{j,f} + \frac{z_{j,G} \cdot z_{G,f} \cdot j \cdot \Delta Y_G}{1 + z_{G,G} \cdot j \cdot \Delta Y_G}}{z_{f,f} - \frac{z_{f,G} \cdot z_{G,f} \cdot j \cdot \Delta Y_G}{1 + z_{G,G} \cdot j \cdot \Delta Y_G}} = \dots \\ &= \frac{z_{i,f} - z_{j,f} - \frac{(z_{i,G} - z_{j,G}) \cdot z_{G,f} \cdot j \cdot \Delta Y_G}{1 + z_{G,G} \cdot j \cdot \Delta Y_G}}{z_{f,f} - \frac{z_{f,G} \cdot z_{G,f} \cdot j \cdot \Delta Y_G}{1 + z_{G,G} \cdot j \cdot \Delta Y_G}} \Rightarrow \end{aligned}$$

$$FSF' = \frac{(A \cdot \mu - k) \cdot \Delta Y_G + A}{(\xi \cdot \mu - \rho) \cdot \Delta Y_G + \xi} \quad (A.63)$$

where $A = z_{i,f} - z_{j,f}$, $k = (z_{i,G} - z_{j,G}) \cdot z_{G,f} \cdot j$, $\mu = z_{G,G} \cdot j$, $\xi = z_{f,f}$, $\rho = z_{f,G} \cdot z_{G,f} \cdot j$

Using the definition of derivative:

$$\begin{aligned} \frac{dFSF}{dY_G} &= \lim_{\Delta Y_G \rightarrow 0} \frac{FSF' - FSF}{\Delta Y_G} \stackrel{(A.62)}{=} \lim_{\Delta Y_G \rightarrow 0} \frac{\frac{(A \cdot \mu - k) \cdot \Delta Y_G + A}{(\xi \cdot \mu - \rho) \cdot \Delta Y_G + \xi} - \frac{A}{\xi}}{\Delta Y_G} \Rightarrow \\ \frac{dFSF}{dY_G} &= \dots = -\frac{k \cdot \xi - A \cdot \rho}{\xi^2} = C \end{aligned} \quad (A.64)$$

where κ , ξ , A , ρ are calculated for the current generator set-up (Y_{G1}, Y_{G2}, \dots) , so C is a constant.

$$\begin{aligned} (A.53) &\xrightarrow[(A.56), (A.57), (A.63)]{(A.54), (A.55)} \\ \frac{d|I'_{i,j}|}{dY_G} &= \frac{[x \cdot (-V_f^x \cdot \text{real}(C) + V_f^y \cdot \text{imag}(C)) - y \cdot (V_f^x \cdot \text{imag}(C) + V_f^y \cdot \text{real}(C))]}{|I'_{i,j}| \cdot |\tilde{z}_{i,j}|^2} \end{aligned} \quad (A.65)$$

$$\begin{aligned} Y_G &= -\frac{1}{X_G} \stackrel{(2.1)}{=} -\frac{1}{X_{\text{typical}} \frac{S_b}{S^G}} \stackrel{(2.9)}{=} -\frac{1}{X_{\text{typical}} \frac{S_b}{P^G / p.f.}} \Rightarrow \\ Y_G &= -\frac{P^G}{X_{\text{typical}} \cdot S_b \cdot p.f.} = -\frac{Q^G}{X_{\text{typical}} \cdot S_b \cdot \sin(\text{acos}(p.f.))} \end{aligned} \quad (A.66)$$

$$\frac{dY_G}{dP^G} \stackrel{(A.65)}{=} \frac{d\left(-\frac{P^G}{X_{\text{typical}} \cdot S_b \cdot p.f.}\right)}{dP^G} = -\frac{1}{X_{\text{typical}} \cdot S_b \cdot p.f.} \quad (A.67)$$

$$\frac{dY_G}{dQ^G} \stackrel{(A.65)}{=} \frac{d\left(-\frac{Q^G}{X_{\text{typical}} \cdot S_b \cdot \sin(\text{acos}(p.f.))}\right)}{dP^G} = -\frac{1}{X_{\text{typical}} \cdot S_b \cdot \sin(\text{acos}(p.f.))} \quad (A.68)$$

$$\begin{aligned} (A.51) &\xrightarrow[(A.66)]{(A.64)} \\ \frac{d|I'_{i,j}|}{dP^G} &= \frac{x \cdot (-V_f^x \cdot \text{real}(C) + V_f^y \cdot \text{imag}(C)) - y \cdot (V_f^x \cdot \text{imag}(C) + V_f^y \cdot \text{real}(C))}{-|I'_{i,j}| \cdot |\tilde{z}_{i,j}|^2 \cdot X_{\text{typical}} \cdot S_b \cdot p.f.} \end{aligned} \quad (A.69)$$

$$\begin{aligned} (A.51) &\xrightarrow[(A.67)]{(A.64)} \\ \frac{d|I'_{i,j}|}{dQ^G} &= \frac{x \cdot (-V_f^x \cdot \text{real}(C) + V_f^y \cdot \text{imag}(C)) - y \cdot (V_f^x \cdot \text{imag}(C) + V_f^y \cdot \text{real}(C))}{-|I'_{i,j}| \cdot |\tilde{z}_{i,j}|^2 \cdot X_{\text{typical}} \cdot S_b \cdot \sin(\text{acos}(p.f.))} \end{aligned} \quad (A.70)$$

A.3 Derivatives of traditional non-linear constrained functions in the Optimal Power Flow formulation

A.3.1 Apparent power flows constrained by lines thermal limits

If $|S_f|$ is the apparent power at the 'from' bus f end of each line, which must be less than the thermal limit of the respective line, then the partial derivatives with respect to the OPF variables are:

$$\frac{d|S_f|}{dP_f} = \frac{\text{real}(|S_f|)}{|S_f|} \quad (\text{A.71})$$

$$\frac{d|S_f|}{dQ_f} = \frac{\text{imag}(|S_f|)}{|S_f|} \quad (\text{A.72})$$

$$\frac{d|S_f|}{d|V_n|} = \frac{d|S_f|}{dP_f} \cdot \frac{dP_f}{d|V_n|} + \frac{d|S_f|}{dQ_f} \cdot \frac{dQ_f}{d|V_n|} \quad (\text{A.73})$$

$$\frac{d|S_f|}{d\varphi_n} = \frac{d|S_f|}{dP_f} \cdot \frac{dP_f}{d\varphi_n} + \frac{d|S_f|}{dQ_f} \cdot \frac{dQ_f}{d\varphi_n} \quad (\text{A.74})$$

where P_f/Q_f are the real/reactive power output of a generator located at bus f , whereas $|V_n|$ and φ_n are the voltage magnitude and phase angle of bus n . The derivatives of the 'to' bus are similar.

A.3.2 Power imbalance at buses equal to zero

$S_n^{unb.}$, the complex power unbalance of bus n , which must be equal to zero at the OPF solution point, is equal to:

$$S_n^{unb.} = V_n \cdot (I_n)^* - S_n^{net} = V_n \cdot \left(\sum_k (Y_{n,k} \cdot V_n) \right)^* - S_n^{net} \quad (\text{A.75})$$

where V_n , I_n and S_n^{net} are the voltage, net injected current and net injected complex power of bus n . The partial derivative of $S_n^{unb.}$, with respect to the OPF variables are:

$$\begin{aligned} \frac{dS_n^{unb.}}{d|V_n|} &= \frac{dV_n}{d|V_n|} \cdot \left(\sum_k (Y_{n,k} \cdot V_k) \right)^* + V_n \cdot \left(\frac{d \sum_k (Y_{n,k} \cdot V_k)}{d|V_n|} \right)^* = \dots \\ &\dots = \frac{V_n}{|V_n|} \cdot \left(\sum_k (Y_{n,k} \cdot V_k) \right)^* + V_n \cdot \left(\frac{Y_{n,k} V_n}{|V_n|} \right)^* \end{aligned} \quad (\text{A.76})$$

$$\begin{aligned} \frac{dS_n^{unb.}}{d\varphi_n} &= \frac{dV_n}{d\varphi_n} \cdot \left(\sum_k (Y_{n,k} \cdot V_k) \right)^* + V_n \cdot \left(\frac{d \sum_k (Y_{n,k} \cdot V_k)}{d\varphi_n} \right)^* = \dots \\ &\dots = j \cdot V_n \cdot \left(\sum_k (Y_{n,k} \cdot V_k) \right)^* + V_n \cdot (Y_{n,k} \cdot j \cdot V_n)^* \end{aligned} \quad (\text{A.77})$$

$$\frac{dS_n^{unb.}}{dP_n} = -\frac{dS_n^{net}}{dP_n} = -1 \quad (\text{A.78})$$

$$\frac{dS_n^{unb.}}{dQ_n} = -\frac{dS_n^{net}}{dQ_n} = -j \quad (\text{A.79})$$

where $Y_{s,r}$ is the s,r element of the network admittance matrix, P_n/Q_n are the real/reactive power output of a generator located at bus n , whereas $|V_n|$ and φ_n are the voltage magnitude and phase angle of bus n .

B. PUBLISHED/SUBMITTED PAPERS CONNECTED WITH THESIS

Journals

Panagis N. Vovos, Gareth P. Harrison, A. Robin Wallace, and Janusz W. Bialek '*Optimal Power Flow as a Tool for Fault Level Constrained Network Capacity Analysis*', IEEE Trans. Power Systems, Vol. 20, pp. 734-741, May 2005.

Panagis N. Vovos and Janusz W. Bialek, '*Direct Incorporation of Fault Level Constraints in Optimal Power Flow as a Tool for Network Capacity Analysis*', IEEE Trans. Power Systems, to be published in November 2005.

Panagis N. Vovos and Janusz W. Bialek, '*A Combinational Mechanism for Generation Capacity and Network Reinforcement Planning*', Proc. IEE - Gen. Transm. Dist., submitted in July 2005.

Panagis N. Vovos and Janusz W. Bialek, 'Impact of Fault Level Constraints on the Economic Operation of Power Systems', IEEE Trans. Power Systems, under review.

Conferences

Panagis N. Vovos and Janusz W. Bialek, 'Impact of Fault Level Constraints on the Economic Operation of Power Systems', PowerTech, St. Petersburg (Russia), June 2005.

Panagis N. Vovos, Aristides E. Kiprakis, Gareth P. Harrison and J. Robert Barrie, 'Enhancement Of Network Capacity By Widespread Intelligent Generator Control', International Conference & Exhibition on Electricity Distribution (CIRED), Turin (Italy), June 2005.

Panagis N. Vovos, Janusz W. Bialek and Gareth P. Harrison, 'Optimal Generation Capacity Allocation and Network Expansion Signaling using OPF', Proc. 39th Universities Power Engineering Conference, Bristol (UK), September 2004.